THE
PHYSICAL REVIEW
A Journal of Experimental and Theoretical Physics Established by E. L. Nichols in 1893
VOL. 51, NO. 5 MARCH 1, 1937 SECOND SERIES

The Absorption of Ionic Crystals in the Ultraviolet*

E. G. SCHNEIDER AND H. M. O'BRYAN
Harvard University, Cambridge, Massachusetts
(Received December 21, 1936)

In order to extend the measurements of Hilsch and Pohl on the ultraviolet absorption bands of the alkali halides below 1600A, lithium fluoride has been used as a support for thin films of the salts. Selected lithium fluoride plates of one millimeter thickness when properly cleaned were consistently transparent to 1050A. The compound to be studied was distilled onto the lithium fluoride within a Thibaud spectrograph. A silver solder Carboloy hot spark and Ilford Q plates were used to make the measurements. Comparison of spectra transmitted by the lithium fluoride plates with and without absorbing films of approximately 0.05 micron thickness show, in addition to the bands reported by Hilsch and Pohl, a number of bands below 1600A whose widths vary between 0.3 and 1.3 electron volts. Observations made on some of these compounds by A. Smith, using a less direct method, agree very poorly with these measurements. A comparison of the observed bands with the computations by A. v. Hippel shows fairly complete agreement. Results on several other halides show only a series of sharp absorption edges with continuous absorption toward shorter wave-lengths.

SINCE lithium fluoride plates which are transparent to wave-lengths as short as 1050A can be obtained, it has been possible to extend absorption measurements on thin films of the alkali halides beyond the limit of fluorite. Hilsch and Pohl,[1] using a double fluorite monochromator with photoelectric cells, have measured the absorption bands of these salts above 1600A. This limit, almost 400A above the limit of transmission of a thin plate of fluorite, was set by the high surface loss and absorption of the lenses and prisms. In order to avoid similar light losses with the lithium fluoride, the thin plates which were used as supports for the extremely thin films of the salts under observation were placed in a grating vacuum spectrograph rather than in a prism instrument.

The spectrograph was of the Thibaud[2] plane grating type, as shown in Fig. 1, with a defining slit, and a knife edge in front of the grating. The slit consisted of a small plate glass mirror separated from the edge of a razor blade by shims. This slit, consisting of a real jaw (the edge of the blade) and a virtual jaw (the image of the knife edge in the mirror), was mounted on a brass cone which could be rotated about an axis through the surface of the mirror. The light source—a spark between silver solder and tungsten carbide (Carboloy) electrodes, excited by a 40,000 volt a.c. transformer coupled with a 0.01 mf condenser—was placed slightly out of the line passing through the slit and grating. By a simple rotation of the slit mirror the image of the spark could be brought into alignment with the optical axis of the spectrograph, thus eliminating the usual tedious adjustment by motion of the electrodes. A further advantage of this slit was that the light reflected from the mirror at grazing incidence was only slightly

* Presented at the New York meeting of the American Physical Society, October, 1936.
[1] Hilsch and Pohl, Zeits. f. Physik **59**, 812 (1930).
[2] Thibaud, Physik Zeits. **29**, 241 (1928).

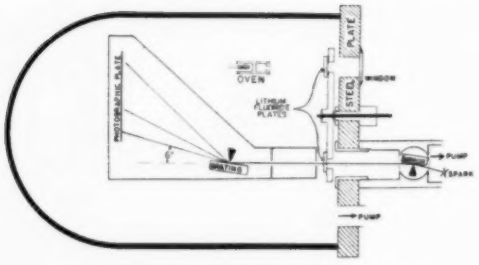

FIG. 1. Diagram of vacuum spectrograph.

diminished in intensity, while all material from the spark which might have contaminated the absorbing surface was condensed on the glass. It was necessary to clean the slit and mirror occasionally.

The grating had 15,000 lines to the inch and was used at 3° from grazing incidence. With the plate holder 7 cm from the grating, the whole spectrum from the central image to 2400A could be photographed on a plate 6 cm long. Although the dispersion was rather small, 40A/mm at 1600, it was sufficient for studies of the structure of the absorption of solids. Because of overlapping orders, the useful range of the instrument was limited to wave-lengths below 400A for studies of solids deposited on celluloid, or to the region above 1050A with lithium fluoride, which eliminated the shorter wave-lengths. With an effective width of the entrance slit of 0.2 mm and the grating slit 0.08 mm, the spectral lines were quite sharp. At longer wave-lengths the lines were considerably narrower than the central image, probably due to the greater width of the diffracted wave emerging from the grating at angles farther from grazing incidence. As the width of the spectral lines in this intermediate region is largely determined by the diffraction pattern of the slit system, it was not possible to use very narrow slits, as with x-rays.

The use of Ilford Q 3 plates was suggested by Professor K. T. Bainbridge. These plates were about ten times as fast as the ordinary plates sensitized with fluorescent oil, and were free from the spots and fog usually found on Schumann plates. Although this type of emulsion was not capable of giving great density, it had sufficient latitude for limited photometric measurement of the absorption.

Since the spectrograph was originally built to study the absorption of thin layers of alkali halides deposited on thin celluloid[3] films, all parts were designed to facilitate the preparation of films by evaporation. Since many of the salts are deliquescent, the preparation of the films and the absorption measurements had to be carried out without exposing the material to the atmosphere. For this reason the spectrograph and evaporation outfit were fastened in adjacent positions on a steel plate 12 inches square and one inch thick, mounted vertically. The plate was ground flat to accommodate an 11-inch Pyrex bell jar which was sealed in place with Apiezon Q compound. Removal of the bell jar made the entire spectrograph readily accessible. The spark chamber, turned from solid brass, was fastened to the opposite side of the plate. Electrical leads to the distilling furnace, mechanical leads for controlling the plate holder and for moving the absorption films, and pump connections, were made through the steel plate.

The distilling ovens were cylinders of molybdenum or iron heated by radiation from a tungsten spiral, as previously described.[4] The molybdenum, because of its greater thermal conductivity, was more suitable for use with high melting point salts. In order to reduce danger of contamination the salts were placed in thin platinum thimbles which were inserted into the ovens.

The lithium fluoride plates on which the salts were deposited were held near the circumference of a 4-inch disk. Rotation of the disk carried the lithium fluoride from a position in front of the oven into the path of the light. By slowly turning the plate of lithium fluoride past the edge of a diaphragm a few millimeters away it was possible to obtain a film which was wedge shaped in thickness. The thickness as judged by the visible light reflected from the film varied from zero to about a micron in a distance of four or five millimeters. The lithium fluoride plates were sufficiently large so that several such wedges could be prepared from different fractions of the distillate from the oven. Since the section of the film used was less than 0.2 mm wide it was possible to examine a number of portions of

[3] O'Bryan, Phys. Rev. **49**, 944 (1936).
[4] O'Bryan, J. O. S. A. **26**, 122 (1936).

each film. Comparison exposures were always taken through an uncoated section of the lithium fluoride. There was no sensible impairment of definition on insertion of the lithium fluoride plates between the slit and the grating.

The lithium fluoride was cleaned by heating to a temperature near red heat after carefully wiping with cotton soaked in ethyl ether. Selected plates of 1 mm thickness when cleaned in this manner were consistently transparent to 1050A. Although this treatment does not give a perfectly clean surface,[5] the more violent cleaning methods which may be used on glass cannot be applied to lithium fluoride because they destroy the surface.

Since the light source varied in intensity during the exposures, accurate transmission measurements were impossible. However, since there was relatively little variation in the spectral distribution of the light, a fairly reliable estimate of the change in transmission with wave-length could be made. Fig. 2 shows typical microphotometer curves for the fluoride, chloride and bromide of potassium. By comparing photometer traces similar to those shown it was possible to obtain the curves given in Fig. 3. Exposures through the salts were compared with exposures of roughly the same density taken through the lithium fluoride alone. The relative heights of the absorption bands are probably correct to within 25 percent, but the actual absorption coefficients are very uncertain. Since the best thickness of salt film to show the absorption maxima was in the neighborhood of 0.05 micron for all of the salts, the absorption coefficients are all of the same order of magnitude. However, this thickness is too thin to show interference colors and can be estimated only by extrapolation from the region of the wedge shaped film where the colors may be seen. Because of this uncertainty in thickness and the variation in intensity of the source, the absorption is plotted in arbitrary units.

Films of the alkali halides estimated at 0.05 micron showed about 10 percent transmission at the point of maximum absorption. These figures give an absorption coefficient in the neighborhood of 4×10^5 per centimeter. Thus these salts which show the greatest transparency over most of the spectrum are more opaque than other materials in the region where absorption sets in.

In the region above 1600A these experiments overlap the measurements of Hilsch and Pohl.[1] The curves in this region have been drawn as dotted lines (Fig. 3) to show the values previously observed, but the wave-lengths of the maxima are the new determinations. In the cases where the measurements agree to within experimental error, only the curve for Hilsch and Pohl's results has been drawn. Certain bands in lithium bromide and lithium iodide previously reported were not found even in films ten times the normal thickness used. Several samples of these chemicals from completely different sources of supply were consistent but failed to show these bands.

Since Hilsch and Pohl used fluorite rather than lithium fluoride, films of potassium chloride were

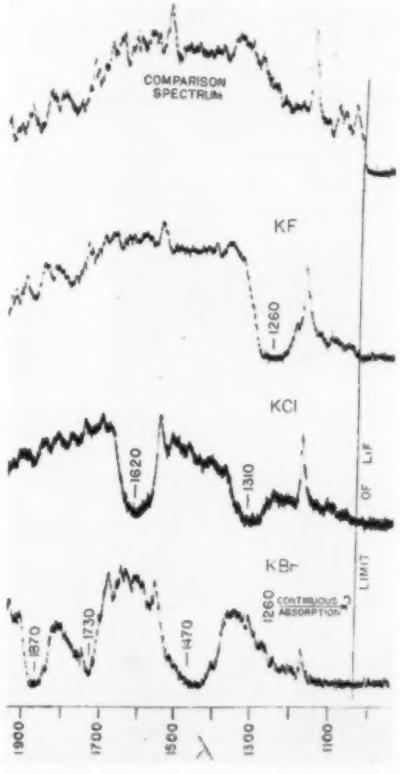

FIG. 2. Microphotometer traces for thin films of potassium salts deposited on lithium fluoride.

[5] Schneider, Phys. Rev. **49**, 341 (1936).

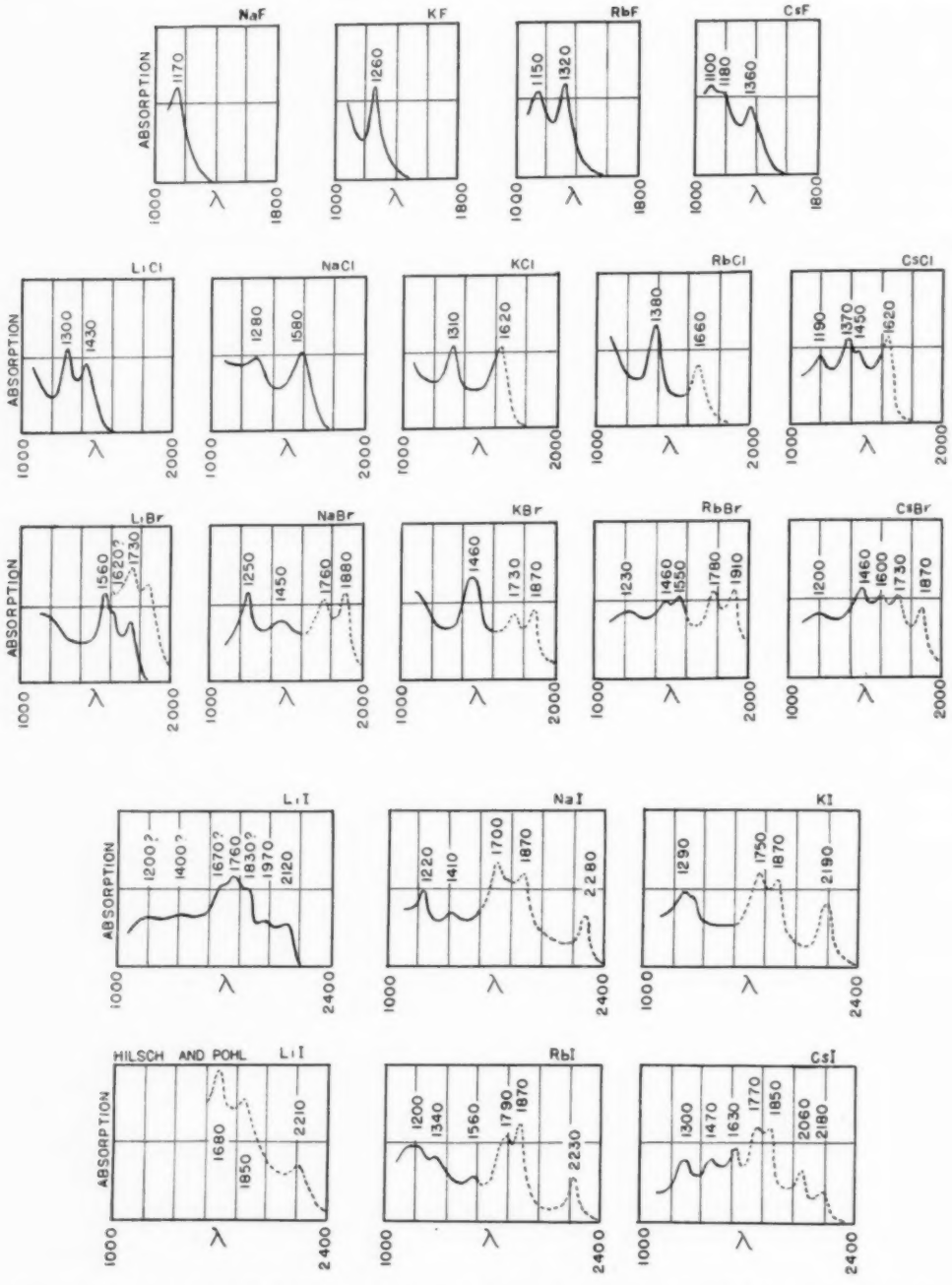

FIG. 3. Absorption of the alkali halides (arbitrary units) plotted against wave-length in angstroms. Dashed curves given by Hilsch and Pohl; solid line curves obtained in these experiments.

deposited on lithium fluoride, fluorite and quartz. There was no measurable difference in the position and width of the bands. This indicates that the evaporated deposit does not assume the structure of the underlying substance but rather retains its own crystal structure. Hilsch and Pohl[1] have compared the absorption structure of evaporated films and films prepared by freezing from the liquid in the region above 2000A, and find a slight shift toward the violet for the evaporated deposits, but no essential difference in structure. Since the films must be composed of very small imperfect crystals, the structures of the bands are probably slightly shifted from the positions expected in a large single crystal.

Since the method of distillation used in these experiments was essentially one of fractionation with only the middle portion used, the more volatile impurities should have been removed, yielding a quite pure salt. In order to determine the effect of impurities a mixture of nine parts of potassium fluoride and one part of potassium chloride was placed in the oven. Since the melting points and boiling points were not identical the film was probably not of this proportion. In the normal thickness only the band of lithium fluoride appeared, while with films about ten times as thick, the bands of both salts were observed. The position of the maxima were not greatly altered and the band widths were only slightly increased. This evidence indicates the presence of an impurity in the lithium salts measured by Hilsch and Pohl. In one case where the lithium iodide was distilled onto the lithium fluoride without sufficient preliminary heating to dry the salt and drive off the more volatile materials, a weak band was observed in the position of the long wave-length band reported by Hilsch and Pohl. Since this band appeared when a very moist sample of the salt was used, it seems probably that it was due to the presence of water. The bands observed in the carefully dried films of lithium bromide and iodide are more consistent with the calculations of von Hippel[6] than those found by Hilsch and Pohl. Most of the band positions computed by von Hippel from an atomic model of the crystal are in excellent agreement with the observed values. The bands of the lithium salts do not agree as well as those of the other alkali halides with calculations from this type of model. Because several different sources of the lithium salts have been studied exhaustively from the experimental side, it seems improbable that impurities can be the cause of this disagreement. Since the positive ion is much smaller than the halide, it may be necessary to consider excited states of the lithium. The structure of the lithium K absorption[3] in these salts points toward the existence of such excited levels.

In the short wave-length region these measurements overlap observations of A. Smith[7] on the intensity of the light reflected at normal incidence by a grating covered with a thin layer of salt. Absorption bands were assumed to give minima of reflection under these conditions. There is no agreement between the results of the two methods. Furthermore the absorption of sodium chloride deposited on celluloid is far less intense for the band at 372A than for the bands in the Schumann region, while the results of Smith indicate the opposite. Because of the extreme difficulty in separating the factors effecting reflection from films on gratings, such measurements cannot be taken as a definite proof of the existence of absorption bands. The existence of selective reflections from cleavage surfaces of

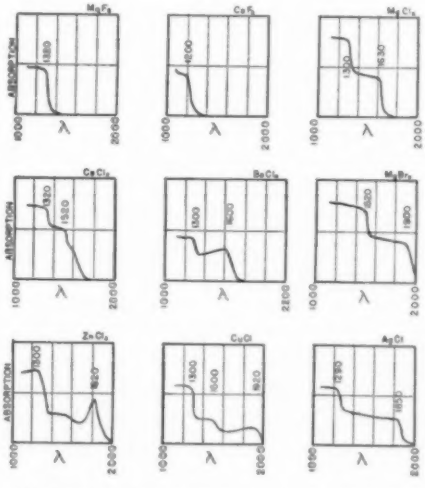

FIG. 4. Absorption of some metallic halides (arbitrary units) plotted against wave-length in angstroms.

[6] Hippel, Zeits. f. Physik **101**, 680 (1936).

[7] Smith, Phys. Rev. **44**, 520 (1933).

single crystals indicates the presence of absorption bands. The observations of A. H. Pfund[8] on sodium and potassium chloride crystals show such reflection maxima just to the long wave-length side of the bands observed by the transmission method. This displacement is to be expected on account of the change in the index of refraction in the neighborhood of a region of high absorption. Estimates of the positions of the absorption bands from the reflection maxima by Pfund agree well with those found by the transmission method.

In Fig. 4 the absorption structures of a number of halides of the alkaline earths and other elements are shown. These substances show little selective absorption, tending rather to a continuum with a relatively sharp edge at long wave-lengths. These results are similar to the observations of H. Fesefeldt[9] on a large group of compounds in the region above 1600A. Since the crystal systems of these salts are in general more complicated than that of the alkali halides, part of the difference in the absorption structure may be due to the lattice. The difference in valence may be another contributing factor. In all of this group of compounds the absorption coefficients were much smaller than those of the alkali halides, film thicknesses of 0.1 micron or greater being necessary to give measurable absorption.

In conclusion the authors wish to express their appreciation of the kindness of Professor G. P. Baxter of the department of chemistry for preparing several salts which are extremely rare, and to thank Professor T. Lyman for his continued interest in the progress of these experiments.

[8] Pfund, Phys. Rev. **31**, 315 (1938).

[9] Fesefeldt, Zeits. f. Physik **64**, 741 (1930).

MARCH 1, 1937 PHYSICAL REVIEW VOLUME 51

The Modification of Spectral Lines by Very Close Collisions[1]

WILLIAM M. PRESTON
Harvard University, Cambridge, Massachusetts

(Received December 18, 1936)

As a result of a survey of the spectra of Hg, Cd and Tl when a few centimeters pressure of a rare gas is added to a discharge through the vapor of these metals, it is concluded that bands of the type first reported by Oldenberg on the short wave-length side of the resonance line Hg 2536.7 probably occur with all metal lines, and with a total relative intensity of the same order of magnitude. The effect of collision induced emission seems in general to be negligible. The occasional appearance of diffuse maxima may be explained by a chance relationship between the potential curves which describe the interaction of the colliding atoms.

INTRODUCTION

CONSIDERABLE study has been devoted to the influence of surrounding atoms on the frequency of the radiation emitted from excited atoms of a gas, or absorbed by normal atoms.[2] A simple case of this general problem is that of a metal vapor at low pressure in the presence of a high pressure of some inert gas, under conditions of excitation such that only the former is excited. Any modification of the spectral lines of the metal must then be primarily caused by neighboring atoms in the normal state, and the effects of chemical binding forces and of resonance forces between excited atoms of the same species are eliminated. Under these conditions the metal lines show an asymmetrical broadening and shift, usually to long wave-lengths, which increase with the density of the inert gas. These pressure effects are due to perturbation of the emitting or absorbing atom by many comparatively distant foreign gas atoms, and must generally be studied at pressures of the order of atmospheres. This

[1] Extract from a thesis submitted to the department of physics of Harvard University in partial fulfillment of the requirements for the degree of Doctor of Philosophy.

[2] For a summary see Margenau and Watson, Rev. Mod. Phys. **8**, 22 (1936).

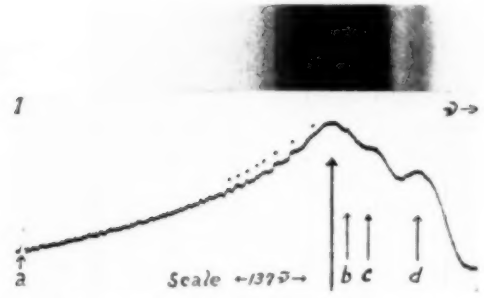

FIG. 1. Hg 2536.7, 10 cm A. On the short wave-length side of the line, whose center is indicated by the large arrow, are two diffuse maxima *c* and *d*; the latter has a relative intensity of 1/1800. *a* and *b* are weak Hg lines, λλ2576.3 and 2534, respectively. A few of the vibration bands superimposed on the long wave-length continuum are marked by dots.

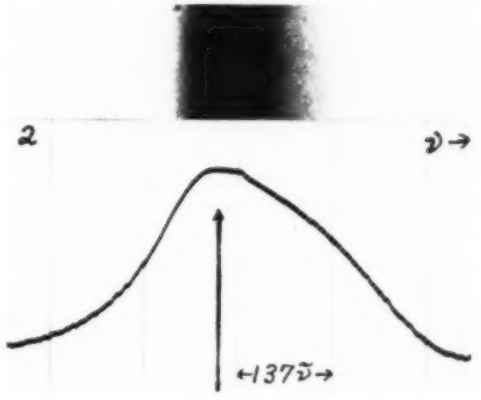

FIG. 2. Hg 2536.7, 10 cm He. There is a structureless continuum on either side of the line which can be traced further to short wave-lengths than in the case of Hg+A, but not so far to long waves.

paper is concerned with the less frequent very close collisions which modify the spectral lines emitted by unperturbed atoms in a more irregular manner. It will be shown that radiation emitted during these close encounters appears most commonly as a faint wing or diffuse band[3] close to the atomic line; it can often be observed, despite its relative weakness, at pressures as low as a millimeter of foreign gas.

Oldenberg[4] has shown that the resonance line Hg 2536.7, $1\,{}^1S_0 - 2\,{}^3P_1$, in fluorescence, with a few centimeters pressure of one of the rare gases added, is accompanied by certain peculiar spectra. With He a continuum extends on both sides of the line with continuously decreasing intensity (Fig. 2). With the heavier rare gases, one or two diffuse intensity maxima are found on the short wave-length side (Fig. 1), lying closer to the line the greater the atomic weight of the rare gas used. These maxima persist at high temperatures. According to Kuhn and Oldenberg[5] they represent radiation emitted from excited Hg atoms during collisions with normal rare gas atoms. At the turning point of a collision the kinetic energy of thermal motion in the internuclear direction has been transformed into potential energy, and part of this may be added to the excitation energy of the Hg atom to give a larger quantum provided emission takes place at this instant. Pairs of colliding atoms may be treated as molecules although they are in continuous states of "positive" total energy and will quickly separate unless transferred to a stable energy level as a result of radiation or a triple impact. Molecular theory indicates that two states arise from the approach of a ${}^3P_1$ atom and a normal ${}^1S_0$ atom of different species between which only weak attractive forces of the polarization type occur,[6] and Kuhn and Oldenberg supposed that the two bands near Hg 2536.7 arise in transitions from these two upper molecular levels to a common ground level.

Krefft and Rompe[7] showed that somewhat similar diffuse bands occur on the short wave-length side of a number of the strongest lines of different metals in the positive column of a discharge to which a rare gas has been added. They classified these bands according to visual judgment of their shape and suggested a number of empirical relations such as proportionality of the width of certain bands to $1/\sqrt{G}$, where G is the atomic weight of the particular rare gas used.

The present investigation of collision spectra was undertaken for two reasons. First, no intensity measurements had been made by previ-

[3] As a matter of convenience, the word "band" will be used rather loosely in this paper when referring to the modified portions of spectral lines believed to be caused by close collisions. These all appear to be *continuous* spectra, some distinctly separated from the actual line, others merely "wings" or marked asymmetries.

[4] Oldenberg, Zeits. f. Physik **47**, 184 (1928) and **55**, 1 (1929).

[5] Kuhn and Oldenberg, Phys. Rev. **41**, 72 (1932).

[6] Mulliken, Rev. Mod. Phys. **4**, 26 (1932).

[7] Krefft and Rompe, Zeits. f. Physik **73**, 681 (1932).

ous workers. Krefft and Rompe reported bands by only a few strong lines in the spectra of each of several metals, and without knowledge of the intensities of the bands relative to their associated lines it was possible that their absence by weak lines was due merely to insufficient exposure. All spectral lines show pressure broadening and shift and there was no apparent reason why they should not also be modified by very close collisions. Accordingly it was proposed to examine all the stronger lines in the spectra of three metals, Hg, Cd and Tl, in the range accessible with a quartz spectrograph, with the addition both of He and of A and with the longest possible exposures, and to measure the relative intensities of all bands found with sufficient accuracy to determine whether there was any considerable variation.

Second, the theory of the intensity distribution of collision radiation needed more careful examination. In explaining the diffuse maxima which appear near Hg 2536.7 in the presence of the heavier rare gases, Kuhn and Oldenberg made the assumption that all close collisions between excited and normal atoms are head on, thus reducing the problem to one dimension. It will be shown later that virtually their same argument extended to three dimensions does not predict any such intensity maxima, and that these require for their qualitative explanation some additional assumption. Kuhn and Oldenberg had suggested that a close collision might in some cases momentarily increase the emission probability of an excited atom, and that this might be a factor in the production of the bands near the mercury resonance line. Evidence of this process was later obtained[8] in the discovery of a small continuous spectrum near the weak forbidden line Hg 2269.8, $1\,{}^1S_0 - 2\,{}^3P_2$, with He or A added. This band has negligible intensity near the line, rises to a maximum near 2259A, and shades off more gradually to shorter wavelengths. With a 10 cm pressure of A the total integrated intensity of the band is over 100 times that of the line itself. Both the shape and the high relative intensity were satisfactorily explained by an enhanced transition probability from the metastable ${}^3P_2$ level during close collisions. It was desirable to obtain more experimental information about the modification of spectral lines by close collisions before deciding whether collision induced emission was of importance in other cases not involving metastable states.

[8] Preston, Phys. Rev. **49**, 140 (1936).

Experimental

The three metals studied, Hg, Cd and Tl, were readily purified by distillation in vacuum. The rare gases, He and A, were treated in a misch metal arc.[9] A high degree of purity was desirable because the whole spectral range from 2200A to 5000A was to be searched for weak new bands. The metal under investigation was distilled into a side arm attached to a simple capillary discharge tube supported within an electric furnace in order to obtain an adequate metal vapor pressure. The discharge was excited by means of a small transformer, using currents of about 10 ma through the capillary. In practice, a 10 cm pressure of rare gas was admitted to the discharge tube at room temperature and the furnace then turned on. While at first the spectrum of the rare gas was emitted strongly, when the metal vapor pressure reached the order of 0.01 mm only the metal spectrum was observed, since the lowest excitation potentials of both He and A lie above the ionization potentials of the metals studied. A quartz discharge tube and a temperature of about 700°C were necessary in the case of Tl. The exact metal vapor pressure was not known because there was some diffusion out into the cool tubing connecting the discharge tube to the vacuum system, but this process was retarded by the comparatively high pressure of the rare gas. It was desirable to have the metal vapor pressure as small as possible in order to keep the proportion of diatomic metal molecules present low. Cd_2 and Hg_2 emit a number of diffuse bands and extensive continuous spectra which can easily be confused with collision spectra.

Collision bands were invariably so weak relative to the lines which they accompany that extreme overexposure of the line was necessary in order to record the band on the photographic plate. A new medium sized quartz prism metal Hilger spectrograph was found to be far superior to older models for this work. Large dispersion

[9] Van Voorhis, Shenstone, and Pike, Rev. Sci. Inst. **5**, 367 (1934).

prism instruments require inconveniently long exposures for weak spectra and seem to produce an irregular diffraction pattern, probably caused by slight inhomogeneities in the optical system, when a line is greatly over-exposed. Diffraction grating spectrographs are unsuitable because ghosts are always too intense.

The photometric problem was that of comparing the intensity of a weak diffuse band with that of a neighboring line. Because the image of a spectral line is merely the central maximum of a diffraction pattern caused by the aperture of the camera lens, a long exposure will bring out many secondary maxima. For example, an exposure of 1000 times the minimum necessary to record a spectral line, which was frequently necessary in this work, will broaden the image to include the tenth diffraction maximum on either side. For this reason the weaker a band the greater the distance from its line to which it must extend in order to be observed experimentally. Most bands are partially and many wholly obscured by the overlapping diffraction pattern of the line.

Provided the slit width of a spectrograph is greater than the spacing of the diffraction pattern, the intensity of a continuous spectrum as measured on the photographic plate increases almost proportionally to the slit width, but a line simply broadens while its intensity remains constant. Hence the ratio of the intensity of a point in a continuous spectrum to a point in a line, as measured by a microphotometer, depends on the width of the spectrograph slit. The latter was kept constant in this work during all intensity measurements so that the results can be compared among themselves. A broad spectrograph slit was used throughout in order to have the photographic image wider than the microphotometer slit image, and also to reduce the necessary exposure time.

For the actual intensity measurements a line was recorded in a series of exposures of increasing time, using a gauze screen to reduce the intensity to the same order of magnitude as that of the neighboring band without a screen. The band was then photographed in a similar series of exposures without a screen. Comparing a line in the first series with some point in the associated band from the second series of the same density, as determined with a microphotometer, the relative intensity could be estimated from the known screen factor and the relative exposure times. Reciprocity law failure was thus neglected over small ranges. Only when a band is quite separate from its line can its intensity be defined unambiguously; it is then naturally taken at the band's maximum. When no maximum is observed the point at which to measure the band's intensity becomes somewhat arbitrary.

Experimental Results

Fig. 1 shows the line Hg 2536.7 in a discharge containing a 10 cm pressure of A. Below the photograph, on the same scale and in register, is a microphotometer trace. To short wave-lengths from the line can be seen a pronounced intensity maximum at 2526.0A and another, less clearly resolved, at 2530A. The outer maximum has a relative intensity of 1/1800; that of the inner appears to be somewhat greater, but is uncertain because of the overlapping line. No trace of fine structure can be observed in either of these diffuse bands. The position of the outer maximum was measured at three different temperatures, 55, 130, and 400 C; it was unchanged within a limit of error of about 0.3A.[10] There was likewise no observable shift when the argon pressure was reduced to 1 mm. The maximum was still clearly visible with as little as 0.1 mm of argon but its intensity relative to the line was enormously less than at 10 cm. In order to avoid errors caused by self-reversal, the intensities of all resonance lines like Hg 2536.7 were measured with a special discharge tube having a vertical quartz capillary 3 mm in diameter, viewed from the side through the capillary wall. At the low metal vapor pressures used the absorption must have been small under these conditions. Correction for residual error from this cause would lower slightly the above figure for the relative intensity of the Hg 2536.7 maximum.

On the long wave-length side of the line Hg 2536.7 in Fig. 1 may be seen a series of narrow bands, the first three with a distinct step-like form, superimposed on a continuous spectrum. These bands were reported by Oldenberg and explained as transitions from *stable* vibration levels of Hg $^3P_1 - A\ ^1S_0$ molecules to a normal

[10] Oldenberg (reference 4) found a slight shift to shorter wave-lengths over a somewhat larger temperature range.

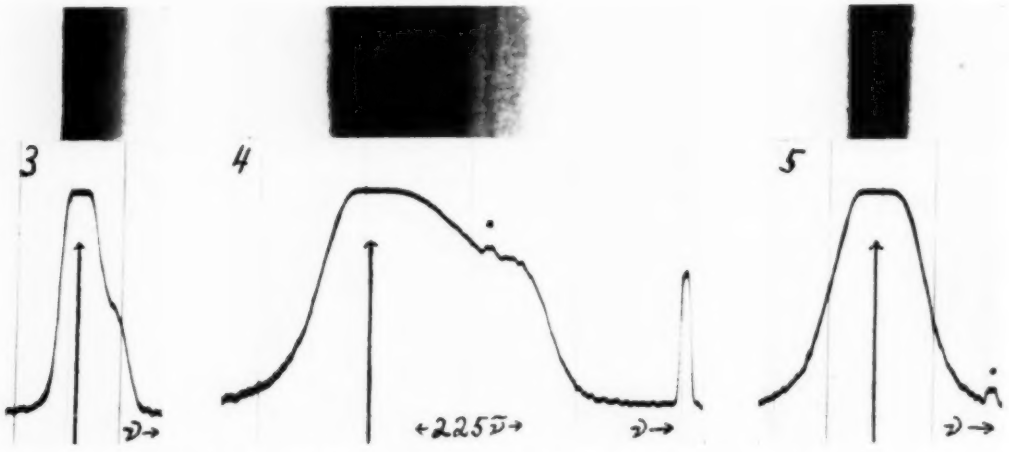

FIG. 3. Tl 3775.7, 10 cm A. There is a narrow band on the short wave-length side of the line, relative intensity 1/350.
FIG. 4. Tl 3775.7, 10 cm He. The broad band on the short wave side appears to have an intensity maximum, but it is confused by the line Zn 3740, which is marked by a dot. This band has a relative intensity of 1/3000.
FIG. 5. Tl 3775.7, 0.05 cm A. This shows the unmodified Tl line with the same exposure as in Fig. 4, namely about 10,000 times that just sufficient to record the line on the photographic plate. With only a trace of rare gas, added merely to make the discharge run smoothly, the line is accurately symmetrical.

state with unresolved vibration levels. Confirming Oldenberg's results, these bands disappear completely at temperatures of a few hundred degrees, a fact which is not surprising in view of the small binding energy to be expected in such polarization molecules. In the present work, similar bands were sought near other lines of Hg, Cd and Tl, but in no other case were they found.

Fig. 2 shows the corresponding band obtained with He. It is apparent that the intensity falls continuously away from the line on the short wave side without any indication of a maximum. The intensity fall is rather gradual, and with long exposures the band can be traced for at least 25A. On the long wave side of the line there is no trace of vibration bands and the continuous tail is relatively much weaker than with A.

Figs. 3, 4 and 5 illustrate the line Tl 3775.7, $2\,^2P_{\frac{1}{2}}-2\,^2S_{\frac{1}{2}}$. Fig. 3 shows the effect of the addition of 10 cm of A. There is a narrow band which to the eye appears to have a step-like form with a well defined edge 120 cm^{-1} from the line. The microphotometer shows that the intensity fall is continuous, but with a point of inflection which may indicate a maximum obscured by the overlapping overexposed line. The relative intensity of the band at the point of inflection in the microphotometer trace is about 1/350.

Fig. 4 shows the same line with the addition of 10 cm of He. Because the resulting band is considerably weaker, the line is more overexposed and therefore broader than in Fig. 3; the longer exposure brings out a neighboring line Zn 3740 due to a trace of impurity, and this is marked by a dot. The relative intensity near the center of the He band is about 1/3000 and its short wave-length edge is approximately 375 cm^{-1} from the line.

Fig. 5 shows Tl 3775.7 in the absence of rare gas and with an exposure nearly the same as that in Fig. 4. By subtracting the intensity relative to the center of the Tl line at a number of points on the short wave wing of Fig. 5 from the intensity at corresponding points of Fig. 4, Fig. 6 is obtained. Although the accuracy of this procedure is small, Fig. 6 shows that the Tl 3775.7 He band has a definite maximum which in Fig. 4 was obscured by the overexposed Tl line and by Zn 3740.

Figs. 7 and 8 illustrate Hg 2967.3, $2\,^3P_0-3\,^3D_1$, the former with A and the latter with He. They show that diffuse maxima may also occur on the long wave-length side of metal lines in the

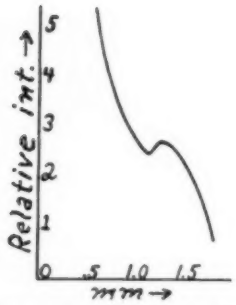

FIG. 6. Result of subtracting the short wave-length portion of Fig. 5 from that of Fig. 6, in terms of relative intensities, thus effecting a correction for the overlapping of the band by the over-exposed line. The ordinates give the relative intensity in units of 0.0001 of the intensity at the center of the line, the abscissae distances towards short waves from the center of the line, in millimeters on the plate.

presence of rare gases. Here the He band lies closer to the line than the A band.

Collision spectra were identified near 13 lines of the spectrum of Hg, 12 of Cd, and 6 of Tl. The majority of these resembled that shown in Fig. 3, having roughly defined short wave edges and no resolved maximum. Only three definite cases of maxima on the short wave side of lines were encountered, all lying fairly close to and definitely associated with an atomic line. Several examples were found of maxima like those in Figs. 7 and 8, at varying distances on the long wave side of lines, some at such great distances that they could not be definitely connected with any particular line.

It was pointed out in remarks concerning Figs. 3 and 4 that the band on the short wave side of Tl 3775.7 with He extended considerably further than that with A. It was found to be quite generally true that when a band with a fairly sharp short wave limit occurred by the same line with both He and A, the He band was roughly three times as wide as the A band. There was considerable variation in the ratios of these widths, however, and some bands had so gradual an intensity fall that no edge could be measured. For this reason it seems unlikely that any significant numerical relationship can be established between these band widths and the properties of the particular rare gas added to the discharge. The observations of Krefft and Rompe in this connection, which have been referred to previously, appear to be illusory.

It would be of interest to measure the ratio of the total energy represented by a band to that of its line. This total integrated relative intensity would afford a measure of the proportion of the total emission occurring during collisions, but it is usually impractical to obtain because of the overlapping of lines and bands. The most that can be said is that the broader bands (in frequency units) were always weaker than the narrow bands, and it is probably true that in all examples studied the total integrated relative intensity was of the same order of magnitude.

A survey of all bands observed indicated definitely that those associated with the lines of a particular spectral multiplet are much more alike in form and width than those belonging to unrelated lines. For example, diffuse maxima occur on the long wave side of several of the $2\,^3P-3\,^3D$ lines of Hg and Cd, and not by any other lines in the spectra of these metals; no bands were found on the short wave side of any members of this multiplet. Similarly, the three Hg lines $2\,^3P_{2,1,0}-3\,^3S_1$ and the line Cd $2\,^3P_1-3\,^3S_1$ all had a narrow He band without resolved maximum and with an edge approximately 60 cm^{-1} on the short wave side (the Cd lines $2\,^3P_{2,0}-3\,^3S_1$ happen to be in unfavorable positions for observation). A tendency was apparent for bands to become narrower in passing to the higher members of a spectral series; no

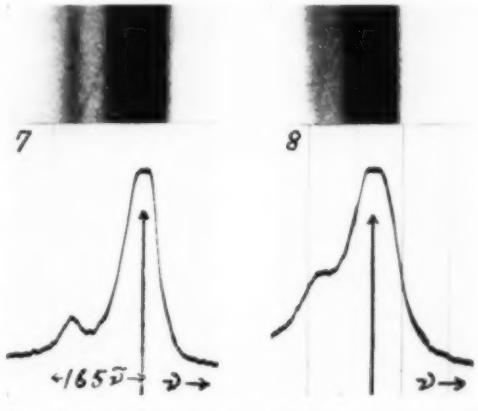

FIG. 7. Hg 2967.3, 10 cm A. This is an example of a clearly resolved maximum on the long wave-length side of a line; the separation is 125 cm^{-1}.

FIG. 8. Hg 2967.3, 10 cm He. Here the maximum is not clearly resolved from the line, since the separation is only 90 cm^{-1}.

connection was observed between band shape or width and the inner quantum number j of either the initial or the final term characterizing the associated line.

It is now possible to answer at least partially the question of the occurrence of collision spectra. It must be emphasized that many lines in the range considered are not suitable for observation, either because they lie close to other lines of greater intensity or because the region about them is covered in long exposures by the extensive continua belonging to diatomic molecules of the metal being studied. Suppose, however, that a distinct band was observed first by one line of a Hg multiplet, in the presence of A. From the foregoing general results we should expect to find approximately similar bands by other members of this multiplet, and wider bands (hence easier to observe) by the same lines when He is added. This was always verified for as many lines as were favorable for study, that is, a band was always found when one of observable width was predicted and the region was not obscured. The evidence therefore suggests that every spectral line of a metal is modified in a characteristic manner by the addition to the discharge of a small pressure of He or A. In addition to the familiar pressure broadening and shift, which are very small under these conditions, a marked asymmetry appears which in extreme cases takes the form of a separate intensity maximum at a considerable distance from the center of the line. The position of these maxima appears to be independent of the pressure of foreign gas while their intensity is probably proportional to it.

Theory

Consider a single excited metal atom under the conditions specified at the beginning of this article. At any instant and for a given foreign gas density the probability of finding a normal atom of the foreign gas in a spherical shell of radius r and thickness dr about the excited atom is proportional to $r^2e^{-\varphi_1(r)/kT}dr$, where $e^{-\varphi_1(r)/kT}$ is the Maxwell-Boltzmann distribution function and $\varphi_1(r)$ the potential energy of interaction between the excited atom and a normal atom of the foreign gas. We will limit ourselves to a region so small that at ordinary pressures the chance of finding two or more foreign gas atoms within it at one time is negligible.[11] At small distances, $\varphi_1(r)$ increases rapidly as r decreases due to the strong repulsive forces between colliding atoms, and hence the probability of finding a foreign gas atoms decreases rapidly.

Suppose we now make the following assumptions:

(a) Let the Franck-Condon rule apply strictly, so that to each internuclear distance r there corresponds a frequency ν which will be emitted if a radiative transition occurs while a perturbing atom is at this distance. This frequency will be given by $h\nu(r)=h\nu'+\varphi_1(r)-\varphi_2(r)$, where ν' is the unperturbed frequency $=\nu(\infty)$, and $\varphi_1(r)$ and $\varphi_2(r)$ represent the interaction between a foreign gas atom and a metal atom in the initial and final states respectively which correspond to the particular transition.

(b) Let the curves φ_1 and φ_2 be nearly similar in their repulsive portions, but the former displaced slightly towards larger values of r. Since the atom in the state of higher excitation may be expected to have a larger collision cross section, repulsion should occur at larger internuclear distances,[12] and for any given value of r in this range we will have $\varphi_1>\varphi_2$ and $d\varphi_1/dr>d\varphi_2/dr$.

(c) The intensity $I(\nu)$ at the frequency ν is proportional only to the number of excited atoms which at any instant are so perturbed by colliding atoms that they can, according to the Franck-Condon rule, radiate this frequency. That is, $I(\nu)d\nu\propto e^{-\varphi_1(r)/kT}dr$ where ν and r are related by $h\nu=h\nu'+\varphi_1-\varphi_2$.

As a consequence of these assumptions the radiation emitted during collisions should appear as a tail on the short wave-length side of the unperturbed line, since $h\nu-h\nu'=\varphi_1-\varphi_2>0$. Its intensity should decrease continuously with distance from the center of the line because of the increasing rarity of the closer collisions which produce the larger shifts, and it should everywhere be small because of the relatively small probability of emission taking place during a close collision. This is indeed what was observed experimentally in a considerable number of cases, such as that illustrated in Fig. 2. However,

[11] Kuhn, Phil. Mag. **18**, 987 (1934).
[12] This assumption was made by Kuhn and Oldenberg, reference 4.

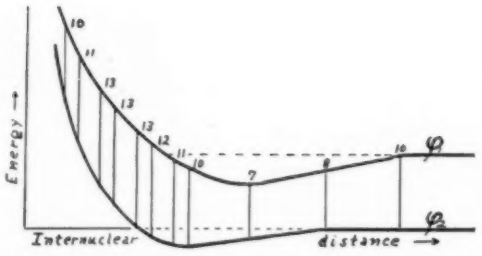

FIG. 9. Hypothetical potential curves illustrating the suggested explanation of diffuse collision spectra having the form of separate maxima. The upper and lower curves represent, respectively, the energy of an excited and of a normal metal atom colliding with a neutral rare gas atom. The lengths of the vertical lines, indicated by the accompanying numbers, are a measure of the energy available if emission takes place at the corresponding nuclear separation.

some modification of our assumptions is necessary to explain the occurrence of separate maxima.

(a) has been discussed by Kuhn and London.[13] It may be expected to apply the more closely the smaller the relative velocity of the colliding atoms, and slight departures from it will merely introduce a certain blurring.

We stated in the introduction that it had been suggested that collision induced emission might be a factor in the explanation of these intensity maxima. Our experimental results show, however, that collision radiation represents a very small[14] and at any given pressure a relatively constant fraction of the total intensity of the line proper. It is not possible to actually calculate this fraction without a quantitative knowledge of the course of φ_1 and φ_2, but estimates show that the intensity is of the right order of magnitude if we assume that (c) is true and that the emission probability of ordinary excited atoms is not markedly influenced by close collisions with normal atoms.

The assumptions under (b) are more arbitrary and possibly quite unnecessary. In Fig. 9, φ_1 and φ_2 have been drawn in such a manner that φ_1 has a somewhat smaller curvature than φ_2 in the region of repulsion[15] and hence the curves are approximately parallel over a short range of r; their vertical separation is here greater than at $r=\infty$. Radiation emitted from hypothetical colliding atoms whose interaction conforms to these potential curves will have a definite high frequency limit somewhere on the short wave-length side of the line, and near this limit the intensity will be large because perturbations over a considerable r range will produce approximately the same frequency shift. The blurring introduced by slight departures from the Franck-Condon rule will result in the formation of a rounded intensity maximum with rapid intensity fall on its short wave-length side.

Of course, these potential curves were devised for the express purpose of "explaining" intensity maxima like those shown in Figs. 4 and 6; almost any sort of band can be similarly accounted for because there is little independent information about the potential curves. Still, it is not unreasonable that there should be a considerable variation in the forces between foreign gas atoms colliding with metal atoms in different states of excitation and that occasionally this special relationship should exist between the potential curves.

In considering Fig. 9 once again, it is apparent that we have neglected radiation coming from the portion of the upper potential curve where the interatomic force is attractive. Since there is an increasingly large chance of finding a perturbing atom at these greater internuclear distances, the corresponding radiation must be more intense than that coming from the range in which repulsive forces predominate. In Fig. 9 the depth of the minimum has been greatly exaggerated; it is necessarily shallow when the attractive force is due only to polarization, as in the case of an excited metal atom colliding with a neutral rare gas atom. For this reason the radiation from this portion of the potential curve is shifted only slightly to long wave-lengths and is therefore obscured by the broadened overexposed atomic line. The weaker collision radiation can only be detected because of its larger frequency shift. The connection between radiation from excited atoms perturbed by close approaches of foreign atoms and the phenomena of pressure broadening and shift has also been discussed by Kuhn.[11]

It is rather surprising that the line Hg 2536.7,

[13] Kuhn and London, Phil. Mag. **18**, 983 (1934).

[14] Except in the case of the Hg 2269.8 band (reference 8), which originates in transitions from a metastable state.

[15] This particular relationship between potential curves was suggested by a diagram in an article by Kuhn (Zeits. f. Physik **72**, 462 (1931)), in which it was used to explain the position of certain TlI bands.

which happened to be the first near which collision bands were found, is the only one thus far which has associated with it two separate maxima, and the only one with discrete vibration bands on the long wave-length side. Molecular theory shows that both the upper and lower states of many of the bands which have been studied should be represented by more than one potential curve; as a rule these must so nearly coincide that observation of separate maxima is impossible. The absence of vibration bands in Cd and Tl may be due simply to the high temperature necessary to obtain an adequate metal vapor pressure in a discharge tube, but it is strange that none were found near other Hg lines.

In conclusion the author wishes to acknowledge his deep gratitude to Professor Otto Oldenberg, under whose direction and inspiration this work was done.

MARCH 1, 1937 PHYSICAL REVIEW VOLUME 51

A Spectroscopic Study of the Magnetron Discharge

OVERTON LUHR AND FRANK J. STUDER
Union College, Schenectady, New York

(Received December 21, 1936)

The spectra from magnetron discharges in various gases have been studied with the aim of investigating the efficiency of this type of source in producing the higher states of ionization. The study of helium was of particular interest since in a mass-spectrograph study of this type of discharge made by one of the writers, it was impossible to distinguish the He^{++} from the H_2^+ ions which were always present. The discharge between a tungsten filament and a nickel cylinder was operated at widely varying voltages, currents and gas pressures. The most satisfactory results were obtained at about 250 volts, 0.5 ampere and pressure of 0.1 mm of mercury. A magnetic field of the order of 150 oersteds parallel to the axis of the cylinder greatly intensified most of the lines in the region of the spectrum investigated between 7000 and 2000A. Higher members of the series in both the He I and He II spectrum were brought out with good intensity compared to results obtained with other types of discharge. The magnetron should thus be an efficient source of He^{++} ions. In the case of nitrogen and mercury many lines of the N II, N III, N IV and Hg II spectra were identified.

INTRODUCTION

THE products of ionization from a magnetron type discharge designed to produce doubly ionized helium by multiple electron impact has been investigated with a mass spectrograph by one of the writers.[1] Such a source, consuming moderate power, would be of use in nuclear studies where alpha-particles were desired for bombardment. There was some doubt about the results because of the continued presence of H_2^+ ions as an impurity which could not be differentiated from He^{++} with the mass spectrograph used. There was evidence that at least two percent of the ion current was due to He^{++} but spectroscopic corroboration of this result seemed desirable. The present investigation was therefore undertaken primarily to obtain spectroscopic evidence for the presence of He^{++} ions by a study of the intensity of the He II spectrum.

[1] Luhr, Phys. Rev. **49**, 317 (1936).

In addition the magnetron discharge seemed to offer some advantages as a spectroscopic source. Due to the axial magnetic field, the electrons spiral close to the cathode, and make many impacts in a small region. It is therefore to be expected that the intensity of the radiation would be great in this region and since the electrons attain their maximum energy (given by the full discharge voltage) in passing through the thin positive ion sheath surrounding the cathode, it should be possible to study the excitation of weak lines with electrons of known energy. Furthermore, with intense ionization close to the cathode there should be a relatively high probability that an electron would strike an atom which had already been ionized and thus produce excitation or highly ionized atoms by multiple electron impact. So a second purpose in this investigation was to find out whether such a source might be of use to spectroscopists for the

purpose of exciting ionized spectra. Most of the experiments were concerned with helium, but some investigation was made of the spectra of hydrogen, nitrogen and mercury in such a discharge.

Apparatus and Experimental Procedure

The discharge tube which was finally adopted as most satisfactory was of simple design and is shown in Fig. 1. The anode *A* was a cylinder of 10 mil sheet nickel, 4 cm long and 4 cm in diameter. A tungsten filament was used so that the discharge voltage could be controlled, and it was found that a piece of 16 mil wire 12 cm long wound into the form of a small spiral was satisfactory. To avoid shorting of the filament and cylinder leads due to sputtering, they were brought into the tube through separate stems. The quartz window *B* was located 10 to 15 cm from the discharge so that it would not be darkened by sputtered metal. In later tubes this window was pointed directly at the filament as it was found that the spectral lines were most intense in that region of the discharge. The continuous spectrum from the filament was of negligible intensity in the ultraviolet, though it gave trouble in the visible region. For work in the visible region tubes were built with the window pointing to one side of the filament, and in one tube end-plates were placed over the cylinder, with a slit cut in front of the window. However, some continuous radiation from the filament was always present, though the stronger lines stood out well against this background.

The life of a tube, barring accident, was limited by the sputtering away of the filament due to positive ion bombardment. With hydrogen and helium the walls of the tube became blackened in a short time, though the filament remained intact for at least 30 or 40 hours of operation. In the case of nitrogen and mercury the rate of sputtering was much higher, and 5 to 10 hours of operation would probably be the limit.

When the tube was operated as a magnetron it was surrounded by a water-cooled solenoid consisting of 800 turns of 45 mil enameled copper wire. After a number of trials it was found that maximum intensity of most lines was obtained with a field of 150 oersteds for a discharge voltage of 200.

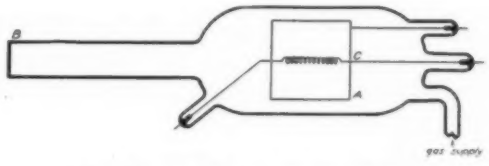

Fig. 1. Diagram of the experimental tube.

Photographs were taken with a small Bausch and Lomb quartz instrument whose dispersion was 125A per mm in the red, and 8A per mm at 2200A. Visual study was made with a constant deviation instrument.

Care was taken to obtain as high a degree of purity as possible in the gases used. The tube was baked out at 450°C for about two hours and the metal parts outgassed by electron bombardment from the filament. Tank hydrogen and nitrogen were purified by passage through hot copper, P_2O_5, and two liquid-air traps. The helium was obtained highly purified from the General Electric laboratories and was passed through a charcoal trap immersed in liquid air and two liquid-air traps before admission to the tube. Except in the case of mercury the tube was not sealed off and fresh gas was admitted after each exposure. Under these conditions lines due to impurities were always weak if there were any present at all; though in the case of helium, hydrogen was always present as indicated by the presence of several members of the Balmer series.

Results

Helium

Some twenty spectrograms, mostly of helium, were taken with the quartz spectrograph, in addition to observations in the visible region with the constant deviation spectrometer. The lines of ionized He were of special interest, but only in one or two cases could lines of the Pickering series be identified owing to the strong continuous spectrum in the region where the series is strong and also due to the continued appearance of the Balmer series. The λ4686 ionized series was quite intense, however, and was therefore employed as a qualitative measure of the concentration of He^{++} ions.

Typical spectrograms of the He magnetron are reproduced in Fig. 2, (*a*)–(*f*) inclusive, and a

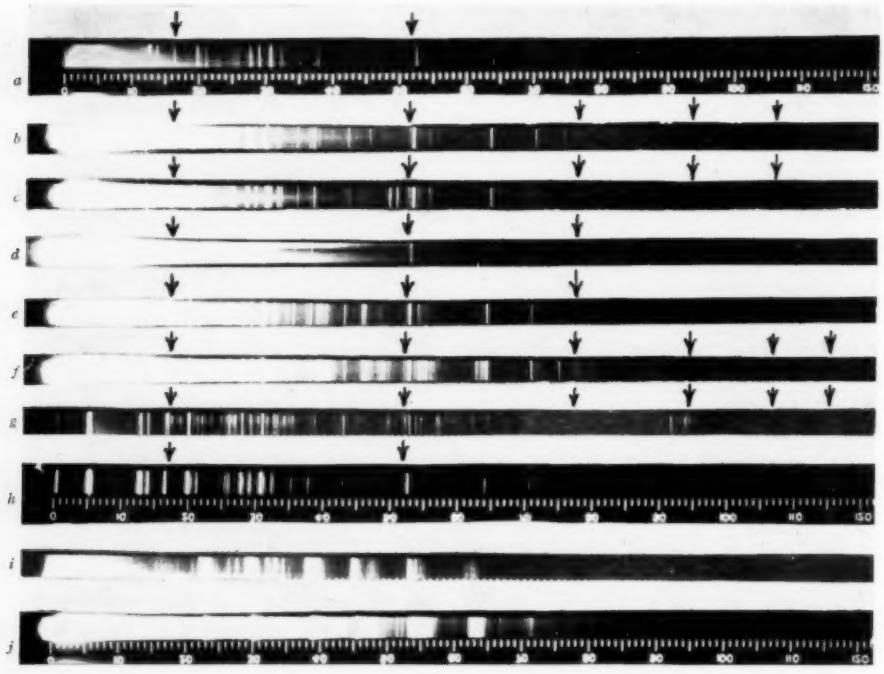

FIG. 2. Typical spectrograms. Arrows indicate position of 4686 series lines of ionized He visible on the original plates. Principal triplet series starts with λ3889 at 30.8 on the scale and ends at about 83 on the scale at λ2645.

summary of the experimental conditions and results are given in Table I.

The intensity of the higher series members in the magnetron seemed to compare favorably with that obtained in other types of discharge, but in order to get some direct comparison a capillary tube was constructed and the He spectrum photographed. The condensed capillary discharge in particular has been employed[2] to obtain ionized spectra. Fig. 2(*g*) shows the results obtained with an hour exposure using a 10,000 volt transformer and a 4.0 mm spark gap. Similar results for the uncondensed capillary discharge are shown in (*h*).

Hydrogen, nitrogen and mercury

In order to investigate the possibility of employing the magnetron discharge to obtain the higher series members and ionized spectra of other gases, the spectra of hydrogen, nitrogen and mercury have been observed. As might be expected, the source did not prove satisfactory in bringing out the Balmer series in hydrogen as the concentration of atomic hydrogen in such a discharge is small.[1] Only six or seven Balmer lines were identified in an hour exposure. The secondary spectrum was relatively strong. The presence of continuous radiation in the ultraviolet was suggested by a violet fluorescence observed on the quartz window, and this showed up on the plates rather strongly throughout the whole region down to 2200A.

Results for nitrogen are shown in Fig. 2(*i*) and (*j*). The strong bands present could probably be suppressed and the nitrogen lines brought out more strongly by employing mixtures of helium and nitrogen[3] but this was not tried.

The mercury spectrum was observed only in the visible region with the constant deviation spectrograph and no photographs were taken. The pressure, though not carefully controlled,

[2] Evans, Phil. Mag. **29**, 284 (1915).

[3] Duffendack and Wolfe, Phys. Rev. **34**, 409 (1929); Merton and Pilley, Proc. Roy. Soc. **A107**, 411 (1925).

TABLE I. *Summary of experimental conditions and results for spectrograms shown in Fig. 2. (a) Window pointed to one side of filament. All other spectrograms shown were taken with window pointed directly toward filament. (b) About the most favorable conditions of operation for bringing out higher members of the series. (c) High pressure gives greater intensity of lower series members, but higher members less intense. Many faint unidentified lines. (d) All lines much less intense without magnetic field. (e) Lower voltage results in weakening the ionized series and higher members of the unionized series. (f) Larger current and longer exposure brings out a few more high members of the series. (g) Only 5 of 4686 series observed in spite of high relative intensity of 4686 itself. He I partially suppressed. (h) Higher series members of He I weaker than in the magnetron.*

PLATE NO.	GAS	DISCHARGE VOLTAGE	DISCHARGE CURRENT (ma)	MAGNETIC FIELD (OERSTEDS)	PRESSURE (mm)	EXPOSURE TIME	NO. MEMBERS PRIN. TRIP SERIES	NO. MEMBERS 4686 SERIES
a	He	220	500	150	0.08	1 hr.	6	2
b	He	220	500	150	0.10	1 hr.	10	5
c	He	260	500	150	1.0	1 hr.	6	5
d	He	260	500	0	0.14	1 hr.	6	3
e	He	100	500	150	0.14	1 hr.	8	3
f	He	220	800	160	0.08	2 hr.	12	6
g	He	condensed capillary discharge			0.7	1 hr.	7	5
h	He	uncondensed capillary discharge			0.7	1 hr.	8	2
i	N	150	500	350	0.06	1 hr.	50 lines due to N II 10 lines due to N III 6 lines due to N IV	
j	N	220	500	160	0.3	1 hr.		

was of the order of a few thousandths of a mm; discharge voltage was 250 and current 0.30 ampere. Application of the magnetic field brought out many lines that were not visible otherwise, about sixty being recorded in the region 7000 to 4000A. Of these, 23 were identified as being due to Hg I, 25 to Hg II, and the remainder have not been identified.

DISCUSSION

It has been shown by Bleakney and Smith[4] that a maximum of 0.55 percent of the ions in helium are He^{++} when ionization is produced by single electron impact. Therefore it would seem that an efficient source of He^{++} must depend on multiple electron impact. Very little is known about the process of ionization in successive stages, but it is usually assumed to be fairly efficient. In the case of helium the problem then resolves itself into one of obtaining as high a degree of ionization as possible, then removing the remaining electron from the He^{+} ions by a second impact. Rough calculations indicate that only about one or two percent of the gas is ionized in a magnetron discharge such as that described here. However, this percentage may be much higher in the intense region of ionization close to the filament. This conclusion is borne out by the increased intensity of the λ4686 series when the window was pointed directly at the filament.

It is obviously impossible to make any quantitative estimate of the concentration of He^{++} ions from spectroscopic results. But these results do indicate the best operating conditions. Thus a fairly low pressure (about 0.1 mm) is evidently desirable since the higher series members are brought out best under those conditions. However, the pressure must not be too low or the electrons escape from the region of intense ionization without making any impact. At first it was surprising that the lower members of the 4686 series should be brought out stronger at much higher pressures (about 1.0 mm) since the percentage of gas ionized under these conditions is presumably smaller. But the intensity of those lines may be due principally to single electron impact, and at any rate, the fact that the higher members are weaker would indicate that high pressures are not desirable for the production of

[4] Bleakney and Smith, Phys. Rev. **49**, 402 (1936).

He^{++} ions. The spectroscopic results also indicate that the electrons should have an energy of two to three hundred volts, but higher energy does not seem desirable, especially if accompanied by a decrease of current. Mass-spectrograph experiments are now under way to study the products of ionization under the most satisfactory conditions of operation.

A consideration of other possible sources of He^{++} ions indicates, where calculation is possible, that the percentage of ionization of the gas would be no greater, and probably less in most cases than in the magnetron. The condensed capillary discharge seems to offer one of the best possibilities since the He II lines are very intense relative to those of He I. However, here again, the higher members of the series are relatively less intense than in the magnetron at low pressures, and the concentration of He^{++} ions may be small. Nevertheless, it would be worthwhile to study the products of ionization in the condensed capillary discharge with a mass spectrograph.

In regard to the excitation of ionized spectra in other gases, the magnetron seems to offer some possibilities. The intensity is high close to the filament, and its superiority over ordinary gas discharges was demonstrated strikingly in the case of mercury where many additional lines were brought out by the application of the magnetic field. Whether it can compete with the other devices employed by spectroscopists, such as the electrodeless discharge or the vacuum spark, could probably be determined only with a vacuum spectrograph as most of the strong lines of the highly ionized states lie in the far ultraviolet. It does, however, offer the possibility of intensity studies with electrons of known energy which is not possible with most other sources.

The writers are indebted to Dr. J. C. Boyce of Massachusetts Institute of Technology for a discussion of the manuscript.

MARCH 1, 1937 PHYSICAL REVIEW VOLUME 51

Low Electronic States of Simple Heteropolar Diatomic Molecules:

III. Hydrogen and Univalent Metal Halides

ROBERT S. MULLIKEN
Ryerson Physical Laboratory, University of Chicago, Chicago, Illinois
(Received December 22, 1936)

Electronic structures for the electronic states involved in the near ultraviolet spectra of AX are discussed (X = halogen, A = hydrogen or univalent metal). The upper electron levels involved are mostly among a set of levels $Q\ ^1\Pi$ and $^3\Pi$, $T\ ^3\Sigma^+$, $V\ ^1\Sigma^+$, or their Ω-s or case c equivalents. Tentative potential energy curves for states Q, T and V of HI, AgI, and NaI are shown in Figs. 1–3. It is concluded that the observed HX absorption (continuous) involves the three Q levels corresponding to $^3\Pi_1$, $^3\Pi_0{}^+$, and $^1\Pi$, but with Ω-s coupling. It is further concluded (in contrast to what is found in the halogen spectra) that the observed absorption goes mainly to the $^3\Pi_1$ and $^1\Pi$ levels rather than the $^3\Pi_0{}^+$. The N and V potential energy curves of HX obtained here are compared (see text) with those given by Pauling; for HI there is good agreement, but for HBr, HCl, HF the V curves go increasingly higher than those of Pauling.

For AgX, it is concluded that the upper potential energy curve of the observed bands (curve B) contains a shallow minimum followed, as r is increased, by a maximum, beyond which it sinks to an asymptote about 1 ev lower. It is concluded that curve B is probably a resultant of an interaction of a stable $^1\Sigma^+$ curve, derived from a d^9s^2 excited silver atom and an unexcited X atom, with curves of the types $V\ ^1\Sigma^+$ and especially $Q\ ^3\Pi_0{}^+$; but that near its minimum state B is essentially $Ag(d^9s^2)\cdot X$ in character, corresponding to a stable union between an Ag atom with a d valence electron and an X atom. It is concluded that transitions to the three Q levels in AgX probably involve continuous absorption, as in HX and MX. The various band systems of CuX and AuX at long wave-lengths are ascribed to electron levels derived mainly from metal atoms in which a d electron has been excited (state d^9s^2, ^2D).

For MX (M = alkali metal), it is concluded, in agreement with previous workers, that the process of light-absorption in the near ultraviolet has approximately the effect of transferring an electron from X^- of M^+X^- to the M atom, leaving two neutral atoms M and X which tend to fall apart (case c separate-atom coupling). The thus indicated lack of valence attraction between neutral M and X probably involves a thoroughgoing failure in MX of the additivity rule for homopolar bond energies. Possible reasons for this probable failure (mainly, highly unequal size and energy of valence orbitals of M and X) are

discussed. The electronic structures of normal and excited MX (also MX^+) are discussed theoretically both from the molecular orbital viewpoint and from that of atomic orbitals, and the occurrence of case *c* coupling is shown to be theoretically reasonable from both standpoints. The upper levels involved in the absorption are identified as three 1 levels each of which is probably a case *c* mixture of $Q\,^3\Pi_1$, $Q\,^1\Pi$, and $T(^3\Sigma^+)_1$, and two 0^+ levels each of which is an approximately 50, 50 mixture of $Q\,^3\Pi_{0^+}$ with $V\,^1\Sigma^+$.

Franck's empirical spectroscopic criterion for distinguishing between atom-molecules and ion-molecules is discussed. From the present analysis of the electronic states involved in the spectra of HX, AgX, and MX, and from previous work on X_2 and XY, it is concluded that, for molecules containing halogen atoms, the criterion does not have a systematic theoretical basis but, insofar as it is valid, depends on the occurrence of certain rather special and fortuitous circumstances.

1. Introduction

THE present paper is a continuation of two recently published,[1,2] which will be referred to hereafter as "I" and "II." For a general introduction to the present paper, also for certain tables needed in the following, reference should be made to these.

The present paper deals with certain more or less heteropolar diatomic molecule types HX, AgX, and MX containing one halogen (X) atom. The types HX, AgX, and MX, respectively, will be taken up in Sections 5, 6, and 7. Preceding these specific treatments, it appears advisable to make a survey of certain questions which arise and certain rules and principles which are or may be applicable in understanding the spectra and electronic structures of all these molecules. This survey is given in Sections 2–4.

2. Franck's Criterion for Atom- and Ion-Molecules

Franck and collaborators some time ago proposed an empirical spectroscopic criterion for distinguishing between diatomic atom- and ion-molecules (cf. I, Section 4). This proposal has stimulated much interesting work on absorption spectra, particularly of salt vapors. Attempts to extend the criterion to polyatomic molecules, e.g., MeX_2, have not been very successful.

The criterion, considerably qualified subsequent to its original formulation, may be stated as follows:[3] the longest wave-length reasonably strong absorption region involving an electronic transition, in the spectrum of the vapor of the substance in question, corresponds in the case of ion-molecules to dissociation into two unexcited atoms, in the case of atom-molecules to dissociation giving products including at least one excited atom.

The qualifying words "reasonably strong" had to be added when it was found that even atom-molecules in some cases show weak absorption correlated with dissociation into unexcited atoms. Recently the work of Acton, Aickin and Bayliss[4] on Br_2 and of Goodeve and Taylor[13] on HBr and HI make it doubtful whether even the qualification "reasonably strong" is adequate. It now appears probable that the longest wave-length absorption in some or all of the atom-molecules just named is fairly strong yet at the same time gives dissociation into unexcited atoms.

Franck's criterion has hitherto received no theoretical explanation,—except that for atom-molecules like H_2, MH, M_2, where both atoms have a ^2S normal state, its necessary validity is rather obvious. As already noted, the criterion states that the first region of photodissociation in the case of an ion-molecule yields two unexcited atoms, but that in the case of an atom-molecule it ordinarily leaves one atom in an excited state. Here it deserves emphasis that in practice, for

[1] R. S. Mulliken, Phys. Rev. **50**, 1017 (1936): I.
[2] R. S. Mulliken, Phys. Rev. **50**, 1028 (1936): II.
[3] *a*. J. Franck, H. Kuhn, and G. Rollefson, Zeits. f. Physik **43**, 155 (1927). *b*. J. Franck and H. Kuhn, Bull. Acad. Sci. United Prov. India **2**, 223 (1933).

[4] R. S. Mulliken, Phys. Rev. **46**, 549 (1934); see also references given there; further, G. E. Gibson and O. K. Rice, Phys. Rev. **50**, 380, 871 (1936); E. Rabinowitch and W. C. Wood, Trans. Faraday Soc., March, 540 (1936); A. P. Acton, R. G. Aickin and N. S. Bayliss, J. Chem. Phys. **4**, 474 (1936); R. S. Mulliken, J. Chem. Phys. **4**, 620 (1936); O. Darbyshire, J. Chem. Phys. **4**, 747 (1936). *Correction:* in the second paragraph on p. 561 of the writer's 1934 paper, next to last sentence, it is stated that "if both were unperturbed, the former [for Ω-*s* coupling] should be about twice as intense as the latter." This is unjustified; no definite relation can be predicted without detailed knowledge of perturbing states. Furthermore, if the high intensity of $^3\Pi_{0^+u} \leftarrow {}^1\Sigma^+_g$ is the result of a strong perturbation of the $^3\Pi_{0^+u}$ state, this is probably due much more to a strong case *c* tendency than to Ω-*s* coupling. *Notes:* In the papers of Rabinowitch and Wood and of Gibson and Rice, support is given to the absorption coefficients and resulting electric moment *P* for I_2 given by the writer in Table II*B* of the 1934 paper. In the other 1936 papers, it is shown that the transition $^1\Pi \leftarrow {}^1\Sigma^+$ shares strongly with $^3\Pi_{0^+} \leftarrow {}^1\Sigma^+$ and probably $^3\Pi_1 \leftarrow {}^1\Sigma^+$ in the intensity of the observed Br_2 continuum.

most of the molecules to which the criterion has been applied, the excited state involved has been the $^2P_{1/2}$ upper component of the ground level ^2P of a halogen atom, the excitation thus consisting solely in the occurrence of the $^2P_{1/2}$ rather than the lower-energy component $^2P_{1\frac{1}{2}}$. To the present writer it has always seemed strange that so relatively minor a constitutional difference as that between the two sublevels of a ^2P state should have any fundamental connection with a constitutional difference presumably so pronounced, and so different in character, as that between an ion-molecule and an atom-molecule.

In previous papers by the writer,[4] special reasons why molecules of the special types X_2 and XY give predominantly one excited ($^2P_{1/2}$) atom on photodissociation have been analyzed, thus showing why Franck's criterion can hold in those cases; but as was noted above, it is now improbable that the criterion actually *does* hold in all such cases. In the present paper a further systematic and comparative study and theoretical interpretation of absorption spectra is made, extending to the types HX, AgX and MX.

From the present work and that already done on X_2 and XY, it is concluded that the usual validity of Franck's criterion in molecules AX is due rather to a combination of special and distinctly fortuitous circumstances than to a general theoretical cause. It is found that in all molecules AX, both atom-molecules and ion-molecules, absorption processes giving photodissociation into unexcited A plus $X(^2P_{1\frac{1}{2}})$ must occur; but that in the case of many but not all atom-molecules, the absorption coefficient for such processes happens to be unusually low (cf. the postulates in Section 4); while in the case of ion-molecules (of which the only known representatives are of the type MX) the absorption coefficient for such processes is always fairly large, in consequence partly or perhaps mainly of the characteristic case *c* nature of the excited states of these ion-molecules. Further reference to Franck's criterion will not be made in later sections of this paper, but the nature of its explanation can be seen by a study of these sections of the paper and of similar work on X_2 and XY.

On the basis of their spectroscopic criterion, Franck and Kuhn[5, 6] class HI and AgX (other than perhaps AgF) as atom-molecules, MX as ion-molecules. Data on AgF are not available, but it seems possible that it may be an ion-molecule like MX. From quantum-mechanical considerations, Pauling[7] and others conclude that all HX are atom-molecules. Even though AgX are atom-molecules, it would probably be generally agreed that they have more ionicness than HX, and so are intermediate in character between HX and MX (cf. Table II of I, also Figs. 1–3). The present study of the several spectra supports this idea.

3. Coupling Cases and Correlation Rules for AX Molecules

In molecules AX, namely HX, AgX and MX, we expect to find energy levels N, T and V just analogous to those which are found in H_2, M_2 and MH (cf. I and II), and in addition we expect the Q group of levels (cf. Table I of I). This group consists of states $^3\Pi_2$, $^3\Pi_1$, $^3\Pi_{0^-}$ and $^3\Pi_{0^+}$, and $^1\Pi$, with energy expected usually to increase in the order named. These designations, however, are really appropriate only if the spin-orbit coupling is of the ordinary case *a* or case *b* type (Λ-Σ coupling). We shall, nevertheless, for the sake of convenience and simplicity, use these same designations, so far as possible, even when the coupling is of another type.

Before considering the individual spectra of HX, AgX and MX, it is advisable to make a survey of the energy relations and other properties to be expected for the Q group of levels (cf. Tables I–IV in I and II for a partial summary). In doing this, one soon finds that it is necessary to consider several different types of spin-orbit coupling. This is partly because the predominant type of coupling varies from one molecule to another, and partly because for any given molecule the coupling varies with the internuclear distance r. A thorough knowledge of the

[5] J. Franck and H. Kuhn, Zeits. f. Physik **43**, 164 (1927): AgI, HI.

[6] J. Franck and H. Kuhn, Zeits. f. Physik **44**, 607 (1927): AgCl, AgBr; B. A. Brice, Phys. Rev. **33**, 1090 (1929); **35**, 960 (1930); **38**, 658 (1931); A. Terenin, Physica **10**, 209 (1930): AgI; H. Kuhn, Zeits. f. Physik **63**, 458 (1930); M. Ashley and F. A. Jenkins, Phys. Rev. **37**, 1712*A* (1931); **42**, 438 (1932).

[7] L. Pauling, J. Am. Chem. Soc. **54**, 988 (1932); F. Hund, Zeits. f. Physik **40**, 762 (1927).

electronic states of a molecule requires understanding them over a range of r values. For dissociation correlations one must cover the range of r from r_e to ∞.

Because of the need of considering several coupling cases, and the rules of correlation between them, the explanations of the observed spectra become of necessity somewhat complex. Although this is regrettable, it appears to be an unavoidable consequence of the actual complexity of the underlying molecular situation.

The main types of coupling which we need to consider are three: (1) Λ, Σ coupling; (2) Ω, s coupling;[4] (3) the writer's case c coupling,[5] i.e., the "far-nuclei" variety of case c coupling. Types (1) and (2) are possible for moderate r values, while type (3) occurs for large or in some cases also for moderate r values. For stable molecular states, and for some unstable ones, the choice is between (1) and (2). Then if spin-orbit coupling is relatively weak, we have Λ, Σ coupling, if strong, we have Ω, s or some similar coupling. For molecules which are essentially just pairs of atoms interacting weakly (this includes *all* molecules for sufficiently large r values), we have type (3). There is a fourth type of coupling (Hund's case c coupling, or "close-nuclei" variety of case c) which will be discussed in Section 5 in connection with the behavior of the HX energy levels as $r \to 0$, but this is not important for AgX or MX, and will not be considered in this section.

In coupling types (1) and (2), the Q group of levels can be considered by itself. In type (3), however, we shall find it necessary to consider N, T, V, and Q (or at least T, V and Q) together, since in this case they become, so to speak, mutually entangled.

For ordinary Λ-Σ coupling, the levels $^3\Pi_2$, $^3\Pi_1$, $^3\Pi_0$ of the Q group should be equally spaced with intervals $^3\Pi_0 - {}^3\Pi_1$ and $^3\Pi_1 - {}^3\Pi_2$ each equal to about $(1/2)a$, where a is the spin-orbit coupling coefficient of the X atom, in its normal electron configuration; a should be about 2/3 of the $^2P_{1/2} - {}^2P_{3/2}$ separation of the latter.[4] The $^1\Pi$ level should be considerably higher in energy.

If, however, as in the levels of X_2 and XY which are analogous to the present Q group, there should be a strong tendency toward Ω-s coupling,[4] then the levels $^3\Pi_2$, $^3\Pi_1$ should form a doublet of width much less than $a/2$, separated by an interval of about a or a^+ from the levels $^3\Pi_0$, $^1\Pi$, which should also form a doublet ($a = a^+$ of X^+ ion[4]). The two doublets should then, respectively, be thought of in AX as

$$[(\sigma^2\pi^3, {}^2\Pi_{3/2})\sigma^*]_{2,\,1} \quad \text{and} \quad [(\sigma^2\pi^3, {}^2\Pi_{1/2})\sigma^*]_{0,\,1},$$

the final subscripts giving resultant Ω values. In ideal Ω-s coupling, each doublet width would shrink to zero. As we shall see below, the actual coupling in the HX molecules, for r near r_e of state N, probably approximates the Ω-s type.

The third possible kind of coupling, which apparently is closely approximated in the excited states of the MX molecules, is the writer's "case c" or "far-nuclei" type.[6] In this the combination between the atoms is loose, and each atom A preserves its own internal coupling and its resultant J_A. The interatomic forces, however, cause a space quantization of each J_A relative to the internuclear axis, giving a quantum number Ω_A for each atom.

In the MX excited states in which we shall be interested, the M atom is in its normal state $\ldots ms$, ^2S, while the X atom is in one of the two states $^2P_{3/2}$ and $^2P_{1/2}$ of the atom's normal electron configuration $\ldots np^5$. Thus $J_M = 1/2$ and $J_X = 3/2$ or $1/2$. When $J_M = 1/2$ and $J_X = 3/2$, we have $\Omega_M = 1/2$, with Ω_X either $3/2$ or $1/2$; when $J_M = 1/2$ and $J_X = 1/2$, we have $\Omega_M = 1/2$, $\Omega_X = 1/2$. There is now in each case a small interaction between Ω_M and Ω_X to give a resultant Ω of the molecule as a whole. The possible Ω resultants are as follows:[5] from M plus $^2P_{3/2}$ of X, $\Omega = 2, 1, 1, 0^+, 0^-$; from M plus $^2P_{1/2}$ of X, $\Omega = 1, 0^+, 0^-$.

Of these several case c electronic states, only $\Omega = 2$ can be correlated uniquely with a single definite state, namely $^3\Pi_2$, of the other coupling cases. The three states $\Omega = 1$, *taken collectively*, do, however, correspond to the Q states $^3\Pi_1$, $^1\Pi$ and the $\Omega = 1$ component[5] of the $T\,{}^3\Sigma^+$ state. The correspondence consists essentially in the fact that the wave functions of the three $\Omega = 1$ states of pure case c can be expressed as linear combinations of the wave functions of the three Λ-Σ coupling states just mentioned, and *vice versa*.

[5] R. S. Mulliken, Rev. Mod. Phys. **3**, 113–119 (1931); **4**, 20, 26–29 (1932). For some case c energy formulas, cf. J. H. Van Vleck, Phys. Rev. **40**, 568 (1932).

In a similar manner the two pure case c states $\Omega=0^+$ together correspond to the Λ-Σ coupling states $Q\,{}^3\Pi_{0+}$ and $V\,{}^1\Sigma^+$. Similarly, the two 0^- states together correspond to the $Q\,{}^3\Pi_{0-}$ and the 0^- component[8] of $T\,{}^3\Sigma^+$.

For each of the above three coupling schemes, there is a one to one correspondence between, on the one hand, the set of states $A(^2S)+X(p^5, {}^2P_{3/2})$, $A(s, {}^2S)+X(p^5, {}^2P_{1/2})$, and $A^+ + X^-(p^6, {}^1S)$, existing at $r=\infty$, and, on the other hand, the set of molecular states $N\,{}^1\Sigma^+$, $T\,{}^3\Sigma^+$, $Q\,{}^{1,3}\Pi$, and $V\,{}^1\Sigma^+$ or their case c equivalents. In all the coupling cases, the sets T and Q are correlated with $A(s, {}^2S)+X(p^5, {}^2P_{3/2,\,1/2})$. The allegiances of N and V on dissociation, however, are found to be less definite. In MX, N goes to $M^+ + X^-$, and V (mixed with $Q\,{}^3\Pi_{0+}$) goes with T and Q to M+X. In HX and AgX, N goes with T and Q to A+X, while V goes to $A^+ + X^-$. These results concerning the correlations of N and V on dissociation are based (see below) on theoretical considerations and on band spectra.

4. Special Postulates for AX Molecules

In interpreting and drawing conclusions from the observed spectra of HX, AgX and MX, it will be helpful to refer to some conclusions reached previously in studying the X_2 and XY spectra.[4] The lowest observed excited levels of these molecules belong to a group analogous to the present Q group. Taking ICl as an example, and calling the lowest states N and Q in analogy to the present case, we had:

$$\begin{aligned} N&: (\sigma_{CII})^2(\pi_{Cl})^4(\pi_I)^4,\ {}^1\Sigma^+;\\ Q&: (\sigma_{CII})^2(\pi_{Cl})^4(\pi_I)^3\sigma^*_{ICl},\ {}^{1,3}\Pi. \end{aligned} \tag{1}$$

States N and Q of ICl are very much like those of HX (cf. Table I of Paper I), except for the presence of an extra group of nonbonding π electrons (π_{Cl}),[4] which need not concern us here.

In ICl, and in XY and X_2 generally, it was found that the strongest transitions between N and group Q are often or usually those to the ${}^3\Pi_{0+}$ component of this group, *which for brevity we shall hereafter refer to* as Q_0. It was concluded that transitions to the ${}^1\Pi$ (and ${}^3\Pi_1$) must often or usually be inherently weak. The coupling in the Q states of X_2 and XY is mostly intermediate in type between Ω-s and case c. In either of these cases, the spectroscopic properties of ${}^1\Pi$ should be shared more or less completely by ${}^3\Pi_1$, since the wave functions of pure singlet and triplet type which would exist for Λ-Σ coupling become mixed together in either Ω-s or case c coupling. [In case c, $\Omega=1$ of ${}^3\Sigma^+$ is also mixed in, as described above.]

The rather high intensity of the spectroscopic transition from N to Q_0 in I_2 was attributed by Van Vleck to the existence of a strong perturbation of Q_0 by a higher lying ${}^1\Sigma^+$ state of such a nature as to have the ability to receive strong spectroscopic transitions from N. Such a perturbation is especially likely in case c, and this admixture of ${}^1\Sigma^+$ wave function would impart to Q_0 the power to combine strongly with N. The higher ${}^1\Sigma^+$ in question was tentatively identified by Van Vleck as the D state of I_2. The writer then pointed out that this "D" state is very probably the expected largely ionic state analogous to the V state of H_2. Strong perturbation of Q_0 by V may then be tentatively considered, for X_2 and XY, as the, or at least a, cause of the strong combination of N with Q_0.

Another possible cause was suggested and favored by the writer,[4] on the ground that a perturbation of Q_0 by V so strong as to give rise to the very high observed intensity of $Q_0 \leftarrow N$ in I_2 (cf. reference 4, Table II*B*) should cause a depression of the energy of Q_0 relative to ${}^3\Pi_1$ larger than would be compatible with the observed relative energies of ${}^3\Pi_1$ and Q_0 (cf. reference 4, Table II*A*). The writer's suggested cause would not depress Q_0 at all. Reconsideration of the matter indicates, however, that the argument is not conclusive. If it be assumed, for instance, that the electric moment of $V \leftarrow N$ has a value corresponding to a displacement of a charge e by 10^{-8} cm, then a 25 percent admixture of V wave function in Q_0 will account for the observed intensity of $Q_0 \leftarrow N$; and estimating the energy interval from Q_0 to V as 4 ev, one finds by perturbation theory that Q_0 should be pushed down by about 0.25 ev. This is indeed rather large, but it may be that there is enough uncertainty in respect to the observed ${}^3\Pi_1 - Q_0$ separation, the exact nature of the coupling, and the size of the $V \leftarrow N$ electric moment, to make such a result admissible. A further possibility might be that Van Vleck's cause and the writer's cause for the strength of $Q_0 \leftarrow N$ operate simultaneously in the case of I_2, in which case both effects could be fairly strong without much depression of Q_0. In any case, it is to be noted that the writer's suggested cause is dependent on the presence of *two* groups of π electrons, and so would be inapplicable to explain high intensity of $Q_0 \leftarrow N$, if this occurs, in HX, AgX or MX. Van Vleck's cause would, however, still be operative.

The foregoing discussion suggests that the

following trial postulates form a reasonable tentative basis for interpreting the spectra of HX, AgX and MX. (1) Transitions between the atomic and ionic $^1\Sigma^+$ state, i.e., $V \leftarrow N$, are always intrinsically very intense. (2) Transitions from N to the $^1\Pi$ and $^3\Pi_1$ components of Q may often be intrinsically weak in these molecules, as is often or usually the case in X_2 or XY. (3) Transitions $Q_0 \leftarrow N$ can be strong because Q_0 may be strongly perturbed by V if strong case c tendencies are present.

Justification for these postulates is as follows. Postulate (1) is theoretically very reasonable, and is supported, experimentally, by the existence of strong transitions $V \leftarrow N$ in H_2, MH and I_2. Postulate (2) is theoretically possible, although not obviously necessary. Its chief basis is its experimental validity for X_2 and XY. This makes it tenable, although not definitely predictable, for any or all of the types HX, AgX and MX. The justification of (3) is similar to that of (2), namely theoretical admissibility and experimental validity in the cases of X_2 and XY.

Anticipating our application of the foregoing postulates in Sections 5–7, it may be well to report here the not very surprising and indeed rather gratifying fact that, in practice, we are forced to conclude that the somewhat arbitrary and special postulates (2) and (3), which are based on experience with halogen molecules, probably are honored as much in the breach as in the observance.

5. The Molecules HX

No discrete electronic band spectra of neutral HX have been found at wave-lengths above λ2000. Continuous absorption and emission bands are, however, found in the ultraviolet. Whether or not the recorded continuous emission bands[10] correspond in part to the same electronic transitions as are involved in the absorption bands appears uncertain. In the following, we shall consider only the absorption bands, since they surely arise from the normal electronic state.

The absorption spectra of HI, HBr and HCl all show absorption beginning in the ultraviolet and reaching a maximum near λ2000. In HF, there is no appreciable absorption at wave-lengths greater than λ1900 or less.[11] In HCl, Leifson[12] reports a broad maximum of absorption at about λ2000, followed by others at about λ1700 and below. More attention has been devoted to HBr and HI; the best results appear to be those published recently by Goodeve and Taylor,[13] who have made quantitative measurements of the absorption coefficient of HBr down to about λ1850 and of HI apparently to about λ2300; quantitative data of others on HI go to about λ2200.[13a] The measurements in each case unfortunately stop just short of the maximum of the absorption curve. The maximum is estimated to come at about λ1790 for HBr ($\nu = 56{,}000$) and at about λ2200 for HI ($\nu = 45{,}000$). The maximum in each case is broad and flat.[13a]

Defining the absorption coefficient k by $I = I_0 e^{-kl}$ (l = path in cm; gas density corrected to 0°C, 760 mm), one finds by calculation from the results of Goodeve and Taylor on HBr, $k_{max} = 56$. [The absorption coefficients given by Goodeve and Taylor, according to a private communication from Dr. Goodeve, refer to gas at 17°C.] On the long wave-length side of the HBr curve, k has fallen to about half its maximum value at about $\nu = \nu_{1/2\ max} = 49{,}450$. Assuming that the absorption curve is somewhat less steep on the high frequency than on the low frequency side, as would be expected, and then proceeding in the manner outlined in Table II*B* of a previous paper[4] on the halogens X_2 and XY, one finds approximately for the effective electric moment amplitude P associated with the transition, the value $P/e = 0.24 \times 10^{-8}$ cm. This is approximately the same as for the strong visible I_2 absorption system ($P/e = 0.26 \times 10^{-8}$ cm) and stronger than for the corresponding Br_2 transition ($P/e = 0.13 \times 10^{-8}$ cm).

[10] M. Kulp, Zeits. f. Physik **67**, 7 (1931): HCl; A. K. Dutta and S. C. Deb, Zeits. f. Physik **93**, 127 (1934). Cf. also H. C. Urey and J. C. Bates, Phys. Rev. **34**, 1541 (1929): but probably X_2 not HX; and W. Weizel, H. W. Wolff, and H. E. Binkele, Zeits. f. physik. Chemie **B10**, 459 (1930): HBr, but probably not involving the normal state.

[11] Cf. H. J. Plumley, Phys. Rev. **49**, 405*L* (1936); K. Siga and H. J. Plumley, Phys. Rev. **48**, 105*L* (1935).

[12] S. W. Leifson, Astrophys. J. **63**, 73 (1926).

[13] C. F. Goodeve and A. W. C. Taylor, Proc. Roy. Soc. **A152**, 221 (1935); **A154**, 181 (1936); and references given there.

[13a] Recently H. J. Plumley in this laboratory has photographed the HI absorption down to about λ1950. The maximum of the absorption appears to be (very roughly) near λ2300, and there appears to be no evidence of more than one maximum. Quantitative measurements from λ2300 down would, however, be desirable.

In the case of HI, k_{max} is 16 according to the data of Goodeve and Taylor, *less* than for HBr. Proceeding in the same manner as above, one finds $P/e=0.14\times10^{-8}$ cm for HI, about the same as for the Br_2 transition. The fact that the transition probabilities increase from Br_2 to I_2, but decrease from HBr to HI, indicates that the nature of the transition or transitions in HX may be considerably different than in X_2.

It has been shown, especially by Goodeve and Taylor, that the long wave-length tails of the HBr and HI continua cannot be ascribed primarily to initially vibrating molecules. This is important in relation to the dissociation process to which these continua must correspond. The dissociation energy of HI into $H+I(p^5, {}^2P_{3/2})$ is 3.02 ev, corresponding to λ4080; for $H+I(p^5, {}^2P_{1/2})$ it is 3.96 ev, or λ3120. Absorption is found to be very appreciable to well beyond λ3120 and has been followed to beyond λ3600 with long gas columns. Hence, noting also that no discrete bands are observed,[13] so that it cannot be a question of a curve going down to a minimum and then rising to $H+I({}^2P_{1/2})$, it is clear[13] that at least a considerable part of the continuous absorption in HI gives rise to $H+I({}^2P_{3/2})$, i.e., to unexcited atoms. But further, the absorption intensity in the tail shows no noticeable acceleration in its rate of following off beyond λ3120; this tends to indicate that *most* or perhaps even nearly all of the absorption at all wave-lengths is associated with a potential energy curve or curves dissociating into $H+I({}^2P_{3/2})$. The data on HBr, although less adequate, point to similar conclusions.

We shall now consider how the foregoing and other experimental evidence may be interpreted in the light of the tentative postulates stated at the end of Section 4. First of all, it is clear that the observed continuum cannot represent transitions $V\leftarrow N$. One can estimate the position of the V level (cf. Pauling's curves[7] for HX) and it is too high. Besides, V should be a stable level and so $V\leftarrow N$ should give discrete bands. Further, the levels Q should certainly lie well below T and V according to band spectrum data on HX^+ (cf. discussion in a later paragraph in connection with Fig. 1), so that $Q\leftarrow N$ absorption might be expected at longer wave-lengths than either $T\leftarrow N$ or $V\leftarrow N$. $T\leftarrow N$ should give continuous absorption, but faint unless case *c* tendencies are strong, which is not likely here (see below). The observed continuum may then safely be attributed to $Q\leftarrow N$; more specifically, to transitions from N to ${}^3\Pi_1$, ${}^3\Pi_{0^+}$, and ${}^1\Pi$ of Q, transitions ${}^3\Pi_2\leftarrow N$ and ${}^3\Pi_{0^-}\leftarrow N$ being rigorously forbidden.

It appears possible that in HX all the transitions ${}^3\Pi_1\leftarrow N$, Q_0 (i.e., ${}^3\Pi_{0^+}$)$\leftarrow N$, and ${}^1\Pi\leftarrow N$ may contribute appreciably to the observed continuum under discussion. The extreme long wave-length part, or tail, of the HI absorption, however, cannot belong to $Q_0\leftarrow N$, since Q_0 necessarily gives $H+I({}^2P_{1/2})$ on dissociation; hence the tail must belong to ${}^3\Pi_1\leftarrow N$ or ${}^1\Pi\leftarrow N$ or both. Either of the two following possibilities then appears compatible with the existing data:

(a) ${}^3\Pi_1\leftarrow N$ and ${}^1\Pi\leftarrow N$ much exceed $Q_0\leftarrow N$ in total intensity;

(b) ${}^3\Pi_1\leftarrow N$ plus ${}^1\Pi\leftarrow N$ about equal $Q_0\leftarrow N$ in total intensity. A third possibility (c) that $Q_0\leftarrow N$ much exceeds the other two in total intensity, is probably incompatible with the evidence (see below).

In order to discuss these possibilities intelligently, it is necessary to consider what kind of coupling (cf. Section 3, above) is to be expected in the states ${}^3\Pi_1$, ${}^1\Pi$, and Q_0, for r values near r_e of state N, from which the absorption processes start. From the character of the HI and HBr continua (great breadth, indicating steeply rising $U(r)$ curves[13] at r equal to r_e of N; and intensity maximum at a frequency corresponding to 2 or 3 ev above the possible asymptotes of the $U(r)$ curves) it is clear that at $r=r_e$ of N there is strong interaction between the two atoms H and X. This and other considerations remove the possibility that the coupling is predominantly of the case *c* separated-atom type, except for large r values. In view of the large multiplet intervals in the Br and I atoms, we may conclude that the coupling in HBr and HI is predominantly of the Ω-*s* (*Jj*-like) type, possibly modified by some tendency toward case *c*. Predominant Ω-*s* coupling probably exists also in HCl and perhaps even in HF, since the relatively high excitation energy of the excited electron makes the electronic states of these molecules comparable with those of the atoms argon and neon.

With Ω-*s* coupling,[4] the levels ${}^3\Pi_1$ and ${}^1\Pi$ in HI should be separated by about 0.6 ev, and the Q_0

level should be close to the $^1\Pi$. As $r \to \infty$, however, we go over to case c coupling, and the $^3\Pi_1$ and $^1\Pi$ should draw together and both dissociate into $H + I(^2P_{3/2})$, while the Q_0 must go to $H + I(^2P_{1/2})$. With Ω-s coupling, transitions to the $^3\Pi_1$ and $^1\Pi$ should be about equally strong, since really the singlet-triplet distinction is completely broken down.

Returning to the possibilities (a), (b), (c) mentioned above, we now see that if (a) is correct, the observed absorption curve in HI must represent mainly the superposition of two similar absorption curves with maxima about 0.6 ev apart. If possibility (b) is correct, there must be three superposed curves, of which $Q_0 \leftarrow N$ and $^1\Pi \leftarrow N$ should have their maxima close together, with $^3\Pi_1 \leftarrow N$ at about 0.6 ev longer wave-length. If (c) should be correct, the absorption curve would be essentially a curve $Q_0 \leftarrow N$ with a single maximum, but with two curves $^3\Pi_1 \leftarrow N$ and $^1\Pi \leftarrow N$ superposed on it, both much weaker than $Q_0 \leftarrow N$ but still strong enough to account for the observed long wave-length tail of the absorption. This, however, is hardly possible, since the intensity of the tail fits on too smoothly to that of the main part of the absorption (see above). Hence possibility (c) is probably excluded on this ground.

Possibilities (a) and (b) require the presence of two strong maxima 0.6 ev apart, while what has been observed experimentally is a single very broad maximum.[13a] However, examination of the observed curve indicates that it could easily be the resultant of two broad-topped curves with their maxima as much as 0.6 ev apart. All things considered, the existing data on HI appear to be compatible with either of the two possibilities. The same is true of HBr and HCl, where, moreover, the maxima of various absorption processes, if more than one should be intensely present, would be closer together than in HI.

Besides the reason already given against possibility (c), it should be noted that this possibility would be expected only if the coupling tended strongly toward case c; but this, as we have already seen, is improbable. Moreover, the fact that the absorption is stronger in HBr than in HI disfavors possibility (c), since any case c tendencies should be stronger in HI than in HBr. In this connection, a comparison with the cases of Br_2 and I_2 is instructive: the absorption is much weaker in Br_2 than in I_2; the high intensity in I_2 is attributed to strong case c influence which, together with weakness of $^3\Pi_1 \leftarrow {}^1\Sigma^+$ and $^1\Pi \leftarrow {}^1\Sigma^+$, is expressed in the realization of possibility (c); in Br_2, on the other hand, we have probably more nearly possibility (b).[4] Thus in the molecules HX, possibilities (a) and (b), or something between, appear by far the most probable, with the chances for (b) greatest for HI.

Goodeve and Taylor, assuming that essentially a single upper electronic state is involved in the continuous absorption of HX above $\lambda 2000$, have constructed a $U(r)$ curve for this state in the same manner as was done by Gibson, Rice, and Bayliss for Cl_2, by a quantum-mechanical treatment of the curve of absorption coefficient against frequency. From the discussion in the preceding paragraphs, however, it will be seen to be very probable that more than one upper $U(r)$ curve is importantly involved in the absorption. If so, the $U(r)$ curve given by Goodeve and Taylor represents some sort of average over the actual curves. Here it may also be noted that the smoothness of the effective curve obtained by Goodeve and Taylor strongly disfavors possibility (c).

Fig. 1 illustrates the nature of the $U(r)$ curves for states N, Q, T and V of HI, the Q curves $^3\Pi_1$ and $^1\Pi$ being drawn so that their average agrees approximately with Goodeve and Taylor's curve. The positions of the states $^3\Pi_2$, $^3\Pi_1$, $^3\Pi_0$, and $^1\Pi$ are estimated assuming Ω-s coupling.[4] The heights of the T and V states above the Q states have been estimated as follows. In the cases of HCl^+ and HBr^+, the energy interval from the normal state $\sigma^2\pi^3$, $^2\Pi$ to the excited state $\sigma\pi^4$, $^2\Sigma^+$ is known experimentally from band spectra. From these values for HCl^+ and HBr^+ (about 3.5 ev in both cases), we can estimate the corresponding interval for HI^+, which is not known experimentally, as 3.6 ev. Now the electron configuration $\sigma\pi^4\sigma^*$ of the states T, V of neutral HI differs from the configuration $\sigma^2\pi^3\sigma^*$ of states Q in exactly the same way that the configuration $\sigma\pi^4$ of the excited $^2\Sigma^+$ of HI^+ differs from the configuration $\sigma^2\pi^3$ of the $^2\Pi$ normal state of HI^+. Hence, for comparable r values (say r_e of $^2\Pi$ of HI^+, which is nearly the same as r_e of state N of HI), the energy difference should be nearly the

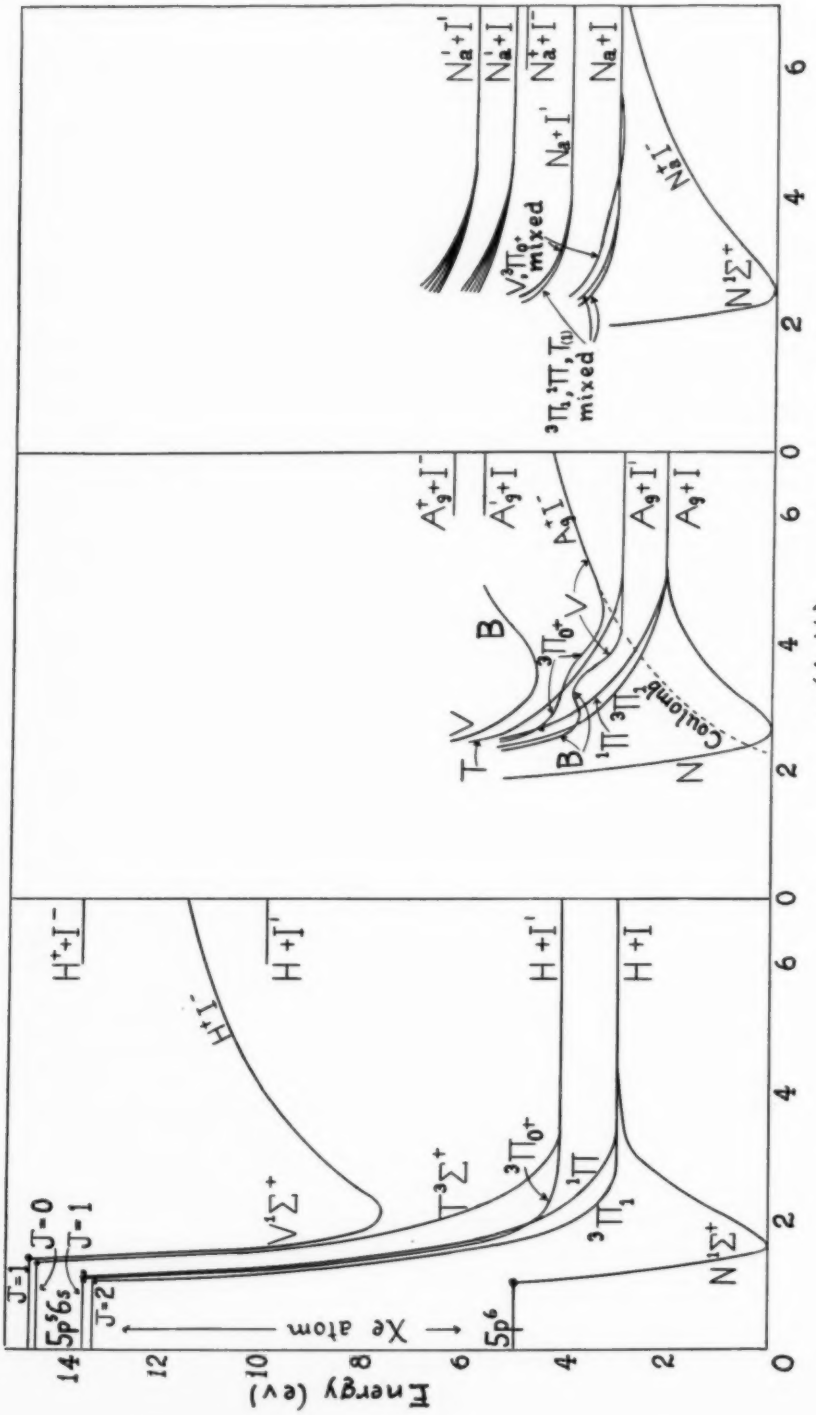

FIG. 1.

FIG. 2.

FIG. 3.

same between the center of gravity of the group Q and that of T, V in HI as between the two states of HI^+. The value 3.5 ev has been assumed in Fig. 1. The mode of dissociation of each of the various individual Q, T sublevels is determined in accordance with the usual case c rules[8] (cf. summary in Section 4). The V level in Fig. 1 is drawn somewhat above the T level at small r, and with the usual ionic type of $U(r)$ curve for larger r; as in the case of other V states, however (cf. I, II), dissociation actually takes place probably into a normal H plus an excited $I(5p^46s)$ atom rather than into two ions. In the neighborhood of the V state, and higher, other levels not shown in Fig. 1 are to be expected. These would be in part analogous to the levels $\sigma^2\pi^4\pi^3\sigma^2$ and others of e.g., ICl (cf. reference 4, Table IV).

In seeking a thorough understanding of the electronic structures and potential energy curves of states N, Q, T, and V of HX, it is valuable to follow them all the way from $r=0$ to $r=\infty$. Consideration of the united-atom ($r=0$), while not in general very important, is of real value for hydride molecules.

A clearer picture can be obtained if at first we neglect, for all values of r, the complicated patterns of energy sublevels corresponding to the various orientations of spin and orbital angular momentum vectors. Starting from $r=0$, we then find (cf. I, Table 1) that . . . $5p^6$, ^1S of Xe ($r=0$) goes over into . . . $\sigma^2\pi^4$, $^1\Sigma^+$ of HI ($r=r_e$) and this into $5p^5$, ^2P of I plus $1s$, ^2S of H ($r=\infty$). Further, . . . $5p^56s$, $^{3,\,1}P$ of Xe splits into $\sigma^2\pi^3\sigma^*$, $Q\,^{1,\,3}\Pi$ and $\sigma\pi^4\sigma^*$, $^{1,\,3}\Sigma^+$ (T and V) of HI; for large r values Q and T, like N, go over into $5p^5$ of I plus $1s$ of H, while V goes (or tends to go) into H^+ plus $5p^6$ of I^-.

At $r=0$, levels Q, T and V are about 9 ev above N; at r near r_e of state N, Q is about 5.6 ev above N, while T and V are about 9 ev above N according to Fig. 1; at $r=\infty$, N, Q and T coincide, while V is 10.3 ev higher. Attention should be called to the energy intervals from N to Q, T and V, which are already two-thirds as large as at $r=0$ for $Q-N$, and probably fully as large as at $r=0$ for $T-N$ or $V-N$. From these one may reasonably conclude that the actual structure of the molecule for r values near r_e of N can be better approximated in terms of united-

FIG. 1. Potential energy curves for lowest electronic states of HI. The curve for state N is based on spectroscopic and chemical data. The approximate locations of the Q curves (marked $^3\Pi$ and $^1\Pi$ in the figure) are based on spectroscopic data. Further details of the Q curves, and the forms of the T and V curves, are uncertain, but have been estimated (cf. text) in accordance with theoretical considerations and with band spectrum data on HCl^+ and HBr^+. At the left an extra scale, referring to the Xe atom, is added, and the state of the Xe atom into which each of the HI curves would go as $r\to 0$ is indicated. The Q curves $^3\Pi_2$ and $^3\Pi_0$ have been *omitted*; the former should be slightly below $^3\Pi_1$, the latter slightly below $^1\Pi$; both should go into the lowest excited level of the Xe atom as $r\to 0$. For $r=\infty$, I refers to $I(p^5\,{}^2P_{\frac{3}{2}})$, I′ to $I(p^5\,{}^2P_{\frac{1}{2}})$ or (upper level H+I′) to $I(p^5s,\,{}^3P_{\frac{3}{2}})$.

FIG. 2. Potential energy curves for lowest electronic states of AgI. The curves for states N and B are based on spectroscopic data and on the chemical dissociation energy (2.04 ev) for state N; the value of r_e for state N was estimated by the use of Badger's rules, and that of state B from that of state N by interpreting the intensity distribution in the $B\leftarrow N$ bands and continuum in terms of the Franck-Condon principle. The $^3\Pi_2$ and $^3\Pi_0$ Q curves (*not shown*) should be slightly below the $^3\Pi_1$ and $^1\Pi$, respectively. The curves for states B, $^3\Pi_0{}^+$, and V are drawn in a plausible way, corresponding to an interpretation suggested in the text. All the curves are strongly uncertain, except in part those of N and B near their r_e's. The labels B, $^3\Pi_0{}^+$, and V are shifted about from one curve to another with changing r in such a way that a given label always corresponds to a wave function approximately of a given character (see text). In regard to certain difficulties about the $^3\Pi_1$ and $^1\Pi$ curves, see the third from last paragraph of Section 6. The dashed curve marked "Coulomb" shows how the energy of Ag^+I^- would run if there were a pure Coulomb attraction. At $r=\infty$, Ag′ refers to $Ag(^2P)$, I′ to $I(^2P_{\frac{1}{2}})$.

FIG. 3. Potential energy curves for lowest electronic states of NaI. The approximate curve shown for state N follows the law $U(r)=(-e/r)+(\beta/r^n)$, with $\beta=3940$ and $n=9.5$ (energy in ev and r in A), β and n being approximately the same as in the Born formula for the lattice energy of NaI crystals; the constant β has, however, been adjusted to correspond to a dissociation energy (into ions) of 5.00 ev, based on chemical and spectroscopic data.[10] The other curves have been estimated in accordance with considerations described in the text. Because of the dominance of case c coupling here (unlike Figs. 1, 2), the states $Q(^3\Pi$ and $^1\Pi)$, $T(^2\Sigma^+)$, and $V(^2\Sigma^+)$ no longer exist as such. Instead we have two 0^+ states (i.e. case c states with $\Omega=0$, and plus character), whose wave functions can be expressed as mixtures of $Q\,^3\Pi_0{}^+$ and $V\,^1\Sigma^+$; further, three 1 states (i.e., $\Omega=1$) representing mixtures of $Q\,^3\Pi_1$, $Q\,^1\Pi$, and an $\Omega=1$ component of $T\,^2\Sigma^+$; and so on. The approximate heights of the curves for r equal to r_e of N are based on spectroscopic information. The relative spacings and positions of the 0^+ and 1 state curves forming each bundle are uncertain, but are shown in a plausible way. The bundle from $Na(^2S)+I(^2P_{\frac{1}{2}})$ should contain two additional curves (a 2 and a 0^-) which are not shown; that from $Na(^2S)+I(^2P_{\frac{3}{2}})$ should contain one 0^- which is not shown. The bundles from $Na(^2P)+I$ are indicated only roughly; each should contain a number of curves. For $r=\infty$, Na′ means $Na(^2P)$, I′ means $I(^2P_{\frac{1}{2}})$.

atom orbitals than of separate-atom orbitals. This strong tendency toward united-atom conditions, together with the rather large interval between $5p^6$ and $5p^56s$ of Xe, may be said to account for the pronounced repulsive character of the $U(r)$ curves of the Q (and T) states of HI (cf. also Dutta and Deb[10]).

Starting from the united-atom, where T, V, Q all belong to $5p^56s$ and coincide, a separation of about 3.5 ev between Q and T, V is attained for r near r_e of N. This separation may be said to be due to the *molecularization* of the Xe orbitals, whereby $5p^56s$ gives rise to $\sigma^2\pi^3\sigma^*$ (Q) or to $\sigma\pi^4\sigma^*$ (T, V). The molecular orbitals σ, π, which for $r=0$ are $5p\sigma_{Xe}$, $5p\pi_{Xe}$ and are equal in energy, now come to differ in energy by about 3.5 ev.

For r near r_e of N, the use of true molecular orbitals here obviously corresponds to a better approximation than the use of united-atom orbitals. It appears reasonable also, in view of the energy relations for the Q, T and V states, to believe that molecular orbitals give a better approximation here than separate-atom atomic orbitals. At larger r values, however, the value of molecular orbital approximations gradually, so to speak, dissolves, and atomic orbital configurations $5p_I^5\cdot 1s_H$ and $5p_I^6$ become appropriate. For moderately large r values short of $r=\infty$, the $5p_I$ orbital type is subdivided into $5p\sigma_I$ and $5p\pi_I$. It is interesting to note how the states Q and T, which both belong to $5p^56s$ of Xe at $r=0$ but spread apart in energy at moderate r values, come together again at $r=\infty$, where they have in common the electron configuration $5p_I^5\cdot 1s_H$.

Let us turn now to the finer details of the states corresponding to $5p_{Xe}^56s_{Xe}$ for $r=0$, to Q for $r>0$, and to $5p_I^5$ for $r=\infty$. For $r=0$ we have Jj coupling between $5p^5$ and $6s$, giving four states with $J=2$, 1, 0 and 1, respectively (corresponding to $^3P_{2,\,1,\,0}$ and ^1P of ordinary L, S coupling). For $r>0$ we at first come upon the "close-nuclei" form[8] of case c coupling (quantum numbers J and Ω). At r values large enough so that molecularization is able to break down this coupling, we have Ω-s coupling, in which we have state Q with five sublevels. Ω-s coupling may be expected to continue until, at relatively large r values, the separate-atom or "far-nuclei" type of case c coupling sets in (cf. Section 3).

The proper correlations of all the various substates at all stages can be worked out,[8] and are indicated in Fig. 1, except for $Q\ ^3\Pi_2$ and $Q\ ^3\Pi_{0^-}$. The latter both come from the level with $J=2$ at $r=0$, and go on dissociation into $H+I(^2P_{3/2})$.

The foregoing discussion is applicable also, after making obvious changes, to the other molecules HX. These should differ only quantitatively from HI, the main changes being in the relative polarity and ionicness, and in the positions, of the several states. Roughly estimated $U(r)$ curves for states N and V of all the molecules HX have been given by Pauling.[7] According to the latter's work, the N and V states become about equally polar and ionic in HF, while in all the other HX, N is predominantly atomic and V predominantly ionic. However, V should probably always be less polar than N according to the theorem of I, Section 6.

In the series HI, HBr, HCl?, HF, the absorption wave-lengths corresponding to $Q\leftarrow N$ steadily decrease. In view of the pronounced tendency toward united-atom conditions shown in HI, the increase in the interval between N and Q in going from HI to HF can be understood in terms of the increase in the corresponding interval np^6 to np^5 $(n+1)s$ in the respective united atoms. It may be pointed out here also that the transitions $Q\leftarrow N$ in HX are much farther in the ultraviolet than the corresponding transitions in X_2, where the states Q are so low as in part to have minima in their $U(r)$ curves. This difference, and also the probable greater intensity of $Q\ ^3\Pi_1\leftarrow N$ and $Q\ ^1\Pi\leftarrow N$ and lesser intensity of $Q_0\leftarrow N$ in HX (in other words, the lesser applicability of postulates 2 and 3 of Section 4 to HX than to X_2 and XY) may well be connected with the closer approach to united-atom conditions in HX than in X_2.

As for states T and V, although we have no direct experimental data, the results on HCl^+ and HBr^+ noted above in connection with the discussion of the construction of Fig. 1 indicate that the heights of T and V above Q do not change much from HI to HBr to HCl, at least for r near r_e of state N. In view of the spectroscopic evidence mentioned above showing the increasing height of level Q above N as we go from HI to HF, we may then conclude, for r near r_e of N, that T and V also rise increasingly

high above N in going from HI to HBr to HCl and, probably, to HF. According to date of Goodeve and Taylor on HI and HBr, even the height *above* $H+X(^2P_{1\frac{1}{2}})$ of level Q increases somewhat from HI to HBr, in spite of the increasing depth of the minimum of N below $H+X(^2P_{1\frac{1}{2}})$. If all this is correct, levels T and V, for $r=r_e$ of N, go increasingly high above the energy of $H+X(^2P_{1\frac{1}{2}})$ as we go from HI to HF. In the case of T, this conclusion is in complete agreement with what the Heitler-London theory would predict.

In the case of V, it is contrary to the behavior of the curves shown by Pauling, according to whom state V (both for its own r_e and for r_e of state N) should go progressively lower, relatively to the energy of $H+X(^2P_{1\frac{1}{2}})$, as one goes from HI to HF. Thus, although for HI, Pauling's V curve agrees closely with that shown here in Fig. 1, his V curve for HF is very much lower than would be obtained if the analogue of Fig. 1 for HF were constructed according to the methods here used. Experimentally, it is certain that the V curve of HF is at least 2 ev higher than Pauling's curve, since HF gas is transparent down to at least λ1950,[11] whereas according to Pauling's V and N curves, $V\leftarrow N$ absorption would be expected to begin near λ2750. According to estimates by the procedure here used, $V\leftarrow N$ absorption might be expected to lie in the neighborhood of roughly λ700 or λ800, i.e., near the first absorption lines of the neon atom (cf. HI, where $V\leftarrow N$ according to Fig. 1 should occur at wave-lengths approximately the same as for the transitions $5p^6 6s \leftarrow 5p^6$ in xenon).

The very high energy above N predicted for V according to the present procedure is based on the assumption that the structure of HF can be well approximated (for r near r_e of N) using united-atom or, better, molecular orbitals. As we have seen, the observed heights of the levels Q in HI and HBr, supported by the trend of the (incomplete) evidence for HCl and HF, tend to bear out this assumption. If the assumption is correct, level V should be above T, and both should be considerably above Q (just how much, in HF, could be better estimated if the HF^+ spectrum were known). A slightly different possibility is that the position of T may be about as just indicated, but that V may be lower due to its ionic character. This would be possible if the influence of the separated-atom atomic orbital approximation (H^+F^-) is still sufficiently pronounced, near $r=r_e$ of state N, to take precedence over the molecular or united-atom orbital approximation. In this connection, comparison may be made with a similar situation in LiH, where it is likely (cf. II, p. 1038, last complete paragraph) that the energy of state V, near $r=r_e$ of N, is near or perhaps even slightly lower than that of T, whereas for the corresponding united-atom (Be), V must be about 2.5 ev above T. Evidently, therefore, it is not impossible for V, due to its ionic tendencies, to come lower than one would expect using molecular orbitals, and even perhaps to come below T for a moderate range of r values (in this connection, cf. also the V state of AgI as shown in Fig. 2). Still, in view of the evidence for the goodness (better than in LiH) of the molecular orbital approximation in HX (of which HF should be the best case), it seems improbable that state V can lie, at worst, *much* below T in HF. Hence it appears probable that V actually lies very high in energy in HF, contrary to Pauling's curves.

6. The Molecules AgX; also CuX, AuX

The observed spectrum of each of the molecules AgCl, AgBr and AgI consists of a single band system, found both in absorption and emission (0,0 band at 3.90, 3.88, 3.84 ev, respectively), together with some continuous absorption mostly in the same spectral region.[5, 6] The bands appear to be single-headed, which would be in harmony with a $^1\Sigma^+ \leftrightarrow {}^1\Sigma^+$ type of transition. According to a private communication from Professor W. G. Brown, AgF also has a similar system of absorption bands at about λ2800, i.e., about 4.4 ev, followed by a gap and a continuum; the observed bands appear to form a sequence.

Let us call the upper electronic level of the observed bands B, the bands then being $B\leftrightarrow N$. The data on state B show a rapidly converging set of vibrational levels for each AgX, so that the energy of dissociation D can apparently be reliably estimated. The resulting D values according to Brice[6] are 0.31, 0.21, and 0.10 ev for AgCl, AgBr and AgI, respectively.

At the dissociation point of B, the total energy is found, using chemical D values (3.1, 2.6, 2.04 ev) for state N, to exceed the energy of unexcited Ag+X by the amounts $E=1.1$, 1.5 and 1.9 ev for AgCl, AgBr and AgI, respectively. If we assume that the X atom is in the $^2P_{1/2}$ instead of the $^2P_{3/2}$ state on dissociation, E is reduced by 0.11, 0.45, 0.94 ev for Cl, Br, I, respectively, becoming about 1 ev for all three AgX. The assumption of an error of 1 ev in the chemical D values would dispose of this, but that would make the chemical D values unreasonably large; besides, Terenin's work[6, 13b] on AgI gives strong support to the accepted chemical D value there. On the other hand, the quantities E are certainly too small to be explained by assuming dissociation from state B to give any higher excited state of X or of Ag. For the lowest known excited state of Ag is the $d^{10}5p$ at 3.65 ev, while the as yet unknown d^95s^2, ^2D cannot be much lower than this, and is probably higher;[14] and the lowest state of I above the p^5, ^2P is p^46s, $^4P_{2\frac{1}{2}}$ at 6.74 ev.

One is driven to conclude, in disagreement with Brice's supposition of dissociation into $Ag(d^9s^2)$ plus $X(p^5)$, that the $U(r)$ curve of the B state must rise slightly with increasing r from its minimum to a maximum, then must drop again strongly to dissociate into $Ag(d^{10}s)$ $+X(p^5, {}^2P_{3/2}$ or $^2P_{1/2})$: cf. Fig. 2, where dissociation giving $^2P_{1/2}$ of X is assumed (for the reasons, see below). Although this type of behavior is unfamiliar in diatomic molecules, it is theoretically perfectly possible, and examples of more or less similar cases have already been found experimentally by Brown in ICl and IBr,[15] and by Hulthén and Rydberg in AlH.[16] It will now be shown that such behavior is not unreasonable in AgX if we identify state B as a resultant of the mutual interaction of three zero-approximation states of which two are the predicted states Q_0 and V.

The near ultraviolet spectra of AgX, like those of HX, might be expected to involve transitions $Q \leftarrow N$. In addition $V \leftarrow N$ might be expected as in MH. In HX, as we have seen, level V must be high up, because of the high energy of $H^+ + X^-$ above H+X, so that $V \leftarrow N$ should be below λ2000. With AgX, however, $Ag^+ + X^-$ is so low (cf. Table III of I) that V should come lower than in HX, although the larger size of Ag^+ as compared with H^+ acts as a restraining influence. If one estimates the course of the pure Ag^+X^- hypothetical $U(r)$ curve using Eq. (5) of I, taking A from Table III of I and β and n from crystal structure data, one finds that its calculated minimum comes below the energy of Ag+X. [The course of the pure Ag^+I^- curve for the case $\beta=0$ (pure Coulomb attraction) is shown by the dotted curve in Fig. 2.]

The situation may then be compared with that in MH (cf. II). In LiH, using Eq. (5) with crystal-structure values of β and n, the calculated minimum of the pure Li^+H^- curve came about 3.2 ev below the energy of Li+H; our analysis of the actual N and V states of LiH showed, however, that the minimum of the pure Li^+H^- curve must really be much less low, most likely only about 1.2 ev below the energy of Li+H. This error of about two ev in the minimum of the Li^+H^- curve calculated using crystal-structure data to get β and n is presumably related to the high polarizability of the H^- ion. In the case of the alkali halides MX, similar calculations of the energy of dissociation of the normal MX molecule, assuming it to be M^+X^-, agree rather closely with the experimental values. In the molecules AgX, it seems likely that we have cases somewhat intermediate between MH and MX in regard to the use of Eq. (5) with β and n from crystal structure data. Thus the calculated minima of the pure Ag^+X^- curves as here calculated may reasonably be expected to be perhaps 1 ev too low, so that these minima would very likely lie actually somewhat above the energy of Ag+X. Thus the pure Ag^+X^- curve would probably lie well above the pure $Ag \cdot X$, $^1\Sigma^+$ curve, and the molecules AgX be less polar than MH.

Nevertheless it is reasonable to suppose that the hypothetical pure Ag^+X^- and $Ag \cdot X$ curves

[13b] Terenin's work gives a threshold value for the production of Ag (^2P) from AgI by photodissociation. This corresponds to an upper limit of 2.17 ev for D of AgI.

[14] Cf. H. A. Blair, Phys. Rev. **36**, 1531 (1930); also A. G. Shenstone, Phys. Rev. **31**, 317 (1928).

[15] W. G. Brown, Phys. Rev. **40**, 529 (1932); **42**, 355 (1932). Cf. also the $U(r)$ curve calculated for He_2^{++} by L. Pauling (cf. Pauling and Wilson, *Introduction to Quantum Mechanics* (McGraw-Hill Co., 1935)); this He_2^{++} molecule is, however, of a type not likely to be met in band spectra.

[16] E. Hulthén and R. Rydberg, Nature **131**, 470 (1933).

come close enough together to interact strongly, as in MH, to give two new curves, the lower being that of the N state, the upper that of the V state. The N state would then be partially polar, for moderate r values, but less so than in MH. Qualitatively, the observed chemical D values for the N states of AgX are considerably larger than would be predicted from the additivity rule for homopolar bond energies (cf. II), using a reasonable estimate for D for Ag_2; and, following Pauling, we may take this difference as evidence that the bond in AgX is not nearly pure homopolar, but that strong interaction of the hypothetical pure homopolar Ag·X with the hypothetical pure ionic Ag^+X^- curve has occurred. [To be sure, the homopolar additivity rule fails in MH (cf. II) and apparently in MX, but the failure is in that the homopolar D values, i.e., the predicted values for the homopolar M·H or M·X curves, are too *small*, not too large. A similar failure here would only *strengthen* the indicated intensity in AgX of interaction between the pure Ag^+X^- and Ag·X curves.]

The interaction between the pure Ag^+X^- and Ag·X curves to give the actual N and V curves should, according to the foregoing, push up the V curve, especially at the smaller r values, very considerably above the position of the pure Ag^+X^- curve. One might then be inclined to identify the observed B state with the V state. This, however, is hardly possible in view of the form of the V, i.e., the Ag^+X^-, curve at large r values. Even at $r=4.5$A in AgI (cf. Fig. 2), where the Ag^+I^- curve can hardly depart much from a pure Coulomb attraction curve, its energy has already descended well below that of the minimum of the B state. At smaller (but probably still rather large) r values, its energy must reach a minimum, and then probably should rise rather steeply due to the combined effects of the β/r^n term in Eq. (5) and the interaction with Ag·I. No reason is apparent, in the discussion thus far, why the Ag^+I^- V curve should descend again to a second minimum at small r, as would be necessary if it were to be identified with the B state.

We have, however, not yet taken into account the predicted states Q. According to the method of molecular orbitals (cf. I, Table I and elsewhere), states N, Q, T, V have the electron configurations

$$\begin{aligned} N&: \cdots\sigma^2\pi^4,\ {}^1\Sigma^+;\ Q,\ \cdots\sigma^2\pi^3\sigma^*,\ {}^3,{}^1\Pi; \\ T,\ V&: \cdots\sigma\pi^4\sigma^*,\ {}^3,{}^1\Sigma^+. \end{aligned} \tag{3}$$

Furthermore it is expected that, as in other known cases (e.g. HX, X_2, XY), the order of binding is σ, π, σ^* so that N should be lowest, Q next, T and V highest. In other words, Q would be expected to lie below V and T, for r values comparable with r_e of state N.

We may then ask whether perhaps state B is Q_0, state V then being higher in energy and as yet experimentally unknown. If so, the occurrence of the elevated minimum in the B curve might perhaps be accounted for by a strong interaction of the V curve on the Q_0 curve. In investigating this idea, let us first consider how Q_0 and V should behave at large r values. As in other analogous cases (cf., e.g., HI) the Q_0 curve should tend on dissociation to give unexcited Ag plus $I(p^5, {}^2P_{1/2})$. Now it is important to note that if the Ag^+I^- V curve follows the Coulomb law fairly closely down to 4.3A, as we should expect, it should tend to cross the Q_0 curve at about this r value. If such crossing takes place, the V curve should descend to a minimum somewhat below the Q_0 curve, then should rise steeply as already suggested in a preceding paragraph, recrossing the Q_0 curve at smaller r values, in order that V may be above Q_0 at r values near r_e of N as demanded by our previous discussion of Eq. (3). Actually, it appears probable that both these crossings are avoided, so that two new curves result which do not cross. The full line curves in Fig. 2 are drawn in accordance with this idea. Of the two new curves resulting from the interaction of the original Q_0 and V curves, the lower one should have the characteristics[16a] of Q_0 for r values greater than about 4.3A, of V for a range of smaller r values, and finally of Q_0 again for still smaller r values. The upper of the two curves will be nearly pure V Ag^+I^- for $r>4.3$A, nearly Q_0 for $r<4.3$A for a while, and nearly pure V again for small r values.

Because of their complicated origin as resultants of two zero-approximation curves which cross and recross, both the actual curves should

[16a] Really, for such large r values, we shall have not Q_0 but a case c 0^+ state corresponding to a mixture of Q_0 and N.

be somewhat irregular in form. The lower of the two curves might perhaps have a broad shallow minimum at large r values, but no reason is evident why it should have a second shallow minimum at small r values so as to permit it to be identified with the observed B curve. Such a second shallow minimum could occur only if the interaction between the zero-approximation V and Q_0 curves increased steadily and rather rapidly in intensity at moderate to small r values, but there appears to be no theoretical reason to expect such a behavior.

We are thus driven to examine the possibility that the B minimum belongs to a state which is primarily neither V nor Q_0. It appears at once that this possibility is very reasonable. Consider the states of AgI which should be derived from

$$\text{Ag}: \cdots 4d\sigma 4d\pi^4 4d\delta^4 5s^2 \text{ plus I } \cdots 5p\sigma 5p\pi^4.$$

There should be a $^1\Sigma^+$ and a $^3\Sigma^+$ state, analogous to the N and T states. The $^1\Sigma^+$ state should show much stronger homopolar binding than would the Ag·I $^1\Sigma^+$ derived from unexcited Ag($\cdots 4d^{10}5s$) plus I, since the $4d\sigma$ of Ag is more suitable in form and energy than the $5s$ of Ag to give strong binding with $5p\sigma$ of iodine. A reasonable estimate of the binding energy would be about 2 ev. The actual binding energy, however, would be expected more or less to exceed this, because of polarity (influence of Ag^+I^- states) and probably also because of effects of interaction with a rather weakly bound $^1\Sigma^+$ state derived from Ag($d^{10}p$) plus I (see next paragraph).

The exact position of the d^9s^2 state above the $d^{10}s$ normal state of Ag is not known, but it is probably not far above the lowest known excited state $d^{10}p$ at 3.65 ev. An estimate of about 4 ev for the energy of excitation of the d^9s^2 state appears not unreasonable. [There should, of course, be a $^1\Sigma^+$ state derived from Ag($d^{10}p$)+I, but this should have a much smaller dissociation energy than that from Ag(d^9s^2) plus I, because of much less favorable energy and form of $5p\sigma$ than of $4d\sigma$ of Ag for interaction with $5p\sigma$ of I. Hence, even though for $r=\infty$ this $^1\Sigma^+$ state derived from Ag($d^{10}p$) may be somewhat lower in energy than that from Ag(d^9s^2), for smaller r values the latter should most probably be decidedly the lower.]

Now it is a rather remarkable fact that in *all* the molecules AgX (cf. first paragraph of this section), the minimum of the B state is just about 4 ev above that of the N state. This would be explained if in each case the B state is essentially the $^1\Sigma^+$ state derived from d^9s^2 of Ag plus p^5 of X, and if also the energy of dissociation D of the B state into d^9s^2 of Ag plus p^5, $^2P_{1\frac{1}{2}}$ of I is approximately equal in each AgX to the D of the N state into unexcited Ag+X. The second condition appears entirely reasonable, as will now be shown. The D of state N is, as we have seen, surely considerably in excess of the homopolar D of normal Ag·X, due to strong polarity in the molecule. The homopolar D of the Ag·X state derived from Ag(d^9s^2) should be very considerably larger than the homopolar D of normal Ag·X. Considering, however, the effects of polarity and possible other influences in the two cases, it is more than merely plausible that the *actual* D of state N into unexcited Ag+X may be nearly equal, for all X, to that of state B into Ag(d^9s^2) plus X. Thus the supposition that state B, for r values near its minimum, is essentially the $^1\Sigma^+$ state derived from Ag(d^9s^2) plus I appears to be strongly indicated.

It remains now to explain why the potential energy curve of state B does not keep on rising until dissociation takes place into Ag(d^9s^2, $^2D_{2\frac{1}{2}}$) plus I(p^5, $^2P_{1\frac{1}{2}}$), but instead rises to a maximum and then descends to give unexcited Ag. The explanation is at hand if we observe that a B state curve going up to Ag(d^9s^2)+I would necessarily cross, at relatively small r values, the Q_0 and V curves discussed in preceding paragraphs. It is entirely reasonable to suppose that fairly strong interaction would take place near each of the attempted crossing points, so that the three curves would be replaced by three new curves somewhat like the three curves shown in Fig. 2. The lowest of the three would then correspond to the observed B curve, with its minimum and maximum. According to Fig. 2, this curve might have a second minimum at large r values; this, however, would not readily be detected in the spectrum. The wave function of this curve would have nearly B character for small r values, would acquire a strong flavor of Q_0 with some of V near its maximum, would take on mostly V character at larger r values, and finally would have case c 0^+ character (mixed Q_0 and N) at large r values.

An explanation which involves such a state of affairs may seem unduly complicated to readers who believe in using simple theories as far as possible. In the writer's opinion, however, the complexity is unavoidably inherent in the nature of the case in hand, so that probably every attempt at simplification would merely destroy all hope of real explanation.

The second lowest curve resulting from the interaction of the zero-approximation V, Q_0, and B curves is very likely a curve without a minimum, as shown in Fig. 2. Further investigation of the AgX spectra may throw further light on the actual forms of the curves which are shown, needless to say very tentatively, in Fig. 2. Data on the intensities of the transition $B \leftarrow N$ in the several AgX might also be useful in testing the present explanation of the B level.

It will be noted that, in our attempt to find analogous low energy levels and spectra in H_2, MH, HX, AgX and MX, we have been forced in the case of AgX to conclude that the lowest known excited electronic level and the known spectrum of AgX are *not* analogous to those of the other molecules. This lack of analogy we have traced to the d electrons in the outer part of the Ag atom, not present in the other cases. In the spectra of CuX and AuX, the effects of the d electrons should be much more conspicuous, since in Cu and Au, the d^9s^2 configuration is only about 1 ev above the normal $d^{10}s$ configuration, as compared with about 4 ev in Ag. This expectation is in accord with the observed spectra, which are quite different from those of AgX. In CuX, numerous band systems and low excited electronic levels (some showing evidence of predissociation) are known. In AuX, two low excited levels are known. An attempt to explain these various low levels in CuX and AuX would be of considerable interest. The present work on AgX should be helpful in preparing the way for this.

Returning to AgX, we have now to explain how it can be that, apparently, no transitions $Q \leftarrow N$ and $V \leftarrow N$ have been observed. Our analysis has shown rather definitely that the B state of AgX (for $r = r_e$ of state N) cannot be either Q_0 or V but must be *below* both of these (cf. Fig. 2). If this is correct, $V \leftarrow N$ and $Q_0 \leftarrow N$ should both be farther in the ultraviolet than $B \leftarrow N$, in a region not yet investigated; further, $Q_0 \leftarrow N$ should probably be represented only by a continuous absorption. Here it is important to note that the absorption work hitherto done on AgX extends only to about λ2500, not far beyond the region of the observed $B \leftarrow N$ bands. Extension of the spectrum toward shorter wavelengths should be important in working out the questions raised here.

Finally, we have to consider $Q\ ^3\Pi_1 \leftarrow N$ and $Q\ ^1\Pi \leftarrow N$. Assuming that the coupling (for r near r_e of state N) is approximately of Ω-s type for the Q states of AgX, the $Q\ ^1\Pi$ level should be close to the Q_0, and the $Q\ ^3\Pi_1$ somewhat lower (e.g., about 0.6 ev lower than the $^1\Pi$ in AgI). The $^1\Pi$ and $^3\Pi_1$ curves for AgI have been drawn in accordance with these specifications in Fig. 2. If Fig. 2 is essentially correct, the transitions $Q\ ^1\Pi \leftarrow N$ and $Q\ ^3\Pi_1 \leftarrow N$, like $Q_0 \leftarrow N$, and like the corresponding transitions in HX and MX (cf. Figs. 1, 3), should be represented only by continuous spectra.

Presumably the observed continua associated with the transitions $B \leftarrow N$ may, at least to some small extent, be attributable to $Q\ ^3\Pi_1 \leftarrow N$. The transition $Q\ ^1\Pi \leftarrow N$, along with $Q_0 \leftarrow N$, should lie considerably farther in the ultraviolet in the case of AgI, and both may so far have escaped detection for this reason (see above). In the case of AgCl, $Q\ ^3\Pi_1 \leftarrow N$ should be close to $Q\ ^1\Pi \leftarrow N$ and $Q_0 \leftarrow N$, but all should be considerably farther in the ultraviolet than $B \leftarrow N$ according to our theory. Further, $Q\ ^3\Pi_1 \leftarrow N$ and $Q\ ^1\Pi \leftarrow N$, and perhaps even $Q_0 \leftarrow N$, may be weak in all AgX (cf. postulate (2) of Section 4). Comparing different AgX, $Q_0 \leftarrow N$ would probably be strongest in AgI.

The continuous absorption which overlies the bands $B \leftarrow N$, extending also toward longer wavelengths, can be adequately accounted for by transitions to curve B on its small r side higher than its maximum, and on its large r side below and outside the maximum. The continuous absorption is most easily obtained in AgI, as one would expect since the height of the maximum of the B state is lowest there. Continuous absorption is obtained in AgCl only by strong heating.[6] This can be accounted for by the Franck-Condon principle. In AgCl it is found that the 0,0 band of $B \leftarrow N$ is the strongest,[6] indicating that r_e is not much different for B than

for N. Thus, in the case of initially nonvibrating molecules, strong absorption transitions occur only to the stable region of the B curve near its minimum. On raising the temperature, the number of N molecules with strong vibrations increases, permitting transitions to other parts of the B curve, in particular to the parts outside its maximum.

In the case of AgI the strongest $B \leftarrow N$ band is no longer the (0,0), indicating that the difference between r_e of B and N is greater than for AgCl. The difference in ω_e values is also greater, as would be expected. In AgI, the maximum of the continuum[6] comes at a wave-length corresponding to 3.89 ev above $v=0$ of N, whereas the minimum of the B curve comes at 3.84 ev, its maximum at 3.94 ev. The agreement with our explanation is a reasonable one. Thus, empirically, it appears that the $^3\Pi_1 \leftarrow N$ continuum may indeed be very weak, as already suggested, since the observed continuum can be explained without assuming this transition at all.

Besides the main continuum in AgI, a much fainter one at longer wave-lengths and obtained only at very high temperatures, has been reported by Kuhn,[6] with a maximum corresponding to 3.08 ev. In view, however, of the high temperature used and the weakness of this continuum, it is probably safer to disregard it than to attempt to explain it, but with the recognition that it constitutes an unsolved problem.

In connection with the present explanation of the AgI spectrum in terms of Fig. 2, a further difficulty should be pointed out. According to Fig. 2, the $^3\Pi_1$ and $^1\Pi$ curves intersect the B curve near its minimum in such a way that one would expect predissociation to occur in the B state. While the existence of predissociation in AgI can hardly be either denied or affirmed on the basis of our present knowledge of the absorption spectrum, it must be admitted that the occurrence of the $B \rightarrow N$ bands of AgI in *emission* is rather strong evidence against the occurrence of predissociation. On the basis of this conclusion it seems probable that the $^3\Pi_1$ and $^1\Pi$ curves do not cross the B curve in the manner shown in Fig. 1. Raising the whole system of Q, T, and V curves, for r near r_e of N, would dispose of the predissociation difficulty and would be entirely consistent with the observed spectrum. The amounts by which the curves would have to be raised in order to avoid crossing of B near its minimum by $^3\Pi_1$ or $^1\Pi$ would, however, be rather considerable (see Fig. 2), and it is rather difficult to believe that these curves could be so high. On the other hand (considering also, especially, the evidence from AgBr and AgCl), the absence of pronounced absorption at longer wave-lengths than $B \leftarrow N$ makes it hardly tenable that the Q curves lie *below* the B curve. In the cases of AgBr and AgCl, the predissociation difficulty should be less troublesome than in AgI, since the several curves should be closer together. In any case, it is obvious that the present Fig. 2 does not represent a final complete solution of the problem of the low AgX energy levels and spectra; but it seems reasonable to believe that it represents progress in the right direction.

In concluding this section, the r_e and ω_e data on the B states of AgX deserve discussion. No direct experimental data on r_e are available, to be sure, but from the application of the Franck-Condon principle to the observed vibrational intensities (see above), it can be concluded that for AgCl, r_e is nearly the same for state B as for state N, while in AgI, r_e is somewhat, but not very much, greater for B than for N. On the other hand, ω_e is considerably less for state B than for state N, and the relative difference increases markedly from AgCl ($\omega_e = 343$ for N, 281 for B) to AgI ($\omega_e = 206$ for N, 131 for B). It is likely that in all AgX, but especially AgI, the ω_e's of state B are smaller than the usual rule, $r_e^2\omega_e$ or $r_e^3\omega_e$ = constant for different states of a molecule, would predict.

It is of interest that a similar situation appears to exist in the $B\,^1\Pi$ state of AlH where, although r_e is the same as for state N, ω_e is apparently relatively much smaller.[16] Less extreme examples are found in the normal states of HgH and analogous molecules; here, as in AlH, the phenomenon of abnormally small ω_e for given r_e is connected with, and probably a result of, an unusually small dissociation energy. The AgX case is similar, except for the large drop in energy with increasing r after the maximum of the potential energy curve is passed. In each case, the small r_e corresponds to the normal behavior of a stable molecular state with large dissociation energy, but the relatively small ω_e and the small

actual dissociation energy, or the occurrence of a maximum in the curve, correspond to a rapid change in the character of the wave function with increasing r. Such behavior may be explained as a result of the strong interaction of two (or more) zero-approximation curves.[16b] In the case of AgX, the observed behavior is in good agreement with our explanation of the B state. In particular, the small r_e agrees with our supposition that the wave function near r_e is approximately that of a stable AgX with d-valent silver.

7. Molecules MX

Both emission and absorption spectra of MX are known.[3, 17] Most characteristic is the continuous ultraviolet absorption, which begins with two rather narrow regions of absorption, the first corresponding to dissociation into $M+X(^2P_{3/2})$, the second into $M+X(^2P_{1/2})$. The interval between the two maxima agrees approximately with the interval $^2P_{1/2}-^2P_{3/2}$ of X. Thus in the iodides the interval is reported as 0.98 ev in NaI, RbI and CsI, as compared with 0.94 ev for the I atom. In the bromides, intervals of about 0.4 ev are reported, as compared with 0.46 ev for the Br atom. Recently Levi[17] has reported an interval of 0.11 ev for NaCl and KCl, as compared with 0.11 ev for the Cl atom. Very little has been done with the fluorides.

This and further evidence indicate[3, 17] that the $U(r)$ curves of the upper levels involved in the continuous absorption all run in nearly horizontally[18] from $r=\infty$. The curves have only slight minima at large r, then begin to rise slowly. The energy of repulsion at $r=r_e$ of N varies only slightly in the several MX molecules for which data exist, from about 0.5 ev (RbI, CsI, KI) to about 0.8 ev (NaCl). [The determination of these repulsion energies is based on the positions of the absorption spectrum maxima combined with the dissociation energy D of the state N. The latter is rather accurately known in most cases from chemical data, supplemented in some cases by reliable determinations based on the ultraviolet spectra themselves, or on fluorescence, or both.[19]]

Besides the two continuum maxima just noted, further maxima are found farther in the ultraviolet. They are explainable by assuming a $U(r)$ curve for each excited state of M+X [e.g., $M(ns, {}^2S)$ or $M(np, {}^2P)$ or $M((n+1)p, {}^2P)$ or $M((n-1)d, {}^2D)$, plus $X(^2P_{3/2})$ or $X(^2P_{1/2})$], *all these $U(r)$ curves running nearly parallel.*[17] That is, the continua maxima are spaced very nearly the same as the known levels of M+X at $r=\infty$; this has been studied most thoroughly for CsI.[17]

In the electrically excited emission spectra of MX, also in chemiluminescence, a pseudo-band structure is found which is explainable by transitions from the large r regions of the upper $U(r)$ curves to the outer limb of the $U(r)$ curve of state N. Similar pseudo-bands are also found in absorption when the temperature is raised so that many molecules are in high quantum vibrational levels of state N. Analysis of such data (see Sommermeyer, and for the most complete results, especially Levi, Dissertation[17]) indicate that the $U(r)$ curves connected with $M+X(^2P_{3/2})$ and $M+X(^2P_{1/2})$ have very shallow minima at large r. Levi further concludes that the pseudo-bands for $M+X(^2P_{3/2})$,—or in one or two cases perhaps for $M+X(^2P_{1/2})$,—involve *two* shallow minima at different r values, hence at least two $U(r)$ curves from which strong transitions to state N occur. The observed continuum maximum for $M+X(^2P_{3/2})$,—or $M+X(^2P_{1/2})$,—is further identified by Levi as associated with one of the two $U(r)$ curves indicated by the pseudo-bands. Thus there appears to be spectroscopic evidence for at least three $U(r)$ curves derived from $M+X(^2P_{3/2})$ plus $M+X(^2P_{1/2})$. Theoretically (cf. Section 3) there should be five curves from $M+X(^2P_{3/2})$ and three from $M+X(^2P_{1/2})$, but spectroscopic transitions to two of the former and to one of the latter are forbidden; as for transitions to the

[16b] For further discussion of this problem, cf. R. S. Mulliken, J. Phys. Chem., January (1937); from Princeton Symposium on Molecular Structure.

[17] E. v. Angerer and L. A. Müller, Physik Zeits. **26**, 643 (1925); L. A. Müller, Ann. d. Physik **82**, 39 (1927); A. Terenin, Zeits. f. Physik **37**, 98 (1926); V. Kondratjew, Zeits. f. Physik **39**, 191 (1926); A. Butkow and A. Terenin, Zeits. f. Physik **49**, 865 (1928); A. Visser, Physica **9**, 115 (1929); K. Sommermeyer, Zeits. f. Physik **56**, 548 (1929); H. Kuhn, Zeits. f. Physik **63**, 458 (1930); H. D. Schmitt-Ott, Zeits. f. Physik **69**, 724 (1931). H. Beutler and H. Levi, Zeits. f. Elektrochem. **38**, 589 (1932); H. Levi, *Dissertation* (Berlin, 1934). For a good review of most of this work, cf. W. Finkelnburg, Physik. Zeits. **34**, 539–541 (1933).

[18] P. K. Sen-Gupta, Zeits. f. Physik **88**, 647 (1934), discussing HX, MX, etc., points out relations between breadths and separations of the maxima, and steepness of $U(r)$ curves: e.g. in MBr, the $U(r)$ curve from $M+Br(^2P_{3/2})$ is apparently a little steeper than that from $M+Br(^2P_{1/2})$.

[19] H. Beutler and H. Levi, Zeits. f. physik. Chemie **B24**, 263 (1934).

rest of the curves, it is possible that some might be relatively weak.

The natural and probably correct conclusion which has been drawn from all this information is that two atoms M+X, in normal or in low excited states, come together without appreciable valence forces, so that the course of the $U(r)$ curves is governed by small van der Waals forces at large r and by the usual closed shell and Coulomb repulsive forces at small r; in short, that the excited MX molecules involved in the ultraviolet spectra behave like mere pairs of atoms. Or in other words, the coupling apparently approaches the ideal case c separate-atom type (cf. Section 3).

Considering now just the two maxima of continuous absorption corresponding to $M+X(^2P_{3/2,\ 1/2})$, we may ask what relation they have to the expected states Q, T and V and to the expected transitions $Q(^3\Pi_1, {}^1\Pi)\leftarrow N$, $Q_0(^3\Pi_{0^+})\leftarrow N$, and $V(^1\Sigma^+)\leftarrow N$. In the first place, we notice that state N no longer has a $U(r)$ curve running down from two unexcited atoms $A+X(^2P_{3/2})$ as in other molecules AX, but now comes from $M^+ + X^-$. This change permits state V now to be correlated with $A+X(^2P)$ instead of with $A^+ + X^-$ as in our previous cases. In short, N and V have exchanged behavior as regards dissociation.

As we have seen in Section 3, the states Q, T and V are replaced for case c coupling by a corresponding set of states $\Omega=2,\ 1,\ 0^-,\ 0^+,\ 1$ derived from $M+X(^2P_{3/2})$ and forming a narrow bundle, together with a second narrow bundle of states $\Omega=0^+,\ 0^-,\ 1$ from $M+X(^2P_{1/2})$. The wave functions of the three states $\Omega=1$ should be mixtures of those of the Q states $^3\Pi_1$ and $^1\Pi$ and of the $\Omega=1$ component of T, $^3\Sigma^+$; those of the two 0^- states should be nearly 50, 50 mixtures of those of $Q\,{}^3\Pi_{0^-}$ and $T(^3\Sigma^+)_{0^-}$; those of the two 0^+ states should be nearly 50, 50 mixtures of those of $V\,{}^1\Sigma^+$ and $Q\,{}^3\Pi_{0^+}$. The selection rules allow transitions from $N\,{}^1\Sigma^+$ to the three $\Omega=1$ and to the two $\Omega=0^+$ levels. Since the three $\Omega=1$ wave functions all contain a $^1\Pi$ component, one expects transitions to all three to occur with comparable intensity, the sum of all these corresponding to the intensity one would have for $Q\,{}^1\Pi\leftarrow N\,{}^1\Sigma^+$ if one had had ordinary case a or b coupling. Similarly, transitions to the two 0^+ levels should be of roughly equal intensity, dividing between them the intensity which $V\,{}^1\Sigma^+\leftarrow N\,{}^1\Sigma^+$ would have had in case b, since each 0^+ level contains a $V\,{}^1\Sigma^+$ component. What the intensities of the transitions to the $\Omega=1$ states would be as compared with those to the 0^+ states is less clear.

If we adapt the postulates at the end of Section 4 to the situation, we conclude that strong transitions definitely should occur to the two 0^+ levels, the one derived from $X(^2P_{3/2})$, the other from $X(^2P_{1/2})$. This is in rough agreement with what is observed, if we ascribe the two continua essentially to $0^+\leftarrow N$ transitions. In addition, there should be transitions to the three $\Omega=1$ levels. If these should be weak, their superposition on two strong $0^+\leftarrow N$ continua would scarcely be noticed. Even if they are fairly strong, they need not much affect the appearance of the continuous spectrum, provided the several Ω levels derived from $M+X(^2P_{3/2})$ lie close together, and those from $M+X(^2P_{1/2})$ again close together. The evidence from Levi's analysis of the pseudo-bands indicates that transitions of appreciable intensity occur to at least two $U(r)$ curves derived from $M+X(^2P_{3/2})$. Assuming that one of these is to the 0^+ state, the others (theoretically there must be *two* others, though only one was definitely detected by Levi's analysis) must be to $\Omega=1$ states. Thus it seems likely that transitions to 0^+ and 1 states may be of comparable intensity. Theoretically, from a consideration of the probable forms of the wave functions, it appears likely that transitions to the 0^+ states should be the stronger.

We may next inquire whether, and if so how, the case c character of the excited electronic states of MX can be understood in terms of electron configuration theory. Especially, one wonders why case c states should occur replacing the V and T states; one would be inclined to expect that the usual Heitler-London valence attraction between $M(\cdots ns,\ ^2S)$ and $X(\cdots np\sigma np\pi^4)$ would give a fairly stable homopolar V state of the type $M\cdot X$, $^1\Sigma^+$ and a rather strongly repulsive T state of type $M\cdot X$, $^3\Sigma^+$. According to the "additivity" rule for homopolar bond energies,[20] one might expect $M\cdot X$, $^1\Sigma^+$ to have a D about equal to the average of those of

[20] L. Pauling, J. Am. Chem. Soc. **54**, 3570 (1932).

M_2 and X_2, i.e., about 1 or 2 ev (cf., Pauling's curves of this type,[7] which are, however, too deep as compared with the later developed additivity rule). Further, it may be asked why the Q states should not lie well below the V and T states, as we have in Section 5 shown to be necessary in HX on the ground of a consideration of the molecular orbital approximation and of the spectra of HX^+.

We shall seek a reasonable answer to these questions by considering first the molecular orbital approximation for MX, then the Heitler-London-Slater-Pauling approximation, and then looking for a way of reconciling the two approximations with each other and with the spectroscopic evidence for case c coupling. Using molecular orbitals, the electron configurations of states N, Q, V and T of MX would be as follows (cf. Table I and Eq. (3) of I):

$$N\colon \cdots\sigma^2\pi^4; \quad Q\colon \cdots\sigma^2\pi^3\sigma^*; \quad V, T\colon \cdots\sigma\pi^4\sigma^*.$$

As discussed following Eq. (3) of I, the orbital σ would be pure $np\sigma$ of atom X if MX in its normal state N were pure heteropolar M^+X^-, while σ^* would then be pure $ns\sigma$ of M; π is nearly pure $np\pi$ of X in any case, but can best be classified as a molecular orbital for the present purpose.

Suppose we consider the electronic structure of MX from the standpoint of the *Aufbauprinzip*, starting, say, with $(MX)^{++}$, and assuming the nuclei always held fixed at a distance r equal to r_e of state N of MX. Here, in the lowest electronic state, the structure may be described as M^+X^+, with the M^+ outer shell complete, but with X^+ containing two electrons less than a closed shell np^6. If now one more electron is added, giving $(MX)^+$, the lowest states by far are clearly the two states

$$\cdots\sigma^2\pi^3, {}^2\Pi \quad \text{and} \quad \cdots\sigma\pi^4, {}^2\Sigma^+,$$

in which the σ and π orbitals are essentially $np\sigma$ and $np\pi$ of X. The Hartree field in which these molecular orbitals exist is of the general type M^+X^+, but the lowest energy solutions of the Schrödinger equation for this field are, clearly, very nearly atomic orbitals of X, since these have much lower energy, for $r=\infty$, than the lowest unfilled orbitals of M. The two above states $^2\Pi$ and $^2\Sigma^+$ are then both approximately of character M^+X. Due to the polarizing action of the M^+ on the X, however, the molecular orbitals σ and π are not quite pure $np\sigma_X$ and $np\pi_X$, but are a little distorted and give a little M–X homopolar bonding, especially the σ, which should have slightly lower energy than the π. The $^2\Pi$ state should then be the normal state of $(MX)^+$, with the $^2\Sigma^+$ just a little higher in energy. [By way of comparison, it may be recalled that in $(HX)^+$ the energy difference between the $^2\Pi$ normal and the $^2\Sigma^+$ excited state is observed to be about 3.5 ev (cf. Section 5).]

If now the last electron is added, the state of lowest energy is certainly that with configuration $\sigma^2\pi^4$, in which the p^6 shell of X is completed. This addition of an electron to the X atom tends to make it X^- and give a molecule of character M^+X^-. The σ and π orbitals, however, are now in a Hartree field of the general type M^+X and are less firmly bound than in M^+X itself, and so are much more strongly polarized by the M^+. Their departure from pure $np\sigma_X$ and $np\pi_X$ should then be much greater than in the $^2\Sigma^+$ and $^2\Pi$ states of $(MX)^+$. As a result, σ should give probably an appreciable amount of M–X homopolar bonding.

Suppose now, however, that the last electron added to $(MX)^+$ to form MX is added not to the lowest energy orbital available, but to the orbital of next lowest energy. Since $(MX)^+$ in either of its two states of lowest energy is essentially of the character M^+X with only a little mutual interaction between the M^+ and the X, the available molecular orbitals are essentially atomic orbitals of M or of X^-. Since the term value is probably nearly zero for all excited orbitals of X^-, the electron will find its resting place preferably in an M atom orbital; practically any such orbital, aside from those which are already occupied in M^+, will give a lower energy than if the electron settled in an excited X^- orbital. We are thus led, by the application of the method of molecular orbitals, to excited states of MX in which an electron is added to either of the two low $(MX)^+$ states $^2\Pi$ and $^2\Sigma^+$ in a molecular orbital which is very nearly a pure M atom orbital. Automatically, these excited states turn out to be of the character MX or M′X, i.e., an association of a

normal or excited (M′) atom with a normal X atom, the last electron being in an orbital of nearly pure M character, and the next to last electrons in orbitals of nearly pure X character. The distortion of the σ and π orbitals as compared with pure $np\sigma_X$ and $np\pi_X$ should be even less in these excited states of MX than in the low states of $(MX)^+$, since we now have a neutral M atom instead of an M^+ as distorting agent.

The lowest excited states of MX should be those in which the last added electron is in an orbital nearly identical with $ms\sigma$ of M, the valence orbital of M. This slightly distorted $ms\sigma_M$ is to be identified with σ^* of Eq. (3) of I. As lowest excited states of MX we then get from the $^2\Pi$ of M^+X the states

$$\cdots\sigma^2\pi^3\sigma^*,\ ^{1,3}\Pi\ (Q \text{ states});$$

and from the $^2\Sigma^+$ of M^+X the states

$$\cdots\sigma\pi^4\sigma^*,\ ^{1,3}\Sigma^+\ (V \text{ and } T \text{ states}).$$

In all of these states, besides inner electrons, we have essentially five unshared, nonbonding, np electrons of X and one unshared, nonbonding, ns electron of M.

In the preceding, we have tacitly neglected the effects of spin-orbit coupling in the X atom. Actually, if there is no appreciable valence coupling between the atoms, this becomes important. We referred above to $\sigma^2\pi^3$, $^2\Pi$ and $\sigma\pi^4$, $^2\Sigma^+$ of $(MX)^+$ and to $\sigma^2\pi^3\sigma^*$, $^{1,3}\Pi$ and $\sigma\pi^4\sigma^*$, $^{1,3}\Sigma^+$ of MX. Really, however, if the σ and π are nearly pure X atom $p\sigma$ and $p\pi$ orbitals, little affected by the M atom, the division into σ and π becomes merely hypothetical, and instead of $\sigma^2\pi^3$, $^2\Pi$ and $\sigma\pi^4$, $^2\Sigma^+$ of X we expect p^5, $^2P_{3/2}$ and p^5, $^2P_{1/2}$ of X. In M^+X, the $^2P_{3/2}$ should be slightly split into two case c levels with $\Omega=3/2$ and $1/2$, while the $^2P_{1/2}$ should remain as a single level, with $\Omega=1/2$. In excited neutral MX, we then expect essentially $(\cdots p^5,\ ^2P_{3/2})_X\cdot(\cdots s)_M$ giving case c levels $\Omega=2,\ 1,\ 1,\ 0^+,\ 0^-$ and $(\cdots p^5,\ ^2P_{1/2})_X\cdot(\cdots s)_M$ giving levels $\Omega=1,\ 0^-,\ 0^+$. Thus the weakness of the valence coupling between M and X in excited MX, or between M^+ and X in $(MX)^+$, indicated by our molecular orbital approach, leads automatically for these states to atomic orbitals with case c coupling. At the same time it causes states Q, V and T to be nearly equal in energy, and the resulting case c coupling then mixes up various components of these states in the way we have seen.

How, now, does the situation look from the H.L.S.P. point of view? In first approximation we get for the normal state the structure $M^+X^-(\cdots\sigma_X^2\pi_X^4)$, and for the low excited states $M\cdot X(\cdots ms_M\cdots\sigma_X^2\pi_X^3$ and $\cdots ms_M\cdots\sigma_X\pi_X^4)$, essentially the same as by the method of molecular orbitals. The states $\cdots ms_M\cdot\cdots\sigma_X^2\pi_X^3$, $^{1,3}\Pi$ are the Q states, and according to the H.L. method we expect no valence attraction here between the M and the X.

In the case of the states $\cdots ms_M\cdot\cdots\sigma_X\pi_X^4$, $^{1,3}\Sigma^+$ we are at first inclined to expect a fairly strong valence interaction between s_M and σ_X, giving a rather stable state V, $^1\Sigma^+$ and a rather strongly repulsive state T, $^3\Sigma^+$. As already noted above, the homopolar bond additivity rule would predict a D of 1 or 2 ev for the V, $^1\Sigma^+$ state. This rule is, however, empirical, and in view of its failure in the molecules MH (cf. II), it may reasonably be expected here also that D for $s_M\cdot\sigma_X\pi_X^4$, $^1\Sigma^+$ should fall much below the value predicted by the rule. The valence attraction in $^1\Sigma^+$ (or repulsion in $^3\Sigma^+$) would then be very weak, and the whole group of excited states should then give place to the corresponding case c states, in harmony with the results of the molecular orbital approach and with the empirical spectroscopic evidence.

Before accepting this, let us see whether the failure of the additivity rule in MH and MX is theoretically reasonable. If we consider the (perhaps hypothetical) *pure homopolar state* A·A, A·B, B·B of each of three molecules A_2, AB and B_2, it is not unreasonable that the additivity rule should hold (D of A·B equal to average of D values of A·A and B·B) provided the valence orbital of atom A is fairly equal to that of B in size and density. This condition is fulfilled in most of the cases discussed by Pauling in connection with the additivity rule. If, however, the valence orbitals of A and B are very unequal, then it appears that the overlapping and the exchange integrals might be much less favorable for the interaction of a valence electron of A with one of B than for the valence electrons of two A atoms, or of two B atoms. From this standpoint, failure of the additivity rule should

be more complete (i.e. D smaller compared with the additivity rule value) in MX than in MH; and in MH we have strong semiempirical evidence that the rule fails badly. [This is apparently contradicted by Heitler-London theoretical calculations on MH, neglecting inner shells, but these are hardly reliable, and on the whole the semiempirical evidence appears to carry much more weight: cf. II. In this connection, theoretical calculations on M·X would of course be of interest, but the effort of making them properly would seem likely to be excessive.] On the whole, thoroughgoing failure of the additivity rule in M·X, leaving only weak valence forces between M and X, and allowing case c coupling to become dominant, gives an explanation of the excited states of MX which may be said to have a fairly high probability of being essentially correct. Granting this, there still remain of course many details to be further investigated and explained, such as the intensities and forms of the various continua and bands, which show interesting features differing from one molecule to another.

In the preceding paragraphs it has been tacitly assumed that all molecules MX may be treated alike with respect to the question of the dominance of case c coupling over valence forces. This assumption now requires consideration. While dominance of case c coupling appears reasonably possible for MI and MBr, where the internal spin-orbit couplings in the halogen atoms are relatively large, it would seem to be more doubtful for MCl and especially MF, unless the valence interactions become extraordinarily small in the latter. In favor of the latter possibility, however, is the trend of the argument in the last preceding paragraph, since maximum inequality between the valence orbitals of M and F occurs in MF. In any case, dominance of weak valence over weak case c coupling in MF should not much affect the positions of any but the V and T levels (and these probably not greatly), nor should it much affect the appearance of the spectrum. Careful study of the as yet little known MF spectra might, however, show something of interest.

Before concluding this section, one further matter connected with the separated-atom or Heitler-London approach must be considered and if possible disposed of. This is the question whether there ought not to be strong interaction between the two first approximation states $M^+X^-(\cdots\sigma_X^2\pi_X^4,\ ^1\Sigma^+)$ and $M\cdot X(\cdots s_M\cdot\sigma_X\pi_X^4,\ ^1\Sigma^+)$. In MH, AgX, and other cases, we have assumed, and found evidence for, strong interaction between the corresponding first approximation states. Certainly in MX there must be some interaction of this sort.

May it be that the homopolar additivity rule really *does* hold after all for $M\cdot X(s_M\cdot\sigma_X\pi_X^4)$, but that the resulting $^1\Sigma^+$ state then interacts strongly with the M^+X^- state, pushing the latter down, and itself getting pushed up, enough to make it *appear* that the additivity rule fails, and to allow case c to take hold? [Case c will take hold of this $V\,^1\Sigma^+$ state if *for any reason* it gets sufficiently close to the $Q\,^3\Pi_0^+$ state.[21]] Under the circumstances just outlined, the T state $M\cdot X(s_M\cdot\sigma_X\pi_X^4,\ ^3\Sigma^+)$ would be strongly repulsive, and would probably escape from case c; this possibility, it must be admitted, is not contradicted by the available spectroscopic evidence, since transitions to such a non-case-c T state from the N state should be weak.

The possibility that the situation just sketched may exist in MX cannot easily be denied on the basis of the empirical data, since it does not differ sufficiently from that obtained assuming thoroughgoing failure of the additivity rule. More probably correct, however, in the writer's opinion, is a situation compounded as follows: (A) the additivity rule fails badly, and there is only very weak valence coupling in *all* states M·X, so that states V and T, as well as Q and also other higher excited states, become approximately of case c type; (B) the pure heteropolar unpolarized M^+X^- character of the first approximation normal state wave function is modified not by strong interaction just with the first approximation $s_M\cdot\sigma_X\pi_X^4$, $V\,^1\Sigma^+$ state, but by the sum total of weaker interactions with the first approximation wave functions of this and a whole series of other M·X (and other) excited states. The possibility that condition (B) exists in MX is favored, as compared with MH, AgX or HX, by

[21] Cf. J. H. Van Vleck, Phys. Rev. **40**, 568 (1932).

the fact that the pure M^+X^- state is well below the whole set of states $M \cdot X$ and $M' \cdot X$ in energy, while in the other molecules the A^+B^- state is close to or even in the midst of the $A \cdot B$ states.

It seems possible that the wave function of state N of MX, resulting from the operation of condition (B), may be describable more or less roughly as "classically polarized" in contradistinction to the "valence polarized" condition that would exist if the pure M^+X^- function were modified mainly just by strong interaction with the valence bond state $s_M \cdot \sigma_X \pi_X^4$, $^1\Sigma^+$. In classically polarized M^+X^-, the whole p^6 shell of X would be shifted relative to the X nucleus and inner electrons (the inner shells are relatively slightly affected), while in valence polarized M^+X^-, just the orbitals of the two σ electrons would be shifted, and also distorted. In a molecule like HF or AgX, state N might be described as (very strongly) valence polarized A^+X^-. If state N of MX is approximately "classically polarized" M^+X^-, the polarization is shared by the σ and π orbitals and therefore need not be so very great for either. In other words, the σ orbital of Eq. (3) of I is in this case nearly pure $np\sigma_X$. Possibly of significance in the present connection is the fact that the Born equation (Eq. (5) of I) with crystal-structure values of β and n gives values, for the energy of dissociation D of state N of MX into ions $M^+ + X^-$, which are close to the actual D values, while for other molecules, the D's calculated in this way are much larger than the actual (cf. II in regard to LiH, Section 6 above for AgX).

The electronic structures of the normal and excited states of MX which result, as just discussed, starting from the H.L.S.P. viewpoint and using the conditions (A) and (B) above, are in excellent agreement with those reached in earlier paragraphs using the molecular orbital viewpoint.

In connection with state N of MX, it is worth noticing here that the dipole moments,[22] although not accurately known, are apparently at least half as large as would be expected for pure heteropolar M^+X^-. If as an approximation we assume that the reduction of the dipole moment to half is due to a "classically polarized" condition, then of the total polarization only one-sixth belongs to each of the electrons in the group $p\sigma^2 p\pi^4$ which makes up p^6. To give the observed dipole moments, each of these six p electrons need be displaced only one-twelfth of the distance from X to M. This corresponds to only a small modification in the σ and π orbitals as compared with pure $np\sigma_X$ and $np\pi_X$ orbitals.[23]

In conclusion, the writer wishes to express his appreciation of the valuable help of Mr. H. J. Plumley in connection with the construction of the figures.

[22] H. Scheffers, Physik. Zeits. **35**, 425 (1934); W. H. Rodebush, L. A. Murray, Jr. and M. E. Bixler, J. Chem. Phys. **4**, 372, 536 (1936): dipole moments of NaI, KCl, KI by molecular ray method.

[23] R. S. Mulliken, J. Chem. Phys. **3**, 584 (1935).

Heights of Reflection of Radio Waves in the Ionosphere

F. H. MURRAY AND J. BARTON HOAG
Ryerson Physical Laboratory, University of Chicago, Chicago, Illinois

(Received September 9, 1936)

A general method has been developed whereby, from the virtual height frequency curves, it is possible to calculate an upper limit to the height of reflection of a radio wave of a particular frequency in the ionosphere. The various portions of the ionosphere are considered as belonging to one of three groups; first, those in which the electron concentration increases continuously with altitude, the manner of increase being unknown at the start but appearing as a result of the calculations, second, those portions in which the concentration remains essentially constant over an appreciable thickness and, third, those portions for which the concentration is less than the maximum of the region immediately below. It was found that a discontinuity in a virtual height frequency curve is a necessary but not a sufficient condition for the existence of two distinct layers. When the method was applied to a particular time and place, it was found that, whereas some of the F_2 virtual heights were rising during the morning hours, the true heights were falling.

INTRODUCTION

QUANTITATIVE determinations of the concentration of free electrons at various altitudes in the upper regions of the earth's atmosphere and the *true* heights to which radio waves rise before suffering reflection or refraction back to the surface of the earth present problems of considerable interest and complexity. The information available for their solution consists of the measured *virtual* heights. These are the distances to which the radio waves would have risen had they traveled throughout their entire paths with the unabated velocity which they possess in the lower regions, i.e., the velocity of light. Virtual heights were reported, for different times of the day and of the year and for radio waves of various frequencies, before the development of automatic recording systems, which now are rapidly increasing the amount of data available in some localities.

Measurements of the virtual heights of the ionized regions in the ionosphere are usually made by noting the echo time for the sky wave as compared with the direct or ground wave, as determined by the impulse method of Breit and Tuve.[1] The frequency change method of Appleton[2] has also been used and yields the same quantity as the echo method whenever only one echo is present. Usually, however, there is more than one echo and, with the frequency change method, the downcoming waves, which are added together, cannot be resolved uniquely by analysis. Large variations were reported in the early work, when the measurements by different observers were made at different locations, frequencies and times of the day or year. The changes in virtual height during a given day or over long periods of time and at different localities have since been studied in considerable detail,[3] using recording equipment and operating at or in the immediate neighborhood of a fixed frequency. A sharp discontinuity, observed as the frequency was increased (as well as other phenomena) was interpreted by Appleton[4] as due to the existence of two physically separate regions. The hypothesis of two (or more) stratifications has been the subject of much controversy and

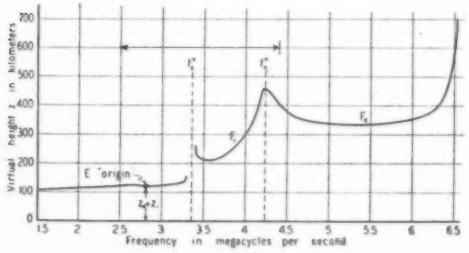

FIG. 1. A virtual height frequency curve.

[1] G. Breit and M. A. Tuve, Nature **116**, 357 (1925). Phys. Rev. **28**, 554 (1926).
[2] E. V. Appleton and M. A. F. Barnett, Proc. Roy. Soc. **A109**, 621 (1925).
[3] E. V. Appleton and A. L. Green, Proc. Roy. Soc. **A128**, 159 (1930). G. Goubau and J. Zenneck, Zeits. f. Hockfreq. **37**, 207 (1931). J. P. Schafer and W. M. Goodall, Proc. I. R. E. **19**, 1434 (1931); **20**, 1131 (1932). J. A. Ratcliffe and E. L. C. White. Proc. Phys. Soc. **45**, 1 (1933). G. W. Kenrick, Physics **4**, 194 (1933). See also references 5 and 7.
[4] E. V. Appleton, Nature **123**, 445 (1929).

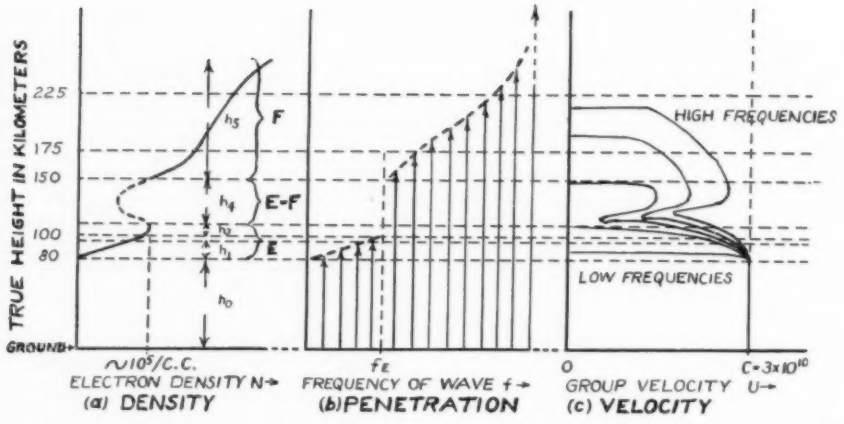

FIG. 2. Qualitative curves of (a) the electron concentration, (b) the true heights to which radio waves penetrate and, (c) the group velocity of the waves, at various distances above the earth's surface.

will be discussed later in this paper. A plurality of regions of *virtual heights* identified in terms of frequency and referred to as E, F, etc., are now commonly accepted. See Fig. 1.

Splitting of the signals into two oppositely polarized components has been observed and interpreted[5] in terms of the effect of the earth's magnetic field on the motion of free electrons in the ionosphere. Magnetic splitting of the echoes from F (or, in general, from F_1 and F_2) is common, whereas from E it is only occasionally observed. The National Bureau of Standards has adopted $f_E{}^0$ for the critical frequency of the ordinary ray at which a discontinuity occurs between E and F_1 and $f_E{}^x$ for the extraordinary ray. They also use $f_{F_1}{}^0$ and $f_{F_1}{}^x$ for the corresponding critical frequencies between F_1 and F_2.

Records are now available[6] of the virtual heights for a wide range of frequencies of the radio waves, as illustrated in Fig. 1. Similar records are made at half-hourly or hourly intervals, so that information is now rapidly accumulating about the virtual heights at different frequencies and times. In Fig. 1, it is to be noted: first, that the E region virtual height is comparatively constant, whereas, the F_1 region values rise markedly[7] at the higher frequencies; second, that a sharp discontinuity occurs at the critical frequency $f_E{}^0$; third, that the virtual heights for frequencies just above $f_E{}^0$ decrease from very large values to a minimum before slowly increasing again; fourth, there is a long "flat" region in F_2. In this article, calculations have been made only over the range from 2.5 to 4.4 megacycles per second, as indicated by the arrows in the figure.

Curves such as shown in Fig. 1, while possessing great value for communication purposes, in that they express the delay time of the sky wave pulse over that of the ground wave pulse, give a greatly distorted picture of the true altitudes to which the waves rise and the locations of the various ionized strata in the upper atmosphere.

From these curves, the authors have evolved a method, presented in this paper, for the calculation of an upper limit to the height of reflection of a radio wave of a particular frequency, includ-

[5] Independently by H. W. Nichols and J. C. Schelleng, Bell Sys. Tech. J. **4**, 215 (1925), and E. V. Appleton, Proc. Phys. Soc. of London **37**, 22D (1924–5). See also E. V. Appleton, J. Inst. Elec. Eng. **71**, 642 (1932).

[6] L. W. Berkner and H. W. Wells, Proc. I. R. E. **22**, 1102 (1934); J. Terr. Mag. **39**, 215 (1934), **41**, 75 (1936). H. W. Wells, J. Terr. Mag. **39**, 209 (1934). L. W. Berkner, H. W. Wells, and S. L. Seaton, Trans. Amer. Geophys. Union, Seventeenth Annual Meeting (1936), J. Terr. Mag. **41**, 173 (1936). T. R. Gilliland, Nat. Bur. Stand. J. Research **14**, 283 (1935); Proc. I. R. E. **23**, 1076 (1935). Kirby, L. W. Berkner and Stuart, Proc. I. R. E. **22**, 481 (1934). Kirby and Judson, Nat. Bur. Stand. J. Research **14**, 469 (1935). H. R. Mimno and P. H. Wang, Proc. I. R. E. **21**, 529 (1933). J. P. Schafer and W. M. Goodall, Proc. I. R. E. **20**, 1131 (1932); **23**, 670 (1935).

[7] The *rapid* rise shown is only typical at certain times. Further, Fig. 1 shows only the ordinary wave component, the extraordinary component having been omitted.

ing a specification of the electron densities[8] at various altitudes. Evaluations[9] of true heights have been attempted previously by various investigators, particularly for the E region.

Group Velocity and Virtual Height

It has been found possible in the past to deduce the *approximate shape* of the distribution curve of electron charge density at various altitudes. As indicated in Fig. 2a, it is negligible up to a height of approximately 80 kilometers, after which it increases for about two score kilometers (in the E region), with a maximum of approximately 10^5 electrons per cubic centimeter. Above the E region the density is usually *assumed* to be of smaller but of unknown amount over a region (call it the $E-F$ region[10]) which varies greatly in extent. The density then rises in the upper or F region to values occasionally as great as ten times the maximum in the E region.

Consider the case of radio pulses of different frequencies, transmitted vertically into a medium whose electron concentration varies in the manner depicted in Fig. 2. During their passage through the ionized media, the waves will travel at a reduced group velocity. The group velocity U at any point along the path is a function of the real part of the index of refraction (n) of the medium and of the frequency of the wave (f) in the following well-known manner,

$$\frac{1}{U}=\frac{1}{c}\frac{d}{df}(f\cdot n), \tag{1}$$

where $c=3\times10^{10}$. The index of refraction at a given altitude is a complicated function of the electron density, the frequency of the waves, the number of collisions per second of electrons with gas atoms and the strength of any magnetic field which may be present, such as that of the earth. A qualitative representation of the group velocities at various altitudes for radio waves of various frequencies, propagated in a vertical direction, may be conceived from the density curve of Fig. 2, and is shown in Fig. 2c. For a wave of given frequency, the group velocity will rapidly approach zero at a certain altitude. At the point where the electron density is sufficient to reduce the group velocity to zero, the wave will be reflected back to the earth.

For the case of vertical propagation, the time of transit, t, of the radio wave from the earth up to the (*true* or geometric) height h, at which reflection takes place, is given by

$$t=\int_0^h (dh/U), \tag{2}$$

in which dh is an increment of distance in the vertical direction. From Eqs. (1) and (2) and the definition of the virtual height z, it follows that

$$z=ct=\int_0^h (d/df)(f\cdot n)dh. \tag{3}$$

The equation states, implicitly, that the value of the virtual height is controlled by two things: first, a *penetration factor*, i.e., the true height to which the wave actually rises, and second, a *retardation factor*, i.e., the velocity with which it travels at various points along its path.

The Penetration and Retardation of the Waves

The virtual height for a given frequency of radio wave is a function not only of the reflecting ability of the ionized region at a given height but also of the retarding influence of all the regions between this position and the earth's surface. The "true" height, on the other hand, is that actual distance above the earth's surface where the ion concentration is such as to cause reflection of the specified frequency. The substructures may alter the intensity and velocity of a wave but not the true point at which it will be reflected

[8] Calculations based on the magnetic splitting of the virtual heights, observed at certain times of the day or night, indicate that wave propagation in the F region is chiefly influenced by free electrons alone, and the same may be true for E layer propagation although there is much evidence that other ions are a large factor. The neglect of ions other than free electrons in the F region, in the formulae developed here, is based on this evidence; the explicit formula for the index of refraction (n) and the calculated values of it are valid only if all other ions are relatively negligible. The general method could still be used, however, with more general formulae. See E. O. Hulburt, Theory of the Ionosphere. Terr. Mag. and At. Elec. **40**, 193 (1935).

[9] See J. C. Schelleng, Proc. I. R. E. **16**, 1471 (1928). G. Breit, Proc. I. R. E. **17**, 1815 (1929). G. W. Kenrick and C. K. Jen, Proc. I. R. E. **17**, 711 (1929). J. Hollingworth, Proc. Phys. Soc. **47**, 843 (1935). E. O. Hulburt, Terr. Mag. and At. Elec. **40**, 193 (1935).

[10] J. P. Schafer and W. M. Goodall use M for this region. Proc. I. R. E. **23**, 1356 (1935).

since this depends uniquely on the frequency of the wave and the ion concentration *at* the point of reflection. It is desired to deduce the true heights of E, F, etc., from the corresponding virtual heights, E, F, etc.

As indicated by the arrows of Fig. 2b, the lower frequencies are reflected from the lower parts of the E layer; the wave with critical frequency f_E is just capable of penetrating through the region of maximum electron concentration in E; higher frequencies are able to travel to greater and greater heights in the F layer; until above a certain frequency all waves will penetrate the ionosphere and pass out into space.

Since the virtual heights are the distances to which the waves would travel in empty space, it is obvious that they are always equal to or greater than the true heights.

For frequencies slightly greater or less than f_E, the group velocity is very small (probably in the region of maximum electron concentration at the top of the E region). This delay in the progress of the wave causes the transit time to be unusually large. If the wave had continued with the velocity of light, it would have traveled to a comparatively great elevation. Thus, the virtual heights for frequencies near f_E are abnormally great. As the frequency is increased above f_E, the group velocity, in the region of maximum electron concentration at the top of E, increases rapidly and the virtual heights decrease, although this is slightly off-set by a small increase in penetration of the higher frequencies to greater altitudes in F.

For somewhat higher frequencies, in the F_1 virtual height region, the group velocity increases more and more slowly and the penetration factor becomes of increasing importance. Hence, the virtual height curves, after passing through a minimum, begin to rise. The rise becomes increasingly rapid as the waves penetrate higher into the F_1 region, due to additional retardation produced by the lower portions of this layer.

It will be noted in Fig. 1 that a peak occurs at $f_{F_1}{}^0$. When sufficiently resolved, this is often found to be a discontinuity, similar to that at $f_E{}^0$. Thus, there exists a region where the electron concentration is increasing less rapidly with altitude than at lower or higher levels and whose comparatively great thickness introduces such a large retardation of frequencies near $f_{F_1}{}^0$ as to give great values to the virtual height. Since this condition does not maintain at all times, the distinction between F_1 and F_2 does not always appear. Then, the peak at $f_{F_1}{}^0$ is absent and the F curve rises slowly from its minimum to the extensive, nearly horizontal portion shown.

We shall, for convenience in the mathematical analysis, replace the actual electron distribution in the ionosphere by ionized strata, each of constant free electron density. Both the density and the thickness may vary from one stratum to the next. For the lower E and for the F regions there shall be a succession of these strata of increasing densities. A single stratum shall be used to represent that portion of the ionosphere (probably the region of maximum concentration at the top of E) which produces the large retardations of the frequencies near f_E. The E–F region, likewise, is to be replaced by only one stratum.

The Index of Refraction

Hartree[11] has derived an expression for the complex index of refraction, n, of a dispersive medium such as the ionosphere, including the effect of the earth's magnetic field. This has been modified by Murray[12] in such a manner as to be more suitable for calculations. For the special case of vertically propagated radio waves, Murray's equation is

$$n=\left[1-\frac{3}{2}\frac{X}{(Z+r/2)X+(k_1^2/2x)[(1+(4k_2^2x/k_1^4)X^2)^{\frac{1}{2}}-1]}\right]^{\frac{1}{2}} \tag{4}$$

where $r=w/x$, $w=(c/2\pi 10^6)^2 2k_0^2/3$, $k_0^2=4\pi Ne^2/mc^2$, $x=f^2/10^{12}$, $X=1-r-if_c/2\pi f$, $Z=1-if_c/2\pi f$, $k_1=-eH_1/2\pi mc$, $k_2=-eH_2/2\pi mc$, in which N is the electron concentration, e is the charge of the electron in e.s.u., m is the mass of the electron, $c=3\times 10^{10}$, f is the frequency of the radio wave, f_c is the number of collisions each second of electrons with gas atoms, $i=\sqrt{-1}$, H_1 and

[11] D. R. Hartree, Proc. Camb. Phil. Soc. **27**, 143 (1931).
[12] F. H. Murray, Am. J. Math. **56**, 259 (1934).

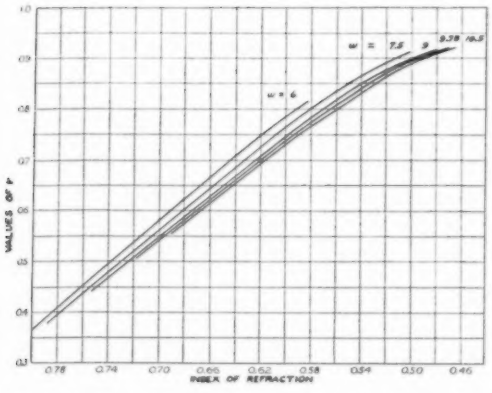

FIG. 3a. Variation of the index of refraction n above Washington, D. C., with electron density N and radio-frequency f. $N=1.86\times10^{4}w$ and $f=10^{6}(w/r)$.[13]

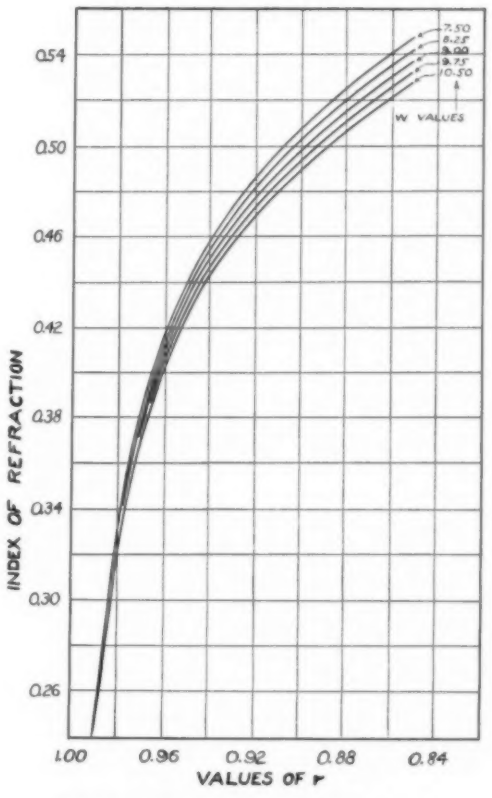

FIG. 3b. Same as Fig. 3a. Small values of n.

H_2 are, respectively, the horizontal and vertical components of the earth's magnetic field, in e.m.u., at the given height above the earth's surface.

The value of H at different altitudes above Washington, D. C., may be obtained from the work of Berkner and Wells.[13] Its variation with altitude throughout the ionosphere causes but minor changes in values of n. We have, therefore, used the value at 180 kilometers. Thus, $H_1=0.16951$ and $H_2=0.49899$.

Collision frequencies, f_c, on the other hand, are difficult to evaluate at the lower E levels since they depend on the pressure, temperature, kind of gas present, etc. Uncertainties in the values of these quantities, and hence in n, make it advisable for the present to omit calculations of true heights for the lower portions of the E region. We shall use the lowest virtual height values of the E region, indicated by the large dot in Fig. 1, as the E "origin" from which to specify the true heights of all higher regions. The true height of the E region has been estimated[14] to lie not more than twenty kilometers below the virtual height at Washington, D. C. Hence, the maximum values of the true heights of the upper layer, which will be computed later in this paper, may be expected, from this cause alone, to be greater than the true heights by distances of this order of magnitude.

For the upper portions of the E region and the more rarefied regions above, calculation has shown that the collision frequency term $f_c/2\pi f$ is negligibly small in comparison with $(1-r)$ and hence may be dropped from Eq. (4). This is only true for the calculation of the real part of n for radio waves whose frequencies are greater than three megacycles and when $(1-r)=1/20$, or greater. Under these conditions, Eq. (4) reduces to

$$n=\left[1-\frac{3r(1-r)/2}{(1+r/2)(1-r)+(k_1^2/2x)\left[(1+(4k_2^2x/k_1^4)(1-r)^2)^{\frac{1}{2}}-1\right]}\right]^{\frac{1}{2}}, \tag{5}$$

[13] Berkner and Wells, Proc. I. R. E. **22**, 1109 (1934).
[14] E. O. Hulburt, Terr. Mag. and Atm. Elec. **40**, 193 (1935).

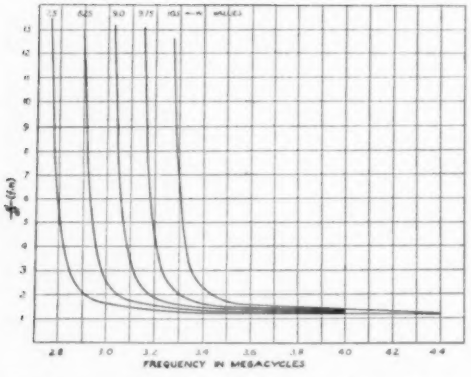

FIG. 4. Variation of the group velocity U above Washington, D. C., with electron density N and radiofrequency f. $N=1.86\times10^{4}w$ and $1/U=(1/c)d(f\cdot n)/df$.

an equation of outstanding simplicity in this field of work. The wave will be reflected when $r=1$, since then $n=0$. Figs. 3*a* and 3*b* show values of n for various values of r (which are inversely proportional to the square of the frequencies) and w (which are directly proportional to the electron densities).

Values of $d(f\cdot n)/df$ for use in Eqs. (1) or (3) may be computed from the data of Fig. 3. Selected values are shown in Fig. 4.

Virtual Height Increments Due to the Ionized Stratum of Maximum Concentration, in E

Let z_3 stand for that contribution to the virtual height due to the equivalent stratum which represents the region of maximum ionization at the top of E. Then, if h_3 is the thickness of this stratum,

$$z_3=(h_3/U)\cdot c=h_3\cdot(d/df)(f\cdot n). \qquad (6)$$

Values of N and h_3 are assumed and z_3 values computed for a series of frequencies above f_E, using Eqs. (5) and (6). Values of N are of the order of magnitude of those in the region of maximum electron concentration at the top of E, (10^5/cc); values which can be calculated from f_E since at this frequency the wave is reflected, i.e., $U=0$, $r=1$, $w=x$, or

$$N=(3\pi m/2e^2)f^2. \qquad (7)$$

Values of h_3 are of the order of 10 kilometers. If reasonably correct values of N and h_3 are chosen, a curve of the form (B) indicated in Fig. 5 will be obtained. Based on the assumption that the limited range of frequencies concerned all penetrate approximately the same distance into the F region, the curve should rise smoothly from a horizontal value near f_E. If the density assumed is too large, one usually finds a small hump in the correction curve just to the right of f_E; if too small, a small dip occurs in the curve. If the value of h_3 has been incorrectly estimated, the curve will not be horizontal just above f_E. After a few trials, this work will be found to progress rapidly.

The Region Between E and F

The distribution of electrons in the E–F region is unknown at present. We shall, for the time being, assume that the ionization in this region is zero. This implies the existence of sharp discontinuities in the electron density at the top and bottom of E–F, which is highly improbable, yet it permits a calculation of the *upper limits* of the true heights of the F layer. Later, we shall discuss the effect of free electrons in E–F.

When the ionization in E–F is zero, all waves which penetrate the E region, regardless of the frequency, would travel through E–F with the velocity of light and the contribution to the virtual height (z_4) due to E–F would be equal to its true thickness h_4'. This is indicated in Fig. 5,

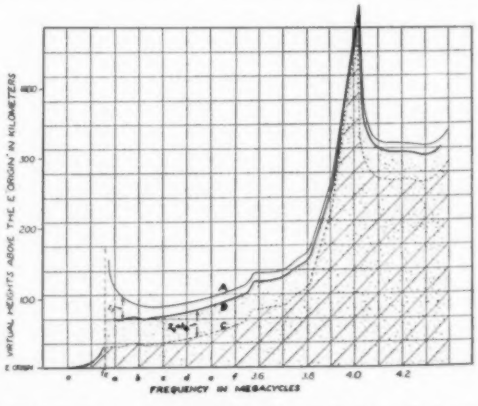

FIG. 5. Curve A, virtual heights of F above E, 3 P.M., August 31, 1933, Washington, D. C. A to B is the increment of virtual height due to the maximum electron concentration in E while B to C is the thickness which the E–F region would have if it contained no ions.

where the vertical distance between the first corrected curve, B, and the dotted curve, C, is the thickness of E–F, provided there are no free electrons in this region. There is a slight uncertainty, of a few kilometers at most, as to the exact point at which the dotted curve forms a smooth extension of the E curve.

Calculations for the F and Part of the E Regions

Let z' represent the contribution to the virtual height due to increasing penetration and retardation in the F region and in that portion of the E region (0–10 km thick) immediately below the region of maximum ionization. These regions are indicated in Fig. 2a by h_2 and h_5. The lowest point of the F region is taken as that point where the ionization, after a decrease in the E–F region, has again become equal to the maximum E value. Let the frequency average of z' be defined by the equation

$$z'_{\text{ave}} = (1/f)\int_0^f z'df. \tag{8}$$

Values of z'_{ave} may be obtained from Fig. 5, using a planimeter to determine the shaded areas from 0 to a, 0 to b, etc., under the dotted curve.

Since z' is a special case of z, Eq. (3) may be substituted in Eq. (8). Then, using an inversion of

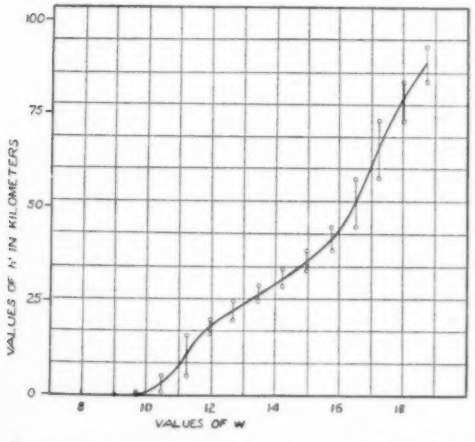

Fig. 6. The contribution to the true height ($h'=h_2+h_5$) due to F and part of E for various frequencies ($f=10^6\sqrt{w}$), 11 A.M., August 31, 1933, Washington, D. C.

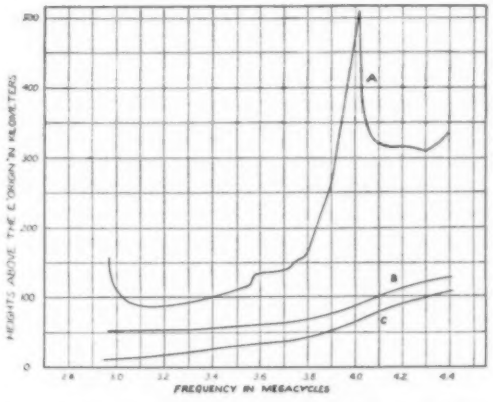

Fig. 7. An example of, (A) virtual heights, as in Fig. 5, (B) maximum and (C) minimum values of true heights of F above E.

the order of integration in evaluating the double integral, we find

$$z'_{\text{ave}} = \int_0^{h'} n dh, \tag{9}$$

where $h'=h_2+h_5$. Our calculations have shown that w increases in a continuous and single valued manner over the regions considered. Hence, there exists an inverse function, $h'(w)$; i.e., the height h' is some unknown function of the electron density. Then,

$$z'_{\text{ave}} = \int_0^x n(dh/dw)dw, \tag{10}$$

where x and w have the meanings stated under Eq. (4). At the upper limit of integration $n=0$ and at the lower limit $h=0$. Integrating by parts leads to the expression

$$z'_{\text{ave}} = -\int_0^x h'(\partial n/\partial w)dw, \tag{11}$$

where h' is the desired quantity. Due to the complexity of even the simplified equation for n, Eq. (11) can only be solved, in practice, by replacing the integral by a finite sum of terms. Thus,

$$\left.\begin{aligned}
(z'_{z1})_{\text{ave}} &= h_1'\Delta n_{11}, \\
(z'_{z2})_{\text{ave}} &= h_1'\Delta n_{21} + h_2'\Delta n_{22}, \\
&\cdots \\
(z'_{zm})_{\text{ave}} &= h_1'\Delta n_{m1} + \cdots h_m'\Delta n_{nm},
\end{aligned}\right\} \tag{12}$$

where h_1' is the value of h' for the electron density corresponding to w_1. Values of Δn for equal interval values of w are taken from the data of Fig. 3 or calculated directly. Numerical values for z'_{ave} and the Δn's are obtained for, say fifteen, equally spaced x values. The resulting simultaneous equations are easily solved for h_1', h_2', $\cdots$, h_m'. These are plotted and averaged, as shown in Fig. 6. Since at the point of reflection $w=x=f^2/10^{12}$, values of h' for various frequencies may be obtained with ease from Fig. 6.

Resumé of the Procedure

The true heights h of the ionosphere layers above the ground (see Fig. 2) are given by

$$h=h_0+h_1+h_2+h_3+h_4+h_5, \qquad (13)$$

and the *maximum* values, h_{max}, which the true heights may have, are

$$h_{max}=(z_0+z_1)+h_3+h_4'+h'. \qquad (14)$$

We have seen that z_0+z_1 is given as the distance up to the E origin, as in Fig. 1, h_3 is determined by Eq. (6), h_4' as in Fig. 5 and h' by the set of Eqs. (12).

Minimum Values of the True Heights of F above E

Let us next assume that the ionization in the E–F region is not zero but is equal to or greater than the maximum in the E layer. If we assume that, for increasing altitudes above E, the density increases steadily from the maximum E value at the same or at a smaller rate than in either E or F, then the E–F region may be considered to be of negligible thickness and the observed virtual height increments, z_4, for frequencies near f_E are, for the most part, a result of the large retardation of the wave in the region just above E. In other words, h_4 can be assumed to be negligibly small and a minimum is established for the height of F above E. The procedure is to apply Eq. (6) and then Eq. (12), using the dotted areas under curve B rather than under C of Fig. 5 to get z'_{ave}. Then, the minimum values (h_m) of the true heights of F above E are given by

$$h_m=h_3+h'. \qquad (15)$$

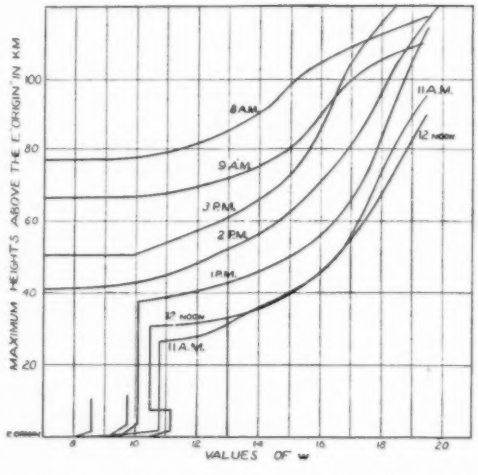

Fig. 8. Maximum values of heights of F above E for various frequencies ($f=10^6\sqrt{w}$).

An Application

Photographs of some virtual height frequency records were kindly given to us by T. R. Gilliland of the National Bureau of Standards and have since been published.[15] These records are for Washington, D. C., August 31, 1933, and extend only over the frequency range from 2.5 to 4.4 megacycles per second; see Fig. 1. Curve A of Fig. 7 shows the virtual heights at 3 P. M. as measured from the records, curve B shows the maximum values while C shows the minimum values of the heights of the F layer above the E "origin" (about 125 km above ground). The large differences between virtual and true heights over this frequency range, at this time and place, are immediately obvious.

Fig. 8 shows maximum values of F above E at various times of the day. Since at reflection $r=1$, $w=x$, the values of w on this curve are directly proportional to the square of the frequency.

Finally, in Fig. 9, the maximum values of the true heights of the F region above the ground at various times of the day are shown for three frequencies, the upper in the F_2° region and the lower in the F_1° region.

[15] T. R. Gilliland, Proc. I. R. E. **23**, 1076 (1935).

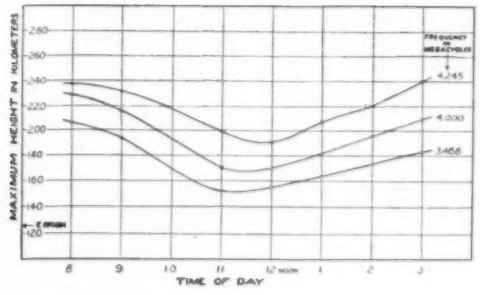

FIG. 9. Variation of maximum values of heights of reflection of radio waves with time of day for August 31, 1933, Washington, D. C.

DISCUSSION

If the electron density in the E–F region is greater than zero but less than the maximum in E, the true height curve will lie between the maximum and minimum curves. It has been found, by calculation, that, assuming equal and increasing increments for the electron density in E–F, the resultant curves are lowered below the maximum values, slowly at first and then rapidly. In other words, the electron density in E–F must be nearly equal to the maximum in E before the true heights are found to lie appreciably below the maximum values. (See curves for $d(f\cdot n)/df$, which is nearly 1 when $w/w_{\max}<2/3$.)

It is to be noted that in the procedure adopted here, the electron density in the E–F region may rise continuously and be even greater than that in E, contrary to the usual conception that a "valley" exists at this elevation. We have observed several cases in which, after the first correction alone (Eq. (6)), the F_1 curve rose continuously from E. It appears that mathematically *a discontinuity in the virtual height curve is a necessary but not a sufficient condition for the existence of two distinct layers.*

The data used in plotting the true height frequency curves may be readily converted to give electron densities at various altitudes by means of Eq. (7). Fig. 8 shows the variation of electron density (which is directly proportional to w) with the maximum values of the true heights at various times of the day, August 31, 1933, above Washington, D. C. The possible range of electron densities at a given elevation can be obtained from curves such as B and C of Fig. 7 and the application of Eq. (7).

In Fig. 7, the true heights are seen to be very much below the virtual heights. However, as in Fig. 1, there is a long, nearly horizontal portion of the F_2 curve, often extending above 10 megacycles. For these frequencies such large differences between the two heights will not be found. It must be kept in mind that the special case used to illustrate our general procedure is limited in frequency range, time, to a given location and to the ordinary ray.

In Fig. 9, it is seen that the maximum height values for the higher frequency (4.245 mc, in the F_2 region) decrease during the morning hours by as much as 50 km. The corresponding virtual heights *do just the opposite*. It is not, in general, to be expected that the virtual and true heights should behave alike since the former depend upon the entire structure from the ground up to the point of reflection, whereas the latter depend only on the structure at this point.

Although it is possible to establish true heights and electron densities within a comparatively small range of values, by the procedure outlined above, it is hoped that further studies of the E and E–F regions will permit still greater accuracy.

We wish to thank Dr. Gilliland of the National Bureau of Standards for the virtual height frequency curves and Mrs. Ardis Monk for her assistance in the calculations of the index of refraction at various frequencies and densities.

Fine Structure in the $^3\Sigma$ Ground State of the Oxygen Molecule, and the Rotational Intensity Distribution in the Atmospheric Oxygen Band

ROBERT SCHLAPP
Lecturer in Natural Philosophy, University of Edinburgh, Scotland
(Received December 5, 1936)

The formula developed by Kramers (and recently on different lines by Hebb) to represent the fine structure of the ground state of oxygen is compared with the experimental data. It is pointed out that the currently accepted values of the parameters are in error. The measurements are compared with a more accurate formula, which takes into account the fact that the rotation does not completely decouple the spin from the axis of the molecule, and values of the parameters are found which give excellent agreement. The rotational intensity distribution in the atmospheric O_2 bands is recalculated on the assumption of incomplete decoupling; the intensities in the ^PP and ^RR branches are found to be unchanged, while those in ^PQ and ^RQ become more nearly equal than with complete decoupling, a result in harmony with the measurements.

1. INTRODUCTION

A MULTIPLET structure of the ordinary kind, due to magnetic interaction between the total spin S ($=1$ for a triplet state) and the quantized component of the orbital electronic angular momentum along the axis of figure, does not arise in Σ states, for in them the latter component vanishes. It was, however, shown by Kramers[1] that the spin-spin interaction of the uncompensated electrons, invoked by Heisenberg to explain the fine-structure of the orthohelium terms, is equivalent to an interaction between S and the axis of figure, with energy proportional to $3\cos^2\theta-1$, where θ is the angle between them. Kramers calculated the energy levels in first approximation by averaging the coupling energy over the "end-over-end" rotation of the molecule (quantum number K), and found that each rotational level K was split by the interaction into three, corresponding to the three different ways of constructing a total angular momentum vector J ($=K-1, K, K+1$) out of K and $S=1$.

There is a further effect[2,3] due to the interaction between the uncompensated spins and the magnetic field set up by the rotation of the molecule as a whole, which is equivalent to a cosine coupling between S and K. These two effects together give[1] for the three energy levels W_J associated with a given value of K the following expressions.

$$\begin{aligned} W_{K+1} &= W_0-2\lambda(K+1)/(2K+3)+\mu(K+1), \\ W_K &= W_0, \\ W_{K-1} &= W_0-2\lambda K/(2K-1)-\mu K. \end{aligned} \tag{1}$$

Here W_0 is the usual rotational energy $h^2K(K+1)/8\pi^2I$. The constant λ ($=3A/2$ in Kramers' notation) is a measure of the $\cos^2\theta$ coupling between S and the axis, and μ ($=$Kramers' $-B$) is a measure of the cosine coupling between S and K.

There is a further cause of fine structure, not taken into account by Kramers. Although on the average the electronic orbital momentum of the molecule in a Σ state is null, this angular momentum has a precessing component perpendicular to the axis of figure, which interacts with the total spin S, an interaction which clearly involves an influence of neighboring $^3\Pi$ states on the $^3\Sigma$ state. The theory of this effect in the rotating molecule has been given recently by Hebb,[4] and the remarkable result has emerged that in first approximation the energy levels are given by expressions of exactly the same form as (1), the constants λ and μ having of course a different interpretation. Until suitable wave functions are available, and the various matrix elements on which the constants depend are worked out, it is not possible to disentangle accurately the contributions of the different causes of the fine structure to the values of λ and μ. But in any case it should be possible to represent the fine structure of a $^3\Sigma$ state by a formula of the type (1), regarding λ and μ as

[1] H. A. Kramers, Zeits. f. Physik **53**, 422 (1929).
[2] F. Hund, Zeits. f. Physik **36**, 657 (1926); **42**, 93 (1927).
[3] J. H. Van Vleck, Phys. Rev. **33**, 467 (1929).
[4] M. H. Hebb, Phys. Rev. **49**, 610 (1936).

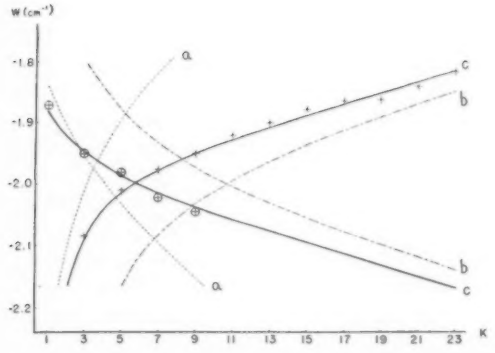

FIG. 1. In the figure the crosses represent the observed positions of two components $J=K-1$ (+) and $J=K+1$ (⊕) of the fine structure of the $^3\Sigma$ ground state of the oxygen molecule (vertical scale in cm^{-1}), plotted against rotational quantum number K (horizontal scale); the positions of the observed points are given relative to the third component $J=K$ at ordinate 0 cm^{-1} (not shown). The curves (*a*), (*b*), (*c*), give the calculated positions of the components $J=K\pm1$, relative to $J=K$ at ordinate 0 cm^{-1}. (*a*) Kramers' formula, with $\lambda=0.726$ cm^{-1}, $\mu=-0.025$ cm^{-1} (the usually accepted values of the parameters), the levels $J=K\pm1$ having been arbitrarily reduced by 1.21 cm^{-1} as explained in the text. (*b*) Kramers' formula (Eq. 1), with $\lambda=1.985$ cm^{-1}, $\mu=-0.008$ cm^{-1}. (*c*) More complete formula (Eq. 2), with $\lambda=1.985$ cm^{-1}, $\mu=-0.008$ cm^{-1}.

parameters to be adjusted to fit the observations. The formula (1) will be referred to as Kramers' formula.

2. Comparison of Kramers' Formula with Experiment in Oxygen

For oxygen, in connection with which Kramers originally developed his theory, the agreement is merely qualitative. As it has been stated several times in the literature that the agreement is good, it may be well to emphasize that Kramers says explicitly that his formula is inadequate for the quantitative description of the fine structure. The values of the parameters which he gives, and which have found their way into the literature ($\lambda=0.726$ cm^{-1}, $\mu=-0.025$ cm^{-1} in our notation) were obviously not meant to be taken very seriously; in order to obtain anything like agreement using these values, Kramers found it necessary to raise the level $J=K$ by an amount 1.21 cm^{-1} ($=1.67\lambda$, or 2.5A in Kramers' notation) relative to the others, an *ad hoc* shift for which he claimed no theoretical justification.

In Fig. 1 the crosses represent the observed relative positions of the components of the $^3\Sigma$ level plotted against K. Only two components of the triplet, *viz.* $J=K-1$ and $J=K+1$ are shown, marked by plain and circled crosses, respectively. The third component $J=K$ is too far distant to appear in the figure, but would be represented by a series of points parallel to the K axis at ordinate 0 (scale on left in cm^{-1}). The data are taken from Dieke and Babcock's measurements[5] of the B band of atmospheric oxygen. This band has been chosen in preference to the A band, with which Kramers originally compared his formula, because Dieke and Babcock assign greater weight to their determinations of wave-length in the B band. In any case the intervals derived from the two bands differ only slightly, and the A band could have been taken without materially affecting the conclusions.

The dotted line (a) in the figure gives the levels as calculated from Kramers' formula (1), using the commonly accepted values of the parameters $\lambda=0.726$ cm^{-1}, $\mu=-0.025$ cm^{-1}. The *ad hoc* shift mentioned above has here been taken account of by lowering the levels $J=K\pm1$ by 1.21 cm^{-1}. Even with this shift the agreement is very poor indeed.

Approximate values for the parameters which will give better agreement can be obtained from a rough consideration of the points representing the observations. From (1) we see that $-\mu$ is the asymptotic slope of W_{K-1} plotted against K; and also that the interval between W_K and the mean of W_{K+1} for $K=K'-2$ and W_{K-1} for $K=K'$ is independent of K' and equal to $-\lambda-\mu/2$. If we take the asymptotic slope from the observations as 0.08 cm^{-1} in 10 units of K, and note that the interval in question is actually approximately constant, having a mean value -1.981 cm^{-1}, we find $\lambda=1.985$ cm^{-1}, $\mu=-0.008$ cm^{-1}. The broken lines (b) in the figure give the energy levels calculated from (1) as functions of K, with these values of the parameters. The agreement, although better than before, is still poor, especially at lower values of K; in particular, the intersection of W_{K+1} and W_{K-1} falls near $K=11$ instead of near $K=6$. I am indebted to Professor Kramers for the information that he had himself noted that his formula as it

[5] G. H. Dieke and H. D. Babcock, Proc. Nat. Acad. Sci. **13**, 670 (1927).

stands could be made to agree moderately well with the observations at large values of K; but he did not place much weight on this agreement, and did not publish the corresponding values of the parameters, as the formula fitted very badly at low values of K, where the experimental points were believed to be more reliable.

3. Correction to Kramers' Formula

Kramers himself indicated a possible cause for the failure of his formula in oxygen, but did not pursue the question. The formula is exact only as far as the first power of the ratio of the fine structure separations to the rotational separations, or in other words, is valid when the $^3\Sigma$ state considered conforms closely to Hund's case (b), where the spin is almost completely decoupled from the axis of figure. This is more likely to be the case in molecules with small moments of inertia, such as the hydrides, than in oxygen.

The correction to be made, assuming that the cause of the fine structure is the spin-spin interaction of the uncompensated electrons, has been given implicitly by Hill and Van Vleck,[6] starting from case (b) as the unperturbed system, and also by the author,[7] starting from case (a). After superposition of the terms representing the coupling of the spin and the magnetic field due to rotation, the formulae for the fine structure are as follows.

$$\begin{aligned} W_{K+1} &= W_0+(2K+3)B-\lambda \\ &\quad -[(2K+3)^2B^2+\lambda^2-2\lambda B]^{\frac{1}{2}}+\mu(K+1), \\ W_K &= W_0, \qquad (2) \\ W_{K-1} &= W_0-(2K-1)B-\lambda \\ &\quad +[(2K-1)^2B^2+\lambda^2-2\lambda B]^{\frac{1}{2}}-\mu K, \end{aligned}$$

where B is the usual constant $h^2/8\pi^2I$, and λ and μ are the parameters introduced above. These expressions agree with Kramers' formula as far as the first power of λ.

If we assume that the cause of the fine structure is the interaction between $^3\Sigma$ and $^3\Pi$ states, it is easy to show from the secular determinant of the problem, given by Hebb,[4] that when the fine structure is no longer small compared with the rotational separation, it is given by formulae of exactly the same form as (2), provided the $^3\Pi$ states are sufficiently remote from the $^3\Sigma$ state, and the terms in μ are much smaller than those in λ. To show this, it is only necessary to diagonalize that part of Hebb's determinant referring to $^3\Sigma$, then to take account approximately of interaction with $^3\Pi$ by putting the appropriate first order terms in $1/h\nu(\Sigma\Pi)$ on the diagonal, and finally to solve the secular problem involving the three $^3\Sigma$ states accurately as regards λ, supposing μ to be small, so that only the terms linear in μ are retained. Thus the agreement between the fine structure formulae arising from two completely different mechanisms, which was noted by Hebb to hold as far as the first powers of λ and μ, holds even when higher powers of λ are included; in oxygen μ turns out to be so much smaller than λ that the neglect of higher powers of μ seems perfectly legitimate.

4. Comparison of the Corrected Formula with the Observed Fine Structure in Oxygen

It is of interest to see whether the observations can be represented more accurately by the corrected formula (2) applicable when the fine structure and rotational separations are comparable, than with Kramers' formula (1), which assumes almost complete rotational decoupling of the spin. It will be noticed that the asymptotic slope and the mean of the levels $J=K\pm1$ determine λ and μ in exactly the same way as before (§2), and lead to the same numerical values of these parameters.

The full lines (c) in Fig. 1 represent the levels $J=K\pm1$ plotted from formula (2) with the values $\lambda=1.985$ cm^{-1}, $\mu=-0.008$ cm^{-1}. The constant B for the ground state of the oxygen molecule has been taken as 1.438 cm^{-1}. The component $J=K$ is at ordinate 0. Agreement with the experimental points is most satisfactory, especially when regard is had to the open scale of ordinates which has been adopted. The intersection of $J=K\pm1$ is now accurately reproduced.

The conclusion is that Kramers' formula, suitably corrected, is adequate to represent the fine structure of the $^3\Sigma$ state in oxygen quantitatively, but the values of the parameters differ considerably from those usually assumed.

[6] E. L. Hill and J. H. Van Vleck, Phys. Rev. **32**, 250 (1928).
[7] R. Schlapp, Phys. Rev. **39**, 806 (1932).

In the hydride molecules NH, PH, PD, OH^+, Kramers' original formula has been found to represent the fine structure sufficiently well; this is what one would expect in view of the smallness of the moment of inertia for these molecules, which makes the constant B large, so that (2) differs little from (1).

5. Intensity Distribution in $^1\Sigma \leftrightarrow {}^3\Sigma$ Bands

Van Vleck[8] has shown that these bands are associated with magnetic dipole transitions rather than with electric dipole transitions of the ordinary type. This fundamental modification of earlier views regarding the nature of these bands does not however invalidate the intensity formulae given by the author.[7] These formulae were based on the assumption of complete decoupling of the spin from the molecular axis. It has been seen above that as regards energy levels this assumption is certainly inadequate, at least in oxygen, and even the next approximation, in which only the first power of λ is retained, is insufficient. We may therefore expect that the incomplete decoupling will have an influence on the intensities.

The origin of the intersystem transitions is that orbit-spin interaction of the type $\Sigma a_i(l_i s_i)$ rather than $A(L\cdot S)$ blends the $^1\Sigma$ state with $^3\Pi$ states, and the $^3\Sigma$ state with $^3\Pi$ and $^1\Pi$ states. It is the blending of $^1\Sigma$ with $^3\Pi$, and of $^3\Sigma$ with $^1\Pi$ that makes intersystem transitions possible, the blending of $^3\Sigma$ with $^3\Pi$ gives no contribution to the intensity of these transitions. It is therefore justifiable to confine attention to the $^3\Sigma$ states (appropriately modified by blending with $^1\Pi$) without considering interaction with $^3\Pi$ in calculating intensities. In the paper referred to above,[7] the intensities were calculated for pure case (b), corresponding to $\lambda/B=0$. It is a comparatively simple matter to recalculate the intensities for any given value of λ/B. It is found at once that the rotational intensity distribution in the branches ${}^RR$, ${}^PP$ is independent of the value of λ/B, i.e., of whether the $^3\Sigma$ state is case (a) or case (b) or intermediate between them. On the other hand the intensity distribution in ${}^PQ$ and ${}^RQ$ depends on the value of λ/B. For $\lambda/B=4/3$, which is roughly the value in oxygen, the intensities in these branches for larger values of J are approximately $\frac{1}{2}(J+\frac{3}{4})$ and $\frac{1}{2}(J+\frac{1}{4})$, respectively, being given for any value of J by the expressions

$$2J(J+1)(2J+1)[8J^2+8J+1 \pm(16J^2+16J+1)^{\frac{1}{2}}] \div[64J^4+128J^3+84J^2+20J+1 \pm(12J^2+12J+1)(16J^2+16J+1)^{\frac{1}{2}}],$$

which do not however differ appreciably from the asymptotic values $\frac{1}{2}(J+\frac{3}{4})$, $\frac{1}{2}(J+\frac{1}{4})$ from $J=2$ upwards.

Table I. *Comparison of experimental and calculated intensities.*

Branch	Intensity				
	Obs.[10]	Obs.[9]	Calc. $\lambda/B=0$[7]	4/3	2
${}^PP={}^PS$	$\frac{1}{2}(J+2)$	$\frac{1}{2}(J+2)$	$\frac{1}{2}(J+2)$	$\frac{1}{2}(J+2)$	$\frac{1}{2}(J+2)$
${}^PQ={}^PS$	$\frac{1}{2}(J+1)$	$\frac{1}{2}(J+1)$	$\frac{1}{2}J$	$\frac{1}{2}(J+\frac{1}{2})$*	$\frac{1}{2}(J+1)$
${}^RQ={}^RS$	$\frac{1}{2}J$	$\frac{1}{2}(J+1)$	$\frac{1}{2}(J+1)$	$\frac{1}{2}(J+\frac{1}{2})$*	$\frac{1}{2}J$
${}^RR={}^RS$	$\frac{1}{2}(J-1)$	$\frac{1}{2}(J-1)$	$\frac{1}{2}(J-1)$	$\frac{1}{2}(J-1)$	$\frac{1}{2}(J-1)$

* Asymptotic values.

With $\lambda/B=2$ the calculated intensities in ${}^PQ$ and ${}^RQ$ are, respectively, $\frac{1}{2}(J+1)$ and $\frac{1}{2}J$, as contrasted with $\frac{1}{2}J$ and $\frac{1}{2}(J+1)$, respectively, for $\lambda/B=0$. It also appears that for a value of λ/B intermediate between 4/3 and 0 the calculated intensities of the two branches should be equal (as Childs and Mecke[9] have concluded them to be from their experiments) for all but the smallest values of J.

Although the intensity measurements are not sufficiently consistent to give an independent determination of λ/B, it is satisfactory that the experimental intensities given by Childs and Mecke are reproduced rather more accurately with the value of λ/B deduced from the energy levels (approximately 4/3) than with $\lambda/B=0$. In this connection it is not without interest to note that in their preliminary report[10] Childs and Mecke gave the intensities of the two branches ${}^PQ$ and ${}^RQ$ as $\frac{1}{2}(J+1)$ and $\frac{1}{2}J$, respectively.

For convenience Table I is given showing the experimental intensities according to Childs and Mecke, and the calculated intensities on the various hypotheses as to the value of λ/B.

I wish to record my thanks to Professor Van Vleck for valuable discussions.

[5] J. H. Van Vleck, Astrophys. J. **80**, 101 (1934).

[9] W. H. J. Childs and R. Mecke, Zeits. f. Physik **68**, 344 (1931).

[10] W. H. J. Childs and R. Mecke, Nature **125**, 599 (1930).

The Photoelectric Work Functions of the 211 and 310 Planes of Tungsten

C. E. MENDENHALL AND CHARLES F. DEVOE*
University of Wisconsin, Madison, Wisconsin

(Received December 15, 1936)

The work functions of a 211 and a 310 plane on one tungsten crystal were determined using Fowler's method. Since the time necessary thoroughly to outgas the crystal would have been very great, the photocurrents characteristics of the clean surfaces were determined from data obtained soon after the crystal was flashed at about 2200°C. The work function of the 211 plane was found to be 4.50 volts and that for the 310 plane to be 4.35 volts.

SEVERAL experiments[1–5] with copper and zinc crystals have shown the dependence of the photoelectric work function on the crystal structure of the surface, but because of the high vapor pressure and low melting point of both copper and zinc the crystals could not have been heated at high temperatures and therefore may not have been well outgassed. The purpose of this experiment was to study a crystal which could be heated at high temperatures without damage.

APPARATUS

The crystal about eleven mm long with a hexagonal cross section of about 3 mm diameter had six natural faces, two 211 planes, two 310 planes, and two "mixture" planes.

The experimental tube evolved in several steps from a simple tube in which the crystal was mounted on a vertical shaft in a collecting cylinder. It was heated by electron bombardment from a filament mounted inside the cylinder. After several months of outgassing, it was found necessary to isolate the bombarding region from the region where photoelectric measurements were made because the high potential (2000 volts) necessary for bombardment polarized and charged the Pyrex walls of the tube to the extent that the amplifier was unsteady and photocurrent measurements impossible for at least a week after the potential was removed. When the tube was heated at about 400°C the amplifier became steady in a very short time due to the increased conductivity of the glass.

In the final tube shown in Fig. 1 the crystal *A* was so mounted on a vertical shaft that it could be placed in the molybdenum collecting cylinder *B* and rotated magnetically to permit photoelectric measurements on any one of the faces of the crystal, or it could be lifted into the molybdenum cylinder *C* where it was heated by electron bombardment from the tungsten filament *D*. The bombarding potential was applied to the filament and cylinder to allow the crystal and mounting assembly to remain at ground potential, thus preventing polarization of the Pyrex below the bombarding region. A grounded platinum guard ring *E* fused to the inner wall of the tube prevented surface leakage along the tube. A bottom in the cylinder *C* prevented space charge leakage into the lower region of the tube. The hole through which the crystal entered the cylinder was covered by a platinum coated molybdenum disk mounted on the shaft which supported the crystal. The soft iron ring *F* moved along molybdenum wire guides on the Pyrex tube which supported the crystal mounting. These wire guides were found necessary, for when the ring was allowed to slide on the Pyrex the amplifier was very unsteady for several days after the crystal was lowered.

Two complete Pyrex vacuum systems, each consisting of two liquid-air traps in series (the ones nearest the tube were cooled only after the major part of the outgassing had been completed) and a water-cooled mercury diffusion pump were connected in parallel to the tube. One system had a bore of $1\frac{1}{4}''$ and the other $1''$. A forepump was connected through a liquid air trap to the mercury pumps. The pressure was measured with an ionization gauge.

* The junior author who was a research assistant to the late Dr. C. E. Mendenhall completed the experiment and wrote this report.

[1] J. H. Dillon, Phys. Rev. **38**, 408 (1931).
[2] E. G. Linder, Phys. Rev. **30**, 649 (1927).
[3] A. Nitzche, Ann. d. Physik **5**, 14, 463 (1932).
[4] B. A. Rose, Phys. Rev. **44**, 585 (1933).
[5] N. Underwood, Phys. Rev. **47**, 502 (1935).

The light source was a water-cooled quartz capillary mercury arc[6] used with a Leiss double prism quartz monochromator. The monochromator, arc, and auxiliary lenses were mounted on a heavy cast iron base provided with two lateral crossed motions and a rotation about a vertical axis so that the light could be thrown either onto the crystal surface for photocurrent measurement or onto the receiver of a vacuum thermopile. The quartz window on the thermopile was identical to that on the photoelectric tube, thus the optical paths were as nearly as possible identical. Thermopile readings were made with a Kipp type Zc galvanometer at a scale distance of three meters. The sensitivity of the thermopile was determined after each set of observations by radiation from a pyrometer lamp which had been calibrated by comparison with a standard lamp.

The photocurrents were measured with a modification of the Barth[7] circuit using a Western Electric D96,475 tube. The tube and high resistances were mounted in the evacuated brass chamber *H* (Fig. 1) which also enclosed the seal connection to the collecting cylinder; thus the entire photocurrent lead was in a vacuum. The high resistances and a ground lead were mounted on a clear Bakelite block inside the vacuum chamber in such a way that an externally controlled contact arm could shunt the tube with any one of the resistances or the ground lead. The ratios of the resistances were determined several times during the experiment by comparing the deflections produced with the tube shunted by each resistance when one face of the crystal was illuminated by light of the same wave-length and intensity. Since these ratios remained constant the absolute values of the resistances were probably constant. The voltage sensitivity of the amplifier (140,000 mm/volt maximum) was measured after each set of photocurrent measurements.

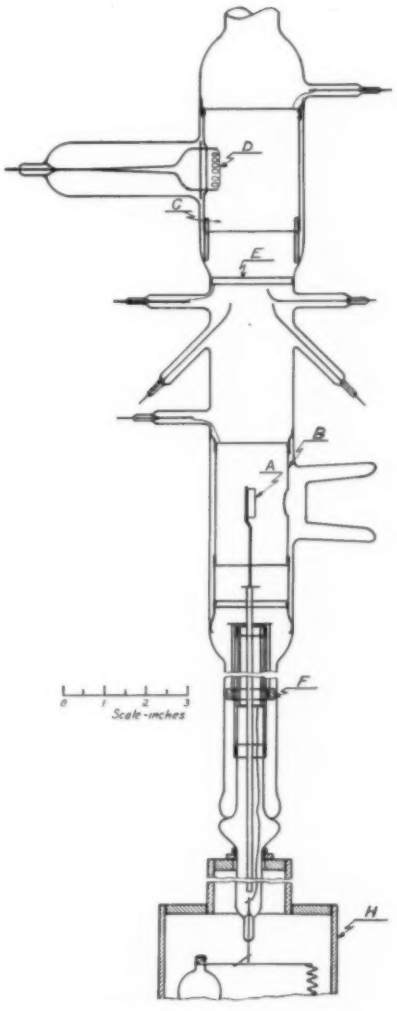

FIG. 1. Diagram of experimental tube.

PROCEDURE

Because of difficulties in the construction of the photoelectric tube, the tube has been rebuilt five times. The following procedure described in detail was the treatment since the tube was last rebuilt, but is characteristic of the procedure throughout the experiment. The crystal had been heated for a total of more than 20,000 hours at temperatures above 1000°C prior to the last rebuild.

Before the tube was assembled the last time, an x-ray comparison of the heated crystal with a half of the original crystal which had not been heated showed that it had not been damaged by the heat treatment. The authors are indebted

[6] F. Daniels, and L. J. Heidt, J. Am. Chem. Soc. **54**, 2381 (1932).
[7] G. Barth, Zeits. f. Physik **87**, 399 (1934).

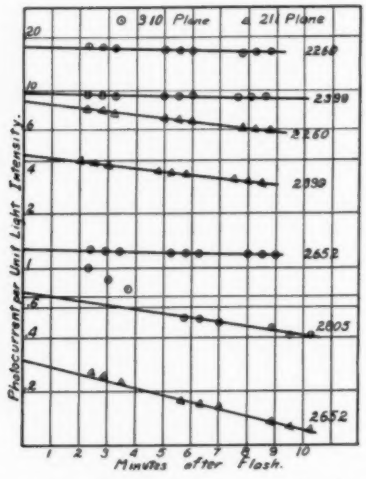

FIG. 2. Monochromatic fatigue curves for the two crystal planes.

to Dr. J. D. Hanawalt of the Dow Chemical Company for this comparison.

The two cylinders and the crystal mounting assembly were heated to bright red in auxiliary vacuum systems until pressures less than 5×10^{-7} mm were attained with the parts heated. They were then quickly transferred to the photoelectric tube and connected to the main system. The tube was baked at 450°C until a pressure of 2×10^{-8} mm was obtained with the tube hot; this required about five weeks. During this period the remaining parts of the vacuum system were heated with a hand torch. The crystal was then placed in the cylinder *C* and bombarded. The temperature was increased at such a rate that the pressure never exceeded 10^{-7} mm. After heating the crystal for three months the pressure was 2×10^{-8} mm with the crystal at about 1500°C. When it was heated continuously at higher temperatures the tube became sufficiently warm that danger of alkali contamination from the Pyrex became appreciable. The crystal was then flashed at 2200°C for 7 seconds once per minute for 1500 hours by a motor driven switch. The temperature of the crystal between flashes was about 1400°C. The pressure remained less than 3×10^{-8} mm during the flash. During the last 1500 hours' outgassing the collecting cylinder was heated very rapidly to a cherry red with an induction furnace. Since the cylinder was supported by legs in contact with the tube, it could be heated only for a very short time and then allowed to cool before another flashing.

An unreasonably long time would have been required to outgas the entire crystal to the same extent that thin strip filaments could be outgassed, since the crystal was many times thicker than filaments which must be heated for at least 1000 hours. However, since the photoelectric effect is a surface phenomenon, it seemed reasonable to measure the photocurrent which would be emitted by the clean surface by extrapolating to zero time the curve obtained by plotting the log of the photocurrent per unit light intensity emitted by the surface as a function of the time after the crystal had been flashed at 2200°C. The long wave limit at absolute zero of each surface was obtained by plotting these extrapolated values in Fowler[8] coordinates and fitting the experimental and theoretical curves in the usual way.

RESULTS

In Fig. 2 the log of the photocurrent per unit light intensity emitted when each of the two crystal surfaces was illuminated by light having the wave-lengths indicated is plotted as a function of the time after the crystal was flashed. These curves show that the higher work function plane (211) points represented by Δ fatigues more rapidly than the other plane (310) points repre-

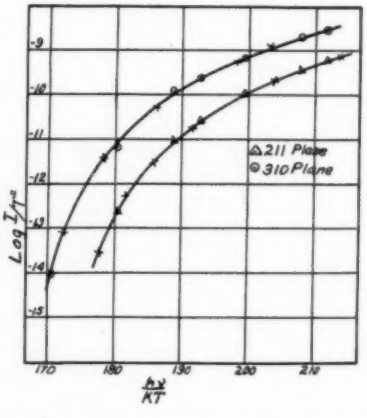

FIG. 3. Photocurrents plotted in Fowler coordinates. The crosses are Fowler theoretical values; the other points are experimental values.

[8] R. H. Fowler, Phys. Rev. **38**, 45 (1931).

sented by circles. As the wave-length of the exciting light approaches the long wave limit of the surface, the experimental points for the first few minutes after the flash deviate to a greater extent from the straight lines determined by the later points. This deviation is undoubtedly due to the fact that the crystal had not cooled to room temperature when the first measurements were made.

In Fig. 3 the extrapolated values of the photocurrents per unit light intensity are plotted in Fowler coordinates. The curves are the shifted theoretical curves, while the points are experimental. The long wave limit at absolute zero was 2840A for the 310 plane and 2740A for the 211 plane. These correspond to 4.35 and 4.50 volts, respectively.

Although the experimental points shown in Fig. 2 for both planes fit the theoretical curve very well, the experimental points for the 211 plane taken four hours after flashing do not fit the Fowler curve, while points obtained at the same time for the 310 plane do fit the curve as shown in Fig. 4. The long wave limit for the 310 plane as given by this curve is 2660A, which corresponds to 4.64 volts, an increase of about 0.3 volt.

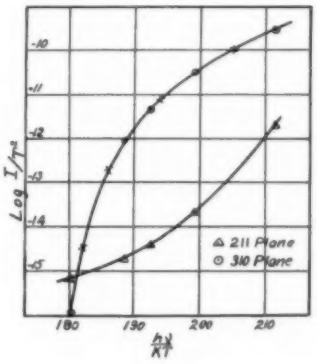

FIG. 4. Fowler plot of the photocurrents taken four hours after the crystal was flashed. The crosses are Fowler theoretical values; the other points are experimental.

The authors are indebted to Dr. H. B. Wahlin for many helpful suggestions, and to the Wisconsin Alumni Research Foundation who sponsored the research assistantship.

MARCH 1, 1937 PHYSICAL REVIEW VOLUME 51

On the Calculation of Errors

LLOYD T. DEVORE
Pennsylvania State College, State College, Pennsylvania

(Received October 24, 1936)

An exact analysis is developed for the calculation of erratic experimental errors. Methods of calculation which have been used are examined and criticized. The analysis developed here is applied to the specific case of the determination of erratic errors resulting from disturbances in a galvanometer system. The formulae here obained reduce, in a second approximation, to the formulae obtained by Zernicke. It is shown that these approximate formulae are too inexact to be used in cases in which the number of observations is small. The exact formulae and more accurate approximations are worked out in detail.

IN conducting experimental investigations it is desirable to be able to use the data obtained to calculate the errors in the measurements which result from erratic disturbances or changes occurring during the course of the experiment. The purpose of this paper is to indicate the general procedure which must be followed in using the data to arrive at the most exact expression for the average resultant error. This problem has been attacked by Zernicke[1] and his method has been reviewed by Barnes and Silverman[2] but owing to a lack of generality in their treatment, resulting from unnecessarily stringent conditions imposed by their statistical assumptions, their results are only approximations to the more exact calculations and may, under

[1] F. Zernicke, Zeits. f. Physik **79**, 516 (1932).
[2] Barnes and Silverman, Rev. Mod. Phys. **6**, 185 (1934).

certain experimental conditions, become very bad approximations. These criticisms will be elaborated somewhat more in detail at appropriate places in the ensuing analysis. The discussion is greatly facilitated by resorting to an illustrative example; accordingly, the galvanometer, which has been treated so often in the literature, will be selected as a typical example.

In the case of the galvanometer it is well known that the Brownian motion in the system is the disturbance which ultimately limits its sensitivity as a measuring instrument, but, for the purposes of the present discussion, such explicitness is superfluous. The arguments to be presented hold quite generally where the disturbances are perfectly random and arise from any external stimulus whatever. First, a few remarks about the manner in which the error is to be represented. If the disturbances are perfectly erratic and the average taken over an infinite number of observations on a given reading of the instrument the average error is obviously zero, for the positive errors will be offset by the negative errors. In errors of this type, i.e., errors which are distributed at random with regard to both magnitude and sign, it is customary to determine the mean square error. The method furnished by the calculus for computing the mean square error, for an instrument which integrates all of the random disturbances, will serve as a guide in computing the mean square error for an instrument in which a set of isolated readings are taken. The deflection of the galvanometer, resulting from these random disturbances, will be a function of the time and may, at any instant, be represented by $r(t)$. The mean square deflection (error) resulting from these random disturbances in any interval $0 \rightarrow T$ will then be, for the integrating instrument,

$$\epsilon_I^2 = \left[\frac{\int_0^T r(t)dt}{T}\right]^2_{\text{ave}} = \frac{\int_0^T \int_0^T [r(\xi)r(\eta)d\xi d\eta]_{\text{ave}}}{T^2} \quad (1)$$

and the corresponding expression, for the instrument in which only a set of isolated readings are taken,

$$\epsilon_\Sigma^2 = (R_0 + R_1 + R_2 + \cdots + R_N)^2_{\text{ave}}/N^2, \quad (2)$$

where $R_0, R_1, R_2, \cdots, R_N$ are the readings taken at times $t_0, t_1, t_2, \cdots, t_N$. The right-hand side of (2) may be expressed in a more compact notation

$$\epsilon_\Sigma^2 = \sum_{i=0}^{N} \sum_{j=0}^{N} (R_i R_j)_{\text{ave}}/N^2. \quad (3)$$

It is desirable to represent the error with the latter notation for two reasons: (1) it stresses the analogy between the discreet and the continuous representations, and (2) it is essentially the most exact notation since, as will be demonstrated subsequently, the factors of the cross-product terms in the expansion of the double sum are not commutable, i.e.,

$$(R_i R_j)_{\text{ave}} \neq (R_j R_i)_{\text{ave}}. \quad (4)$$

This latter point is to be especially emphasized because the analysis made by the authors previously mentioned[1, 2] does not bring out this important point.

After the establishment of the manner in which the error is to be represented, the problem now is to demonstrate how the terms $(R_i R_j)_{\text{ave}}$ are to be calculated. The equation of motion of the galvanometer suspension may be written

$$I\ddot{r} + \beta\dot{r} + K^2 r = f(t), \quad (5)$$

where r is the deflection of the galvanometer suspension; I the moment of inertia; β the resisting torque per unit angular velocity; K^2 the restoring torque per unit angular deflection; and $f(t)$ is the fluctuating disturbance. The general solution of this equation is

$$r(t) = \frac{R_i}{m_1 - m_2}[m_1 e^{m_2 t} - m_2 e^{m_1 t}] + \frac{\Omega_i}{m_1 - m_2}[e^{m_1 t} - e^{m_2 t}] + \frac{1}{m_1 - m_2}\int_0^t [e^{m_1(t-\xi)} - e^{m_2(t-\xi)}]g(\xi)d\xi, \quad (6)$$

where $g(\xi) = f(\xi)/I$ and m_1 and m_2 are roots of the equation

$$Im^2 + \beta m + K^2 = 0. \quad (7)$$

R_i and Ω_i are the deflection and angular velocity respectively at $t = 0$. The reason for subscripting the initial constants with an i rather than with the customary zero will become evident directly.

The averaging process will not be explained. Suppose that simultaneous records are made of the random fluctuations of a very large number of identical galvanometers, each subject to its own independent disturbances. From this set of records a subset is selected, the subset being characterized by the fact that at some arbitrarily chosen instant of time, which may be called the initial time, every member of the subset has the same deflection. The averages to be mentioned hereafter are to be interpreted as averages taken over such a subset as the one described above unless otherwise stated. Another view which will lead to identically the same results is alternatively to regard the records as having been obtained by a very great number of repetitions of the same experiment with just one galvanometer. Then the average characteristics of this galvanometer will be obtained by treating this set of records in the same manner as was described for the previous case in which the records were obtained from many galvanometers. In either case it is clear that the subset is not in any way identified with either the initial velocity or the initial value of the fluctuating torque, i.e., the initial velocity and initial torque may be any values whatever and since they are perfectly random their resultants for the subset must necessarily be identically zero. The number of records to be taken in the hypothetical experiments is determined by the conditions that the averages over the subset of the initial velocity and initial disturbances are to be simultaneously zero for each initial deflection. Since an infinite number of hypothetical experiments may be performed it is always assured that the statistical conditions are perfectly satisfied. It is in connection with the averaging process that the essential weakness of Zernicke's method arises. He has assumed that $[f(t)]_{\text{ave}}=(\Omega_i)_{\text{ave}}=0$ and obtained his averages by taking averages over the finite number of readings taken within a finite time interval on the instrument. It is clear that the assumptions are very poor and the calculations based upon this averaging process may be greatly in error for small numbers of readings and small time intervals. It is, however, an unfortunate consequence of the refinement indicated for the averaging process that the correlation coefficient used so fruitfully by Zernicke loses its significance.

It is now possible to arrive at the value of $(R_iR_j)_{\text{ave}}$. The solution of the equation of motion for the instant $t=t_j$ is

$$R_j=\frac{R_i}{m_1-m_2}[m_1e^{m_2t_j}-m_2e^{m_1t_j}]+\frac{\Omega_i}{m_1-m_2}[e^{m_1t_j}-e^{m_2t_j}]+\frac{1}{m_1-m_2}\int_0^{t_j}[e^{m_1(t_j-\xi)}-e^{m_2(t_j-\xi)}]g(\xi)d\xi. \quad (8)$$

Averaging (8)

$$(R_j)_{\text{ave }R_i}=\frac{R_i}{m_1-m_2}[m_1e^{m_2(t_j-t_i)}-m_2e^{m_1(t_j-t_i)}], \quad (9)$$

since, as has already been explained, $(\Omega_i)_{\text{ave }Ri}=(g(\xi))_{\text{ave }Ri}=0$. The notation is designed to signify that the average has been taken over a subset characterized by members whose initial displacements are R_i. It follows immediately, since R_i is here regarded as a constant, that

$$(R_iR_j)_{\text{ave }R_i}=\frac{R_i^2}{m_1-m_2}[m_1e^{m_2(t_j-t_i)}-m_2e^{m_1(t_j-t_i)}]. \quad (10)$$

The interpretation of (9) may be given as follows. From the infinite number of hypothetical experiments implied all the records are discarded except those whose initial displacements were R_i. This latter group of records is then averaged after an interval (t_j-t_i) and the average displacement is found to be that indicated by (9). Eq. (10) indicates no correlation between either initial displacement and initial velocity or initial displacement and initial torque. This, of course, is a direct consequence of the statistical conditions.

Now every reading must be considered as initial reading and hence, when the jth reading is taken subsequent to a previous ith reading, the solution of the equation of motion appropriate to negative times must be used in calculating $(R_jR_i)_{\text{ave }R_j}$. It is readily proven

$$(R_i)_{\text{ave }R_j}=\frac{R_j}{m_1-m_2}[m_1e^{m_2(t_i-t_j)}-m_2e^{m_1(t_i-t_j)}] \quad (11)$$

and

$$(R_jR_i)_{\text{ave }R_j}=\frac{R_j^2}{m_1-m_2}[m_1e^{m_2(t_i-t_j)}-m_2e^{m_1(t_i-t_j)}]. \quad (12)$$

Here (11) and (12) may be subjected to the same type of physical interpretations as were applied to (9) and (10), the only difference being a reversal of the direction in which the events are viewed along the time axis.

It is now clear from (10) and (12) that the factors of the cross product terms in the expansion of (3) are not commutable. In other words, (4) has been established since $R_i^2 \neq R_j^2$.

The calculation of the error in determining the zero of a galvanometer from a group of N equally timed readings taken at times $t_0, t_1, t_2, \cdots, t_{N-1}$ will now be carried out.

$$\epsilon_\Sigma^2 = \frac{1}{m_1 - m_2} \sum_{i=0}^{N-1} \sum_{j=0}^{N-1} \frac{R_i^2}{N^2} \times [m_1 e^{m_2(t_i - t_j)} - m_2 e^{m_1(t_i - t_j)}]. \quad (13)$$

Summing over the j's, let $(t_{i+1} - t_i) = S$, then

$$\epsilon_\Sigma^2 = \frac{1}{N^2(m_1 - m_2)} \sum_{i=0}^{N-1} R_i^2 \times \left\{ m_1 \left[\frac{1 - e^{m_2 S} - e^{m_2(i+1)S} - e^{m_2(N-i)S}}{1 - e^{m_2 S}} \right] - m_2 \left[\frac{1 + e^{m_1 S} - e^{m_1(i+1)S} - e^{m_1(N-i)S}}{1 - e^{m_1 S}} \right] \right\}. \quad (14)$$

This expression (14) cannot be summed over the i's because the R_i's are a set of unknown coefficients in the series. Actually, the R_i's are the experimental readings taken from the instrument and for a very small number of readings it would not necessarily be an unreasonable task to substitute directly into (14) and add the series thus obtained arithmetically to obtain ϵ_Σ^2. In most cases, however, even for a comparatively limited number of readings, this procedure is much too laborious. A much better method consists in transforming the original series into a very rapidly convergent form. This may be accomplished as follows. Let

$$(IS) = [m_1 e^{Im_2 S} - m_2 e^{Im_1 S}],$$

then

$$N^2 \epsilon_\Sigma^2 = [R_0^2 + R_1^2 + R_2^2 + \cdots + R_{N-1}^2] + [R_0^2 + 2R_1^2 + 2R_2^2 + \cdots + 2R_{N-2}^2 + R_{N-1}^2](1S) + [R_0^2 + R_1^2 + 2R_2^2 + 2R_3^2 + \cdots + 2R_{N-3}^2 + R_{N-2}^2 + R_{N-1}^2](2S) + \cdots + [R_0^2 + R_1^2 + R_2^2 + \cdots + R_{i-1}^2 + 2R_i^2 + \cdots + 2R_{N-i-1}^2 + R_{N-i}^2 + \cdots + R_{N-1}^2](iS) + \cdots. \quad (15)$$

Collecting terms in (15) and grouping them into sums,

$$N^2 \epsilon_\Sigma^2 = \sum_{i=0}^{N-1} R_i^2 + \{2 \sum_{i=0}^{N-1} R_i^2 - (R_0^2 + R_{N-1}^2)\}(1S) + \{2 \sum_{i=0}^{N-1} R_i^2 - (R_0^2 + R_1^2 + R_{N-2}^2 + R_{N-1}^2)\}(2S) + \{2 \sum_{i=0}^{N-1} R_i^2 - (R_0^2 + R_1^2 + R_2^2 + R_{N-3}^2 + R_{N-2}^2 + R_{N-1}^2)\}(3S) + \cdots + \{2 \sum_{i=0}^{N-1} R_i^2 - [\sum_{j=0}^{I} (R_j^2 - R_{N-1-j}^2)]\}(I+1)S + \cdots. \quad (16)$$

Now let

$$\sum_{i=0}^{N-1} \frac{R_i^2}{N} = R_{\text{ave}}^2$$

where the type of average is defined by the equation as an average taken over the number of observations made in the experiment. Then summing (16) in a vertical direction the result obtained is

$$N \epsilon_\Sigma^2 = R_{\text{ave}}^2 + 2R_{\text{ave}}^2 \sum_{K=1}^{N-1} (KS) - \frac{(R_0^2 + R_{N-1}^2)}{N} \sum_{K=1}^{N-1} (KS) - \frac{(R_1^2 + R_{N-2}^2)}{N} \sum_{K=2}^{N-1} (KS) - \frac{(R_2^2 + R_{N-3}^2)}{N} \sum_{K=3}^{N-1} (KS) - \cdots - \frac{(R_i^2 + R_{N-1-i}^2)}{N} \sum_{K=i+1}^{N-1} (KS) - \cdots. \quad (17)$$

Carrying out the summation where indicated, (17) becomes finally

$$N\epsilon_\Sigma^2 = R^2_{\text{ave}}\left\{1+\frac{2}{m_1-m_2}\left[m_1\left(\frac{e^{Nm_2S}-e^{m_2S}}{e^{m_2S}-1}\right)\right.\right.$$

$$\left.\left.-m_2\left(\frac{e^{Nm_1S}-e^{m_1S}}{e^{m_1S}-1}\right)\right]\right\}-\frac{R_0^2+R^2_{N-1}}{N(m_1-m_2)}$$

$$\times\left[m_1\left(\frac{e^{Nm_2S}-e^{m_2S}}{e^{m_2S}-1}\right)-m_2\left(\frac{e^{Nm_1S}-e^{m_1S}}{e^{m_1S}-1}\right)\right]$$

$$-\frac{(R_1^2+R^2_{N-2})}{N(m_1-m_2)}\left[m_1\left(\frac{e^{Nm_2S}-e^{2m_2S}}{e^{m_2S}-1}\right)\right.$$

$$\left.-m_2\left(\frac{e^{Nm_1S}-e^{2m_1S}}{e^{m_1S}-1}\right)\right]-\cdots$$

$$-\frac{(R^2_{I+1}+R^2_{N-1})}{N(m_1-m_2)}\left[m_1\left(\frac{e^{Nm_2S}-e^{Im_2S}}{e^{m_2S}-1}\right)\right.$$

$$\left.-m_2\left(\frac{e^{Nm_1S}-e^{Im_1S}}{e^{m_1S}-1}\right)\right]-\cdots. \quad (18)$$

Eq. (18) may be transformed into a slightly more compact form

$$N\epsilon_\Sigma^2 = R^2_{\text{ave}}\left\{1+\frac{1}{m_1-m_2}\left[\frac{m_1e^{Nm_2S}}{e^{m_2S}-1}-\frac{m_2e^{Nm_1S}}{e^{m_1S}-1}\right]\right.$$

$$\left.+\frac{2}{m_1-m_2}\left[\frac{m_2}{1-e^{-m_1S}}-\frac{m_1}{1-e^{-m_2S}}\right]\right\}-\frac{1}{N(m_1-m_2)}$$

$$\times\left\{\begin{aligned}&\frac{m_2}{e^{m_1S}-1}[(R_0^2+R^2_{N-1})e^{m_1S}\\&\quad+(R_1^2+R^2_{N-2})e^{2m_1S}+\cdots\\&\qquad+(R^2_{I+1}+R^2_{N-I})e^{Im_1S}+\cdots\\&-\frac{m_1}{e^{m_2S}-1}[(R_0^2+R^2_{N-1})e^{m_2S}\\&\quad+(R_1^2+R^2_{N-2})e^{2m_1S}+\cdots\\&\qquad+(R^2_{I+1}+R^2_{N-I})e^{Im_2S}+\cdots.\end{aligned}\right. \quad (18a)$$

Eq. (18) are exact formulae and could be applied to yield the theoretically most accurate estimate of the experimental error. To use them exactly would again involve too much labor; their advantage lies in the fact that, for a given period of observation S, they converge very rapidly for moderately large values of N. The first large bracketed expression is the main term of the expansion and the subsequent terms may be regarded as correction terms. The number of correction terms carried in the calculation is determined by the precision desired. An examination of (18a) shows how the series converges so rapidly. If N is large enough, i.e., for

$$e^{Nm_1S} \ll e^{Im_1S}$$

and $e^{Nm_2S} \ll e^{Im_2S}$, where I is small.

[Since m_1 and m_2 contain real parts which are negative—see Eq. (7)] an approximate formula may replace (18), namely,

$$N\epsilon_\Sigma^2 = R^2_{\text{ave}}\left\{1+\frac{2}{m_1-m_2}\left[\frac{m_2}{1-e^{-m_1S}}-\frac{m_1}{1-e^{-m_2S}}\right]\right\}$$

$$-\frac{1}{N(m_1-m_2)}\left\{\begin{aligned}&\frac{m_2}{e^{m_1S}-1}[(R_0^2+R^2_{N-1})e^{m_1S}\\&\quad+(R_1^2+R^2_{N-2})e^{2m_1S}+\cdots\\&-\frac{m_1}{e^{m_2S}-1}[(R_0^2+R^2_{N-1})e^{m_2S}\\&\quad+(R_1^2+R^2_{N-2})e^{2m_2S}+\cdots.\end{aligned}\right. \quad (19)$$

If further, N is increased to such an extent that the correction terms may be dropped; i.e., if the factor

$$1/N \to 0$$

the resulting formula

$$N\epsilon_\Sigma^2 = R^2_{\text{ave}}\left\{1+\frac{2}{m_1-m_2}\left[\frac{m_1e^{m_2S}}{1-e^{m_2S}}-\frac{m_2e^{m_1S}}{1-e^{m_1S}}\right]\right\} \quad (20)$$

is precisely the formula obtained by Zernicke. A little reflection will show just how bad the approximation made in the use of Eq. (20) may be for very small values of N. This becomes even more striking in view of the fact that if N is small enough the error may easily be calculated without any approximation from Eq. (18).

The calculations will now be carried out to show how the error is to be obtained in the case of an integrating instrument.

$$\epsilon_I^2 = \left[\frac{1}{T}\int_0^T r(t)dt\right]^2_{\text{ave}} = \frac{1}{T^2}\int_0^T\int_0^T [r(\xi)r(\eta)d\xi d\eta]_{\text{ave}}$$

utilizing Eq. (10) to remove the bar in the integrand

$$\epsilon_I^2=\frac{1}{(m_1-m_2)T^2}\int_0^T\int_0^T r^2(\xi)[m_1e^{m_2(\xi-\eta)} - m_2e^{m_1(\xi-\eta)}]d\xi d\eta. \quad (21)$$

Splitting the integral into two parts to insure the proper sign relationships in the exponents of the integrand (21) becomes

$$\epsilon_I^2=\frac{1}{(m_1-m_2)T^2}\int_0^T\int_\xi^0 r^2(\xi)[m_1e^{m_2|\xi-\eta|} - m_2e^{m_1|\xi-\eta|}]d\xi d\eta+\frac{1}{(m_1-m_2)T^2} \times\int_0^T\int_\xi^T r^2(\xi)[m_1e^{m_2|\xi-\eta|}-m_2e^{m_1|\xi-\eta|}]d\xi d\eta. \quad (22)$$

Integrating with respect to η

$$\epsilon_I^2=\frac{1}{(m_1-m_2)T^2}\int_0^T r^2(\xi)\left[\frac{m_1}{m_2}(e^{m_2\xi}+e^{m_2|\xi-T|}-2) -\frac{m_2}{m_1}(e^{m_1\xi}+e^{m_1|\xi-T|}-2)\right]d\xi. \quad (23)$$

Here again, as in the case of the isolated readings, difficulty is encountered in the final integration since the form of the function $r^2(\xi)$ is unknown. For most practical purposes this difficulty may be removed by the following procedure. Let $|\xi-\eta|=u$ and $\xi=V$. The integral then becomes

$$\epsilon_I^2=\frac{1}{(m_1-m_2)T^2}\int_0^T\int_0^\infty r^2(v) \times[m_1e^{m_2u}-m_2e^{m_1u}]dudv. \quad (24)$$

The factor 2 in (24) results from fixing v at some point intermediate between zero and T and integrating in both directions from v. If this procedure were not followed, the calculation would be greatly in error because only the small values of u contribute appreciably to the value of the integral. In the form (24) the approximation makes its appearance in the limits of integration. If the integration over u is taken from zero to infinity, the approximation is equivalent to that introduced in going from Eq. (18) to Eq. (19) in the discrete calculation. By integrating Eq. (24) the error is found to be

$$\epsilon_I^2=(2R^2_{\text{ave}}/(m_1-m_2)T)(m_2/m_1-m_1/m_2), \quad (25)$$

since

$$\frac{1}{T}\int_0^T r^2(v)dv=R^2_{\text{ave}}. \quad (26)$$

It is possible to check the validity of the approximations made in arriving at (25). If the total observation time $T=NS$ is held constant while the number of observations made is increased indefinitely, i.e., the conditions may be expressed

$$N\to\infty, \quad S\to 0, \quad \text{such that} \quad NS=T,$$

then the summation formula must reduce to the integration formula. This is readily seen to be the case for

$$\lim_{\substack{N\to\infty\\ S\to 0\\ NS=T}}\epsilon_\Sigma^2=\lim_{\substack{N\to\infty\\ S\to 0\\ NS=T}}\left\{\frac{R^2_{\text{ave}}}{N}\left[1+\frac{2}{m_1-m_2}\left(\frac{m_2}{1-e^{-m_1S}}-\frac{m_1}{1-e^{-m_2S}}\right)\right]-\frac{1}{N^2(m_1-m_2)}\right\}\cdots =\frac{2R^2_{\text{ave}}}{(m_1-m_2)T}\left(\frac{m_2}{m_1}-\frac{m_1}{m_2}\right)=\epsilon_I^2. \quad (27)$$

This result clearly establishes the validity of the approximations made in evaluating the limits of integration for the continuous case.

It has been the objective of this paper not to treat exhaustively the errors involved in the use of a galvanometer but rather to set forth a general method of analyzing the erratic errors in experimental problems. Specifically, the object has been to show how to approach the problem of using the experimental data to estimate the mean erratic error in the experiment. The galvanometer example was used in the interests of an abbreviated discussion and also to simplify the problem of pointing out weaknesses in methods extant in the literature.

The author wishes to acknowledge the assistance rendered by Mr. W. L. Rast in many helpful comments on the present paper.

Resistance of Monovalent Metals[1]

E. L. Peterson and L. W. Nordheim
Purdue University, Lafayette, Indiana
(Received November 19, 1936)

With the detailed knowledge available at present of the nature of the metallic state, an attempt has been made to estimate quantitatively the resistivity of the monovalent metals. It is shown that the older conception of a "deformable" potential gives for Na a resistivity about 9 times too high. In our new formulation the resistivity is simply due to the fact that in a distorted crystal the proper solutions are not of the type of progressive waves, but linear combinations of these. The transition probabilities can be worked out under the assumptions that the charge distribution of the conduction electrons almost compensates the electrostatic potential due to the shift of the ions from their equilibrium positions and that in the undistorted crystal the periodic factor u_k in the wave functions $u_k \exp(2\pi i \mathbf{k}\cdot\mathbf{R})$ does not depend sensibly on the wave number $\mathbf{k}$. In this case only the average electronic density and not the exact form of the wave functions and potentials is found to be relevant. The result can be expressed by an interaction constant C, which measures the average scattering effectiveness of the elastic waves. The computation gives $C/E_0=0.84$, where E_0 is the Fermi energy. The empirical values are for Na 0.77, K 0.81, Cu 1.12, Ag 1.21, Au 1.19.

§1. The Model

THE present theory of metals explains the normal resistance by the interaction of the heat motion of the lattice ions and the conduction electrons. By describing the heat motion by the Debye concept of elastic waves, it has been found under rather general assumptions that the mechanism of interaction which produces the resistance consists of Bragg reflections of the electronic waves from the elastic longitudinal waves, the transverse waves being ineffective. Though this picture is certainly correct in its essence, a satisfactory theoretical computation of the resistivity has not yet been given even for the simplest metals. It is the purpose of this paper to attempt such a computation for monovalent metals.

The main problem in such a computation is to achieve an unambiguous description of the mode of interaction of electronic and elastic waves. In the nearest previous approach to a definite theory, Bethe,[2] following the ideas of Bloch,[3] has used the hypothesis of a "deformable potential." In an undistorted crystal the electrons are subject to a perfectly periodic potential $V(\mathbf{R})$, $\mathbf{R}$ being the coordinate vector. The heat oscillations cause a shift of the points of the crystal which we will represent by $\delta\mathbf{R}$. By "deformable potential" it is meant that the potential at the point $\mathbf{R}+\delta\mathbf{R}$ in the distorted crystal is the same as that at the point $\mathbf{R}$ when the crystal is not deformed. Starting from this assumption and taking the change in the potential due to the distortion as a perturbation acting on the electronic wave functions of the undistorted crystal, S.B. obtained a simple expression for the resistivity,[4] in which only one "interaction constant" was left undetermined. This constant was expressed as an integral requiring only the unperturbed wave functions (compare (22)). Wigner and Seitz[5] have since determined the wave functions for Na and we have used them to evaluate the constant. The value obtained when substituted in the S.B. formula gives a resistivity about nine times that observed.

That the assumptions made in this theory should lead to a very high value for the resistivity is quite understandable. The wave functions and the potentials are both large and vary rapidly near the centers of the ions. A displacement of the ions would, according to the Bloch hypothesis, cause a shift of the large part of the potential against the large part of the wave functions, and would produce an asymmetry in the potential near the center of the ion. Neither effect actually

[1] Presented at the Washington meeting of the American Physical Society, May, 1936. Submitted as a thesis to the Faculty of Purdue University by E. L. Peterson.
[2] A. Sommerfeld and H. Bethe, *Handbuch der Physik*, Vol. 24, second edition (Berlin, 1933). Quoted henceforth as S.B.
[3] F. Bloch, Zeits. f. Physik **52**, 525 (1928).
[4] S.B., p. 523 (36, 11).
[5] E. Wigner and F. Seitz, Phys. Rev. **43**, 804 (1933); **46**, 509 (1934). Henceforth quoted as W.S.

occurs. The inner part of the wave function will remain in the same position relative to the ion and the inner part of the potential cannot be much changed by the small shifts of the ions against one another. It is therefore clear that the Bethe-Bloch formulation overestimates the interaction and therefore the resistivity. The entire method of describing the effect of the elastic waves as a perturbation of the wave functions of an undistorted crystal is hardly adequate, because the displacements due to heat motion, while small compared to the normal distance between ions, are not small compared to the dimensions of the region where the potential and wave functions are large. Therefore, though the wave functions and the potential in a distorted crystal will be quite similar to those in the undistorted crystal it is not possible to represent them by a Taylor development in terms of the undisturbed functions.

The consideration that the large part of the wave functions should follow closely the motion of the ions suggests a procedure better suited to the actual physical situation. Due to the relatively slow motion of the massive ions it will probably be a fair approximation to assume that the electronic wave functions follow them adiabatically. Such an adiabatically deformed wave function will be a much better starting point for calculating transition probabilities than the wave functions of an undistorted crystal.

The wave functions in an undistorted crystal are of the well-known Bloch type

$$\psi_k = u_k \cdot \exp\,(2\pi i(\mathbf{k}\cdot\mathbf{R})), \qquad (1)$$

where u_k has all the periodicities of the lattice and $\mathbf{k}$ is the propagation vector. Since the exponential factor does not affect the electronic charge density, Wigner and Seitz first determined the function u_0 for an electron at rest by the self-consistent field method. The functions belonging to moving electrons, $(\mathbf{k}\neq 0)$, were then treated by a perturbation calculation. It was found that the u_k were practically independent of $\mathbf{k}$, i.e., that the wave functions of the higher states were given in good approximation by multiplying the function u_0 by the proper exponential factor. This seems to hold very well for Na and fairly well for the other monovalent metals[6] with the exception of Li, Rb, Cs. If the crystal is distorted the function u_0 will go over into a new function U_0 which would again have to be found by the self-consistent field method and which is, in principle, unique.

As $u_0 \exp\,(2\pi i\mathbf{k}\cdot\mathbf{R})$ represents well the wave functions in the undistorted crystal, it is suggestive to approximate the wave functions in the general case by $U_0 \exp\,(2\pi i\mathbf{k}\cdot\mathbf{R})$. It is then found that one such function alone does not give a sufficient approximation but that a better one can be found by a superposition of such waves. This only expresses but the well-known fact that, in presence of a perturbation, not the progressive exponential waves but standing sine and cosine waves would be the proper solutions. The same fact can also be expressed in this way that in a description by progressive waves one will have transitions from one state to the other.

The transition probabilities can be worked out by a straightforward scheme[7] which is slightly more general than the usual one. The matrix element in question can then be transformed into an expression which contains only one Fourier component of the electronic density U_0^2 in the distorted crystal and does not contain the potential. A complete solution would thus require the determination of the function U_0 perhaps by a method similar to the W.S. method for the undistorted crystal. This seems to be an extremely complicated problem. But for the value of our matrix element only the deviation from the practically constant density in the crystal at rest is relevant. The general features of this density can be obtained directly. In a monovalent metal the electrons are easily movable. Therefore no differences of electric potential can exist over distances greater than atomic ones, that is, the electronic fluid will have a very high dielectric susceptibility. Since the volume of the elementary cells and therefore the distribution of positive electricity will be changed by an elastic wave,

[6] For a general survey of metallic eigenfunctions compare J. C. Slater, Rev. Mod. Phys. **6**, 209 (1934). Wave functions for Li have been calculated by F. Seitz, Phys. Rev. **47**, 400 (1935), for Cu by H. M. Krutter, Phys. Rev. **48**, 665 (1935) and K. Fuchs, Proc. Roy. Soc. **A151**, 585 (1935).

[7] It is to be noted that we use a perturbation calculation only to go over from the states $k=0$ to those with $k\neq 0$, and not for obtaining the eigenfunctions in the distorted crystal from the eigenfunctions in the undistorted one.

there will be an additional electronic density which in the average will compensate the former. This average density alone determines the magnitude of the interaction integral and can be obtained easily. The statement that the charge distribution of the conduction electrons will be such that it will destroy a potential due to the displacement of the ions is clearly the correct formulation of the deformable potential hypothesis.

With the above picture the resistivity can be obtained by a very simple calculation the results of which fit the experimental data remarkably well. The resistance of Na and K is given quantitatively if one uses the new values for the Debye temperature for these substances as given by Fuchs.[8] For Cu, Ag, Au one obtains somewhat too low values for the resistivity which is probably due to the fact that the principal assumption that the u_k are independent of $\mathbf{k}$ for the *undisturbed* crystal is not so nearly fulfilled.

In our theory, the factor which determines the resistance is essentially the change of volume of the elementary cells due to the elastic displacement. From this follows that in our case only the longitudinal waves are effective. It follows further that also for molten metals only the compression waves will contribute to resistivity and not other types of disorder which may be present. We obtain thus a justification for Mott's[9] treatment of the liquid metals. The argument for this may be put more directly. In the case of a displacement which does not change the volume of the elementary cells, a practically self-consistent set of proper functions of the progressive wave type can be constructed.

In §2 we collect the formulae of the general theory of conductivity which are necessary for our purpose and we evaluate the Bloch-Bethe interaction constant. §3 contains our new theory and our final results. In §4 we have attempted a more detailed discussion of the function U_0 by a more direct method. In the appendix we give a generalization of the scheme for calculating transition probabilities so as to include functions which are not strictly orthogonal.

§2. General Formulae of Conductivity, Bloch-Bethe Theory

We will need certain formulae of the general theory. The wave functions of the electrons are of the form (1). For monovalent metals the energy as a function of the propagation vector $\mathbf{k}$ is practically spherically symmetric. It is closely approximated by

$$E_k=(h^2k^2)/2m. \tag{2}$$

The group velocity has the form

$$v_x=\frac{1}{h}\frac{\partial E_k}{\partial k_x}=\frac{hk_x}{m}. \tag{3}$$

The resistivity[10] for temperatures well above the Debye temperature θ may be written in the well-known Drude-Lorentz-Sommerfeld form

$$\sigma=\frac{Ne}{hk_0}\left(\frac{1}{h}\frac{dE}{dk}\right)_0\cdot\tau\Big|_{k=k_0}=\frac{Ne^2}{m}\cdot\tau_0, \tag{4}$$

in which N is the number of conduction electrons per unit volume and where the subscript $_0$ means that the quantities have to be taken at the top of the zero Fermi distribution. $1/\tau$ is the probability that an electron will have its state changed by a "collision" in unit time. If there exists an elementary probability $V_{kk'}$ for the transition $k\rightarrow k'$, we have

$$1/\tau=2\pi\int V_{kk'}k'^2(dk'/dE')(1-(k'/k)\cos\vartheta)\times\sin\vartheta d\vartheta dE', \tag{5}$$

ϑ being the angle between k and k'.

Following the concepts of the general theory of resistivity, we assume that such transitions are caused by the interaction of electronic and lattice ion motion. The Debye theory describes the ion motion as a superposition of independent elastic waves, whose wave number we may represent by $\mathbf{f}$. The displacement of a point $\mathbf{R}$ in the lattice due to such a superposition of elastic

[8] K. Fuchs, Proc. Roy. Soc. **A153**, 622 (1936).

[9] N. F. Mott, Proc. Roy. Soc. **A146**, 465 (1934) has shown that the change in resistivity at the melting point can be fully accounted for by the change in the Debye temperature θ which may be deduced from other physical properties. He also gives the interpretation that in the liquid state only longitudinal waves contribute.

[10] L. Nordheim, Helv. Phys. Acta **7** (supplementum II), 3 (1934).

waves will be

$$\delta\mathbf{R}=\sum_f \delta\mathbf{R}_f,$$
$$\delta\mathbf{R}_f=\mathbf{n}_{fj}[a_{fj}\exp(2\pi i(\mathbf{f}\cdot\mathbf{R}))+a_{fj}^*\exp(-2\pi i(\mathbf{f}\cdot\mathbf{R}))] \quad (6)$$

a_{fj} is the wave amplitude and $\mathbf{n}_{fj}$ is a unit vector giving the direction of displacement, being parallel to $\mathbf{f}$ for longitudinal waves and perpendicular to $\mathbf{f}$ for transverse waves. The wave number $\mathbf{f}$ takes all integral values up to the maximum given by

$$hf_m=h(3N/4\pi)^{\frac{1}{3}}=h\nu_m/c=k\theta/c. \quad (7)$$

where N is the number of ions per unit volume which for monovalent metals is equal to the number of electrons per unit volume, ν_m the maximum frequency corresponding to the maximum wave number f_m, c is the velocity of sound, and θ is the Debye temperature. The wave amplitudes a_{fj} have to be quantized:

$$\left.\begin{matrix}a_{fj}^*\\ a_{fj}\end{matrix}\right\}=\left(\frac{h}{8\pi^2 d\nu_f}\right)^{\frac{1}{2}}\begin{cases}N_f^{\frac{1}{2}} \text{ for the transition } N_f\rightarrow N_f-1 \text{ (absorption)};\\ (N_f+1)^{\frac{1}{2}} \text{ for the transition } N_f\rightarrow N_f+1 \text{ (emission)}.\end{cases} \quad (8)$$

N_f is the quantum number of an oscillator and d the density of the material. For high temperatures ($T>\theta$) the average number of quanta per oscillator is

$$N_f\approx N_f\pm 1=kT/h\nu_f \quad (9)$$

and
$$|2\pi f a_f|^2=\frac{kT}{2d}\cdot\frac{f^2}{\nu_f^2}=\frac{kT}{2dc^2}. \quad (10)$$

It will be seen later that in our theory, as in the Bloch-Bethe theory, the possible scattering processes will consist of Bragg reflections of the electronic waves from the elastic waves with the emission or absorption of a sound quantum, i.e., an oscillator $\mathbf{f}$ may suffer a transition for which the interference condition,

$$\mathbf{k}'-\mathbf{k}=\pm\mathbf{f}, \quad (11)$$

is satisfied. The transition probability will be of the general form

$$V_{ss'}=|G_{ss'}|^2\frac{\partial}{\partial t}\frac{4\sin^2(\pi/h)(E_{s'}-E_s)t}{(E_s-E_{s'})^2}, \quad (12)$$

where s denotes a state of the total system, electron plus oscillators, the time factor leading to the factor $4\pi/h$ after integration over the energies in the well-known way.

The interference condition (11) restricts the direction in which an oscillator can scatter an electron. For this reason f can be introduced as variable instead of θ by the relation,

$$f^2=k^2+k'^2-2kk'\cos\vartheta. \quad (13)$$

If one introduces this in (5) and carries out the integration over the energies, neglecting the small difference between E_k and $E_{k'}$ one obtains,

$$\frac{1}{\tau}=\frac{4\pi^3}{h}\cdot\frac{1}{h^2}\cdot\frac{1}{dE/dk}\cdot 2\int_0^{f_m}|G_{kk'}|^2 f^3 df, \quad (14)$$

the factor 2 arising from the fact that an oscillator can scatter an electron in the process of emission as well as of absorption of a sound quantum, the matrix elements being essentially the same for both processes.

Since the matrix elements are approximately linear in the oscillator amplitudes, it is convenient to define new elements which will be practically independent of them by

$$G_{kk'}=2\pi i|f|a_f F_{kk'}(k). \quad (15)$$

$F_{kk'}$ will thus be independent of temperature. If we insert (7), (9), (10), (12), (14), (15) in (4) we have the final formula

$$\sigma=\frac{n_0e^2}{h^3}\frac{16M}{9\pi}k_0\left|\frac{dE}{dk}\right|_0^2\frac{(k\theta)^2}{T}\cdot\frac{1}{\overline{F^2}} \quad (16)$$

with
$$\overline{F^2}=\frac{4}{f_m^4}\int_0^{f_m}F_{kk'}^2 f^3 df. \quad (17)$$

n_0 is the number of electrons per atom, and M is the mass of an atom. For E we take the approximate expression (2) and we have

$$\left.\frac{dE}{dk}\right|_{k=k_0}=\frac{h^2k_0}{m} \quad \text{with} \quad k_0=\left(\frac{3N}{8\pi}\right)^{\frac{1}{3}}. \quad (18)$$

In (16) everything except the "interaction constant" F is known.

If one uses the Bloch-Bethe hypothesis, $G_{kk'}$ will be the matrix element of the "deformable potential." Up to linear terms in the oscillator amplitudes, we have

$$\delta V = V_0(\mathbf{R}+\delta\mathbf{R}) - V_0(\mathbf{R}) = \delta\mathbf{R}\cdot\text{grad } V_0, \quad (19)$$

where V_0 is the potential in the undistorted lattice. The matrix elements will be

$$G_{kk'} = \int \psi_{k'}^* \delta\mathbf{R}\cdot\text{grad } V_0 \psi_k dv. \quad (20)$$

By using (6) and the periodicity properties of V_0 and ψ_k it is easily shown that only longitudinal waves give nonvanishing matrix elements and they do so only if (11) is fulfilled. The expression reduces to

$$G_{kk'} = a_f \int u_k^*(\mathbf{f}/|f|)\cdot\text{grad } V_0 u_k dv, \quad (21)$$

which is to be integrated over only one elementary cell. The function u_k is normalized in one cell. By partial integration and use of the Schrödinger equation (21) reduces to[11]

$$G_{kk'} = 2\pi i a_f F,$$
$$F = \tfrac{2}{3}C = \tfrac{2}{3}(h^2/8\pi^2 m)\int |\text{grad } u_0|^2 dv. \quad (22)$$

In this expression the fact that u_k and $u_{k'}$ are practically identical has been used. The interaction constant F, according to this hypothesis, is independent of the wave number.

If (22) is inserted in (16) σ becomes identical with Bethe's expression[12] except for the differences of notation. There we find $2\pi\mathbf{k}$ replaced by $\mathbf{K}$, h replaced by $2\pi h$ and $\overline{F^2}$ replaced by $(4/9)C^2$.

We have used the function u_0 calculated by W. S.[1, 13] to find the theoretical value by numerical integration of the expression (22) for C. The value obtained was 7.6 ev or about 2 to 3 times the empirical value. (Compare the table at the end of §3.) Since the resistivity is proportional to C^2, the theoretical value is 5 to 9 times the observed value.[14]

[11] Compare S.B., pp. 512–513.
[12] Compare S.B., p. 523 (36, 11).
[13] We are indebted to Dr. F. Seitz for kindly furnishing us a tabulation of u_0 for Na.
[14] In an earlier paper one of the authors (L. Nordheim, Ann. d. Physik **9**, 607 (1931)) has discussed as an alternative to the Bethe-Bloch hypothesis that of a "rigid ion." Here the ionic potential is thought to be shifted rigidly as a whole by the elastic displacement and again the difference to the unshifted potential is taken as a "perturbation." This would give, as can be shown easily, a smaller resistance than the "deformable ion" and would agree better with experiment. Also the rigid ion probably represents more closely the actual physical situation as the effective potential is now known to be nearly that of the ion (without much contribution from the conduction electrons) which certainly will not be deformed to any appreciable extent. We have, however, not taken up the discussion from this point of view since the same inconsistency, a shift of the rapidly varying parts of the potential and the wave functions against each other, would appear also in this case.

§3. New Calculation of Resistivity

We assume that in an undistorted crystal the wave functions are of the type (1) with u_k independent of the wave number, which is equivalent with the assumption that the energies have the form (2). We consider now a crystal deformed by heat oscillations of the type (6). In this case we have to work with a Hamiltonian for the electron,

$$H = -(h^2/8\pi^2 m)\Delta + V(\mathbf{R}, a_f) + \Sigma H_f = H_{el} + \Sigma H_f, \quad (23)$$

where ΣH_f is the Hamiltonian of the oscillators, and H_{el} represents the kinetic and potential energies of the electron. V, we may suppose, has been determined by the Hartree method and contains the oscillator amplitudes as parameters. It is to be noticed that we do not separate V into a part V_0 and a perturbation term according to the usual procedure. The potential V is real since we have taken $\delta\mathbf{R}$ as real. Of the several solutions of the Schrödinger equation

$$H_{el}U = -(h^2/8\pi^2 m)\Delta U + VU = EU \quad (24)$$

there will be one, U_0, which will go over into u_0 as the oscillator amplitudes vanish. This function must be real since it must be nondegenerate if u_0 is nondegenerate and it must satisfy the same boundary condition (periodicity with respect to a cube of 1 cm in length) as u_0. The proper value E_0 for the distorted crystal will be practically the same as for the undistorted crystal. A development of E_0 in terms of the amplitudes a_f must start with quadratic terms since a change in the sign of the amplitudes could not change the energy.

For the calculation of the conductivity we must have in addition to U_0 the higher functions ψ_k corresponding to $k \neq 0$. As we have assumed that u_k is practically independent of k we will try the following combination for ψ_k.

$$\psi_k = U_0 \exp 2\pi i(\mathbf{k}\cdot\mathbf{R}). \quad (25)$$

The functions (25) are not true characteristic functions of the Hamiltonian in contrast to the case of the undistorted crystal, but they have certain properties which show that they must be closely related to them.

I. Since U_0 is real they give the same current as the corresponding functions of the undistorted crystal

$$\frac{h}{4\pi i m}\int(\psi_k^*\ \text{grad}\ \psi_k-\psi_k\ \text{grad}\ \psi_k^*)dv=\frac{hk}{m}. \quad (26)$$

This ensures that the ψ_k (25) are suitable for the treatment of conductivity.

II. The average value of the energy is different from E_0 by the same amount as for an undistorted crystal

$$\int\psi_k^* H_{el}\psi_k dv=E_k=E_0+h^2k^2/2m. \quad (27)$$

We have for $H_{el}\psi_k$ the expression,

$$\begin{aligned}H_{el}\psi_k&=\left[-\frac{h^2}{8\pi^2 m}\Delta+V\right]U_0\exp(2\pi i(\mathbf{k}\cdot\mathbf{R}))\\&=\exp(2\pi i(\mathbf{k}\cdot\mathbf{R}))\left[-\frac{h^2}{8\pi^2 m}\Delta U_0+VU_0\right.\\&\qquad\left.+\frac{h^2k^2}{2m}U_0-\frac{ih^2}{2\pi m}\mathbf{k}\cdot\text{grad}\ U_0\right]\\&=\exp(2\pi i(\mathbf{k}\cdot\mathbf{R}))\left[E_k-\frac{ih^2}{2\pi m}\mathbf{k}\cdot\text{grad}\ U_0\right].\end{aligned} \quad (28)$$

In the integral (27) the term

$$\int U_0\mathbf{k}\cdot\text{grad}\ U_0 dv=\tfrac{1}{2}\int\mathbf{k}\cdot\text{grad}\ U_0^2 dv \quad (29)$$

vanishes, as it can be transformed into a surface integral, and U_0 takes the same value at two opposite boundaries of the crystal. (27) ensures that there will not be any appreciable second order terms if we take (25) as the starting point of a perturbation consideration.

The functions (25) have the same average energy and current as the proper functions of the normal lattice and become identical with them if the oscillator amplitudes become vanishingly small. They have, furthermore, the same charge distribution U_0^2 as those corresponding to an electron at rest, so that the latter alone would enter into the determination of the self-consistent field. The effect of the distortion can therefore be adequately described by considering the secular perturbations between the functions (25) or, which amounts to the same thing, by transitions between those states, as we shall show. The functions are different from the functions usually used only in that that they are not strictly orthogonal to each other. This requires, as is shown in an appendix, that the matrix elements must be corrected for the non-orthogonality. The matrix elements $H_{kk'}$ have to be replaced by

$$G_{k'k}=H_{k'k}-E_k d_{k'k}=\int\psi_{k'}^*(H-E_k)\psi_k dv, \quad (30)$$

where E_k is the average energy of the state k and $d_{k'k}$ the nonorthogonality integral. The expression $G_{k'k}$ can be introduced directly in (14) to (17) to obtain the conductivity. (It is understood that the integration over the oscillator functions has already been carried out. Since H contains the amplitudes a_f the oscillator matrix elements for the transitions considered have to be inserted.) From (25), (28), (30), one finds

$$G_{k'k}=-\frac{ih^2}{4\pi m}\int\exp(2\pi i(\mathbf{k}-\mathbf{k}')\cdot\mathbf{R})\cdot\mathbf{k}\cdot\text{grad}\ U_0^2 dv,$$

and integration by parts yields

$$G_{k'k}=\frac{\mathbf{k}\cdot(\mathbf{k}-\mathbf{k}')h^2}{2m}\int\exp(2\pi i(\mathbf{k}-\mathbf{k}')\cdot\mathbf{R})\cdot U_0^2\cdot dv. \quad (31)$$

It will be shown that to a reasonable approximation $G_{k'k}$ vanishes unless the interference condition, $\mathbf{k}'-\mathbf{k}=\pm\mathbf{f}$, is satisfied. Conservation of energy requires that k and k' are practically identical and if we neglect the small difference, $\mathbf{k}\cdot(\mathbf{k}-\mathbf{k}')$ can easily be expressed in terms of f,

$$\mathbf{k}\cdot(\mathbf{k}-\mathbf{k}')=|k|\,|f|\cos\vartheta=f^2/2.$$

With this (31) becomes

$$G_{k'k}=-(f^2h^2/4m)\cdot K_{k'k} \quad (32)$$

with $K_{k'k}$ defined by

$$K_{k'k}=\int\exp(2\pi i(\mathbf{k}-\mathbf{k}')\cdot\mathbf{R})\cdot U_0^2 dv. \quad (33)$$

The only formal difference between our theory

and the Bloch-Bethe theory is therefore that their matrix elements have to be replaced by the new ones (33). The essential point here is that U_0 is supposed to be the actual self-consistent wave function for an electron at rest in a crystal distorted by an elastic wave with wave number $\mathbf{f}=\mathbf{k}-\mathbf{k}'$ and contains the amplitudes a_f as does (22). The integration is over the whole crystal.

U_0^2 represents the electronic density in the crystal; (33) is therefore one Fourier component of this density, and one belonging to a comparatively long wave-length. Therefore, the value of this integral will be determined chiefly by the variation of the total charge from cell to cell and deformations of the distribution inside the single cells will not be important. This total charge of the cell will be such, that it compensates, to a high degree of accuracy, the positive charge of the ion since otherwise electrostatic potential differences over large distances would be produced. This will hold at least as long as $(1/|\mathbf{k}-\mathbf{k}'|)$ is large compared to the atomic distance. In this case it does not matter for the value of $K_{kk'}$ how the charge is distributed over the individual cell. $K_{kk'}$ will therefore be given to a fair approximation by a smooth function U_0^2 which just compensates the change in volume.

The volume v of a space element changed by the distortion $\delta\mathbf{R}$ (compare (6)) is given by

$$v=v_0(1+\operatorname{div}\delta\mathbf{R}). \tag{34}$$

The density which compensates the change of volume expressed by the second term is therefore,

$$\rho=(\rho_0/1+\operatorname{div}\delta\mathbf{R})\leqq\rho_0(1-\operatorname{div}\delta\mathbf{R}). \tag{35}$$

If U_0 is normalized in unit volume, one obtains for the interaction integral (32)

$$\begin{aligned} G_{kk'}&=\frac{\mathbf{k}\cdot(\mathbf{k}'-\mathbf{k})}{2m}h^2\int\exp(2\pi i(\mathbf{k}'-\mathbf{k})\cdot\mathbf{R})\\ &\qquad\times(1-\operatorname{div}\delta\mathbf{R})dv\\ &=-\frac{\mathbf{k}\cdot(\mathbf{k}'-\mathbf{k})}{2m}h^2\int\exp(2\pi i(\mathbf{k}'-\mathbf{k})\cdot\mathbf{R})\\ &\qquad\times\operatorname{div}\delta\mathbf{R}dv, \end{aligned} \tag{36}$$

since the integral over the undistorted part vanishes.

div $\delta\mathbf{R}$ is different from zero only for longitudinal waves ($\mathfrak{n}_f\|\mathbf{f}$) and therefore

$$\operatorname{div}\delta\mathbf{R}_f=2\pi i f a_f\exp(2\pi i(\mathbf{f}\cdot\mathbf{R}))+\text{conj. complex.} \tag{37}$$

(33) is different from zero only if the interference condition,

$$\mathbf{k}'-\mathbf{k}=\pm\mathbf{f},$$

is satisfied for a certain oscillator. The emission of a sound quantum ($-$ sign) involves only the amplitude a_f, the absorption ($+$ sign) only a_f^*. In both cases we get the same absolute value for $G_{kk'}$. With (37) we get for emission

$$\begin{aligned} G_{kk'}&=\frac{h^2f^2}{4m}\cdot 2\pi i f\cdot a_f=2\pi i f a_f\cdot F;\\ F&=h^2f^2/4m, \end{aligned} \tag{38}$$

and this has to be inserted in (17) and (16) to obtain the conductivity.

In the Bethe-Bloch theory F was to be replaced by $\frac{2}{3}C$ (compare (22)). In distinction to their interaction constant C, our F still contains the wave number of the elastic waves. With (38) and (17) we obtain

$$\overline{F^2}=\left(\frac{h^2}{2m}\right)^2\cdot\frac{1}{f_m{}^4}\int_0^{f_m}f^4df=\frac{1}{8}\left(\frac{h^2f_m{}^2}{2m}\right)^2. \tag{39}$$

From (7) and (18) we get $f_m=k_0\cdot 2^{\frac{1}{2}}$ and therefore instead of the Bethe C

$$C_{\text{calc}}\rightarrow\frac{3}{2}(\overline{F^2})^{\frac{1}{2}}=\frac{3\cdot 2^{\frac{1}{2}}}{2\cdot 2^{\frac{1}{2}}}\cdot\frac{k_0{}^2h^2}{2m}=0.84E_0, \tag{40}$$

where E_0 is the Fermi zero point energy.

The comparison with experiment has been made in the same way as in S.B.,[15] that is from the empirical conductivity and Debye temperature a value C_{obs} has been determined and compared to the value (40). Table I gives the relevant data for those metals for which one can expect that our assumptions are sufficiently fulfilled. There is rather an uncertainty in the Debye temperatures for the alkalies. The higher values for θ are those used by S.B. The lower ones are those given by Fuchs[8] in a recent paper which are probably better. The best values will probably be slightly higher than his lowest values (perhaps $\sim 170°$ for Na and $\sim 110°$ for K), as he extrapolates to $T=0$ whilst for the conductivity the values of θ for room temperature are relevant.

[15] Reference 2, page 524.

TABLE I. *Calculated and observed values of C and pertinent data for Na, K, Cu, Ag, Au.*

Element	Na	K	Cu	Ag	Au
Atomic weight	23	39	63.6	108	197
Conductivity $\times 10^4$ (in Ω^{-1} cm^{-1}) at 0°C	22.6	15.3	64	67	68
Debye temperature θ	202–150	126–100	315	215	175
Zero point energy E_0 (in ev)	3.16	2.06	7.10	5.52	5.56
Radius of s sphere $\times 10^8$ (in cm)	2.11	2.56	1.41	1.59	1.59
C_{obs} (ev)	3.28–2.44	2.35–1.66	7.9	6.7	6.6
C_{calc} (ev)	2.66	1.81	5.91	4.68	4.68

C_{obs} is directly proportional to θ (compare (16)). We have given therefore in the table the limits for C_{obs} corresponding to the values of θ quoted.

We see an almost perfect agreement of our C with the C_{obs} obtained with Fuchs' values for θ. By comparing this with the value of 7.6 ev as obtained from Bloch-Bethe theory for Na we see the improvement compared to the older theory. The calculated values for the noble metals come out too low, i.e., the observed resistivities are higher than those calculated. This is most probably due to the circumstance that our principal assumption that in the undistorted crystal the functions u_k are independent of k, holds less well.

Because the theory uses the Debye model for heat motion and the Hartree approximations for the electrons, both of which are certainly none too good, the excellent agreement for the alkalies is not really significant. In our calculation the effect of the shorter wave-lengths (near f_m) is probably overestimated since in this case the compensation of the ionic charges might not be so complete. On the other hand, the effect of the long wave vibrations (small f) is probably underestimated. Our matrix element is proportional to f^2 and therefore becomes very small for small f. Other effects neglected in our approximation may be important in this range, though for the average they do not matter much.

The matrix elements for small f will be most important at low temperatures, since then they alone are thermally excited. A substitution of our expression (38) for the matrix element in the Bloch formula for the conductivity at low temperatures would lead to proportionality to T^9 instead of the usually assumed T^5 law. We do not consider this as a serious objection against our theory. As mentioned above any neglections will be much more serious for small T. It will probably not be justified to take U_{k_0} for the Fermi energy as equal U_0, and the distinction between the two should introduce a term similar to the Bethe-Bloch theory, though much smaller. We have not investigated the resistance at low temperatures more closely in this paper because the whole theory for this case is still not in order. The new W.S. results on the eigenvalue distribution in monovalent metals exclude the possibility of the *Umklapp-Prozesse* of Peierls and therefore the mechanism of producing equilibrium between thermal and electronic motion is uncertain.

§4. Wave Functions in the Distorted Crystal

We discuss in this section the properties of the wave functions which we have used, and the problems which an accurate treatment of a distorted crystal by the self-consistent field method would involve. This leads to another approximation for the calculation of the integral (33) which gives practically the same results as those given in the last section.

To obtain the self-consistent field and wave function in a crystal Wigner and Seitz divide the crystal into elementary polyhedrons constructed by passing planes perpendicularly through the midpoints of lines joining the neighboring atoms with each other. If the potential and wave function are found for a single polyhedron they can be found for the entire crystal from the periodicity properties. It has been found that the self-consistent field in any polyhedron is given in good approximation by that due to the ion in the polyhedron and that the boundary condition for u_0, vanishing derivative normal to the faces of the cell, can be replaced by the requirement that the derivative normal to the surface of a sphere[16]

[16] We use the following notation: $\mathbf{R}$ is the coordinate vector in the crystal. The equilibrium position of the nth ion is denoted by $\mathbf{R}_n^0$. A shift in the position of an ion is denoted by $\delta\mathbf{R}_n$ so that $\mathbf{R}_n = \mathbf{R}_n^0 + \delta\mathbf{R}_n$. The coordinate vector taken from the center of an ion to a position in the cell is denoted by $\mathbf{r}$ so that in the nth cell we have $\mathbf{R} = \mathbf{R}_n + \mathbf{r}$.

("s sphere") of equal volume shall vanish.[17] That this substitution involves only a very small error is insured by the extreme flatness of the wave function in the outer parts of the polyhedron.

If one inserts the form (1) for the higher functions in the Schrödinger equation one obtains

$$\Delta u_k + 4\pi i \mathbf{k} \cdot \text{grad}\, u_k + (8\pi^2 m/h^2)(E_k - h^2k^2/2m - V)u_k = 0. \quad (41)$$

This is different from the equation for u_0 by the shift in the energy, $h^2k^2/2m$ and the term $4\pi i \mathbf{k} \cdot \text{grad}\, u_k$. If the term $4\pi i \mathbf{k} \cdot \text{grad}\, u_k$ is treated as a perturbation term one finds that the first order change of energy vanishes. Wigner and Seitz have computed for the Na ion the second-order term also and have found it to be very small, due to the flatness of u_0. It is for this reason that the higher functions are fairly well approximated by multiplying u_0 by the term $\exp 2\pi i \mathbf{k} \cdot \mathbf{R}$.

We have now to consider the distorted crystal. The first difference from the normal case is that the ions and their contribution to the potential will be shifted to new places.

While the ionic potential alone gives approximately the complete self-consistent field in an undistorted crystal a distortion will give rise to other terms, one due to imperfect compensation of negative and positive charge and another due to deformation of the electron charge distribution. If such terms did not appear one could take the wave functions simply as the Wigner-Seitz functions around each ion. They would join smoothly even in a distorted crystal due to the flatness in the outer portions of the cell.

If the distortion were such that no change in volume of the cell were produced the only new potential would be a weak electrostatic action of one cell upon neighboring cells. This would be caused by the distortion of the cells from almost perfect spheres to ellipsoids. If this small term is neglected one would obtain a solution for any wave number $\mathbf{k}$ by taking the solution which behaves like $\exp(2\pi i \mathbf{k} \cdot \mathbf{r})$ in the cell and multiplying it by a factor $\exp(2\pi i \mathbf{k} \cdot \mathbf{R}_n)$ in the nth cell. This function would be practically continuous over the whole crystal since it would approach $\exp(2\pi i \mathbf{k} \cdot \mathbf{R})$ between the ions and it would be a solution of the Schrödinger equation. To this approximation there would therefore be no transitions between different states and thus no contribution to resistivity. The fact that the molten monovalent metals show no additional resistivity which can be attributed to the disorder of the liquid state can be taken as an empirical justification of the above argument.

If, however, we consider displacements which cause a change in the volume of the elementary cell the situation is quite different. If we took for U_0 simply the Wigner-Seitz function around each ion they would still join smoothly. They would, however, give a nonuniform electron charge distribution. Cells which were reduced in volume would be positively charged while those increased in volume would be negative. Such an effect would cause a strong electrostatic disturbance. However, since the electrons in the metals considered behave nearly like free electrons, as we have pointed out above, this effect will be almost perfectly compensated by redistribution of the negative charge.

It would be desirable to justify this assumption rigorously by setting up and solving the self-consistent field problem including the electrostatic forces mentioned. We have not been able to do so thus far, but as these forces must be small because of the compensation mentioned, the main part of the potential will still be given by the ionic potential. It must be possible, therefore, to construct a fairly close approximation to the function U_0 by a proper combination of W.S. solutions. We have made such a calculation and we reproduce it here not because we believe that it is a better approximation than that used in the previous section, but more to show that the final result does not depend sensibly on the exact form of U_0. Furthermore one can see by this method that the irregularity of the wave function near the centers of the ions is of no importance for our problem.

The simplest approximation one can make is to take the spherically symmetric W.S. function around each ion and to multiply it by a factor that will give the proper negative charge in each cell. This function is given in the nth cell by

$$U_0 = (1/\sqrt{v_0})(1 + 2\pi f y_n) u_0, \quad (42)$$

where v_0 is the volume of the undistorted W.S.

[17] The potential and charge distribution are then spherically symmetric and a cell does not contribute to the potential outside its boundaries.

sphere and $2\pi f y_n$ is $-\frac{1}{2}$ div $\delta\mathbf{R}$ taken at the center of the ion in its actual place in the crystal. This means, of course, an approximation of the true continuous function by a step-like function which otherwise has all the required properties. To better the fit at the boundaries one could try to introduce other solutions of different symmetry, but we have not found a systematic way of doing this.

With U_0 given by the function (42) the integral (33) can be evaluated by integrating over each cell separately and then summing over all cells. In this evaluation the change of the amplitude of exp $(2\pi i\mathbf{f}\cdot\mathbf{r})$ within the cells contributes to the integral. We have found by numerical calculation that neglecting the variation of u_0 in the cell introduces an error of only about 1 percent, since the rapidly varying part is small compared to the wave-length of the elastic wave. The integrals over the cell can be divided into two parts, one over the undistorted cell, and another over the change in volume, and all integrations carried out by elementary methods.

As a result of this calculation one obtains finally

$$F_{kk'}=(ih^2r_s/4mv_0)\times[4\sin x/x-4\cos x-x\sin x] \quad (43)$$

with $x=2\pi fr_s$, and where r_s and v_0 are radius and volume, respectively, of the undistorted W.S. spheres. This $F_{kk'}$ is the equivalent of (38). Since it contains f only in the combination fr_s, which is dimensionless, the integration (17) to obtain $\overline{F^2}$ is the same for all monovalent metals with the upper limit $x_m=2\pi f_m r_s=2\pi(3/4\pi)^{\frac{1}{3}}$. The only dependence of (45) on the particular metal considered is contained in the factor $r_s/v_0\sim 1/r_s^2$ which is the same as that of the zero point energy as shown in the previous section. The final result can also be given the same form as in §3.

$$C=(3/2)(\overline{F^2})^{\frac{1}{2}}=1.04E_0. \quad (44)$$

We obtain thus a somewhat higher value than by the previous calculation. (Compare (40).) The difference is of course due to the different assumptions about the distribution of negative charge and it shows roughly the uncertainty which is involved in our theory at the present stage.

Appendix

Transition Probabilities for Nonorthogonal Wave Functions

Our functions ψ_k (25) are not strictly orthogonal as one sees from the discussion of the matrix element (33) which represents directly the nonorthogonality integral. This is small as long as div $\delta\mathbf{R}\ll 1$ which is fulfilled in our case. The calculation of transition probabilities can then be carried out in close analogy to the treatment of secular perturbations with nonorthogonal functions.

We consider the total system of an electron and the lattice oscillators. The full wave equation

$$H\psi=-(h/2\pi i)(\partial\psi/\partial t) \quad (45)$$

may be solved approximately by a set of functions ψ_s with the matrix elements and nonorthogonality integrals

$$E_s=\int\psi_s^*H\psi_s;\quad H_{ss'}=\int\psi_{s'}^*H\psi_s;\quad d_{ss'}=\int\psi_{s'}^*\psi_s. \quad (46)$$

The ψ_s are in our case the functions (25) multiplied by the corresponding oscillator functions. We try to solve (45) by the linear combination

$$\psi=\sum_s c_s(t)\psi_s\exp(-(2\pi i/h)E_s t). \quad (47)$$

Substituted in (45) this gives

$$\sum_s c_s\exp(-(2\pi i/h)E_s t)(H\psi_s-E_s\psi_s)=-(h/2\pi i)\sum_s\dot{c}_s\exp(-(2\pi i/h)E_s t)\psi_s.$$

Multiplication by a particular function ψ_{s_1} and integration yields

$$-(h/2\pi i)\dot{c}_{s_1}=\Sigma' c_s\exp(-(2\pi i/h)(E_s-E_{s_1})t)(H_{s_0s_1}-E_{s_0}d_{s_0s_1})+(h/2\pi i)\Sigma'\dot{c}_s\exp(-(2\pi i/h)(E_s-E_{s_1})t)d_{ss_1}.$$

Introducing the initial conditions; $c_{s_0}=1$, $c_{s_i}=0$, if $i\neq 0$, we obtain for small t

$$-(h/2\pi i)\dot{c}_{s_1}=\exp(-(2\pi i/h)(E_{s_0}-E_{s_1})t)(H_{s_0s_1}-E_{s_0}d_{s_0s_1})+(h/2\pi i)\Sigma'\dot{c}_s\exp(-(2\pi i/h)(E_s-E_{s_1})t)d_{ss_1}.$$

Here the terms in Σ' (over all the states excluding s_1) contain the factor d_{ss_1} and can therefore be regarded as small compared to the derivative on the left side. Therefore the value for $\dot{c}_{s_1}$ as obtained by neglecting this correction term can be introduced in this term itself, giving

$$-(h/2\pi i)\dot{c}_{s_1}=\exp(-(2\pi i/h)(E_{s_0}-E_{s_1})t)\{[H_{s_0s_1}-E_{s_0}d_{s_0s_1}]-\sum_s[H_{s_0s}-E_{s_0}d_{s_0s}]d_{ss_1}\}. \quad (48)$$

This has now the same form as the usual perturbation equations. The second term on the right side being small compared to the first one we obtain by the usual method

$$V_{s_0s_1}=|H_{s_0s_1}-E_{s_0}d_{s_0s_1}|^2\frac{\partial}{\partial t}\left[\frac{4\sin^2(\pi/h)(E_{s_0}-E_{s_1})t}{(E_{s_0}-E_{s_1})^2}\right], \quad (49)$$

as used in §3.

Dependence of Luminescence on Physical Structure in Zinc Borate Compounds

D. H. KABAKJIAN
University of Pennsylvania, Philadelphia, Pennsylvania
(Received November 28, 1936)

Luminescent zinc borate compounds have been prepared which can be obtained in either vitreous or crystalline form and which can be converted from one form to the other by purely physical processes. The dependence of luminescence of compounds of this type on physical structure has been investigated. It is found that changing a given compound from vitreous to granular state increases its luminescence many times. It is also found that zinc borate compounds can be made luminescent without the addition of an activator. The addition of an activator is found to result in a condensation of the emission bands and an increase in their wave-lengths. The bearing of these on the "solid solution" idea is discussed.

INTRODUCTION

LUMINESCENCE excited in certain chemical compounds by light or other types of radiation is generally considered to be a characteristic of "solid solutions." It has been asserted by various investigators that pure substances do not luminesce. A small quantity of one element, known as the solute or the activator, intimately mixed with a large quantity of another compound, known as the solvent, is supposed to give rise to a number of active centers (Lenard centers) which have the property of absorbing and reemitting energy in the form of luminescence.

There is a wide divergence of opinion as to the nature of these hypothetical centers, and the function of the activator atom in producing luminescence. It is claimed by some that in the luminescence of solid solutions the solute plays the active role while the function of the solvent is to insure the dissemination of the molecules of the activator.[1] In agreement with this view several investigators have claimed that the impurities responsible for luminescence of certain minerals can be identified by determining the wave-lengths of the bands emitted by them,[2, 3] although this has been questioned by others.[4, 5]

The emitting centers have been usually considered as consisting of molecular aggregations of the solvent linked in some way with a single activator atom (Lenard theory).

In recent years the dependence of luminescence on crystal structure has been emphasized.[6, 7] It is supposed that the emitting centers consist of crystal units of the solvent into which an activator atom has entered, either isomorphically or by absorption, thereby causing a distortion of the lattice. Working on this hypothesis, Ewles[8] computed the number of the molecules of the solvent in a crystal unit linked to one molecule of the solute, for certain luminescent compounds, by determining the optimum concentration of the solute for producing luminescence in these compounds. Cohen,[9] however, finds that Ewles' conclusions do not agree with his determinations of the optimum concentration for thermoluminescence of zinc borate glass and rejects the theory of crystal structure.

It was considered desirable, therefore, to investigate further the dependence of luminescence on the physical structure of the compounds and also to determine whether or not the presence of an activator was absolutely necessary. Certain mixtures of zinc oxide and boric acid were found very suitable for this purpose since they can be obtained in either vitreous or crystalline form, and can be converted from one form to the other, by purely physical processes, without altering their chemical compositions. The effects of such modifications on the luminescence of these compounds are given below.

[1] L. Bruninghause, J. de phys. et rad. **2**, 398 (1931).
[2] Tanaka, J. Opt. Soc. Am. **8**, 411 (1924).
[3] H. Haberlandt, B. Karlik and K. Przibram, Akad. Wiss. Wien. Ber. **143**, 151 (1934).
[4] S. Iimori, Inst. Phys. and Chem. Research Tokyo, Sci. Papers **419**, 274 (1933).
[5] F. Schmidt, Ann. d. Physik **12**, 211 (1932).
[6] M. Servigne, Comptes rendus **200**, 2015 (1935).
[7] E. Iwase, Inst. Phys. Chem Research Tokyo, Sci. Papers **567**, 1 (1935).
[8] J. Ewles, Proc. Roy. Soc. **129**, 509 (1930).
[9] B. E. Cohen, J. Am. Chem. Soc. **55**, 953 (1933).

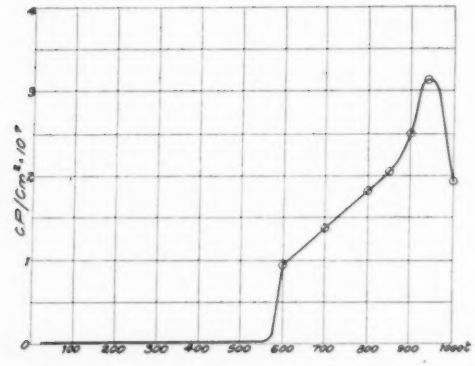

FIG. 1. Variation of brightness with heat treatment temperature for fused C.P. zinc borate disk. Ordinates brightness in candlepower per cm², abscissae maximum temperatures to which the compound has been heated, transition at 600°C.

MATERIALS AND MODE OF PROCEDURE

Preparation of zinc borate glass

Zinc oxide and boric acid mixed in proportion corresponding to the formula ZnB_2O_4 and heated to a temperature of about 500°C, combine to form an amorphous mass. If this mass is heated to about 1000°C, it will fuse into a clear glass known as zinc borate glass. Zinc borate glasses with a much higher zinc oxide content than that corresponding to the above formula can be prepared. Such glasses can be made to luminesce by the addition of activators.[10] If the zinc oxide content of the mixture be gradually increased, a point is reached when the fused mass may become, on cooling, either vitreous or crystalline, depending upon the rate of cooling. This critical mixture, corresponding approximately to 57 percent zinc oxide and 43 percent boric acid, was used in the experiments described below and is referred to as zinc borate compound for want of a more definite term.

A mixture of zinc oxide and boric acid in the above proportion is fused in a platinum crucible in an electric furnace. A drop of the fused material is then quickly squeezed between two brass plates to a small disk of clear glass, 0.5 mm thick and 10–15 mm in diameter. This quick cooling is necessary to obtain a clear glass. If the fused material is allowed to cool slowly, a crystalline mass will result. These disks are quite stable at ordinary room temperatures. They have the characteristics of the vitreous state, and will begin to soften at about 650°C with no definite melting point.

[10] Nyswander and Cohn, J. Opt. Soc. Am. **20**, 131 (1930).

Conversion into crystalline state

One of these clear disks is placed on a platinum plate and introduced into an electric furnace, at a temperature of 600°C. In a few minutes the disk loses its transparency. It becomes opaque and granular in appearance. After the transformation is completed the disks can be raised to much higher temperatures without losing their shape. They have the characteristics of a crystalline mass with a fairly definite melting point at about 1000°C. They can be fused again at higher temperatures and converted back into vitreous state as described above.

Measurements of luminescence

A large number of such disks were prepared both from C.P. materials and also from materials to which an activator had been added, and the luminescence produced in these, both in vitreous and crystalline states, was examined.

Excitation was produced by means of an iron spark, a quartz mercury arc, cathode rays and rays from radioactive materials. For quantitative measurements of brightness excitation was produced only with radium disks to insure the absorption of equal amounts of energy by the transparent and nontransparent forms of the

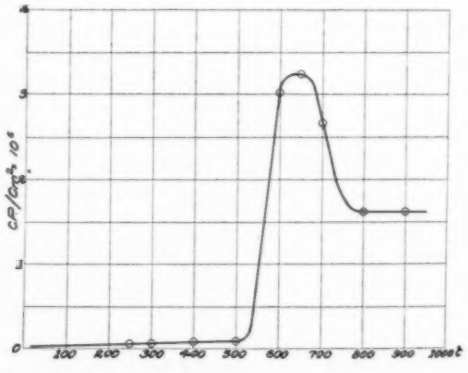

FIG. 2. Variation of brightness with heat treatment temperature in fused zinc borate disk activated with manganese. Ordinates brightness in candlepower per cm², abscissae maximum temperatures to which the material has been exposed. Transition takes place between 500° and 600°C.

material. The radium disks and the special type of photometer used in these measurements have been described in a previous paper.[11] A quartz spectrograph was used to determine the wavelength distribution of the emission bands. All measurements were made at the room temperature.

Results

Luminescence of pure zinc borate compounds

A clear zinc borate glass disk prepared from C.P. materials in the above proportion does not show any appreciable luminescence with such exciting sources as mercury arc, iron spark, or rays from radioactive elements. An appreciable luminescence appears in it on converting it into the opaque form at 600°C.

The opaque disk can now be exposed to various higher temperatures and its luminescence measured after cooling. Fig. 1 gives the variation in the luminescence of such disks with the maximum temperatures to which they have been exposed. It is seen that the maximum brightness is obtained at about 950°C, after which the luminescence begins to decline as the material approaches its melting point. At higher temperatures it can be fused and converted into vitreous form with complete loss of luminescence. The luminescence can, however, be recovered by going through the same process of reconverting it into crystalline form. This conversion from crystalline to vitreous form and *vice versa*, with appearance and disappearance of luminescence, can be repeated indefinitely, showing that the cycle has not produced any permanent changes in the material.

Luminescence of activated zinc borate compounds

Addition of 1 percent manganese, produces some distinct changes in the luminescence of this compound. The fluorescence is increased, the phosphorescence is diminished, the wavelength of maximum emission becomes much larger and the emission bands become much narrower, but the dependence of luminescence on the physical structure of the material is the same as in the pure compound. The activated compound, fused into a clear glass disk, shows very faint luminescence. This is increased tremendously when the disks are divitrified at 600°C. Fig. 2 shows the rise in brightness of such a disk with the maximum temperatures to which it has been exposed. It is seen that the temperature of maximum brightness in this case is 650°C.

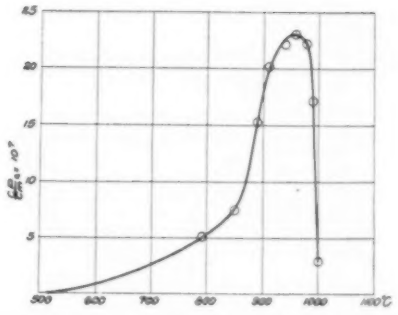

FIG. 3. Variation of brightness with heat treatment temperature in activated zinc borate powder. Ordinates brightness in candlepower per cm², abscissae maximum temperatures to which the compound has been raised.

Both pure and activated compounds can also be made luminescent by heating the amorphous mixtures to temperatures below the fusion point. The materials obtained in this way, however, do not luminesce as intensively as those obtained by divitrifying the fused compounds. Fig. 3 gives the rise in brightness of such a mixture, with the temperature of heat treatment, for a compound activated with manganese.

Nature of the emission bands

The emission of pure zinc borate consists of a single diffuse band in the violet, extending far into the ultraviolet region, with a maximum emission at about 4000A. The activated compound can be made to give a band in the red or in the green region. These are comparatively narrow bands. Ordinarily both bands are present and overlap, giving the appearance of a continuous band but by careful control of temperature they can be distinguished as two distinct bands. In Fig. 4, "*a*" is a spectrogram of the emission from the pure compound and "*b*" from the activated compound giving the red band, when bombarded by cathode rays in a cold cathode-ray discharge tube operated at about

[11] D. H. Kabakjian, Phys. Rev. **44**, 618 (1933).

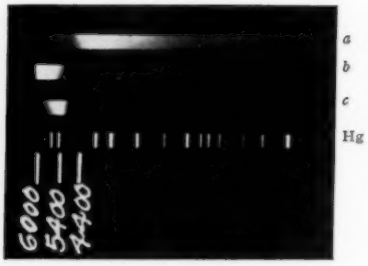

FIG. 4. Cathode-ray spectrogram of the pure and activated zinc borate compounds, "*a*" pure zinc borate, "*b*" and "*c*" manganese activated zinc borate heated to different temperatures.

8000 volts.[12] Both compounds were heated to 950°C. "*c*" is also from an activated compound heated to a much lower temperature. The green band predominates in this case.

Discussion

Several conclusions can be drawn from these experiments. It is seen that luminescence is closely connected with the physical structure of these compounds. A change from vitreous to granular state increases the brightness of the activated zinc borate more than 30 times. The ratio is even greater in the case of pure zinc borate. Whether the structure is microcrystalline or not cannot be definitely stated at this time but this seems quite probable. Assuming a crystalline structure, it appears that the nature of the emissions, and hence the nature of the emitting crystals, is controlled by the temperature of heat treatment as well as by the presence of the activators. It is also seen that pure zinc borate can be made luminescent without the addition of an activator. Although absolute purity is not claimed for this compound, the intense luminescence of the C.P. mixtures can hardly be explained as due to some undetected impurity, since the nature of luminescence given by the activated compound is quite different from that of the pure compound, as seen above.

[12] This voltage was found sufficient to excite all the wave-lengths as no additional wave-lengths appeared on such spectrograms when the specimens were excited by α-rays of polonium at high speed β-rays from radium $B+C$.

The luminescence of pure compounds has been claimed in previous communications from this laboratory.[13, 14] In recent years similar claims have been made by others.[15] If it be assumed that luminescence results from displacement of electrons to higher energy levels which may exist in an orderly arrangement of molecules, there is no reason to assume that pure substances cannot luminesce. Whether or not luminescence can be excited in a given solid will depend upon the existence or not existence of unoccupied energy levels to which electrons can be displaced, and not necessarily upon the presence of an impurity. On the other hand, the function of the impurity seems to be to lower these energy levels, as indicated by the abrupt change in the wave-length of the emission bands when an activator is used. If this law holds generally for other crystals, we might expect many pure crystals to show luminescence in the ultraviolet region. Addition of activators to these would simply bring the luminescence within the visible range, thereby creating the impression that the luminescence is produced by the activator. This seems to be true for a number of crystals under investigation, the results of which will be published in the near future. It is also possible that activator atoms create unoccupied energy levels in some crystals where none existed before. In any case the generally accepted idea of luminescence as due to active centers requiring an impurity as a nucleus seems subject to modification.

The author wishes to express his indebtedness to Mr. Howard Ashton for very efficient assistance in the preparation of the materials and in making the photometric measurements, and to Dr. Horace C. Richards and Dr. E. E. Witmer for many valuable suggestions. This investigation was made possible by a special grant from the Faculty Research Committee of the University of Pennsylvania which is hereby gratefully acknowledged.

[13] J. A. Rodman, Phys. Rev. **23**, 478 (1924).
[14] L. E. Smith, Phys. Rev. **28**, 432 (1926).
[15] O. Glasser and I. E. Beasler, Phys. Rev. **47**, 470 (1935).

LETTERS TO THE EDITOR

Prompt publication of brief reports of important discoveries in physics may be secured by addressing them to this department. Closing dates for this department are, for the first issue of the month, the eighteenth of the preceding month; for the second issue, the third of the month. The Board of Editors does not hold itself responsible for the opinions expressed by the correspondents.

Communications should not in general exceed 600 words in length.

Refraction of Neutrons

In looking for neutron effects analogous to the optical, a somewhat colimated beam of slow neutrons was prepared by the method of Szilard.[1] A paraffin "howitzer," as it is called in the Columbia laboratory, was made of a paraffin cylinder 40 cm high and 25 cm in diameter (*H* in Fig. 1) with a cavity 20 cm high and 12 cm in diameter. Just below the cavity lies the source, *S*, (Be+200 mg Ra). In an attempt to increase collimation, cylindrical tubes of paraffin (*C*) of 5 cm bore were fitted into the cavity. By measuring the activity of a silver target at *T*, numerous experiments were made with different heights of the cavity and different lengths of the inner tube, with no unexpected results. A curious phenomenon was observed, however, when the lower inner edge of the inner tube was beveled by conical cuts illustrated in the figure by the lines *L–N* to *L–P*. With the inner tube 18 cm long and unbeveled (*L–M*) the activity of the silver target in arbitrary units was 15.0. With a bevel of 30° the activity had fallen to 12.3, at 45° to 11.0 and at 60° to 10.3. The result obtained by removing the small amount of paraffin from the edge of the tube is rendered the more striking by the fact that if instead of the oblique cuts, transverse cuts had been made at *N*, *O* and *P* the activity would have steadily increased, as shown by numerous other experiments.

So singular a result had, of course, to be corroborated.

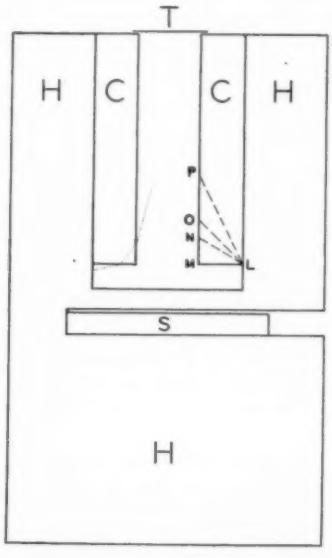

FIG. 1. Paraffin "howitzer."

It appeared fallacious after the experiments were repeated with another tube of paraffin and the measured activities proved to be nearly independent of beveling. However, the first tube was made of clear translucent paraffin while the second, apparently through the separation of a new solid phase, contained many holes of a few mm diameter. We had already suspected from other measurements that this heterogeneous paraffin (possibly through some phenomenon of refraction) was abnormal. Therefore other tubes were made up as nearly as possible like the first. With these, many experiments which cannot be described here have shown beyond any doubt that the effect first observed was correct. The magnitude of the effect varies with the distance between bottom of inner tube and bottom of cavity, being a maximum when this distance is about 2 cm. Under these conditions the average of all our experiments shows a diminution in activity of 20% for a bevel of 30°.

We have been unable to conceive of any purely corpuscular explanation of this remarkable phenomenon. If, however, we imagine the movement of a neutron to be directed by a coherent train of waves, a simple explanation suggests itself. The lower inner edge of the paraffin tube acts like a prism, as it would for light, and neutrons moving nearly horizontally in the cavity just below the tube would frequently follow such a path as indicated by the dotted line in the figure. This view at once suggests the use of a paraffin lens for the focusing of neutron beams. Preliminary experiments have been made which strongly indicate the existence of such focusing.

In many of the experiments that we have described parallel determinations were made with a rhodium in place of a silver target. The number of experiments was insufficient to give quantitative results but the effect of the beveled edge is certainly considerably less for rhodium than for silver. We think of the refraction phenomenon as affecting only the group of coherent neutrons, which probably coincides roughly with the group of very slow neutrons. The small effect with rhodium might, therefore, be attributed to a diminution in coherence by the rhodium or to a relatively lower sensitivity of rhodium toward very slow neutrons. The latter explanation is more probable since in an experiment which we have made with Dr. W. F. Libby a change from 300°K to 90°K diminishes the ratio of the activity produced in rhodium to that in silver.

GILBERT N. LEWIS
PHILIP W. SCHUTZ

Department of Chemistry,
University of California,
Berkeley, California,
February 14, 1937.

[1] Hopwood and Chalmers, Nature **135**, 341 (1935).

On the Interaction of Fast Neutrons with Lead

In a recent letter to *Nature*[1] Kikuchi and co-workers have postulated a hitherto unknown direct interaction of fast neutrons with extra-nuclear electrons. He and the others have noticed a large number of counts from a Geiger-Müller counter operated near a "deuteron-deuteron" source of neutrons. The counter was always placed in a lead box for x-ray shielding. Using a D-D source we have also observed a large number of counts in a Geiger-Müller counter, but our experiments were consistent with the supposition that fast neutrons excited gamma-rays in our lead x-ray shield.

We have investigated this assumption further, using 200 mc of Ra-Be in the arrangement shown in Fig. 1, in which the nearest hydrogenous material was the floor 112 cm below the lead block. The counter wall was covered with 1.0 g/cm² of lead. When the Ra-Be was introduced into the large lead block the counting rate changed from the natural background of 56/min. to 120/min. An investigation of the cause of this 64/min. increase was conducted as follows. Tests with radon alone in place of the Ra-Be, as well as other measurements, showed that the primary gamma-rays coming directly from the Ra-Be source were responsible for 6/min. of this increase.

With the 200 mc Ra-Be source in the lead block additional lead (in plates 15×30 cm²) was placed behind the counter (position *A*) and produced a further increase in the count. In Fig. 2 the percentage increase of the count due to the lead behind the counter (with the appropriate natural backgrounds subtracted) is plotted against the thickness of lead so placed. The curve obtained in the same manner for iron is included for comparison.

This curve establishes the existence of a gamma-ray produced by the action of fast neutrons on lead and the magnitude of its self-absorption indicates an energy somewhat less than 1 Mev. It is to be noted that the energy of this gamma-ray agrees roughly with the energy of the electron reported by Kikuchi. Assuming an efficiency of 1 in 100 for counting a gamma-ray of this energy, we arrive at a cross section of 1×10^{-24} cm² for the interaction of a fast neutron with lead to form a gamma-ray. From the magnitude of the effect produced by the lead at *A* we conclude that two-thirds of the 64/min. counts observed with no lead at *A* are due to such gamma-rays from the large lead block. Experiments indicate that the remaining one-third can be accounted for by the gamma-rays excited in the floor and walls, which were not infinitely remote.

A full account of the work is to be submitted for publication soon. We wish to express our thanks to Dr. L. R. Taussig of the University of California Medical School for the gift of the radon used for the gamma-ray control experiments and to Dr. W. F. Libby of the chemistry department and Dr. Edwin McMillan of the radiation laboratory of the physics department for valuable advice and assistance.

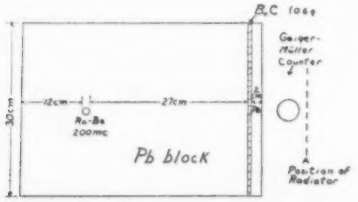

FIG. 1. Arrangement of source, counter, and radiator.

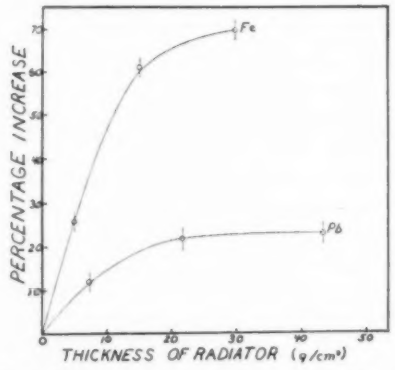

FIG. 2. Gamma-rays from fast neutrons on lead and iron.

G. E. GIBSON
G. T. SEABORG
D. C. GRAHAME

Department of Chemistry,
University of California,
Berkeley, California,
February 15, 1937.

[1] Kikuchi, Aoki, Husimi, Nature **138**, 841 (1936).

The Virial Theorem in Nuclear Problems

During the course of some calculations on the "group structure" of light nuclei,[1] the extension of the virial theorem to include exchange forces has been found of use, and seems to be of sufficient intrinsic interest to record here. Let Greek subscripts refer to the individual particles, while the Cartesian orbital coordinates are designated by x_j, $j=1, 2, \cdots$. It will suffice to consider the typical wave equation

$$-\sum_j(\hbar^2/2M_j)(\partial^2\psi/\partial x_j^2)+\sum_{\alpha}\sum_{\beta<\alpha}J_{\alpha\beta}S_{\alpha\beta}\psi=E\psi, \qquad (1)$$

where ψ is a function of all the coordinates, inclusive of spins, and $S_{\alpha\beta}$ is any kind of exchange (transposition) operator; e.g., the Majorana or Heisenberg type. The simplest procedure is to follow Slater's proof of the ordinary virial theorem,[2] the ψ function being assumed normalized. This involves only operation on Eq. (1) with the operator $\psi^*\sum_i x_i(\partial/\partial x_i)$, a rearrangement of the terms, and an integration over coordinate and spin space. The steps can easily be set down from Slater's procedure. The result is

$$2T_a=\sum_{\alpha}\sum_{\beta<\alpha}\int\left[\psi^*\left(\sum_i x_i\frac{\partial J_{\alpha\beta}}{\partial x_i}\right)(S_{\alpha\beta}\psi)\right]d\tau$$

$$+\sum_{\alpha}\sum_{\beta<\alpha}\sum_i\int J_{\alpha\beta}x_i\left\{\psi^*\frac{\partial}{\partial x_i}(S_{\alpha\beta}\psi)-\frac{\partial\psi}{\partial x_i}(S_{\alpha\beta}\psi^*)\right\}d\tau, \qquad (2)$$

where T_a is the average kinetic energy of the system.

If ψ is an eigenfunction for any $S_{\alpha\beta}$ the corresponding term of the last member of Eq. (2) vanishes. Thus if the ψ function is made antisymmetrical in the protons and neutrons separately, and the S's are Heisenberg operators, the last member will contain only cross terms between protons and neutrons. Again, this term vanishes for the separate states of the deuteron.[3]

Writing $J_{\alpha\beta}$ as a function of $r_{\alpha\beta}$ only, we get

$$\sum_i x_i \frac{\partial J_{\alpha\beta}}{\partial x_i} = (\mathbf{r}_\alpha - \mathbf{r}_\beta)\cdot\nabla_\alpha J_{\alpha\beta} = r_{\alpha\beta}(dJ_{\alpha\beta}/dr_{\alpha\beta}),$$

so that for the total energy we find

$$E = \sum_\alpha \sum_{\beta<\alpha} \int \psi^* \left\{ J_{\alpha\beta} + \frac{1}{2} r_{\alpha\beta} \frac{dJ_{\alpha\beta}}{dr_{\alpha\beta}} \right\} (S_{\alpha\beta}\psi) d\tau$$

$$+ \frac{1}{2} \sum_\alpha \sum_{\beta<\alpha} \sum_i \int \left[J_{\alpha\beta} x_i \left\{ \psi^* \frac{\partial}{\partial x_i} (S_{\alpha\beta}\psi) - \frac{\partial \psi}{\partial x_i} (S_{\alpha\beta}\psi^*) \right\} \right] d\tau.$$

In some simple cases this formula permits a relatively quick method of estimating the energy from approximate wave functions.

E. L. Hill

University of Minnesota,
Minneapolis, Minnesota,
February 8, 1937.

[1] W. H. Wells and E. L. Hill, Phys. Rev. **49**, 858 (1936).
[2] J. C. Slater, J. Chem. Phys. **1**, 687 (1933).
[3] Cf. H. Bethe and R. F. Bacher, Rev. Mod. Phys. **8**, 82 (1936), especially pages 105–119, for a discussion of the properties of the deuteron wave functions.

Neutron Optics

The remarkable results already obtained from the study of neutrons show what an extraordinarily fertile field of theoretical and experimental research would be opened if a beam of neutrons, like a beam of light, could be collimated, focused, or broken into a spectrum. Results have been obtained in two experiments[1,2] which have hitherto been attributed to the diffraction of slow neutrons by a crystal lattice, but it seems unlikely that diffraction by crystals can carry us far toward the goal of a complete mastery of the neutron beam.

Indeed the achievement of such a goal seems at first a little hopeless. The de Broglie wave-length, even of the slower neutrons with which we have to deal, does not much exceed 1A, compared with which any ordinary optical surface is extremely rough. Nevertheless, if some form of radiation is capable of penetrating deeply into a given medium, it may not be greatly affected by conditions at the surface.

In the theory of light there is another distance which is almost as important in the interpretation of wave phenomena as the wave-length. This distance is the length of the wave train, or, for short, the coherence distance, which may be roughly measured as the maximum difference in path, between two parts of a divided beam, that still permits interference. This coherence distance, according to modern theory, is determined in part by the history of the emitting atom, and chiefly by the life of that excited state of the atom which precedes the emission of a photon. Some time ago, however, I pointed out[3] that, according to the law of the symmetry of time in physics, which is one of the most universal of physical laws, "If a transition depends upon the properties of the state preceding the transition, it must in equal measure depend upon the properties of the state following." We may therefore state that the coherence distance depends symmetrically upon the lifetime of the emitting atom preceding the transition and the lifetime of the absorbing atom after the transition. This dependence of optical coherence upon the nature of the absorbing as well as of the emitting substance has never been sought for experimentally, but will undoubtedly be found.

It has seemed to me that a search for ordinary optical effects in a neutron beam would be profitable if, and only if, the neutrons can be expected to possess a high degree of coherence. Such coherence is indeed to be predicted from the view of capture in neutron orbits that I have recently set forth.[4] It seems to me that there can hardly be any other explanation of the remarkable effect of paraffin[5] in slowing neutrons down even to 20°K, except that neutrons fall into and are held by paraffin molecules, and are later reejected through thermal agitation. At least this view suggested a large degree of coherence of the slow neutrons from paraffin and led to the experiments described in the accompanying communication.

Gilbert N. Lewis

Department of Chemistry,
University of California,
Berkeley, California,
February 14, 1937.

[1] von Halban and Preiswerk, Comptes rendus **203**, 73 (1936).
[2] Mitchell and Powers, Phys. Rev. **50**, 486 (1936).
[3] Lewis, Science **71**, 569 (1930).
[4] Lewis, Phys. Rev. **50**, 857 (1936).
[5] Libby and Long, Phys. Rev. **50**, 577 (1936).

Experiments on the Magnetic Moment of the Neutron

Further experiments[1] have been performed to observe directly the effect of the magnetic moment of the neutron, and magnetic scattering. In one experiment, the neutrons were directed normally through two iron plates, each 0.5 cm thick, 24 cm apart, and magnetized to saturation by separate electromagnets. Counts were taken with the "polarizing" plate successively magnetized in opposite directions and then demagnetized. The "analyzing" plate was continuously magnetized in one direction. Table I shows the results of this experiment.

From these results it is seen that while there is no significant difference between the parallel and antiparallel cases, the differences between these cases and the zero case is significant. By considering only the slow (absorbed in Cd) neutrons it is seen that these differences represent 3.3 percent$\pm$1.2 percent and 2.7 percent$\pm$1.3 percent effects. These figures are in good agreement with a number of experiments which we have performed, including the results given in Table I of the previous letter,[1] in which the differences between the parallel and antiparallel cases are small, but in which much larger differences occur

TABLE I.

	Total No. Counts	No./min.	Differences from Demagnetized Case
Fields parallel	16,256	208.9±1.7	5.5±2.1
Fields antiparallel	16,220	207.8±1.7	4.4±2.1
"Polarizer" demagnetized	27,686	203.4±1.2	0
Background with Cd	787	26.7±1.0	176.7±1.5

TABLE II.

	Total No. Counts	No./min.	Differences
Magnetized	99,880	149.85±0.47	4.00±0.66
Demagnetized	98,542	145.85±0.47	
Background with Cd	6,310	28.30±0.36	117.55±0.59

between these and the demagnetized cases. These results in the parallel-antiparallel case are also consistent with those obtained by Hoffman, Livingston and Bethe.[2] (They give no data for the demagnetized case.)

The difference between the parallel and demagnetized cases suggested that an experiment should be performed using a single magnet. In order to reduce multiple scattering the experiment was performed using three 0.65 cm plates of Armco steel, spaced 5.7 cm apart. The plates were magnetized and then demagnetized. The results obtained in this experiment are shown in Table II. This difference represents a 3.4 percent±0.6 percent effect which is approximately six times the probable error.

In all experiments of this type, the effect of the magnetic field on the operation of the ionization chamber and the first tube of the amplifier must be considered. Spurious effects may be caused if they are not sufficiently shielded. In this experiment test runs were made which showed no such effects larger than 0.5 percent.

All of these results are at least in qualitative agreement with the theory which has been developed.[3] According to this theory, the scattering cross section for neutrons whose spin is parallel to the magnetic field in the iron is different from those whose spin is antiparallel. The transmission in the parallel case is proportional to

$$e^{-n\sigma(x_1+x_2)}\cosh n\sigma p(x_1+x_2)$$

and in the antiparallel case to

$$e^{-n\sigma(x_1+x_2)}\cosh n\sigma p(x_1-x_2),^{3-4}$$

where n is the number of atoms per cc, $\sigma(1+p)$ and $\sigma(1-p)$ are the cross sections for the two directions of polarization, and x_1 and x_2 are the thicknesses of the plates. The expression for the antiparallel case becomes the same as that for the demagnetized case, namely, $e^{-n\sigma(x_1+x_2)}$ provided that $x_1=x_2$.

In general, therefore, the transmission should be greatest in the parallel case, and the same in the antiparallel case as in the demagnetized case. In the first experiment, only one plate was demagnetized; hence this transmission should be slightly greater than the antiparallel case. Evidence for the reorientation of the neutrons in the antiparallel case is found, since the number transmitted was nearly as great as in the parallel case; i.e., the plates were so far apart that the neutrons passed through a region in which the gradient of the field was of the same order as the Larmor precession frequency of the neutrons, and hence a large fraction of them reoriented themselves parallel to the field of the second plate. Thus it approximates the parallel case and the difference would be small as all of the experiments indicate.[1, 2]

From these and the earlier experiments[1, 2] the existence of magnetic interaction with magnetized materials arising from the neutron magnetic moment is definitely proven; but the results must be interpreted with caution.

P. N. POWERS
H. G. BEYER
J. R. DUNNING

Pupin Physics Laboratories,
Columbia University,
New York, N. Y.,
February 17, 1937.

[1] Dunning, Powers and Beyer, Phys. Rev. **51**, 51 (1937).
[2] Hoffman, Livingston and Bethe, Phys. Rev. **51**, 214 (1937).
[3] Schwinger, in process of publication.
[4] Bloch, Phys. Rev. **50**, 259 (1936).

Proceedings of the American Physical Society

Minutes of the Atlantic City Meeting, December 28–30, 1936

THE 38th annual meeting (the 211th regular meeting) of the American Physical Society was held at Atlantic City, New Jersey, on Monday, Tuesday and Wednesday, December 28, 29 and 30, 1936, in affiliation with Section B-Physics of the American Association for the Advancement of Science. The presiding officers were Professor F. K. Richtmyer, President of the Society, Professor H. M. Randall, Vice President, Dr. Lyman J. Briggs, Professor H. A. Erikson, Dr. Lauriston S. Taylor, and Professor D. L. Webster. There were about four hundred physicists in attendance at the meeting. All sessions were held at the Hotel Chalfonte.

The joint session with Section B of the A. A. A. S. and the American Association of Physics Teachers was held on Tuesday morning at ten o'clock. The presiding officer was Professor D. L. Webster in the place of Dean George B. Pegram, vice president of Section B. The retiring vice president of Section B, Professor John T. Tate, presented a paper on "Electron Impacts in Gases." Professor F. K. Richtmyer, president of the American Physical Society, delivered an address on "Multiple Ionization of Atoms."

On Monday morning and afternoon there was a symposium of fifteen invited papers on "Some Problems in Radiological Physics." The program was arranged by Dr. Lauriston S. Taylor of the National Bureau of Standards.

On Tuesday evening the Physical Society and the American Association of Physics Teachers held a dinner at the Hotel Chalfonte. Professor F. K. Richtmyer, president of the Physical Society, presided. A brief speech was made by Professor H. M. Randall. Dr. A. G. McCall of the U. S. Department of Agriculture spoke on the subject of soil conservation and erosion. The award of the prize for excellence in teaching was given posthumously to Professor William S. Franklin by the American Association of Physics Teachers. This award consisted of two bronze plaques to be placed in the laboratories of the Massachusetts Institute of Technology and Lehigh University. A certificate was also presented to Professor Franklin's son. There were two hundred guests at the dinner.

Annual Business Meeting. The regular annual business meeting of the American Physical Society was held on Tuesday morning, December 29, 1936 at nine-thirty o'clock, President Richtmyer presiding. The president had appointed Messrs. Richard M. Bozorth and William H. Crew to canvass the ballots for the officers of the Society. They reported the following elections:

President, H. M. Randall
Vice President, Lyman J. Briggs
Secretary, W. L. Severinghaus
Treasurer, George B. Pegram
Member of the Council, one year term, H. A. Erikson
Members of the Council, four year term, M. J. Kelly, J. C. Slater
Members of the Board of Editors, three year term, Kenneth T. Bainbridge, H. P. Robertson, H. B. Wahlin

Approval was voted of the following modification of the by-laws as recommended by the council:

Change Article V, Section 4, to read as follows:
"No papers may be accepted for presentation at any meeting of the Society subsequent to the closing date stated in the printed call for that meeting."

The Secretary reported that during the year there have been 238 elections to membership. The deaths of 12 members have been recorded; 30 have resigned; 91 have been dropped; and 60 have been placed on the inactive list. The membership of the Society as of December 24, 1936 was as follows: 2160 members; 725 fellows; 6 honorary members; 2891 total membership. The membership at the present time shows a gain of 45 members, a rather small increase since last year but this is accounted for by the fact that a great many members who were carried on the rolls of the Society during the depression have either been dropped or placed on the inactive list.

The Treasurer presented a summary of the financial condition of the Society. It was impossible to present a final report for the year at the annual meeting because the fiscal year ends on December 31. The Treasurer's financial report will be audited, printed and distributed to members.

The Managing Editor made an informal report.

Meeting of the Council. At the meeting of the Council held on Monday afternoon, December 28, 1936 two members were transferred from membership to fellowship and sixty-four were elected to membership. *Transferred from membership to fellowship:* N. Henry Black and Erich Hausmann. *Elected to membership:* Herbert L. Anderson, Kanetako Ariyama, Charles H. Bachman, Robert M. Besancon, Harold G. Beyer, Nautamlal B. Bhatt, C. B. Braestrup, Robert B. Burnham, C. W. Chapman, Peh-ping Cheo, Djen-yuen Chu, R. F. Clash, Jr., Arnold A. Cohen, William J. Culmer, C. W. Curtis, Lee Devol, Emmanuel Dubois, Charles K. Eckels, Charles H. Ehrhardt, Walter M. Elsasser, Einosuke Fukushima, Erwin R. Gaerttner, John E. Gorham, Horace J. Grover, Homer D. Hagstrum, Sally Harrison, Harry H. Hubbell, Jr., Richard W. Jones, David M. Kerns, Gilbert D. Kinzer, Solomon J. Klapman, Reginald G. Lacount, Andrew W. Lawson, Jr., Lawson M. McKenzie, Albert V. Masket, Bertrand J. Miller, Alexander M. Monnier, Joseph Morgan, Otto Morningstar, Philip Nolan, Thomas J. W. O'Neil, Chester H. Page, Hermon M. Parker, Wallace W. Perkins, John R. Pierce, W. G. Pollard, Philip N. Powers, Maurice H. L. Pryce, David L. Rich, A. Rostagni, Walter E. Sargeant, Klaus Schocken, Ross E. Shrader, R. K. Sharma, Keizo Sinma, Lynn H. Stauffer, Robert B. Taft, A. H. Taub, John Victoreen, E. R. Walker, Arthur C. Weid, Royal Weller, Victor J. Young, and Arthur A. Zuehlke.

The regular scientific program of the Society consisted of sixty-eight papers, of which numbers 2 and 16 were read by title. The abstracts of these papers are given in the following pages. An *Author Index* will be found at the end.

W. L. SEVERINGHAUS, *Secretary*

ABSTRACTS

1. Some Problems in Radiological Physics. LAURISTON S. TAYLOR, *National Bureau of Standards.*—This paper does not present any new experimental results but is intended to serve as an introduction to the succeeding papers on radiological physics. It appears that radiation dosage measurements are satisfactory up to 200 kv, although for higher voltages and gamma-rays there is not yet complete unanimity of opinion regarding what methods are best. Thimble ionization chambers are used in these voltage ranges but there is no adequate standard for calibrating them. With the possibility that neutrons may have biological application, further problems of dosage measurement are in the offing. The means for protection from super-voltage x-rays, gamma-rays, and neutrons are very uncertainly effective—some workers practically neglecting it entirely while others overdo it. Measurements of voltages above 300 kv are not entirely satisfactory, and in most medical installations no simple and adequate means is available at present. The measurement of radiation quality in the supervoltage range is still uncertain and of the several methods proposed none is as yet in general use. For neutrons the question of energy distribution or quality of radiation is essentially untouched.

2. The Measurement of Very Hard X-Rays in Roentgens. G. C. LAURENCE, *National Research Council of Canada.*—The standard x-ray ionization chamber is impracticable for very hard radiation and it is customary to use thimble chambers with thick walls composed of the light elements. In interpreting these measurements in roentgens, it has been assumed usually that the intensity of the ionization in the air space is equal to the value it would have in the center of a very large volume of air. This is approximately true, but it is shown that the intensity in the thimble chamber is greater by a factor B that differs generally from unity by a few percent. An expression for B is derived and curves are given to assist in calculating it for any quality of very hard radiation with different compositions of wall material. Using radium B+C radiation filtered through 0.5 mm platinum, B has the value 0.977 for a carbon chamber, and 1.082 for aluminum. B for carbon varies between 0.96 and 0.975 for x-rays excited at potentials between 400 kv and 1000 kv and filtered through 1 mm lead. Absorption corrections and other details that must be considered in thimble chamber measurements are discussed.

3. The Measurement of Backward Scattered X-Radiation. EDITH H. QUIMBY, *Memorial Hospital, New York, N. Y.*—In radiation therapy an important factor in determining the amount which can be delivered through a given field is the tolerance of the skin. The radiation which produces the skin reaction is a combination of the direct beam and that scattered backward by the underlying tissues; it varies among other things with the quality of the radiation and with the size of the field. The back scatter cannot be satisfactorily measured with small closed ionization chambers of the thimble type, because of potential errors introduced by the wall thickness, air volume, etc. The extrapolation type of chamber described by Failla is well adapted to making such measurements, since the wall effect can be eliminated; the volume can be varied between wide limits and the ionization for a vanishingly small

volume found by extrapolation. Data are presented for back scatter measurements with both types of chamber, from a volume of organic material comparable with the human body, for a wide range of qualities and of field sizes.

4. Dosage Determinations on Ten Different 400 kv Roentgen Ray Generators. OTTO GLASSER, *Cleveland Clinic, Cleveland, Ohio.*—Ten high voltage generators both of the pulsating and constant potential type were examined. The radiation quantity was measured for given conditions in roentgens by means of an "air wall" thimble chamber. Absorption curves in copper and tin were made. The values obtained were compared with those measured on 200 kv roentgen ray generators under otherwise identical conditions.

5. A Study of the Secondary Radiations Emitted by Filters Used in Roentgen Therapy. L. D. MARINELLI, *Biophysics Laboratory, Memorial Hospital, New York, N. Y.*—The secondary emission from aluminum, copper, tin and lead has been studied by shifting the relative position of the primary and additional filters with respect to an open ionization chamber of the mesh type. The softer part of the emission from Al, Cu and Su has been found to be satisfactorily eliminated by 0.16 mm celluloid in the case of Al primary filter; 0.18 mm Al plus 0.16 mm celluloid, or 0.40 mm celluloid in the case of Cu; and 0.17 mm Cu plus 0.4 mm celluloid in the case of Su. No conclusive figure could be reached in the case of lead with 200 kv x-rays. The harder portion of the emission cannot be controlled efficiently by the insertion of secondary filters, and data are presented for the calculation of the skin to filter distance in order to reduce the residual scatter to 1 percent of the available beam, when primary filters of Cu and Su are used. Experimental evidence points out that a Cu filter removed from the skin by more than 10 cm does not contribute any appreciable amount of soft radiation to the skin dose.

6. The Production of Very Thin Beryllium Flakes for a Po-Be Neutron Source. T. R. FOLSOM, *Physics Department, Memorial Hospital, New York, N. Y.*—A technique for producing extremely thin flakes of metallic beryllium by a vacuum-evaporation process is described. The use of these flakes to produce an intense Po-Be neutron source concentrated in a very small volume is discussed.

7. Physical Measurements Concerning the Biological Action of Neutrons. PAUL C. AEBERSOLD, *Radiation Laboratory, University of California.*—The large yield of neutrons produced by the bombardment of beryllium with the high voltage deuterons obtainable with a cyclotron allowed investigation of the biological actions of neutrons. With 20 microamperes of 5.8 Mev deuterons, the intensity of ionization in an x-ray r-meter thimble chamber at 15 cm from the beryllium target is the same as that due to 10 r/min. of x-rays. This neutron intensity was found to be biologically equivalent to 20 to 50 r/min. of x-rays, depending on the organism irradiated. To produce biologically equivalent intensities of gamma-rays would require 50 to 125 grams of radium. However, to obtain this yield of neutrons would require more than 10,000 grams of radium mixed with beryllium. The biological effectiveness per unit of ionization measured with a small Bakelite-walled thimble chamber was found for neutrons to be two to five times as great (depending on the organism) as for x-rays. Although the ionization due to neutrons varies with the hydrogen content of the chamber wall and its enclosed gas, the variation observed is not sufficient to indicate that neutrons cause two to five times as much ionization in tissue as x-rays when these radiations cause equal ionization in a Bakelite-walled chamber. Thus using other "tissue-like" chamber walls, there still appears to be a differential, as well as an increased biological effectiveness for neutrons; consequently until further knowledge is gained concerning "tissue" ionization, a small Bakelite-walled thimble chamber calibrated with x rays may serve as a standard ionization measure for neutrons.

8. The Mechanism of Delayed Killing of Maize Seedlings with X-Radiation. LOUIS R. MAXWELL, *Bureau of Chemistry and Soils.**—Dry seeds of maize after receiving heavy x-ray dosages (60,000 to 100,000 r units) show no reduction in germination; however, soon after the plumule has emerged growth ceases and the plant dies. This phenomenon has been called "delayed killing." An S-shaped survival ratio curve has now been obtained which shows that 50 percent delayed killing will occur at 35,000 r units. This result can be interpreted from the standpoint of the hit theory involving the conception of a certain number of required hits within a vital volume of the seed. On this basis the experimental results can be expressed in either of two ways: (1) that a single vital volume of 6×10^{-16} cm³ must be hit 14 times by primary electrons to cause delayed killing or (2) that there may exist several vital volumes each of which must be hit a number of times in order to produce delayed killing. Since the seed embryo is multicellular the latter explanation is more tenable. When various restricted zones 0.5 to 2.8 mm wide taken across the seed are exposed it is found that no appreciable killing occurs until a slit width greater than 0.5 mm is used. This definitely proves that no single vital volume of the above small dimensions exists.

* In cooperation with the Bureau of Plant Industry.

9. Columnar Ion Concentration and the Biological Effectiveness of X-Rays, Neutrons and Alpha-Particles. RAYMOND E. ZIRKLE, *Johnson Foundation for Medical Physics, University of Pennsylvania.*—Biological effectiveness per ion depends to a marked extent upon the concentration of ions produced in the track of the ionizing particle. Four different columnar concentrations have been investigated: (*a*) that produced by electrons set in motion by x-rays; (*b*) that produced by recoil nuclei set in motion by neutrons; (*c*) that produced by the polonium alpha-particle at the beginning of the column; (*d*) the same at the end of the column. These concentrations are listed in increasing order. All four have been used on one type of biological object; (*a*) and (*b*) upon two others. In all cases, the higher the concentration of ions in the column, the greater is the biological effectiveness per ion. The magni-

tude of this effect varies markedly among the three different organisms. (The neutron experiments were carried out in the Radiation Laboratory, University of California, with the collaboration of P. C. Aebersold and E. R. Dempster.)

10. Neutron-Yield Curves for Light Elements. L. R. HAFSTAD AND M. A. TUVE, *Department of Terrestrial Magnetism, Carnegie Institution of Washington.*—During a visit by E. Amaldi, measurements on neutron-yield curves for several light elements bombarded with deuterons were carried out in our laboratory. Observations were made from 200 to 1000 kv by using the Rome technique for determining the absolute number of neutrons produced. These observations show the values of current and voltage required for producing neutrons in large quantities in this voltage range, and determine the amounts of artificial radioactive substances which can be produced.

11. The Absorption of Ultra-Short X-Rays. F. K. RICHTMYER, *Cornell University.*—Accurate data giving absorption coefficients of monochromatic ultra-short x-rays (i.e. $\lambda<100$ X.U.) are desirable: (1) to check and extend current theories of the interaction between high frequency radiation and matter; (2) to place in the hands of the roentgenologist and the industrial technician pertinent information with regard to the uses of high voltage x-rays in radiology and in industry. Recent developments in the technique of producing high voltage x-rays and in the design of spectrometers for work in this x-ray region have made it possible to obtain acceptably correct values of monochromatic absorption coefficients for x-rays of wavelength as short as $\lambda=30$ X.U. These data have been reported by Cuykendall[1] and Jones.[2] From these and similar data by other authors, "half-value" thicknesses for representative materials are computed. Also, the filtering action of representative materials on high voltage x-rays is presented.

[1] Cuykendall, Phys. Rev. **50**, 105 (1936).
[2] Jones, Phys. Rev. **50**, 110 (1936).

12. The Chemical Activity of X-Ray Activated Water Molecules. HUGO FRICKE AND HOMER P. SMITH, *Walter B. James Laboratory for Biophysics, The Biological Laboratory, Cold Spring Harbor, N. Y.*—An important fact in the biological effects produced by x-rays (as compared, for example, with those of light) is that the initial chemical reactions result from the activation of all molecular species present in the irradiated medium. In view of the large content of water in living cells, the reactions resulting from the activation of the water molecule are of particular importance. The present report is a summary of our studies in this field, including investigations of solutions of a number of organic, and certain biologically important inorganic, molecules. Particular attention is given to the influence of certain general factors, particularly the oxygen molecule and the hydrogen ion.

13. The Effect of Irradiation on Oil Drops. WILHELM STENSTROM AND IRWIN VIGNESS, *University of Minnesota Hospital, Minneapolis, Minn.*

14. The Measurement of Scattered Radiation in Roentgenography of the Chest. R. B. WILSEY, *Kodak Research Laboratories, Rochester, N. Y.*—Scattered radiation was recorded photographically in the shadows of lead shot placed on the tube side of the patient. The evaluation of the ratio of scattered radiation to the total of scattered and primary radiation just outside the shot shadow was determined with the aid of time-scale sensitometric exposures placed at the corners of the film. The correction for the difference in time-scale and intensity-scale sensitometric exposures was found by a separate experiment. In a series of adult chests of medium size, the proportion of scattered radiation recorded in the roentgenogram averaged 55 percent, while values as high as 65 percent occurred in some portions of the chest. In larger patients, the proportion of scattered radiation averaged as high as 65 percent over the lung fields with some areas recording values over 80 percent. These data indicate the necessity of applying the Potter-Bucky diaphragm to the roentgenography of the larger sizes of chest.

15. Secondary Radiation Intensity as a Function of Certain Geometrical Variables. HERMAN E. SEEMANN, *Kodak Research Laboratories, Rochester, N. Y.*—X-ray intensity measurements of a beam passing through filters or diaphragms may be affected by the secondary radiation produced. Definite means for estimating the secondary radiation intensity must therefore be used if this quantity is to introduce no error in the final results. Making certain assumptions, it is possible to treat the problem geometrically and, with source and receiver fixed, obtain simple relations between the secondary intensity and the distance between scatterer and receiver. Several cases are considered: (1) the position of a filter of fixed size is varied, (2) the filter size is varied so as to always fill a fixed cone of radiation, (3) the edge of the diaphragm furnishes secondary radiation due to partial transmission of the primary beam, or (4) due to the incidence of the primary beam directly upon the faces of the hole. The results apply to other forms of radiation, since the treatment is geometrical. There is satisfactory experimental verification of the formulas developed for cases (1) and (2), but (3) and (4) will require great constancy of radiation intensity and sensitivity of measuring apparatus.

16. Thermal Diffusivity of Nickel. CHAUNCEY STARR, *Harvard University.**—The dynamic method of determining thermal diffusivities devised by King has been improved. A sinusoidal temperature is impressed on one end of a wire specimen, and the thermal diffusivity is determined from the characteristics of the temperature wave traveling along the specimen. In King's method the velocity of the wave is measured. In the present method the amplitude decrement is determined. The unknown surface heat loss from the specimen can be eliminated from the calculations by measurement with heat waves of two different periods. Greater precision is possible with this method than with previous methods. The thermal diffusivity of nickel, measured at 25°C, was 0.15885 cm²/sec., with a probable error of 0.06 percent. The specimen had been annealed in

hydrogen at 870°C, and had a total nickel content greater than 99.98 percent, a density of 8.79 g/cm³, and an electrical resistivity of 7.21 microhm-cm at 22°C. The thermal conductivity of nickel corresponding to this determination is 0.618 watt/cm °C.

* To be read by title.

17. Biophysical Methods in Studies of Mammalian Temperature Regulation. ALLAN HEMINGWAY, *Yale University and the University of Minnesota.*—Electrical conductivity measurements of the tissues of warm blooded animals have been made using alternating currents of frequencies ranging from 1000 to 1,000,000 cycles per second. At the higher frequencies the phase angle of the tissues becomes zero. This makes possible the measurement of the heat received by an animal which is heated by a high frequency current, the power consumption of the animal being simply the product of high frequency voltage and current, these values being obtained from suitable high frequency instruments. By placing metallic electrodes in contact with the skin of an animal and placing these electrodes in a high frequency circuit the current passing through the animal generates heat which can be accurately measured. This provides the physiologist with a tool for giving to animals a known amount of heat produced by physical means and with a minimum amount of discomfort to the animal. Such a method is especially useful in studies of heat tolerance. Dogs have been heated by a diathermy current (one million cycles per second) which does not produce electrical stimulation of the neuromuscular system. The heat received by the animal has been measured together with changes in the physiological mechanisms for heat dissipation which include (1) increased skin and rectal temperatures and (2) changes in respiratory activities.

18. Characteristics of Shock-Wave Propagation Near an Explosive Source. L. THOMPSON AND N. RIFFOLT, *Naval Proving Ground, Dahlgren, Va.*—Continuing an experimental study[1] of the condensation pulse generated by a detonating high explosive, the following results have been obtained. (*a*) Cathode oscillograms of the pressure pulse taken at similar points of the field for charges of different magnitudes show the conditions actually to be similar, at least with respect to maximum pressure. A shape factor is identified by the slightly greater values of reduced times obtained for spherical sources, comparing data for cylindrical charges. (*b*) The shock-wave is shown to be definitely diverging from the gas bubble at x values less than 15 (half-diameters). (*c*) The formulas therefore represent a "free" sound field (as distinguished, for example, from the permanent regime at the nose of a high-speed bullet in flight) with velocities extending to several times the normal velocity. The characteristics are those which would develop in fact if there were free propagation in accordance with the formulas all the way from the boundary of the charge, at which point the pulse velocity is sometimes as much as 5000 meters per second.

[1] *The Propagation of a Shock-Wave in Air*, L. Thompson and N. Riffolt, abstracts 64, 65, Phys. Rev. **49**, 421 (1936).

19. High-Speed Multi-Jet Oil Diffusion Pumps of Metal Construction. C. M. VAN ATTA AND L. C. VAN ATTA, *Massachusetts Institute of Technology.*—Several models of a new design of all-metal, multi-jet oil diffusion pump have been constructed, tested and used at this laboratory during the past two years. Some of the distinctive features of the design are a compact boiler and jet system, direct heating of jets by conduction through metal parts of low thermal resistance, cooling of all surfaces exposed to the high vacuum space, low power requirements and small over-all dimensions for resulting pumping speeds, and ease of dismantling and servicing without disconnecting high-vacuum or fore-vacuum lines. The performance characteristics of this design may be judged from the following data taken on three pumps all with jet clearances of approximately 4.5 mm. As the gas leak into the system

Diam. of Pump Jacket (in.)	Power Required (watts)	Pumping Speed for Air (liters/second)
3½	240	40
4¼	260	75
7	480	200

is increased, the pumping speed remains constant up to a fore-pressure of about 1.5×10^{-2} mm Hg and is still appreciable at a fore-pressure of 3×10^{-2} mm Hg, so that mechanical pumps are adequate for backing purposes. Curves showing pumping speed as a function of fore-pressure and of oil temperature will be shown, the influence of jet clearances discussed and the methods used for measuring pumping speeds described.

20. A Cold Cathode Rectifier. CHARLES. T. KNIPP, *University of Illinois.*—The cold cathode rectifier exhibited at the Science Exhibit sponsored by the A.A.A.S. at St. Louis last holidays has been very much improved as an efficient device for the rectification of comparatively high alternating voltages. The rectifier as first made, with comparatively small electrode surfaces (about 10 sq. cm area each), transmits 30 ma on half wave rectification, and about 50 ma on full wave rectification. This is for 25,000 alternating volts. Rectifiers having electrodes of larger area and spaced differently are in the process of construction. Photographs of wave-forms for both half and full wave rectification will be shown. The rectifier will be in operation during the period of the science exhibit, booth 90.

21. The Mechanism of Electron Emission from Coated Cathodes. EMERY MESCHTER, *Cornell University.*—Emission from oxide-coated and other complex cathodes is explained qualitatively in terms of certain fundamental quantum-mechanical ideas to which Gurney has called attention. Perturbation of the highest levels in the atoms forming the coating results in the broadening of these levels into bands. The degree to which these bands are filled determines the strength and sign of the double layer formed at the surface, and hence the work function of the surface. Double layers formed by metallic atoms of low ionization potential may be changed in strength or reversed in sign by the admixture of nonmetallic atoms which possess a high virtual level. The most common of such atoms is oxygen, but among other possibilities might be listed sulfur, fluorine, chlorine and iodine. The char-

acter of the resulting double layer depends on the arrangement of the atoms of the one or more elements composing the coating. Experimental work has indicated the upper limit of the ionization potential of the metallic atom.

22. The Charge on the Electron. J. A. BEARDEN, *Johns Hopkins University.*—The satisfactory agreement of the ruled grating measurements of x-ray wave-lengths by different observers[1] and the failure to find an explanation of the discrepancy in the value of e thus obtained with the Millikan oil-drop value have made a repetition of Millikan's experiment necessary. The first part of the experiment has been a precision determination of the viscosity of air by the rotating cylinder method. This has been done as a check on former results (Millikan, Kellstrom and Bond). In the final measurements it is intended that a pure inert gas will be used. The design of the apparatus, the machining of the cylinders and guard rings, and the alignment of the apparatus are such as to insure a final value of the viscosity with an accuracy of about one part in 10^4. The speed of the driving mechanism is constant within 5 parts in 10^6. The value of the viscosity of air obtained, together with Millikan's oil-drop data, gives e in agreement with the x-ray value.

[1] Phys. Rev. **48**, 385 (1935).

23. Contact Potential Difference Between Different Faces of Silver Single Crystals. H. E. FARNSWORTH, *Brown University.*—Two crystals were cut and etched so as to expose (100) facets on a plane surface of one, and (111) facets on a plane surface of the other. Measurements by the Kelvin null method of the potential difference between these faces are being made in a high vacuum as a function of heat treatment. Outgassing has been continued at various temperatures below visible red heat for a period of 160 hours. After this time the (111) face is positive with respect to the (100) face by about 0.4 volt. While this is a preliminary value only, the results indicate that the true value is probably greater than this.

24. The Shenstone Effect in Bismuth. ALFRED H. WEBER, *St. Joseph's College, Philadelphia,* AND CHARLES B. BAZZONI, *University of Pennsylvania.*—Shenstone's original experiments[1,2] on the variation of the photoelectric sensitivity of Bi as a function of electric currents passed directly through the metal were repeated and extended. In the present preliminary investigation (1) the effect reported by Shenstone was verified; (2) the change of the effect with successive runs on the same Bi specimen was studied (Shenstone used fresh Bi samples for each of his curves); (3) the effect of occluded gases, presumably, on the photoelectric sensitivity was investigated; and (4) curves of the decay of the effect were obtained. Two cast Bi plates and a Bi single crystal were employed as specimens. The obvious conclusion to be drawn from the present experiments is that the variations in the photoelectric sensitivity of Bi when electric currents are passed directly through this metal are due to changes in the quantity of gas occluded by the metal.

[1] A. G. Shenstone, Phil. Mag. **41**, 916 (1921).
[2] A. G. Shenstone, Phil. Mag. **45**, 918 (1923).

25. Note on Quantum Absorption Probability in the Case of the Photoelectric Effect. A. T. WATERMAN, *Yale University.*—If, in the derivation of the expression for the photoelectric current by the Dubridge method, the probability of absorption of a quantum of radiation by an electron is assumed to be proportional to u^β, i.e., to some unknown power of the velocity component normal to the emitting surface, then the photoelectric current for frequencies near the threshold retains the same form of dependence upon frequency and temperature, in the first approximation, independent of β. The coefficient of the expression for the current (or the constant term in the expression for log I/T^2), however, contains the factor $(m/2\zeta)^\gamma$, m being the electronic mass and ζ the thermodynamic potential, while $\gamma = \frac{1}{2}, 0, -\frac{1}{2}$, for $\beta = 0, 1, 2$, respectively. Using experimental values for absolute magnitudes of the photoelectric current, it appears that the value of β should be in the neighborhood of 2, i.e., that the probability of absorption of a quantum is proportional to the square of the electron's normal velocity component, in approximate agreement with the prediction of quantum mechanics.

26. Critique of the Quantum Theory of Metallic Conduction. ERNST WEBER, *Polytechnic Institute of Brooklyn.*—Although quantum theory has shown many successes in its applications to metal physics, still there are some fundamental inconsistencies, as for example the concept of the "free path" of the quantized and spinning electron, its treatment by periodic functions without boundary conditions applicable to the metal, nevertheless the assumed potential barrier at the surface; the "gas" character of the electrons and the tremendous internal pressure, yet no admitted compressibility; and the fact that there is no room for superconductivity. The inference is drawn that other than ideal "gas concepts" should be applied to the electron swarm and a theory of electric conduction is proposed which, while essentially a continuum theory, leaves room for quantum theoretical treatment of the new parameters for microscopic phenomena. Conductivity variations with thickness of films, resistance variations in the magnetic field, and the galvanomagnetic phenomena can be described in simple terms.

27. Application of a New Mathematical Method to Vibration-Rotation Interaction. JENNY E. ROSENTHAL AND LLOYD MOTZ, *Columbia University.*—Standard methods of treating the vibration-rotation interaction, such as perturbation or W.K.B. calculations, require the expansion into infinite series of the rotational term in Schrödinger's equation. This procedure is highly questionable because it involves integrations over a region where this infinite series diverges. A method of solution is proposed here which does not require such expansions. Its applicability is contingent upon the presence in the differential equation of a small parameter multiplying the second order derivative. For example, if z is the radial component of the eigenfunction, the equation for the rotating harmonic oscillator is:

$$\frac{d^2z}{d\xi^2}-\frac{\xi}{\alpha}\frac{dz}{d\xi}+\left[\frac{\lambda}{\alpha}-\frac{j(j+1)}{(1+\xi)^2}\right]z=0,$$

where $\xi=r/r_e-1$, $\alpha=B_e/\omega_e\ll 1$, $\lambda=E/\omega_e-\frac{1}{2}$. The substitution: $z=y\exp\left[-\alpha j(j+1)\int\sum_{k=0}^{\infty}\alpha^k\varphi_k d\xi\right]$, with y the eigenfunction for no rotation, leads to a solution if we equate to zero the coefficients of successive powers of α. The eigenvalues are obtained from the behavior of the solution not at the limits but at the intermediate point $\xi=0$, which is a singular point of the equation. This method has been used for the determination of energy levels of both the harmonic and the anharmonic oscillator. It is particularly suited to the calculation of higher order corrections which may be obtained with a comparatively small amount of labor. The results check Dunham's standard W.K.B. calculation to the fifth order. An explanation is given for this somewhat unexpected confirmation.

28. The Calculation of Intermolecular Forces and Energies. MAURICE L. HUGGINS, *Kodak Research Laboratories.*—The resultant force between two molecules may be considered as the sum of forces of the following types: (1) interpenetration repulsions; (2) attractions of the London "dispersion" type; (3) forces between dipoles; and (4) valence or exchange forces. In many instances the last can be neglected. Methods for evaluating the other three are discussed in the paper and applied to specific examples.

29. On the Interaction of Heavy and Light Particles at Very High Energies. L. W. NORDHEIM AND G. NORDHEIM, *Purdue University.*—An attempt has been made to estimate the probabilities of the emission of electrons and neutrinos by very energetic protons passing through matter, due to the Fermi interaction, as suggested by Heisenberg.[1] An interaction "Ansatz" which gives both the correct magnitude and the correct range for the nuclear forces has been used.[2] It involves therefore a cutting off at high energies of the interaction of the light particles in a system of reference where the heavy particle is at rest. For the case when the proton does not actually penetrate the nucleus the probability of the effect mentioned can be worked out by a generalized Weizsäcker method involving a more careful estimate of the integration limits and of the action of the Coulomb field of the nucleus on the protons. The effect proves to be small. The total energy loss of protons of about 10^{11} ev is in Pb of the order of the ordinary collision losses and in air a few percent of it. The photon and neutrino absorption coefficients due to induced nuclear β-transformations were also worked out and found to be very small. The magnitude of these effects depends essentially only on the integral strength of the nuclear forces and not much on the particular interaction Ansatz.

[1] W. Heisenberg, Zeits. f. Physik **101**, 533 (1936).
[2] Suggested by J. R. Oppenheimer at the Harvard Tercentenary Physics Symposium.

30. A Test of the Cellular Method of Obtaining Lattice Functions. W. SHOCKLEY, *Massachusetts Institute of Technology.*—In the absence of a rigorous theory for solving the wave equation in the cellular potential field introduced by Wigner and Seitz, approximate methods have been developed by Slater, Wigner and Seitz, and others. These utilize the solutions obtained in spherical coordinates in the cell to construct lattice functions, which are required to be continuous in value and derivative only at certain points of the intercellular boundary, for example the midpoints of the faces for body and face-centered lattices. The purpose of this paper is to test certain of these methods for the case where the exact solutions are known, namely the case of the "empty lattice" for which the potential is everywhere constant and the lattice points are geometrical figments, the exact solutions then being plane waves. For body and face-centered lattices it is found that within the first Brillouin zone the agreement is excellent. In the next zone the energy may be in error by a factor of $\frac{1}{2}$. Slides comparing the approximate and exact solutions will be shown, and the implications of these results in regard to the work done on various crystals will be discussed.

31. The Sign of the Nuclear Magnetic Moment of K^{39}. H. C. TORREY AND I. I. RABI, *Columbia University.*—The method of nonadiabatic transitions in an atomic beam[1] has been used to determine the sign of the nuclear magnetic moment of K^{39}. It is found that this sign is positive and that the hyperfine structure of the $^2S_{\frac{1}{2}}$ state is normal. This result is in apparent contradiction to spectroscopic data.[2] In view of this disagreement, and inasmuch as it has not been possible, heretofore, to compare results of these two methods, it was thought advisable to determine the sign of the nuclear magnetic moment of N_a^{23} for which the spectroscopic evidence[3] is very good. In this case the two methods agree on a positive sign.

[1] I. I. Rabi, Phys. Rev. **49**, 324 (1936); J. M. B. Kellogg, I. I. Rabi, J. R. Zacharias, Phys. Rev. **50**, 472 (1936).
[2] D. Jackson, H. Kuhn, Nature **137**, 108 (1936).
[3] L. P. Granath, C. M. Van Atta, Phys. Rev. **44**, 935 (1933).

32. An Attempt at Direct Measurement of the Magnetic Moment of the Rb^{85} Nucleus.* S. MILLMAN AND I. I. RABI, *Columbia University*, AND J. R. ZACHARIAS, *Hunter College.*—The atomic beam method of "zero moments" gives values of the nuclear spin i and $\Delta\nu$ of the hfs multiplet. Nuclear moments μ_r are then calculated with electronic wave functions assuming cosine interaction. We wish to point out that, when the magnitude of μ_r is not neglected in comparison with μ_j, these zero moment states are close doublets in H for $j=\frac{1}{2}$. Indeed

$$\Delta H/H=\left(\frac{2i+1}{i}\right)\left(\frac{\mu_r}{\mu_0}\right)\left\{1-\left(\frac{2m}{2i+1}\right)^2\right\}^{\frac{1}{2}}$$

independent of the form of the (ij) interaction. In virtue of the high resolution attainable with these experimental methods we can measure $\Delta H/H$ and evaluate μ_r directly. Although our apparatus cannot resolve a zero moment peak into two we were able to measure ΔH by supplementing the weak deflecting field with a strong field which separates spatially the atoms which form the doublet.

The fields for the zero moment peaks are then measured separately for each component. We find $\Delta H/H = 1.8 \times 10^{-3}$ and $\mu_r = 1.8$ nuclear magnetons. These results cannot be regarded as in definite disagreement with 1.44 n.m. from the methods mentioned above, since our precision is not yet better than 30 percent. We thank Dr. Marvin Fox for important aid in the early stages of this experiment.

* Reported at the Harvard Tercentenary Conference.

33. The Signs of the Nuclear Magnetic Moments of Li^7, Rb^{85}, Rb^{87} and Cs^{133}. S. MILLMAN, *Columbia University*, AND J. R. ZACHARIAS, *Hunter College*.—The atomic beam method of nonadiabatic transitions for determining the signs of nuclear magnetic moments has been applied to Li^7, Rb^{85}, Rb^{87} and Cs^{133}. The method requires a magnetic state filter supplemented by a device which induces transitions between magnetic levels. The filtering mechanism usually[1, 2] consists of a weak deflecting field, a strong refocusing field and a selecting slit inserted between the two fields. The apparatus used by Millman, Rabi and Zacharias[3] for the direct measurement of the nuclear magnetic moment of Rb^{85} possesses this filtering feature. The insertion of a nonadiabatic field between the selector slit and the weak field adapted this apparatus for the present work. The procedure used in filtering and identifying the atoms in the magnetic states which make nonadiabatic transitions will be described. The results show that the moments of all of these nuclei are positive in agreement with known hfs measurements.

[1] Kellogg, Rabi and Zacharias, Phys. Rev. **50**, 472 (1936).
[2] Torrey and Rabi, Abstract No. 31.
[3] Millman, Rabi and Zacharias, Abstract No. 32.

34. The Viscosity of Sols Made from X-Irradiated Agar. H. KERSTEN AND C. H. DWIGHT, *University of Cincinnati*.—Powdered agar was irradiated with x-rays from a copper target, added to water, heated, and the viscosity of the resulting sols measured. It was found that irradiation decreases their viscosity, as well as their pH.

35. L-Satellites in the Atomic Number Range $73 < Z < 79$. F. K. RICHTMYER, C. H. SHAW AND R. E. SHRADER, *Cornell University*.—The satellites of the x-ray lines $L\alpha$ and $L\beta_2$ are relatively strong in the atomic number range $40 < Z < 50$; but they grow rapidly weaker and are either absent or experimentally not observable in the rare earths. The satellites of $L\alpha$ appear again a little above,[1] and those of $L\beta_2$ a little below[2] Yb(70); and continue up to U(92). The Koster-Kronig theory, based on the Auger effect, qualitatively explains this behavior. The present work was undertaken to determine, quantitatively by the ionization-chamber method, (1) the increase in intensity of these satellites from the neighborhood of Yb(70) to higher atomic numbers, as a check on, and a refinement of the Koster-Kronig theory; and (2) the satellite structure for comparison with the known structure in the lower atomic number range. Preliminary data on intensities of the entire satellite group, relative to the parent line for $L\alpha_1$, are as follows:

I satellites

Z	$I_{L\alpha_1}$
Ta(73)	<0.2 percent
Os(76)	0.8
Pt(78)	1.3
Au(79)	(5.)*

* Data from Richtmyer, Barnes and Ramberg, Phys. Rev. **46**, 843 (1934).
[1] Richtmyer and Kaufman, Phys. Rev. **44**, 605 (1933).
[2] Coster, Phil. Mag. **43**, 1070 (1922).

36. The Structure of Glasseous Selenium. K. LARK-HOROVITZ AND E. P. MILLER, *Purdue University*.—Thin rods of glasseous selenium have been investigated with silver $K\alpha$ and copper $K\alpha$ radiation. Three bands have been observed in the diffraction pattern, $\lambda/2 \sin\theta$ of which are equal to 3.42, 1.73, 1.13. These values agree with recent results on liquid selenium obtained by J. A. Prins:[1] 3.38, 1.79, 1.15. Exposures in a vacuum camera with monochromatic copper radiation have been evaluated by the Fourier method in the manner described before.[2] Three sharp peaks are found in the distribution curve at distances $r = 2.35$, 3.7, 4.8A. These peaks correspond to the distances for next neighbors in the crystal, 2.32, (3.46, 3.69), 4.34A. Also the number of atoms at these distances corresponds to the number of atoms in the crystal. These results are discussed in connection with the different theories of the structure of glasses.

[1] To appear in Trans. Faraday Soc., September 1936. We are indebted to Professor Prins for communication of these results before publication.
[2] Bull. Amer. Phys. Society, Abstract No. 21, November (1936).

37. Electron Diffraction Patterns of Sulphur and Selenium Molecules. J. D. HOWE AND K. LARK-HOROVITZ, *Purdue University*.—By use of the Universal camera[1] described sometime ago, the diffraction of electrons from the vapor of selenium and sulphur at low temperature has been investigated. The diffraction pattern for sulphur is different from the one described by other observers,[2] the values of $\sin\theta/\lambda$ being given as 0.130, 0.238, 0.343, 0.465, 0.745. The pattern cannot be interpreted on the basis of a diatomic molecule; after several attempts with other models it was found that a puckered ring S_8 structure, as the one observed in the S crystal, described the results adequately. The diffraction pattern of selenium is very similar to the one obtained for sulphur, $\sin\theta/\lambda$ being given as 0.157, 0.290, 0.454, 0.698. Also this pattern must be attributed to a higher molecular structure, and a structure like the one found for sulphur but corresponding to Se_8 seems to account best for the results.

[1] H. J. Yearian and J. D. Howe, R. S. I. **7**, 26 (1936).
[2] L. R. Maxwell, S. B. Hendricks, V. M. Mosley, Phys. Rev. **49**, 199 (1936).

38. An Arrangement for Simplifying the Analysis of a Spectrum Plate. J. G. BLACK, *Morehead Teachers College and University of Michigan*.—A recording drum fastened rigidly to the screw shaft of a microphotometer having a millimeter thread, prints a scale on a piece of paper tape as the plate advances, in such a way that each mark of the scale identifies a plate position. The tape moves under a fixed straight edge and across the tape a sharp line is quickly made with a pencil each time a line center passes. By this line the galvanometer deflection is recorded on the

moving tape. The 10 inch glass plate is put aside; replaced by a paper tape about 88 feet long. This tape is laid beside a standard tape having the iron lines and interpolations made between recorded iron lines. Each unknown spectrum is supplied with a light iron comparison to furnish landmarks at intervals on the tape.

39. The Absorption Spectrum as a Quantitative Test for Free Hydroxyl Radicals. O. OLDENBERG AND F. F. RIEKE, *Harvard University and Johns Hopkins University.*—In preceding papers by A. A. Frost and O. Oldenberg the absorption spectrum served as a test for free OH radicals. Their presence during rapid gas reactions could be traced by means of spectra taken in snapshots. First, only a *qualitative* test was made. Secondly, the test was made *quantitative* in a *relative* sense. Finally, in order to obtain an *absolute quantitative* test for free OH the absorption spectrum was calibrated against a known concentration of free OH produced, according to the method of Bonhoeffer and Reichardt, in thermally dissociated water vapor. At high temperature and one atmosphere pressure the width of the individual absorption lines is sufficiently large for observation in the second order of a 21-foot grating. On the basis of this calibration the combination of OH and H after the interruption of an electric discharge through water vapor was studied quantitatively. Because of the small width of the absorption lines at the low temperature and pressure of the discharge the high resolving power of quartz Fabry-Perot plates was needed.

40. Rotation of Water Molecules in Nonpolar Solvents. E. L. KINSEY AND J. W. ELLIS, *University of California at Los Angeles.*—Infrared absorption records of water dissolved in carbon bisulphide, previously reported as indicating a more vaporlike than liquidlike absorption, show the following interesting results. For the 1.38μ band the two long wave-length components of the set of three, into which the spectrograph resolves this band in the vapor, appear in the solution in the unshifted vapor position. The relative intensities however are reversed. The third component is completely absent. Of the three weak bands at the extreme long wave side of this group only one, the long wave-length component, appears in the solution. In the 1.87μ band, which the spectrograph resolves into more than a dozen bands for the vapor, only three occur in the solution, again unshifted. If Mecke's analysis of the vapor bands is used it is seen that in each region in the solution the P branch is strong, the Q branch is weak, and the R branch is absent. The strongest transitions occurring in absorption therefore are those for which the total angular momentum decreases. Those for which it remains constant are weak. Those for which it increases are absent.

41. The Lithium I like Spectrum of Phosphorus P XIII. HOWARD A. ROBINSON, *Ohio State University.*—Recent spectrograms taken on the new 5 meter grazing incidence spectrograph located in Professor Siegbahn's Institute at Uppsala, Sweden, have made possible the extension of the Li I like isoelectronic sequence to include P XIII. The first members of the principal series cannot be observed for reasons given previously.[1] The second members ($2s-3p$) lie at 35.137A and 35.098A respectively. Other transitions such as $2p-3d$ and possibly $2p-3s$ have been located. The deviation from the hydrogen like term values is very small; for the ground state being approximately 1.94 and for the $2p$ state 1.98. The ionization potential is roughly 608 electron volts.

[1] H. A. Robinson, Zeits. f. Physik **100**, 636 (1936).

42. Hyperfine Structure in the Resonance Lines of Mg I and Mg II. RUSSELL A. FISHER, *Northwestern University.*—By employing an atomic beam excited in an electrodeless discharge in argon as source, measurable structure has been observed in the resonance line of Mg I λ2852 and in the two resonance lines of Mg II λ2803 and λ2796. The resolving element was a Fabry-Perot interferometer with aluminum films and spacers of 1, 2, 3 and 5 cm. λ2852 was found to consist of a strong component accompanied by a second weaker component of approximately 1/10 its intensity, the weaker component lying 0.066 cm^{-1} to the higher frequency side. While this separation is entirely at variance with that reported by Jackson and Kuhn* in their absorption measurement, it is supported by observations made with each of the four spacers mentioned above. The lines λ2803 and λ2796 show identical structures consisting of a strong central component with a much fainter component lying on each side at $+.100$ cm^{-1} and $-.025$ cm^{-1} respectively. The satellite of λ2852 may be attributed to one or both of the two less abundant isotopes of Mg. The fact that the two satellites in the Mg II lines are fainter relative to the strong component than is the satellite in the Mg I line suggests that they may be interpreted as belonging to Mg^{25} and that their total separation of 0.125 cm^{-1} is that of the $3s\ ^2S$ state of Mg II. If this interpretation is accepted the satellite of the Mg I line must be attributed to Mg^{25} also.

* Jackson and Kuhn, Proc. Roy. Soc. **154**, 679 (1936).

43. Remark on the Creation of Pairs by Nuclear Electrons. JULIAN K. KNIPP, *Purdue University.*—As has been pointed out by Uhlenbeck and Goudsmit, if the interaction between a number of particles does not depend critically on the energies of the particles, the energy distribution function for the particles will be given roughly by the statistical factor, which gives the number of states per energy interval. Consider the case of beta-decay with the creation of two electrons, a positron and a neutrino. The coulomb field of the nucleus will cause the creation of fast positrons and slow electrons to be favored. Otherwise the interaction will not depend greatly on the energies. Thus the statistical factor should give the form of the energy distribution of the observed positrons for light nuclei, where the coulomb interaction of the nucleus is of less importance. For heavy nuclei it should not give enough high energy positrons. Experimental data exist only for heavy nuclei. Comparison of the statistical distribution with the experimental distribution of positrons from Th C+C″ obtained by Alichanow, Alichanian and Kosodaew has been carried out and shows that the statistical factor for this case (heavy nuclei) gives too few fast positrons. A detailed calculation of the interaction is being made by Møller. In the

Born approximation it cannot be expected that there will be much improvement in the form of the distribution function over that given by the statistical factor.

44. Theory of Neutron Velocity Distributions in Aqueous Solutions. W. H. FURRY, *Harvard University.*—The discussion of velocity distributions of slow neutrons in aqueous solutions has been extended to cases more general than treated previously.* If more than one solute obeying the Breit-Wigner law of absorption is present, one finds, for resonances not too broad or too close together and concentrations not too high, that the distribution is of a sort readily interpreted in terms of the formalism already given. Aside from the resonance regions the curve is essentially of the v^{-2} form given by Fermi, its amplitude being decreased on crossing each resonance region by the amount absorbed there, which is a typical nonlinear function of the concentration. Corresponding results are obtained for the case when a solute absorbing according to a v^{-1} law (boron) is also present. For broad resonances or very high concentrations the approximations used break down; such a situation is, however, not a very likely one experimentally. In the case of a single solute a procedure is available for calculating the exact curves numerically without much difficulty.

* Phys. Rev. **50**, 381 (1936).

45. Interaction Between Light Nuclei. M. PHILLIPS,[1] L. EISENBUD AND E. U. CONDON, *Princeton University.*—On the basis of the concept of a static potential we have attempted to calculate the scattering cross sections for neutrons or protons on H_1^2, H_1^3, He_2^3, He_2^4 and for deuterons on deuterons. The interaction potential between individual particles was assumed to be of the form $J(r_{ik}) = Ae^{-\alpha r_{ik}^2}$. A straightforward attack on the problem leads to difficulties which are connected with symmetrization of the wave functions and the use of exchange interaction operators. Simple considerations using ordinary forces and unsymmetrized wave functions yield elastic scattering cross sections in approximate agreement with existing experimental data. The present state of nuclear theory does not appear to justify a refinement of this crude treatment. An exact formulation of the problem is given and the new features which are introduced by exchange forces are discussed.

[1] A.A.U.W. Fellow.
[2] Massey and Mohr, Proc. Roy. Soc. **156**, 634 (1936).

46. On the Nuclear Three Body Problem. R. D. PRESENT, *Purdue University,* AND W. RARITA, *Columbia University.*—All evidence points to a nuclear Hamiltonian comprising a Majorana-Heisenberg interaction $\{(1-g)P^M+gP^H\}V$ between unlike particles and an attractive singlet interaction between like particles which is equal to that for unlike particles. The experimental mass defects of H^2 and H^3 together with the cross section σ for slow neutron-proton scattering will determine the range (b) and depth (B) of nuclear forces and the proportion g of Heisenberg force (we use throughout the potential $Be^{-2r/b}$). An exact analytic expression relating σ, g and b is derived for this potential and g is found to be very insensitive to σ. An exact solution of H^2 gives the relation between B and b. The final relation which fixes the constants is furnished by a precise variational treatment of H^3 with the above Hamiltonian and the following wave function:

$$\psi = \partial^{-\frac{1}{2}}\alpha_1(\alpha_2\beta_2 - \alpha_3\beta_2)\phi_1 + \partial^{-\frac{1}{2}}\alpha_1(\alpha_2\beta_3 + \alpha_3\beta_2)\phi_2 + \beta_1\alpha_2\alpha_3\phi_3$$

where ϕ_1, ϕ_2 and ϕ_3 each represent an exponential times a power series in the interparticle distances of proper symmetry (ϕ_2 and ϕ_3 are brought in by the Heisenberg term). The convergence of energies obtained from successive improvements in ψ is rapid and the eigenvalue may be closely estimated. With $E(H^2) = -4.35$ mc², $E(H^3) = -16.55$ mc² and $\sigma = 13\times10^{-24}$ cm², preliminary results give: $b = 1.73 \times 10^{-13}$ cm, $B = 242$ mc² and $g = 0.215$. The binding energy of He^3 is readily obtained and accurate wave functions for H^3 and He^3 will be calculated. The Breit-Feenberg operator is used for the small triplet neutron-neutron interaction.

47. Absorption of Resonance Neutrons. H. H. GOLDSMITH AND J. H. MANLEY, *Columbia University.*—Measurements of the absorption of various neutron groups in Cd, Rh and Ir have yielded the following preliminary results: (1) The ratio of the capture cross section of Cd for Rh neutrons to the cross section for In neutrons is 1.7. The Cd cross section, in this case, should vary approximately as $1/v^5$. This gives a velocity ratio between Rg and In neutrons of about 1.1 in good agreement with the ratio obtained from the boron absorption method. (2) The absorption of Rh neutrons in Rh is not exponential. The absorption coefficient varies from 2.5 to 0.7 cm²/g for absorbers which vary in thickness from 0.2 to 2.0 g/cm². The absorption in Rh of the B neutrons is considerably greater than that of the A neutrons. (3) The absorption coefficient of Ir for the neutrons detected by Ir varies from 1.5 to 0.85 cm²/g for thicknesses of 0.3 to 1.0 g/cm². The absorption in Ir of the neutrons detected by Rh, In, Ir, Ag (A and B groups) and I indicates that the cross section of Ir varies more slowly with neutron energy in the region 1–100 ev than that of any other element yet investigated. Additional measurements of the absorption of the neutrons detected by Rg, Ag and I in various elements have been made.

48. Experiments on the Magnetic Properties of the Neutron. J. R. DUNNING, P. N. POWERS AND H. G. BEYER, *Columbia University.*—Certain experiments have been made to detect an alignment or polarization of neutrons, due to their magnetic moment, on passing through strongly magnetized material.[1, 2] First the scattering of a beam of thermal neutrons on passing through two sheets of iron magnetized to saturation was investigated, varying the directions of magnetization. No changes in neutron transmission larger than the probable error were observed. In further experiments, the neutrons were first passed through a magnetized sheet of iron (polarizer) at 30° and 45°, and then scattered from the pole face of a second magnet which should serve as an "analyzer" if the scattering cross section depends on parallel or anti-parallel orientation of the neutron with respect to the field. The difference 2.01 ± 0.65

Polarizer Field Direction	Parallel to Analyzer Field	Anti-parallel to Analyzer Field	Zero Field, i.e. Unpolarized
No. Counts	12,700	11,500	15,600
No./Min.	50.81±0.48	49.40±0.44	48.80±0.40
Difference		1.41±0.66	2.01±0.65

between the unpolarized or random orientation and the parallel case is not considered to prove conclusively any effect. The smaller difference, if real, between the parallel and anti-parallel conditions may be caused by a large fraction of the neutrons losing their space quantization and re-orienting themselves parallel after leaving the polarizing plate. The nuclear cross section (scattering plus capture) is so large compared to the observable magnetic interaction cross section that detection of such possible effects is clearly difficult.

[1] Bloch, Phys. Rev. **50**, 259 (1936).
[2] Schwinger, unpublished.

49. The Bombardment of Palladium with Deuterons. J. D. Kraus and J. M. Cork, *University of Michigan.*—Observations have been made of the active isotopes formed when palladium (46) is bombarded by 6.5 Mev deuterons. Chemical separations show strong activities in the palladium and at least two active silver isotopes. This silver activity is not the Fermi activity which would have resulted from the bombardment of silver itself (22 sec. and 2.3 min.) but has half-life periods of 32 minutes and 7½ days. An estimate is made of the maximum energies of the observed beta radiations.

50. Radioactive Isotopes from Aluminum. M. L. Pool and J. M. Cork, *University of Michigan.*—It has been apparent for some time that aluminum bombarded by high energy deuterons yields radioactive isotopes other than $_{12}Al^{28}$, which decays with a half-life period of 2.3 minutes. As ordinary aluminum generally contains contamination of SiO_2 the 2.5 hr. period due to $_{14}Si^{31}$ is usually observed. Chemical separations of a specimen of very pure aluminum activated by 6.5 Mev deuterons show an additional activity in the magnesium precipitate which emits solely positives and has a half life of 15.8 hours. If this cannot be ascribed to a contamination it must mean the formation of $_{12}Mg^{23}$ which would be due to the emission of an $_2He^4$ particle plus a neutron or some equivalent transformation.

51. Induced Radioactivity in Lead. R. L. Thornton and J. M. Cork, *University of Michigan.*—The abundance of the normal stable isotopes of lead (203 to 209) suggests the possibility of producing radioactive isotopes of thallium or bismuth in addition to any activity in the lead. The existence of isotopes 205 and 209 is questionable. Should 209 exist, then neutron activation or deuteron bombardment should yield radio lead (210), which is radium D. Bombardment of a pure lead specimen by a beam of 2 microamperes of deuterons at 6.5 Mev for about 12 hours gave no sure indication of the formation of radium D. Another active lead isotope of a half-life period 3.0 hours, however, is observed. This emits negative beta-particles and hence is undoubtedly isotope 209. Other shorter period activities have been observed but have not yet been chemically resolved.

52. The Magnetic Susceptibility of Molecular Hydrogen Calculated by Quantum Mechanics. Enos E. Witmer, *University of Pennsylvania.*—For gaseous molecular hydrogen the molar magnetic susceptibility is given by the formula

$$\chi_M = -\frac{Le^2}{6mc^2}\Sigma\overline{r^2} + \frac{Le^2}{6m^2c^2}\sum_{n'\neq n}\frac{|P(n;n')|^2}{h\nu(n;n')}.$$

As stated in a recent abstract (No. 3, New York Meeting, October 29–31, 1936) the first term on the right was evaluated for different internuclear distances R, using the eleven-term wave function of James and Coolidge. These values were averaged by using a Morse wave function for the vibrational state $v=0$. The value of the average depends on the nature of the extrapolation of the curve through the calculated points. The maximum possible value of the first term is -4.09×10^{-6}, the value -4.15×10^{-6} is probably a minimum, the estimated best value being nearer to the latter value. Using the approximation of Van Vleck and Frank for the second term, the maximum possible value calculated from the five term function is 0.31×10^{-6}; it is probable that 0.25×10^{-6} is a minimum, and the best value is 0.285×10^{-6}. The maximum and minimum possible values of χ_M are then -3.78×10^{-6} and -3.90×10^{-6}. The best calculated values are from -3.83×10^{-6} to -3.87×10^{-6}. The average of the best experimental values is -3.97×10^{-6}. Increasing the factor ν_1 in the approximation of Van Vleck and Frank would bring the calculated values into better agreement with the experimental values.

53. A Theory of the Ferromagnetism of Alloys. F. Bitter, *Massachusetts Institute of Technology.*—Excluding pressure effects, the magnetization of an alloy may be considered to be a function of three variables, the concentration of the alloy, the temperature, and the magnetic field. A theory is developed which gives the dependence of spontaneous magnetization on temperature for any homogeneous phase. The expression obtained reduces to the usual form $I/I_0=\tanh(CI/KT)$ for pure substances. The equations contain five arbitrary constants, four of which are C, and I_0 for the two pure phases. Among the new points brought out are that in alloys, spontaneous magnetization need not increase with decreasing temperature and that there may be more than one critical temperature. Further, the conditions for the existence of a single homogeneous phase are discussed, and it is shown that a chemical separation may take place at the critical temperature analogous to the chemical separation that takes place on freezing, and that this chemical separation may be modified by the application of a magnetic field.

54. On the Choice of the Action Function in the New Field Theory. B. Hoffmann and L. Infeld, *The Institute for Advanced Study, Princeton, N. J.*—There are difficulties connected with the action functions, hitherto used in the

new field theory initiated by Born, apart from their lack of uniqueness. They permit isolated magnetic poles to exist, and the field equations have to be supplemented by extra conditions equivalent to equations of motion. Further, the f_{kl} field is not regular in the case of an electrical particle, and space-time is also singular for this case. By requiring that solutions having physical significance must have f_{kl} fields free from singularities we are led to a unique action function, so far as the significant lower order terms are concerned, which gives a theory in which isolated magnetic poles cannot exist and in which the equations of motion are a consequence of the field equations. Moreover, the gravitational field is now regular and electromagnetic and gravitational mass are shown to be the same. The Hamiltonian of the new action function turns out to be $\mathbf{H}=\frac{1}{2}\log(1+P)$, $P\equiv D^2-H^2$, and the electric field vector in the spherically symmetric case is now given by $E_r=r^2(1+r^4)^{-1}$. Thus, E_r goes over to the Maxwellian case for large r and, in accordance with the regularity condition, tends to zero as $r\to 0$.

55. The Influence of Dipole-Dipole Coupling on Electric and Magnetic Susceptibilities. J. H. VAN VLECK, *Harvard University.*—The partition function, and hence the entropy, specific heat, and susceptibility, are calculated as power series in $1/T$ for a dielectric or paramagnetic body inclusive of dipole-dipole coupling. This kinetic treatment is in principle rigorous but practically handicapped by poor convergence. However, it shows that the usual, essentially static, Lorentz method wherein dipole-dipole interaction merely adds a term $4\pi P/3$ to the local field is justified only in the first approximation and involves assumptions comparable to supposing in the Heisenberg theory of ferromagnetism that all states of the same crystalline spin possess the same energy. The Fowler-Debye hypothesis of hindered rotation consequently may not be necessary to explain the nonoccurrence of the spontaneous polarization which the Lorentz $4\pi P/3$ procedure would predict below a "Curie point" $\theta=4\pi N\mu^2/9k$ in polar liquids. This hypothesis seems inadequate in HCl, as here $\theta=260°$, whereas Pauling showed that free rotation is destroyed only below 100°K. If a Gaussian distribution rather than identity of energies is assumed, the spontaneous behavior is impossible. In the magnetic case, the dipole-dipole coupling is important at, and only at, the new very low temperatures. It is uncertain whether coupling of this type (in distinction from exchange interaction) can ever produce ferromagnetism.

56. Entropy and Magnetic Susceptibility of Paramagnetic Salts Below 1°K. M. H. HEBB AND E. M. PURCELL, *Harvard University.*—The results of Giauque, Kürti, DeHaas and their collaborators on the production of extremely low temperatures by the adiabatic demagnetization method are discussed. At these temperatures the Debye specific heat is negligible and the entropy depends on the distribution of the paramagnetic ions among the Stark components produced by the crystalline electric field and on the magnetic and exchange coupling of the ions. The splitting produced by the crystalline field is calculated by the method of crystalline potentials. This splitting is of the order of a few tenths of a cm^{-1}. The contribution to the entropy from the coupling of the ions is evaluated by Van Vleck's method.* Below 1°K the Curie temperature scale deviates from the true thermodynamic scale due to the influence of the crystalline field and the ion coupling. The extent of this deviation is uncertain on account of the latter effect but calculations based on the Lorentz local field seem to fit the experimental data better than do those based on a more elaborate theory* which attempts to take account of fluctuations of the moments of surrounding ions about their mean values.

* See preceding abstract.

57. On the Density of Energy Levels of Heavy Nuclei, JOHN BARDEEN, *Harvard University.*—The present calculation of the density of energy levels of a heavy nucleus is based on the statistical model of Van Vleck.[1] As in Bethe's calculation,[2] the particles are assumed to move in a simple potential hole, but the depth of the hole varies with the velocity of the particle. If exchange forces act, the interaction energy of a given particle with the remainder of the nucleus decreases as the velocity of the particle increases. This results in a lower density of states of the individual particles at the top of the Fermi distribution. Bethe's formula for the density of excited levels of the nucleus as a whole may be applied to the present situation if this change in the density of the individual particle states is taken into account. The spacing between the levels is several hundred times larger than that found by Bethe, and, if one uses the Gamow value for the radius of a radioactive nucleus ($\sim 9\times 10^{-13}$ cm), is much too large to be reconciled with the frequent occurrence of resonance levels for slow neutrons. If one uses the new value for the radius suggested by Bethe[3] ($\sim 13\times 10^{-13}$ cm), the present theory gives values agreeing roughly with experiment.

[1] J. H. Van Vleck, Phys. Rev. **48**, 367 (1935).
[2] H. A. Bethe, Phys. Rev. **50**, 332 (1936).
[3] At the New York Meeting, October, 1936.

58. Concentration of Chlorine Isotopes by Centrifuging. J. W. BEAMS AND A. VICTOR MASKET, *University of Virginia.*—A specially designed type of air driven centrifuge[1] has been employed to concentrate the isotopes of chlorine. A hollow metal rotor (60 cc capacity) was both supported and spun in a vacuum by a metal tube (stainless steel hypodermic needle tubing 1.3 mm bore). The rotor was partially filled (16 cc) with CCl_4 and evacuated through the tube while at full speed. One cubic centimeter of liquid CCl_4 was collected in dry ice traps every 6.5 minutes. Light, medium and heavy fractions were collected and separately re-centrifuged. Density measurements of the successive fractions were roughly in agreement with the theory.

[1] Beams and Pickels, R. S. I. **6**, 299 (1935); Beams and Haynes, Phys. Rev. **50**, 491 (1936).

59. Atomic Masses of Hydrogen, Helium, Carbon, and Nitrogen Isotopes. KENNETH T. BAINBRIDGE AND EDWARD B. JORDAN, *Harvard University.*—The mass separations CH_4-O, H_2-D and $D_3^+-C^{++}$ yield the masses:

$$H = 1.00815 \pm 0.00002; \quad D = 2.01478 \pm 0.00003;$$
$$C = 12.00428 \pm 0.00017;$$

where the doublet separation $D_3^+ - C^{++} = 0.04219 \pm 0.00005$ mass units and the other doublets[1] have already been reported. The mass of helium $= 4.00395 \pm 0.00007$ from the doublet separation $D_2 - He = 0.02561 \pm 0.00004$ mass units. The mass of $C^{13} = 13.0079 \pm 0.0002$; $N^{14} = 14.0076 \pm 0.0002$; and $N^{15} = 15.0050 \pm 0.0003$ from earlier measurements.[1, 2] An additional link between the lighter and heavier masses is provided by the doublet $Li^{7+} - N^{14++} = 0.01443 \pm 0.0001$ which yields $Li^7 = 7.01822 \pm 0.00014$. The carbon and nitrogen mass values were checked from mass spectrographic data by the use of the doublets $CO - N_2$, $CH_4 - NH_2$, $OH - NH_3$ and $O - NH_2$. The doublet measurements were made in the linear section of the recording plate on lines of very nearly equal density.

[1] E. B. Jordan and K. T. Bainbridge, Phys. Rev. **49**, 883 (1936).
[2] J. and B., Phys. Rev. **50**, 98 (1936).

60. Atomic Masses of Beryllium, Boron, Neon and Argon. EDWARD B. JORDAN AND KENNETH T. BAINBRIDGE, *Harvard University.*—The mass differences of the following doublets have been calculated from measurements made on lines of approximately equal density in the linear region of the recording plate of the mass spectrograph:

1. $O^{16}D_2^+ - Ne^{20+} = 0.03065 \pm 0.00010$ mass units.
2. $B^{10+} - Ne^{20++} = 0.01675 \pm 0.00015$ mass units.
3. $B^{10}H_2^+ - C^{12+} = 0.02875 \pm 0.00020$ mass units.
4. $B^{10}H^+ - B^{11+} = 0.01160 \pm 0.00010$ mass units.
5. $B^{11}H^+ - C^{12+} = 0.01714 \pm 0.00010$ mass units.
6. $Be^9H^+ - Ne^{20++} = 0.02391 \pm 0.00020$ mass units.
7. $Be^9H^+ - B^{10+} = 0.00696 \pm 0.00020$ mass units.
8. $B^{11+} - Ne^{22++} = 0.01360 \pm 0.00015$ mass units.
9. $B^{10}H^+ - Ne^{22++} = 0.0251 \pm 0.00050$ mass units.
10. $Ne^{20}H^+ - Ne^{21+} = 0.00726 \pm 0.00020$ mass units.
11. $OD_2^+ - A^{36++} = 0.04189 \pm 0.00020$ mass units.
12. $Ne^{20+} - A^{36++} = 0.01130 \pm 0.00010$ mass units.

The first three mass differences given above can be used in conjunction with those reported[1, 2] for the $C^{12}H_4 - O^{16}$ and the $H_2 - D^2$ doublets to make up a complete mass circuit from which the masses of the atoms involved can be calculated:

$$C^{13} = 12.00402 \pm 0.00017 \text{ mass units.}$$
$$B^{10} = 10.01633 \pm 0.00013 \text{ mass units.}$$
$$Ne^{20} = 19.99917 \pm 0.00019 \text{ mass units.}$$

The mass of B^{11} can now be computed either by means of doublet number 4 or doublet number 5. The values obtained by the two methods agree within the probable error and give a value

$$B^{11} = 11.01295 \pm 0.00013.$$

Similarly the mass of Be^9 can be computed by using doublets number 6 and 7. The average value obtained is

$$Be^9 = 9.01517 \pm 0.00016.$$

Other masses which can be obtained and checked from the values reported above are:

$$A^{36} = 39.97580 \pm 0.00031, \quad Ne^{21} = 21.99870 \pm 0.00040.$$

The value obtained for Ne^{21} is

$$Ne^{21} = 21.00013 \pm 0.00029.$$

The authors wish to thank Dr. E. L. Gamble of the Massachusetts Institute of Technology for preparing the boron hydrides which were used in these experiments.

[1] E. B. Jordan and K. T. Bainbridge, Phys. Rev. **49**, 883 (1936), Abstract 124.
[2] K. T. Bainbridge and E. B. Jordan, Phys. Rev. **49**, 883 (1936), Abstract 123.

61. Nuclear Disintegrations Accompanying Cosmic-Ray Showers. ARTHUR BRAMLEY, *Swarthmore, Pa.*—Nuclear disintegrations can occur as follows: (1) Through the nuclear photoelectric effect of a shower of electrons or photons a neutron[1] is emitted. The action of a shower, whether pairs[2] produced by heavy particles or photons[3] by light, is enhanced through the production of secondaries.[4] (2) On the Heisenberg-Oppenheimer picture of showers, as pairs produced by heavy particles, the nucleus can lose either electrons or positrons[5] through unsymmetrical emission. The nucleus assumes a new isotopic number. (3) Excitation of the β-particle field of proton by photon, electron or proton with subsequent emission of positron[5] and neutrino yields a new nucleus. In extreme cases, the nucleus loses all its charge, Ze. In the shower of N rays with average energy $\lesssim 10$ Mev, the probability of (1) is $\gtrsim N/Z^2$; for (2) with average energy $\gtrsim 100$ Mev, it is ~ 0.5; for (3) in same energy range it cannot be estimated until more knowledge is acquired of the β-particle interaction for high energy electrons and neutrinos and for the nucleus as a unit.

[1] Locher, Phys. Rev. **50**, 394 (1936).
[2] Heisenberg, Zeits. f. Physik **101**, 533 (1936).
[3] Bramley, Science, August 28, 1936.
[4] Bhabha and Heitler, Nature, September 5, 1936; Oppenheimer, Phys. Rev. **50**, 389 (1936).
[5] Anderson and Neddermeyer, Phys. Rev. **50**, 263 (1936).

62. Radio-Transmitted Coincidence Counter Measurements of Cosmic-Ray Intensities in the Stratosphere. THOMAS H. JOHNSON, *Bartol Research Foundation and The Carnegie Institution.*—Instruments for registering double coincidences of GM counters have been sent into the stratosphere by small balloons. The results, though still preliminary, are in substantial agreement with those of Regener and Pfotzer and of Swann, Locher and Danforth. Each coincidence is transmitted as a pulse of high-frequency radio waves and is received and recorded photographically on the ground. At regular intervals the cosmic-ray signals are interrupted for transmission of signals produced by a neon tube flicker circuit whose frequency depends upon the height of a mercurial barometer. Counter voltage is produced by six-fold multiplication of the 180 volt B-battery. The apparatus hangs from the balloon by a cord which slowly unwinds from a spool. This turns the multiplier switch and signal commutator. The first model, four of which have been launched, weighed 14 pounds but improved design has reduced this to 8 pounds including batteries for five hours. Elimination of radio interference and greater distance reception have been achieved by locating the receiver on Mt. Washington. On the most successful flight signals came in with undiminished intensity for 110 minutes, and then suddenly stopped. During this time the balloon had ascended 55,000 ft. and cosmic-ray intensity had passed through a maximum equal to about

sixty times the ground intensity. The method will be used for measurements of vertical cosmic-ray intensity in the stratosphere in unpopulated latitudes.

63. Automatically Recorded Coincidence Counter Measurements of the Cosmic-Ray Latitude Effect. D. N. READ AND THOMAS H. JOHNSON, *Bartol Research Foundation and The Carnegie Institution of Washington.*—The instrument described last year will have completed its eighth voyage on the Grace Line from New York to Talcahuano, Chile, 36°S. Of the first seven voyages all but the first two have yielded successful records of cosmic-ray intensities from definite angles as a function of geographical position. Some trouble has been experienced from temperature effects but the following conclusions seem to be established. (1) The local magnetic field, as well as the geomagnetic latitude, is an important variable in determining the vertical intensity. (2) The vertical latitude effect is between 12 and 16 percent as compared with Millikan and Neher's value of 8 percent for rays from all directions. (3) A very slight latitude effect towards the west at 45° from the vertical, compared with a much greater effect at the same angle towards the east, indicates not only the excess of positive but the almost complete absence of negative primaries in the radiation responsible for the sea-level geomagnetic effects. Measurements at a zenith angle of 45° in north and south azimuths are being made as a further test of the Lemaitre-Vallarta theory of the north-south asymmetry. The apparatus will be on exhibition during the meeting.

64. Cosmic-Ray Ionizations under Various Thicknesses of Lead Shield in Northern and Equatorial Latitudes at Different Altitudes. R. T. YOUNG, JR., *Worcester Polytechnic Institute*, AND J. C. STREET, *Harvard University.*—Measurements with an ionization chamber have been carried out at Cambridge, Mass. (sea level), Mt. Evans, Colo. (3200 and 4300 m) and at corresponding elevations in Peru. Since it was desired to study the occurrence of small bursts with the same equipment, a small chamber (230 cc volume) was used. Due to statistical fluctuations the ionization measurements may be in error by 3 percent. It was found that within limits of error the latitude ionization ratios, Northern: Equatorial, were independent of shield at each elevation studied. The results are listed in the table.

BAROMETRIC PRESSURE cm Hg	GEOMAGNETIC LATITUDE	LATITUDE RATIO
76	53N – 1S	1.16
51	49N – 1S	1.27
45	49N – 1S	1.30

An analysis of the lead absorption curves has been made in terms of a penetrating and a soft component of the radiation. Counter data on the absorption of vertical rays and on showers are available at two stations (53N, bar. 76 and 49N, bar. 51) at which ionization measurements were made. By comparison with the counter data an estimate has been made of the contributions of both the penetrating and soft components to the ionization. The analysis shows that the ionization due to secondaries associated with the soft component varies with the shielding in the same manner as the production of showers determined by counters. This contribution of secondaries is important even under thick shields, e.g., 40 percent of the total ionization at an elevation of 3200 m and with a 20 cm lead shield. It is believed that the secondary ionization under thick shields is associated with the second shower peak observed by Ackemann and Hummel.

See the following:

1. R. H. Woodward and J. C. Street, Phys. Rev. **49**, 198 (1936).
2. R. H. Woodward, Phys. Rev. **49**, 711 (1936).
3. M. Ackemann, Naturwiss. **22**, 169 (1934).
4. J. N. Hummel, Naturwiss. **22**, 170 (1934).

65. Cosmic-Ray Bursts Photographed with a Cloud Machine Controlled by Noncollinear Counters. GORDON L. LOCHER, *Bartol Research Foundation of the Franklin Institute.*—A series of 640 pairs of pictures has been made at sea-level with a semi-automatic Wilson cloud machine controlled by various noncollinear arrangements of Geiger-Müller counters, to study the disintegration products of cosmic-ray bursts in paraffin, aluminum, and lead. The general type of burst picture obtained under a given set of circumstances depends not only on the kind and amount of burst-generating material, but also on the number, area, and configuration of the coincidence counters used for control. Photographs of bursts typical of the several arrangements, and of some unusual bursts, will be shown.

66. Photoelectric Geiger-Müller Counters for Visible and Ultraviolet Light.* GORDON L. LOCHER, *Bartol Research Foundation of the Franklin Institute.*—New developments in the technique of making photoelectric counters of high sensitivity, responding to visible light, are described. Composite cathode surfaces consisting of oxidized hydrides of barium, thallium, lithium, and sodium have been used with good success. Barium (threshold~4900A) and thallium (threshold~3500A) composite surfaces have spontaneous counting rates that are consistently lower than those of lithium and sodium. Measurements made by O. Mohler, using a composite barium counter on the Cook Observatory reflecting telescope (mirror silvered, Cassegrain aluminized), show a rate of 80 impulses per min. on a 5.2 magnitude, type B3 star, as compared with a "sky rate" of 40 per min., and a rate of 8.5 per min. in darkness. The response of this counter, which has a cross section of 3 cm by 1 cm, to the unresolved light from a tungsten ribbon lamp in fused quartz, at 1763°K, is 3.1×10^{10} impulses per min., per cm^2 of tungsten, per steradian. Its response to unresolved light from a Hefner candle is about 180 times that of a good zinc counter of the same dimensions. Curves of the spectral distributions of response of various counters, made with a double quartz monochromator, will be shown, and various problems relating to the construction and use of photoelectric counters will be discussed.

* To be called for after paper No. 65.

67. Stopping of Fast Electrons.* ARTHUR BRAMLEY, *Swarthmore, Pa.*—Electrons with energy $\gtrsim 137\ mc^2$ lose energy primarily by radiation and production of photon showers. Since the cross section for shower process is $\sim 1/10$ that for radiation, the rate of loss of energy is practically unchanged from that given by radiation theory.[1] The electron can also lose energy by the disintegration of the nucleus. (1) The losses from that process, which is the equivalent of the nuclear photoelectric effect, are negligible. (2) The electron excites the β-particle field of the nucleus which dissipates the energy by (I) radiation, (II) emission of neutrino,[2] (III) emission of positrón with formation of a new nucleus. The cross section is uncertain.

Experiments[3] on electrons of energy $\sim mc^2$, indicate that energy losses exist besides those from ionization which are several times the theoretical radiation losses. If this conclusion can be extrapolated to higher energies, then it casts doubt on the assumption that the energy losses recorded for electrons in Pb plates[3] are radiative. Experiments[3] on elastic scattering at large angles require that radiation losses be less than estimated.

* To be called for after paper No. 66.

[1] Bethe and Heitler, Proc. Roy. Soc. **146**, 83 (1934).
[2] Skobeltzyn and Stepanowa, Nature **137**, 234 (1936); Klarmann and Bothe, Zeits. f. Physik **101**, 489 (1936).
[3] Anderson and Neddermeyer, Phys. Rev. **50**, 263 (1936).

68. Perturbation Theory and Heavy-Particle Interactions.* D. R. INGLIS, *University of Pittsburgh.*—Perturbation theory is applied to the nuclei He^4 and Li^6.[1] The form of interaction used by Feenberg and Knipp is here about adequate, the calculated binding energy of Li^6 being 58 mc^2 when the parameter C is adjusted to fit He^4 *by this method*. (Although this method gives He^4 only about 2 mc^2 less binding than does the equivalent two-body method with the same parameters, the Li^6 energy is quite sensitive to this small difference.) Symmetrization of this form by using its proton-neutron interaction operator between all pairs is not satisfactory. A more satisfactory simple symmetric form (which is also expected to have comparatively slight quadratic dependence on the number of particles in heavy nuclei) is suggested: $U=\Sigma((1-g)P^{(q)}+gP^{(\sigma)})\mathrm{Be}^{-\alpha r^2}$, containing a linear combination of space permutation and spin permutation.

* To be called for after paper No. 33.
[1] Cf. Phys. Rev. **50**, 399 (1936).

AUTHOR INDEX TO ABSTRACTS OF ATLANTIC CITY MEETING

Aebersold, Paul C.—No. 7

Bainbridge, Kenneth T.—see Jordan, Edward B.
——— **and Edward B. Jordan**—No. 59
Bardeen, John—No. 57
Bazzoni, Charles B.—see Weber, Alfred H.
Bearden, J. A.—No. 22
Beyer, H. G.—see Dunning, J. R.
Beams, J. W. and A. Victor Masket—No. 58
Bitter, F.—No. 53
Black, J. G.—No. 38
Bramley, Arthur—No. 61
———No. 67

Condon, E. U.—see Phillips, M.
Cork, J. M.—see Kraus, J. D.
———see Pool, M. L.
———see Thornton, R. L.

Dunning, J. R., P. N. Powers and H. G. Beyer—No. 48
Dwight, C. H.—see Kersten, H.

Eisenbud, L.—see Phillips, M.
Ellis, J. W.—see Kinsey, E. L.

Farnsworth, H. E.—No. 23
Fisher, Russell A.—No. 42
Folsom, T. R.—No. 6
Fricke, Hugo and Homer P. Smith—No. 12
Furry, W. H.—No. 44

Glasser, Otto—No. 4
Goldsmith, H. H. and J. H. Manley—No. 47

Hafstad, L. R. and M. A. Tuve—No. 10
Hebb, M. H. and E. M. Purcell—No. 56
Hemingway, Allan—No. 17
Hoffmann, B. and L. Infeld—No. 54
Howe, J. D. and K. Lark-Horovitz—No. 36
Huggins, Maurice L.—No. 28

Infeld, L.—see Hoffmann, B.
Inglis, D. R.—No. 68

Johnson, Thomas H.—see Read, D. N.
———No. 62
Jordan, Edward B.—see Bainbridge, Kenneth
——— **and Kenneth Bainbridge**—No. 60

Kersten, H. and C. H. Dwight—No. 34
Kinsey, E. L. and J. W. Ellis—No. 40
Knipp, Charles T.—No. 20
Knipp, Julian K.—No. 43
Kraus, J. D. and J. M. Cork—No. 49

Lark-Horovitz, K.—see Howe, J. D.
———**and E. P. Miller**—No. 36
Laurence, G. C.—No. 2
Locher, Gordon L.—No. 65
———No. 66

Manley, J. H.—see Goldsmith, H. H.
Masket, A. Victor—see Beams, J. W.
Maxwell, Louis R.—No. 8
Marinelli, L. D.—No. 5
Meschter, Emery—No. 21
Miller, E. P.—see Lark-Horovitz, K.

Millman, S. and I. I. Rabi—No. 32
———**and J. R. Zacharias**—No. 33
Motz, Lloyd—see Rosenthal, Jenny E.

Nordheim, G.—see Nordheim, L. W.
Nordheim, L. W. and G. Nordheim—No. 29

Oldenberg, O. and F. F. Rieke—No. 39

Phillips, M., L. Eisenbud and E. U. Condon—No. 45
Pool, M. L. and J. M. Cork—No. 50
Powers, P. N.—see Dunning, J. R.
Present, R. D. and W. Rarita—No. 46
Purcell, E. M.—see Hebb, M. H.

Quimby, Edith H.—No. 3

Rabi, I. I.—see Millman, S.
———see Torrey, H. C.
Rarita, W.—see Present, R. D.
Read, D. N. and Thomas Johnson—No. 63
Richtmyer, F. K., C. H. Shaw and R. E. Shrader—No. 35
———No. 11
Rieke, F. F.—see Oldenberg, O.
Riffolt, N.—see Thompson, L.
Risher, Russell A.—No. 4
Robinson, Howard A.—No. 41
Rosenthal, Jenny E. and Lloyd Motz—No. 27

Seemann, Herman E.—No. 15
Shaw, C. H.—see Richtmyer, F. K.
Shockley, W.—No. 30
Shrader, R. E.—see Richtmyer, F. K.
Smith, Homer P.—see Fricke, Hugo
Starr, Chauncey—No. 16
Stenstrom, Wilhelm and Irwin Vigness—No. 13
Street, J. C.—see Young, R. T., Jr.

Taylor, Lauriston S.—No. 1
Thompson, L. and N. Riffolt—No. 18
Thornton, R. L. and J. M. Cork—No. 51
Torrey, H. C. and I. I. Rabi—No. 31
Tuve, M. A.—see Hafstad, L. R.

Van Atta, C. M. and L. C. Van Atta—No. 19
Van Atta, L. C.—see Van Atta, C. M.
Van Vleck, J. H—No. 55
Vigness, Irwin—see Stenstrom, Wilhelm

Waterman, A. T.—No. 25
Weber, Alfred H. and Charles B. Bazzoni—No. 24
Weber, Ernst—No. 26
Wilsey, R. B.—No. 14
Witmer, Enos E.—No. 52

Young, R. T., Jr. and J. C. Street—No. 64

Zacharias, J. R.—see Millman, S.
Zirkle, Raymond E.—No. 9